











Metropolitan Segment Traffic Speeds from Massive Floating Car Data in 10 Cities

Moritz Neun , Christian Eichenberger , Yanan Xin , Cheng Fu , Nina Wiedemann , Henry Martin ,
Martin Tomko , Lukas Ambühl , Luca Hermes , Michael Kopp 

Abstract—Traffic analysis is crucial for urban operations and planning, while the availability of dense urban traffic data beyond loop detectors is still scarce. We present a large-scale floating vehicle dataset of per-street segment traffic information, *Metropolitan Segment Traffic Speeds from Massive Floating Car Data in 10 Cities (MeTS-10)*, available for 10 global cities with a 15-minute resolution for collection periods ranging between 108 and 361 days in 2019–2021 and covering more than 1500 square kilometers per metropolitan area. *MeTS-10* features traffic speed information at all street levels from main arterials to local streets for *Antwerp, Bangkok, Barcelona, Berlin, Chicago, Istanbul, London, Madrid, Melbourne, and Moscow*. The dataset leverages the industrial-scale floating vehicle *Traffic4cast* data with speeds and vehicle counts provided in a privacy-preserving spatio-temporal aggregation. We detail the efficient matching approach mapping the data to the OpenStreetMap (OSM) road graph. We evaluate the dataset by comparing it with publicly available stationary vehicle detector data (for Berlin, London, and Madrid) and the Uber traffic speed dataset (for Barcelona, Berlin, and London). The comparison highlights the differences across datasets in spatio-temporal coverage and variations in the reported traffic caused by the binning method. *MeTS-10* enables novel, city-wide analysis of mobility and traffic patterns for ten major world cities, overcoming current limitations of spatially sparse vehicle detector data. The large spatial and temporal coverage offers an opportunity for joining the *MeTS-10* with other datasets, such as traffic surveys in traffic planning studies or vehicle detector data in traffic control settings.

Index Terms—GPS probes, massive floating car data, traffic speed dataset, spot binning

I. INTRODUCTION

Urban traffic analysis and prediction are highly complex as traffic arises from crowd behavior and human interactions that are difficult to model. It also shows a strong spatial variation depending on the layout, regulations, and operations of the

Final manuscript of accepted paper submitted 23 June 2023 to the IEEE Transactions on Intelligent Transportation Systems (T-ITS). (*Moritz Neun and Christian Eichenberger contributed equally to this work.*) (*Corresponding authors: Moritz Neun; Christian Eichenberger.*)

Moritz Neun, Christian Eichenberger, Henry Martin, and Michael Kopp are with the Institute of Advanced Research in Artificial Intelligence (IARAI), Vienna, Austria (e-mail: {first.last}@iarai.ac.at).

Yanan Xin, Nina Wiedemann and Henry Martin are with the Institute of Cartography and Geoinformation, ETH Zurich, Switzerland.

Cheng Fu is with the Department of Geography, University of Zurich, Switzerland.

Martin Tomko is with the Department of Infrastructure Engineering, The University of Melbourne, Australia.

Lukas Ambühl is with the Dept. of Civil, Environmental and Geomatic Engineering, Traffic Engineering Group, ETH Zurich, Switzerland.

Luca Hermes is with the Machine Learning Group, Bielefeld University, Germany

TABLE I: *MeTS-10* dataset overview.

City (Traffic4cast competition year)	Days	Date ranges	8:00–18:00 coverage (#edges w. speed / total #edges)	Mapped ratio (% GPS probes mapped)
Antwerp (2021)	361	2019-01–06, 2020-01–06	0.17	0.89
Bangkok (2021)	361	2019-01–06, 2020-01–06	0.05	0.91
Barcelona (2021)	361	2019-01–06, 2020-01–06	0.09	0.81
Berlin (2021)	180	2019-01–06	0.36	0.94
Chicago (2021)	180	2019-01–06	0.11	0.93
Istanbul (2021)	180	2019-01–06	0.63	0.96
Melbourne (2021)	180	2019-01–06	0.08	0.93
Moscow (2021)	361	2019-01–06, 2020-01–06	0.71	0.81
London (2022)	110	2019-07–12, 2020-01	0.24	0.95
Madrid (2022)	109	2021-06–12	0.36	0.93
Melbourne (2022)	108	2020-06–12	0.08	0.90

street network. Meanwhile, in light of the impact of urban traffic on sustainability, health, and the environment, policy leaders have a strong interest in understanding traffic patterns and in the deployment of data-driven methods for efficient and innovative mobility, called smart cities [1].

Accordingly, the identification, analysis, modeling, simulation, and forecasting of traffic patterns have received much attention in research for years [2]–[4]. Traffic analysis has become a high-tech business aiming at accurately capturing and predicting traffic patterns online [5] to ultimately create a “digital twin” of city-wide traffic that could support operational decisions, navigation, and infrastructure planning [6].

However, the lack of accurate and fine-grained open-source traffic data hinders methodological progress in traffic analysis. Currently, most analyses are based on data from stationary vehicle detectors installed at fixed locations in the urban environment, such as loop counters [7]–[9] or cameras [10], [11]. Such vehicle detector datasets have three main shortcomings: 1) The installation of stationary detectors is costly and laborious. Thus, there are only a few cities globally with sufficiently dense sensor coverage to gain a comprehensive picture of traffic behavior. 2) These data are captured with varying temporal and spatial granularity. 3) Even with high investments, the sensors are integrated only at selected fixed locations, providing incomplete reflection of the traffic flow in urban streets. In particular, the available datasets are usually

guided by the requirements of traffic control, therefore are biased towards highways or urban streets of high throughput.

In summary, datasets based on stationary detectors are usually prone to biases and insufficient spatial coverage for fine-grained traffic analysis. An alternative to data based on stationary detectors with high spatial coverage is provided by vehicle tracking datasets. Such datasets are currently provided by owners (or administrators) of vehicle fleets, such as taxi fleets [12], private vehicle tracks [13], or from ride-hailing services such as the Uber dataset [14], [15]. However, access to these datasets is usually expensive and has additional issues. For example, the Uber dataset provides a high spatial resolution with many street segments, but it comes at the cost of a lower temporal resolution with only hourly traffic speed data available. An important obstacle to publishing such datasets is usually privacy concerns [16], which prevents the sharing of data from sensors installed in private vehicles or smartphones. As exceptions, there are a few publicly available vehicle-probe datasets, but these are limited to single cities (*e.g.* the Didi dataset [17]), short time periods, a low temporal [13] or spatial resolution [18], or a single type of vehicle. Another difficulty is the representation of such datasets: For simplicity and privacy, data are usually aggregated as origin-destination matrices or in a raster format (*e.g.* [13]), making the mapping of traffic speed and flow to the street network impossible.

Here, we introduce *Metropolitan Segment Traffic Speeds from Massive Floating Car Data in 10 Cities (MeTS-10)*, a multi-city traffic speed dataset that provides high-coverage probe-vehicle data mapped onto street segments of the city network. We present a pipeline to derive the dataset from the *Traffic4cast* data [19]. The *Traffic4cast* data was recently published by HERE Technologies, a company providing a platform for the visualization and analysis of location data. To ensure data privacy, the *Traffic4cast* dataset was published as rasterized and aggregated cell-based data, nevertheless providing a high spatial and temporal resolution. We use data from the OpenStreetMap street network to yield the *MeTS-10* with the following properties:

- *Multi-city coverage*: the dataset includes 10 large metropolitan regions in geographically and culturally diverse locations across the globe;
- *High city coverage*: spanning all roads segments covered by the vehicle fleet, in contrast to the sparsity of vehicle detectors and biases of other datasets towards roads of high throughput;
- *Long-term coverage*: between 108 and 361 days of continuously sampled data;
- *Fleet coverage*: in contrast to other vehicle-probe datasets, the dataset is not restricted to *e.g.* taxis only;
- *Graph representation*: in contrast to raster-datasets, we provide data mapped to street segments, enabling the ascription of traffic properties to local regulations or infrastructure;
- *High temporal resolution*: *MeTS-10* provides traffic speed data at 15-min bins as default to balance the trade-off between quality and data size. If needed, data can be readily generated in 5-min bins using the provided pipeline.

With the large spatio-temporal coverage and high resolution, our dataset enables multi-city analysis and studies on spatial transfer learning. Segment-wise representation allows enriching of the data with urban properties and spatial context data at an unprecedented coverage and level of detail, see Table I. Therefore, we believe that the *MeTS-10* data can facilitate the development of new methodologies for future smart cities.

The contributions of this paper are as follows:

- the introduction of the *MeTS-10* dataset of traffic speeds disaggregated and matched on the segments of a road graph from massive floating car data aggregated in a privacy-preserving format (*spot binning*);
- the open-source implementation of the data pipeline, enabling re-processing with refined methods and different road graphs;
- the comparison with stationary vehicle detector speeds (ground-truth-like but spatially sparse measurements) and Uber Movement speeds (also from GPS probe data using trajectory-based aggregation and a different vehicle fleet);
- the analysis and discussion of the effects of spot binning and trajectory-based speed aggregation.

The remainder of this paper is organized as follows: We first describe related work in Section II, and then describe our novel pipeline to derive the dataset from the HERE raster-data with OSM data in Section III. Section IV gives a description of the technicalities of the dataset and usage instructions. In Section V, we compare and validate our data with stationary vehicle detector data as well as probe vehicle data from the Uber dataset, exploiting partial temporal and spatial overlaps of our dataset with others. Finally, we discuss the opportunities and limitations of *MeTS-10* in Section VI.

II. RELATED WORK

We compare existing traffic datasets in Table II in terms of type, size, temporal, and spatial resolution. While many cities worldwide publish (parts of) their sensor data, we focus on a few datasets that were selected based on one of the following properties: 1) size (pooling of multiple sensor-based datasets), 2) their relevance for research (mentioned in methodological work on traffic analysis and prediction), or 3) their similarity to our dataset (probe-vehicle data).

A. Vehicle Detector Datasets

Most available data come from stationary vehicle detectors installed on highways and main roads. The reason for the availability of such data is their low privacy sensitivity, in contrast to information about individual vehicle tracks. Although many studies have been conducted in collaboration with local authorities on proprietary vehicle detector data, such data was systematically collected, pre-processed, and published for specific regions, for example, in the PEMS [20] and METR-LA [21] datasets. Smaller public datasets exist, for example, for Seattle [8], Guangzhou [22], or Portland [23]. The UTD-19 [9] dataset is an effort to combine data from 40 cities into a unified representation but has been used primarily for the analysis and simulation of traffic data [24], [25]. Others have introduced image-based datasets from cameras installed

TABLE II: Overview of related public traffic datasets.

Dataset	Type	Number of records	Temporal resolution	Spatial resolution	Collection Area	Biases (vehicle / road types)
PEMS [20]	Loop detectors		5 min	39k detectors	California	highway network
METR-LA [21]	Speed (loop detectors)	34,272	5 min	207 nodes	Los Angeles County	highways
UVDS [7]	Flow (loop detectors)	25,632	5 min	104 nodes	Daejeon (South Korea)	urban main roads
Seattle Loop [8]	loop detectors		5 min	323 detectors	Seattle	freeways
NYC Taxi	pick-up / drop-offs	1.5 B.	timestamp	full city	New York	taxis
UTD-19 [9]	loop detectors		3-5 min	23541 sensors	40 cities	main roads
VLUC [13]	vehicle-probes	4800 x 2 cities	30 min	450 m × 450 m grid	2 cities	all urban streets
Q-traffic [18]	Speed data (Baidu)	265 mio	15 min	15k road segments	Beijing, 1x1 km grid	urban areas
Uber [14]	Speed data		1 hour	OSM segments	11 cities	Uber drivers
Didi (Gaia Initiative)	Speed data		10min	Road segments	Chengdu & Xi'an	Didi ride
Mobile Millenium [27]	GPS trajectories	(not open data)	timestamp	GPS trajectories	San Francisco	crowd-sourced collection
T-Drive [28], [29]	GPS trajectories	15 million	timestamp	GPS trajectories	Beijing	taxis
Kaggle congestion	Vehicle count	48,120	1h	4 Junctions	Unknown	only 4 junctions
Traffic4cast [19]	Speed and probe count	108–361 days	5 min	~ 100 m × 100 m × 4 headings	10 cities, ~ 50 km × 50 km	vehicle fleet

on streets [10], [11], [26]. Since we focus on traffic speed and since the use cases of such datasets are very different from ours, we refer to other work for more details.

B. GPS Probes Datasets

A similar approach as in the HERE traffic movie dataset is taken by the VLUC dataset [13], pooling several GPS-based datasets in traffic movie representations. In Table II, we only report the statistics for their new dataset from two big cities in Japan (Tokyo and Osaka), although they also include previously published datasets such as NYC Taxi and NYC bike datasets in the VLUC dataset. These new data were collected over 100 days, using a GPS enabled app installed by about 1 million users, “approximately 1% of the total population of Japan” [13]. The data was later aggregated into 30-minute intervals and $450\text{ m} \times 450\text{ m}$ grid cells. In contrast, Microsoft presented work on two datasets of GPS trajectories that were not aggregated in grid cells. While only a small fraction of the Mobile Millenium dataset [27] is publicly available, the T-Drive data [28], [29] offers a large set of taxi trajectories for trajectory analysis. Such data is rich in information but requires extensive preprocessing before any analysis. Finally, crowdsourced GPS probes have been used for collecting lane-based road information [30].

Furthermore, the ride-hailing services Didi and Uber published segment-wise data that are closest to ours in terms of representation [14], [15], [17]. While the data are biased toward taxi traffic behavior, they provide high spatial coverage of speed estimates. The main drawback of the Uber dataset is the low temporal resolution of one hour, preventing not only the evaluation of short-term prediction methods, but also in many cases peak hour is around 1h, so 1h bins come at the risk of missing peak hours or averaging them out.

III. THE DATASET: SEGMENT MEDIAN SPEEDS

In this section, we give an overview of *MeTS-10*, before going into the technical details in Section IV. The *MeTS-10* dataset provides segment-wise speeds derived from aggregated GPS probes via a spatial join with a road graph. We use a road graph derived from OSM. The GPS data was made publicly available by HERE Technologies as a spatio-temporal aggregation [19], [31]–[33]. Table I shows the cities and date ranges of the available aggregated data. The raw source probes or trajectories are not publicly available. The dataset comprises 10 cities with data from 108 up to 361 days publicly available

for download from HERE Technologies for the corresponding *Traffic4cast* competition years.

The GPS speeds and the number of probe points (probe volumes) come at a 5-min resolution. Segment-wise speeds can thus be aggregated to 5-min or any coarser resolution (as an integer multiple); here, we default to 15 minutes to balance between quality and storage. The *Traffic4cast* bounding box covers $\sim 50\text{ km} \times 50\text{ km}$ in every city. Table I also shows that the different cities have different coverages (relative number of speed data points at 15-minute resolution), depending on the size and constitution of the contributing vehicle fleets, but also on the road topology (segment lengths). The high coverage in Moscow is partially due to the exclusion of the “fat tail” as reflected by the lower ratio of mapped GPS probes. Here, most inner-block roads are modeled as service roads, which we do not include by default in the road graph derivation from OSM data. More details can be found in Supplement E [34] and the documentation in the code repository.

For illustration, we pick the city of London, one of the cities for which we have other datasets to compare with in Section V. Figure 1 shows the densities and geographical coverage of the available speed segments across the whole city of London. Densities (or temporal coverage) is the ratio of edges with speed values between 8am and 6pm (from 20 sampled days) with respect to the selected OSM road graph (see also 8:00–18:00 coverage in Table I). For motorway highways, the coverage is close to 100% during day time, and also trunk and primary streets have a speed value during 50% of the day, see Supplementary Material [34]. Figure 8 shows the daily speed profiles for two motorway situations, reflecting the speed limits as well as the daily fluctuation due to increased traffic (dips during the morning and afternoon peak hours). London has cross-country motorways cutting through the bounding box, resulting in high speed levels.

IV. INPUT DATA AND DATA PIPELINE

In this paper, we are demonstrating how the aggregated GPS data can be matched with an OSM road graph. The same methodology can also be used on further road graph variants other than OSM. Due to the license limitations of the two input data sources (see Supplement A-A [34]), users need to generate the dataset by running the data pipeline. As we provide the complete code for generating our multi-city segment-wise traffic speed dataset, users are welcome to improve the methodology we describe in this article and refine it for specific applications.

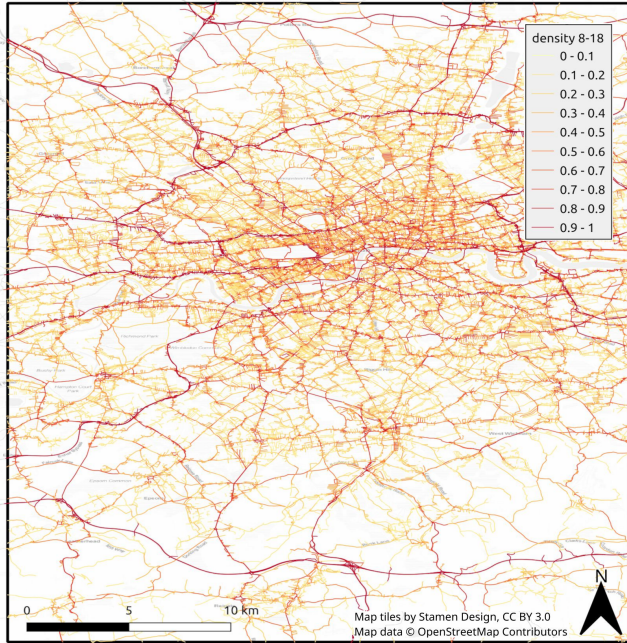


Fig. 1: Segment density during 08:00–18:00 for London.

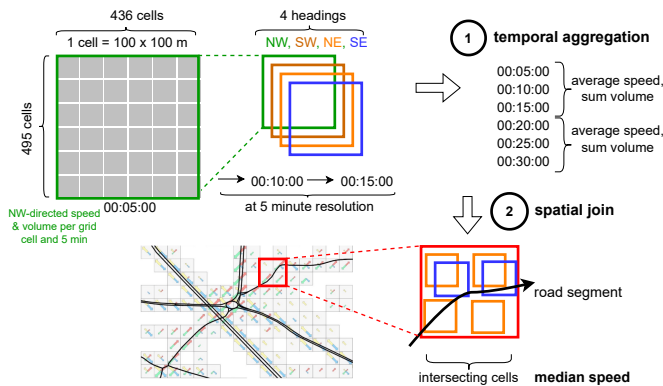


Fig. 2: *MeTS-10* method overview. We leverage data from HERE traffic map movies (GPS probes that are aggregated spatially into $\sim 100\text{m} \times 100\text{m}$, and 4 headings, and temporally in 5-minute bins). We derive segment-wise 15-min speeds by temporal (①) and spatial (②) aggregation.

Figure 2 gives an overview of our method implementing the spatial join: The road graph comes from OpenStreetMap (OSM) and the spatio-temporally aggregated GPS probes come as Traffic Map Movies from HERE Technologies. After downloading the aggregated GPS probes from HERE Technologies, the pipeline code can be executed and automatically takes care of downloading a suitable navigable road graph from OSM. Further technical details on input data and data pipeline can be found in Supplement A [34].

A. Input Data

1) *Traffic Map Movies*: HERE Technologies provides spatially and temporally aggregated GPS probe data from multiple culturally and socially diverse metropolitan areas around the world. The data comprises between 3 months to one year of data per city from 2018, 2019, and 2020 (see Table I). In

Traffic Map Movies [19], [31]–[33], each snapshot (or movie frame) covers $\sim 50\text{km} \times 50\text{km}$ of the urban area at a 5-minute time bin, thus providing comprehensive coverage of complex cities. The city bounding boxes were defined in the context of the *Traffic4cast* competition series with the same height and width for all cities (for some cities, the shape is rotated). The spatial binning divides the data into grid cells of 0.001° (*i.e.* $\sim 100\text{m} \times 100\text{m}$) and 4 headings (NE,SE,SW,NW), as shown in Figure 3. In each bin, probe volume (number of GPS recordings, not vehicles) and mean speed are collected. More precisely, data for one city and one day comes in the shape of (288, 495, 436, 8) uint8, representing 288 time slots, 495 rows, 436 columns, and 8 channels (volume and speed for 4 headings).

Intuitively, this *spot binning* favors lower speeds as slower cars stay longer in the same spatio-temporal bin and are counted multiple times. Under idealized conditions (see Supplement B [34]), the spatio-temporally aggregated speed represents the total distance divided by the total travel time, which is the harmonic sum of the speeds. In particular, this requires controlling the probe rate of vehicles and depends on traffic volume and homogeneity.

2) *OpenStreetMap*: OpenStreetMap (OSM) is a database of GIS data built by an open community of contributors [35]. The OSM data model does not directly describe a road graph, a traversable graph needs to be derived from the OSM elements.

B. Data Pipeline

Figure 3 gives an overview of the GPS probe aggregation. The HERE traffic map movies are the source of GPS probe data to be leveraged by our method. Optionally, depending on the application, further temporal aggregation helps to smoothen sparsity in the data collection and to align with other data sources like vehicle counters. Finally, the gridded data is mapped to a road graph through the spatial join. We refer to Supplement B [34] for technical details.

1) *OpenStreetMap Data Download and Road Graph Construction (dp03)*: As described above, OSM does not directly come in the form of a road graph. We generate a basic road graph using source data from OSM data for the city’s bounding box using *OSMnx* [36].

2) *Spatial Intersection of Road Graph and City Cells (dp04)*: This step generates lists of intersecting cells for each road segment in the corresponding Traffic Movie grid. By interpolation over the edge geometries we get a list of directed cells (row, column, and heading) partially overlapping with this segment.

3) *Temporal Aggregation of HERE Traffic Map Movies (dp01)*: HERE Traffic Movies come in 5-minute aggregation, *i.e.* the data of one day for each city is represented by 288 movie frames per day. Further aggregation might be advisable to match with other data sources (such as vehicle counters in the *Traffic4cast* competition [37]) or to smoothen the sparsity of data. Here, we aggregate the gridded data temporally in 15-minute resolution, see Figure 2 (top right, ①) and Figure 3.

4) *Segment Speeds from Spatial Join (dp06a)*: We derive the segment speeds and volumes by taking the median speed

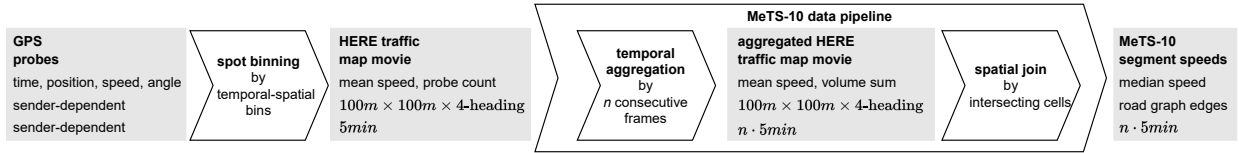


Fig. 3: GPS probe aggregation overview showing the different steps (arrowheads) and the data (grey areas). For the data, their main attributes and the spatial and temporal resolution are listed.

and total probe volume over all intersecting cells from the aggregated *Traffic4cast* movie, see Figure 2 (bottom, ②). The intersecting cells take into account the heading, and there is a positional and angular margin. In Figure 2, we show the intersecting cells within the red box for one directed road segment; the orange NE cells are intersecting by the positional margins; the blue SE cells are intersecting because of the angular margins. We choose the median in order to be robust to distortions coming from erroneous GPS signals and the different intersecting cells going into the edge. In particular, cars stopping for delivery, alighting, or boarding, even in a parking space close to the road, emit many GPS signals at the same location, which can have a large impact on the mean speed from the *Traffic4cast* movies under low flow conditions.

5) *Confidence Filtering of Segment Speeds (dp06b) Based on Speed Clustering (dp02) and Free Flow Speeds from Spatial Join and Quantile Selection (dp05)*: As confidence filtering is optional and it does not change the data values, we discuss it last. Spot binning of GPS probes does neither include any map-matching nor segmentation. Therefore, many of the traditional data cleansing methods of trajectory data mining [38] do not apply in our setting. As a pragmatic approach to trading off quality and coverage, we apply confidence filtering on segment-wise 15 min median speeds. The rationale for our filtering is the following: First, as just mentioned, there are many situations where small speed values can distort the current traffic situation, which is particularly grave in low-volume situations. Second, we want to avoid too many false positive low-speed congestion outputs. Therefore, in order to be confident that a situation is congested, we require more “proof” to confidently accept the overall low speed; if we are not confident enough, we reject the median speed computed, *i. e.* we do not correct or impute, but filter it out.

Our confidence filtering is based on the concept of a congestion factor [39], which is the ratio of the current segment speed by the free flow speed. The derivation of free flow speeds is based on k-Means clustering of the speed data. This is in line with similarly motivated approaches to derive free flow, *e. g.* [15] uses the 85th percentile of all speed values observed.

V. VALIDATION

In this section, we validate the *MeTS-10* dataset by comparing it with two other datasets: (A) the Uber Movement Speeds dataset, which partially overlaps with the *MeTS-10* dataset spatially and temporally for cities Barcelona, Berlin, London. (B) ground-truth-like speed readings from stationary vehicle detectors for cities Berlin, London, and Madrid. As additional baseline and sanity check, in (C), we compare the

Uber Movement Speeds with the stationary vehicle detector speed readings.

A. Comparison with Uber Movement Speeds

1) *Dataset Comparison*: Uber Movement [40] provides speeds, travel time, and mobility heatmap across world cities. Uber uses the mean trip speed of a segment as the signature of speed [14]. Trips as GPS waypoints are map-matched to OSM road segments. Trip speed is then defined as the length of a segment divided by the time of a trip that passes the segment, including the waiting time at exits. For the mean trip speed calculation, trip speeds are further aggregated hourly, excluding trips that have a drop-off or pick-up in the segment. In addition, if a road segment has fewer than 5 valid trips during an hour, the mean trip speed is not provided [14]. Table III compares HERE Traffic Map Movies [19], [41]–[43] and Uber Movement Speeds data sources [14], [15], [40].

TABLE III: Comparison of HERE Traffic Map Movies and Uber Movement Speeds data sources.

	HERE Traffic Map Movies [19]	Uber Movement Speeds [40]
contributing vehicles	connected vehicles, different providers	Uber driver app
temporal resolution	5 min	60 min
spatial resolution	~100m x 100m x 4 headings	segments (map matched)
speed aggregation	mean of instantaneous GPS probe speeds	mean of trajectory distance over time
cities	10	11
license	academic and non-commercial, custom HERE T&Cs	CC BY-NC
probe vol	number of readings	–
continents	AS, EU, NA, OC	AF, AS, EU, NA, OC, SA
coverage	108–361 days	3–27 months
collection period	2019.01–2021.12	2018.01–2020.01
overlap		Barcelona: 3 months (2020-01 – 2020-03) Berlin: 6 months (2019-01 – 2019-06) London: 7 months (2019-07 – 2020-01) Madrid: no temporal overlap

2) *Spatial and Temporal Coverage*: As Uber data is aggregated hourly, we take the 1h-mean of our 15-min *MeTS-10* speeds for the comparison. Figure 4 shows the differences by road class for all the segments within the *MeTS-10* bounding box for London. We show the mean density difference by road class (*i. e.* OSM highway attribute); positive density difference means higher temporal coverage of *MeTS-10* and negative mean lower temporal coverage. We see that *MeTS-10* provides generally higher temporal coverage.

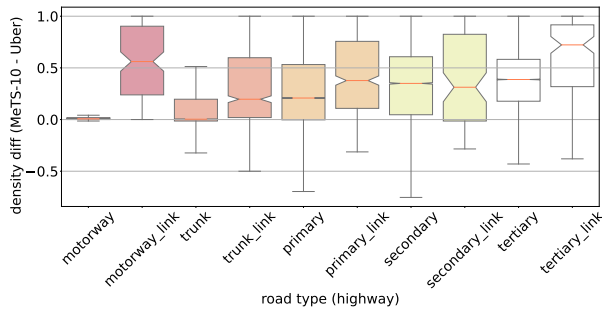


Fig. 4: Segment density differences Uber and *MeTS-10* London daytime (8am–6pm, *Traffic4cast* bounding box only) by road type. Color scheme: OSM Carto.

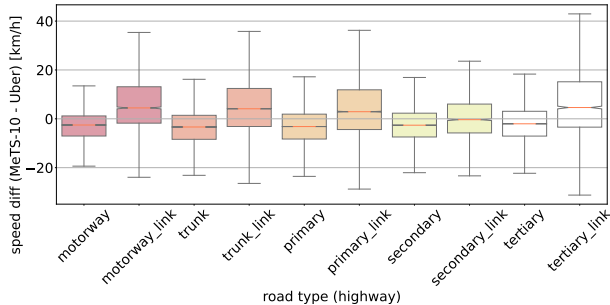


Fig. 5: Speed differences Uber and *MeTS-10* for London daytime (8am–6pm, *Traffic4cast* bounding box only) by road type. Color scheme: OSM Carto.

3) *Speed Differences*: Figure 5 shows the mean speed differences of the matching data, *i. e.* within *MeTS-10* bounding box only and where data is available at the same time and segment. Positive speed difference means higher values in *MeTS-10*. We see that our speeds are slightly lower, except for the link road classes, where our speeds tend to be much higher. We suspect this is due to the aggregation strategy: [14] seems to take the mean of the trajectory speeds, resulting in a time-mean speed (arithmetic mean of vehicle speeds), whereas our spot binning aggregation results in an approximation of space-mean speed (harmonic mean of vehicle speeds) as discussed above in Section IV-A1 and Supplement B [34]. We hypothesize that the higher speeds on link roads are due to links running in parallel to the corresponding higher-class roads they link to; as the Uber map-matching follows the vehicle trajectory, Uber can make a distinction here whether the vehicle is on the link or not. These findings are confirmed in a quantitative analysis. We use absolute percentage error as used in the traffic simulation calibration literature [44]. We show differences in APE between complex and non-complex road segments, differentiated by road type.

For additional material and the analysis of Barcelona and Berlin, we refer to the Supplementary Material [34] and our code repository.

B. Comparison with Stationary Vehicle Detector Data

Stationary vehicle detectors such as inductive loop detectors or road cameras are commonly used to monitor traffic. Earlier work for Berlin [45] has already shown that there is a good

TABLE IV: Overview of stationary vehicle detector sources.

	Berlin	London	Madrid
provider	VIZ Berlin [47]	TfL [48] / Highways England [49]	Ayuntamiento de Madrid [50]
temporal resolution	60 min	15 min	15 min
# all sensors	547	3819	4413
# speed sensors	547	236	404
speed sensor coverage	entire city	motorways in outskirts	inner-city motorways

global alignment between the *Traffic4cast* data used in *MeTS-10* and the traffic volumes in vehicle detector data. The good overlap between floating car data and stationary vehicle detector ground truth has also been shown in the Netherlands [46]. In this section, we compare vehicle detector data speed readings with the *MeTS-10* values in three cities (Berlin, London, and Madrid) to highlight the differences between the two datasets and their suitability in different applications.

Table IV gives an overview of openly available vehicle sensor data we use in our comparisons. We focus on detectors that directly measure the speed of passing vehicles in addition to the traffic flow. In Berlin all sensors provide speed measurements at a temporal resolution of 60 minutes while in London and Madrid fewer counters do have speed measurements but at a temporal resolution of 15 minutes.

Figure 6 shows the distribution of the measured speed values of an entire day in the three cities. *MeTS-10* speeds are shown on the x-axis and corresponding sensor speeds on the y-axis using 10 bins for clustering. Speed readings are from a full day between 6am and 11pm in 15-minute (resp. 60 minutes for Berlin) intervals.

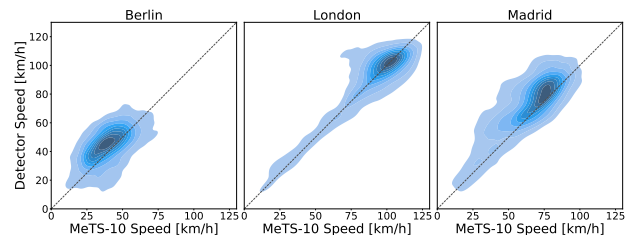


Fig. 6: Binned Kernel Distribution Estimation (KDE) Plots of speeds of *MeTS-10* and sensors.

On the y-axis, the average sensor speeds per time interval are used and on the x-axis the *MeTS-10* speed readings on the corresponding segment. Hence, the best correspondence of the speeds is found on the diagonal line. All three cities show a good alignment of the majority of the points along the diagonals. The shapes of the KDE plots reflect the differences in the city sensor placement (*cf.* Table IV and Figure 7, and placements in Supplement C [34]). In Berlin, most sensors are placed on major streets (primary/secondary) with speed limits between 50 and 60 km/h. In contrast, speed sensors in London are all along motorways yielding a high speed density at around 100 km/h in Figure 6. In Madrid, most sensors are also along motorways, but all are within the city on the main ring road. Hence, here lower speed limits are common and there is more variance of speeds caused by the general traffic situation (traffic lights or alike).

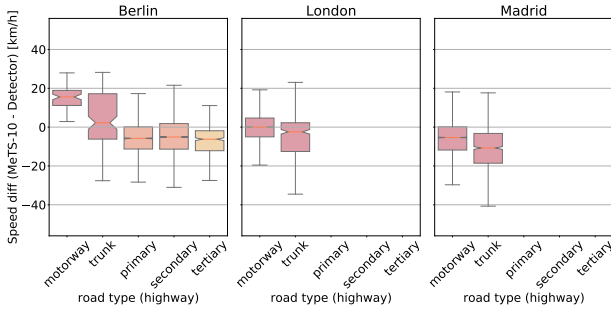


Fig. 7: Box plots of speed differences between *MeTS-10* and vehicle detectors by highway type. Color scheme: OSM Carto.

For London, Madrid, and non-motorway/trunk highways in Berlin, the sensor speeds usually are a bit higher than the *MeTS-10* speeds (see Figure 7). This is in line with the differences observed in the comparison with Uber speeds (see Section V-A). In particular, speed sensors measure every vehicle only once, while the space mean speed of GPS data weighs slow vehicles more often than fast vehicles along the same segment (spot binning resulting in harmonic mean under idealized conditions, see Supplement B [34]). On motorway or trunk roads in Berlin, sensors show a 10 to 15 km/h lower speed level. However, this only affects 10 sensors (2%, see Supplement C.B [34]) and was also observed in the comparison between Uber and sensor data (see Section V-C).

The alignment of speed readings during an entire day can be seen in Figure 8 with examples on motorways in London. The general alignment between the *MeTS-10* speed (yellow) and the sensor speed (blue) is good but *MeTS-10* shows a higher variance and responsiveness to changes. For example, during evening and night times in the undisturbed situation with no intersecting roads or lane changes (Figure 8a) the sensor speed is significantly smoother. A possible reason is the fact that the sensor speed is the mean over 15 minutes in exactly the same location while the *MeTS-10* speed contains a median over multiple values along the segment.

In addition, in situations where the sensor is near a motorway exit (Figure 8b), the general *MeTS-10* speed level might be increased and smoothed by signals from the nearby motorway segments which results in less accentuated slowdowns during rushhour ($t \approx 50$ and $t \approx 70$) with the lowest *MeTS-10* speed approx 20km/h higher than the sensor speed.

Overall the comparisons and examples in the three cities show that *MeTS-10* speeds show a good general correspondence with the sensor speeds. The differences seen can be explained sufficiently through the differences in data collection and aggregation methods.

C. Baseline comparison of Uber Movement Speeds with Stationary Vehicle Detector Data

As a baseline and additional sanity check of the used ground-truth-like data, we compared the Uber Movement Speeds data with the stationary vehicle detector speeds in Berlin and London. The matching approach was the same as for the comparison with *MeTS-10* in Section V-B. The detailed plots of the analysis in Supplement C.C [34] show similar effects and differences as discussed with regards to Figures

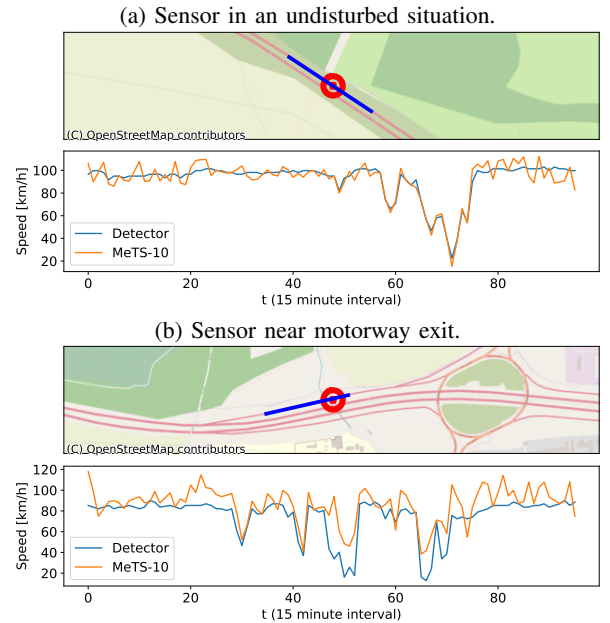


Fig. 8: Sensor placement examples along motorways in Greater London with corresponding speeds during one day.

6 and 7. For example, the speed differences for motorways in Berlin are also present with average speed differences 12.7 ± 7.2 km/h for *MeTS-10* and 13.5 ± 7.8 km/h for Uber. Over all road types, we have -2.9 ± 13.4 km/h for *MeTS-10* and -2.6 ± 14.2 km/h for Uber.

VI. DISCUSSION

In this section, we discuss the opportunities and limitations of our design choices of our method and validations.

A. Discussion of Method Design Choices

a) *Traffic Map Movies*: The GPS probe data originates from connected vehicles from different probe data providers [41], [42]. HERE Technologies leverage many different probe data providers in collaboration with leading automotive companies, logistics providers, city governments and transportation agencies [41]. Information on the exact set of probe data providers and provider changes in each city is not publicly available. The HERE Traffic Map Movies are not restricted to a single GPS probe provider, e.g., taxis or buses, as other floating car data. Hence, as for other floating vehicle datasets [51], the dataset only reflects a (biased) subset of road traffic in the cities. Clearly, volumes do not reflect total traffic and we assume they are also biased towards the vehicle fleet of connected cars providing GPS probes; Uber, for instance, does not publish probe volume for this reason [15]. On the other hand, speeds can be expected to be accurate and representative apart from notorious situations like lower speed limitations for transport vehicles on motorways and vehicles stopping for delivery of goods or people boarding or alighting.

From a more theoretical point of view, it would be interesting to explore the characteristics of spot binning under different assumptions (spatial and temporal resolution, GPS emittance rate, sampling bias and flow conditions, road network complexity), e. g. using traffic simulations.

Whereas the Traffic Map Movies dataset does not cover long enough periods for long-term trend analysis, it could still be useful for daily and/or seasonal traffic analysis.

b) OpenStreetMap Road Graph (dp03): We chose to use OpenStreetMap data due to its availability for research. The method and the source data can be applied to any directed road graph. For instance, we use our pipeline to also map the Traffic Map Movies to the non-simplified historic OSM road graph used by Uber. The flexibility of using any road graph helps to prevent practical usage limitations when the road graph evolves or a different type of road graph is preferred.

c) Spatial Intersection of Road Graph and City Cells (dp04): In order to investigate whether our method suffers from having only 4 headings in the Traffic Map Movies, we compare the coverage on segments mainly along diagonals and along the horizontal/vertical main axes. We see only a slightly higher coverage on the segments along the main axes. For more details, we refer to the Supplementary Material [34].

d) Temporal Aggregation of Traffic Map Movies (dp01): We chose to default to 15-minute aggregation of Traffic Map Movies as it is the least common multiple of the temporal resolution of many public stationary vehicle detector datasets. Depending on the use-case, the raw 5-minute of HERE Traffic Map Movies can also be used.

e) Spatial Join (dp06a): We chose the median of all intersecting cells for its robustness against outlier data, *e.g.* data from a higher-speed road distorting the value of a lower-speed road nearby. The described temporal-spatial join gives equal weight to all cells that intersect a road segment – we chose it for its simplicity. Our method could be refined by giving different weights to these intersecting cells based on volume or geometric properties, *e.g.* intersection length or alignment with spot binning heading.

f) Confidence Filtering of Segment Speeds (dp06b): The confidence-based filtering approach of *MeTS-10* is a pragmatic implementation for the matching of the aggregated speed values. The congestion factor thresholds (as coming from [39]) and derived free flow values do not need to be perfectly calibrated as they are only used during filtering but not directly for the computation of the median segment speeds. We used sample segments to validate the chosen setting, aiming at a balance between reducing noise through filtering and ensuring high data quality.

The filtering is not overly aggressive. For instance, in Madrid (moderate data availability), around 20% of input speeds are discarded. The chosen thresholds do work well for our use-case of a general-purpose segment speed dataset as well as in the comparisons with Uber and the stationary vehicle counters.

From a methodological point of view, the effect of this filtering would merit additional investigations and refinements, *e.g.* for data smoothing and data imputation. In particular, we never filter speeds much higher than signalized speeds, which could be done during aggregation.

B. Discussion of Validations

There is no existing baseline method for mapping spot-binned traffic data such as the HERE Traffic Map Movies to

a road graph. Also, there is no per-se ground-truth data: First, there is only partial spatio-temporal overlap with the Uber dataset in addition to the collection method being different. Second, stationary vehicle detectors are spatially sparse and may not capture the full road segment (relevant at traffic lights) and have no fleet-bias as GPS probe based datasets. Third, the vehicle trajectories used by HERE to create the Traffic Map Movies are not openly available for research. Hence, we resort to comparing to two other available datasets with partial temporal-spatial overlap.

The differences between *MeTS-10* from loop counters are not higher than between Uber and loop counters. This shows that the spot binning method of Traffic Map Movies gives similar results as trajectory-based methods used by Uber, at lower computational costs.

While the comparison to Uber and vehicle detector data demonstrated good representativeness and coverage, *MeTS-10* is of course not free of biases. The speed channel can be biased in complex road network situations (where probes from parallel roads closeby may interfere) and under low-volume conditions. (where a single stopped car emits many signals). The effects are stable and can be mitigated using *e.g.* the standard deviation, which is provided in addition to the median speeds, for filtering. The volumes provided are biased by the provider's vehicle fleet composition; however, they can be a valuable additional signal for sanity checks if interpreted carefully. Similarly, our free flow speeds are data-driven and could be compared with other data sources, and the divergences between them and signalized speeds could be used for map correction or roadworks detection.

Furthermore, the daily temporal coverage is highly dependent on the road class and is usually very good for highway types such as motorways. There is also a bias depending on the mix of the city's providing vehicle fleet and on the location within the city.

In order to further validate our speed dataset, corridors could be sampled and ETAs derived from our speeds could be compared with ETAs from routing engines or real ETAs from taxi fleets for typical daytime situations.

VII. CONCLUSION

In this paper, we have presented the new *Metropolitan Segment Traffic Speeds from Massive Floating Car Data in 10 Cities (MeTS-10)*. The source data covers 10 large metropolitan areas with 108 to 361 days of sampled data per city and with a temporal resolution of 5 minutes. In contrast to other datasets, *MeTS-10* neither suffers from low spatial coverage as common vehicle detector datasets, nor is it restricted to a single GPS probe provider, *e.g.*, taxis or buses, as other floating car data. Specifically, our validation experiments showed that *MeTS-10* has better spatial and temporal coverage than the Uber speeds within the main city area. Therefore, depending on the use-case, there can be an additional gain from combining the two data sources. Floating car data availability is also often limited due to privacy constraints. The Traffic Map Movie format of the source data circumvents such restrictions through its spatio-temporal aggregation. With the proposed

pipeline, we are offering an efficient and standardized way of disaggregating and matching such aggregated floating car data to a road graph.

The comparisons with the Uber dataset on the one hand as well as the stationary vehicle detector datasets on the other hand show the good representativeness and coverage of the *MeTS-10* dataset. The limitations *e.g.* for complex network situations, low-volume situations, and location and road class dependent effects of vehicle fleet composition are understood and discussed. Spot binning, the aggregation method of Traffic Map Movies, is shown to correspond to space-mean speeds (harmonic mean of vehicle speeds) under idealized conditions, resulting in potentially lower speeds than time-mean speed (arithmetic mean of vehicle speeds). The effects are stable and researchers can use the additional attributes at their location of interest for filtering, *e.g.* using the standard deviation and volume channel.

The large spatial and temporal coverage offers the opportunity to also complement other datasets and extend on the disaggregation, matching, or fusing techniques for other data-driven use-cases. The sources and the complete code for creating the dataset are publicly available. This open approach allows the extension and modification of the matching algorithm as well the use of other or customized road graphs, preventing many practical limitations, for example when the road graph evolves or with unavailable historic road graph data. It can also be a suitable approach for other GPS data sources and potentially even for coarser data such as mobile phone location information. *MeTS-10* is also a candidate for the creation or extension of benchmark datasets for common domain specific tasks such as short-term traffic prediction and also for more general machine learning tasks *e.g.* in the area of graph neural networks. This can help to compare the performances of different approaches, as well as to identify potential biases and limitations in models and datasets.

DATA AND CODE AVAILABILITY

The *Traffic4cast* movies input data is available from [19]. The code to create the dataset and to reproduce the analysis and figures in this paper is available in our GitHub repository¹. The Uber data is available from [40], the OSM data for the historic road graphs is available from Geofabrik², and the vehicle detector data from VIZ Berlin [47], TfL [48], Highways England [49] and Ayuntamiento de Madrid [50].

ACKNOWLEDGMENT

The authors would like to thank HERE Technologies for making the *Traffic4cast* competition data available.

AUTHOR CONTRIBUTIONS STATEMENT

Following CRediT (Contributor Roles Taxonomy³), the authors have contributed as follows.

Writing – original draft (integral), Software, Data Curation: M.N. and Ch.E. *Validation, Visualization, Writing – original*

draft (Validation Section): Y.X., Ch.F., M.N., and Ch.E. *Writing – original draft (Introduction and Related Work):* N.W. and H.M. *Conceptualization, Writing – review & editing:* all.

REFERENCES

- [1] M. Angelidou, "The role of smart city characteristics in the plans of fifteen cities," *Journal of Urban Technology*, vol. 24, no. 4, pp. 3–28, 2017.
- [2] R. Vaughan, *Urban spatial traffic patterns*. Pion Limited, 1987.
- [3] S. Paveri-Fontana, "On boltzmann-like treatments for traffic flow: a critical review of the basic model and an alternative proposal for dilute traffic analysis," *Transportation research*, vol. 9, no. 4, pp. 225–235, 1975.
- [4] H. Greenberg, "An analysis of traffic flow," *Operations research*, vol. 7, no. 1, pp. 79–85, 1959.
- [5] M. Batty, *The new science of cities*. MIT press, 2013.
- [6] T. Deng, K. Zhang, and Z.-J. M. Shen, "A systematic review of a digital twin city: A new pattern of urban governance toward smart cities," *Journal of Management Science and Engineering*, vol. 6, no. 2, pp. 125–134, 2021.
- [7] K.-H. N. Bui, H. Yi, and J. Cho, "Uvds: a new dataset for traffic forecasting with spatial-temporal correlation," in *Asian Conference on Intelligent Information and Database Systems*. Springer, 2021, pp. 66–77.
- [8] Z. Cui, R. Ke, Z. Pu, and Y. Wang, "Deep bidirectional and unidirectional lstm recurrent neural network for network-wide traffic speed prediction," *arXiv preprint arXiv:1801.02143*, 2018.
- [9] A. Loder, L. Ambühl, M. Menendez, and K. W. Axhausen, "Understanding traffic capacity of urban networks," *Scientific reports*, vol. 9, no. 1, pp. 1–10, 2019.
- [10] C. Snyder and M. Do, "Streets: A novel camera network dataset for traffic flow," *Advances in Neural Information Processing Systems*, vol. 32, 2019.
- [11] H. S. Bharadwaj, S. Biswas, and K. Ramakrishnan, "A large scale dataset for classification of vehicles in urban traffic scenes," in *Proceedings of the Tenth Indian Conference on Computer Vision, Graphics and Image Processing*, 2016, pp. 1–8.
- [12] B. Donovan and D. Work, "New york city taxi trip data (2010-2013)," 2016. [Online]. Available: <https://doi.org/10.13012/J8PN93H8>
- [13] R. Jiang, Z. Cai, Z. Wang, C. Fan, X. Song, K. Tsubouchi, and R. Shibasaki, "Vluc: an empirical benchmark for video-like urban computing on citywide crowd and traffic prediction," *arXiv preprint arXiv:1911.06982*, 2019.
- [14] "Uber movement: Speeds calculation methodology," last accessed 11 October 2022. [Online]. Available: https://movement.uber.com/_static/97e6e916ed8e8176.pdf
- [15] "Faqs – uber movement: Let's find smarter ways forward, together," last accessed 11 October 2022. [Online]. Available: <https://movement.uber.com/faqs?lang=en-US>
- [16] A. Boeckelt, S. Breitenberger, and M. Hauschild, "Probe vehicle data: data efficiency and privacy interest," in *12th World Congress on Intelligent Transport Systems/ITS America/ITS Japan/ERTICO*, 2005.
- [17] D. C. T. Co, "Didi chuxing gaia initiative," last accessed 31.12.2022. [Online]. Available: <https://gaia.didichuxing.com>
- [18] B. Liao, J. Zhang, C. Wu, D. McIlwraith, T. Chen, S. Yang, Y. Guo, and F. Wu, "Deep sequence learning with auxiliary information for traffic prediction," in *Proceedings of the 24th ACM SIGKDD International Conference on Knowledge Discovery & Data Mining*, 2018, pp. 537–546.
- [19] "Sample data — here developer," September 2020, last accessed 11 October 2022. [Online]. Available: <https://developer.here.com/sample-data>
- [20] "Caltrans performance measurement system (pems)," last accessed 2022-12-23. [Online]. Available: <https://pems.dot.ca.gov/>
- [21] Y. Li, R. Yu, C. Shahabi, and Y. Liu, "Diffusion convolutional recurrent neural network: Data-driven traffic forecasting," in *International Conference on Learning Representations (ICLR '18)*, 2018. [Online]. Available: <https://arxiv.org/abs/1707.01926>
- [22] X. Chen, Z. He, and J. Wang, "Spatial-temporal traffic speed patterns discovery and incomplete data recovery via svd-combined tensor decomposition," *Transportation research part C: emerging technologies*, vol. 86, pp. 59–77, 2018.
- [23] T. R. Metro, Southwest Washington Regional Transportation Council (RTC) and E. C. T. at Portland State., "Portal," last accessed 13 November 2022. [Online]. Available: <https://portal.its.pdx.edu/home>

¹<https://github.com/iarai/MeTS-10>

²<https://download.geofabrik.de/>

³<https://credit.niso.org/>

- [24] L. Ambühl, A. Loder, L. Leclercq, and M. Menendez, "Disentangling the city traffic rhythms: A longitudinal analysis of mfd patterns over a year," *Transportation Research Part C: Emerging Technologies*, vol. 126, p. 103065, 2021.
- [25] D. M. Bramich, M. Menéndez, and L. Ambühl, "Fitting empirical fundamental diagrams of road traffic: A comprehensive review and comparison of models using an extensive data set," *IEEE Transactions on Intelligent Transportation Systems*, 2022.
- [26] D. Xia, X. Liu, W. Zhang, H. Zhao, C. Li, W. Zhang, J. Huang, and H. Wang, "Dutrafic: Live traffic condition prediction with trajectory data and street views at baidu maps," in *Proceedings of the 31st ACM International Conference on Information & Knowledge Management*, 2022, pp. 3575–3583.
- [27] T. Hunter, T. Moldovan, M. Zaharia, S. Merzgui, J. Ma, M. J. Franklin, P. Abbeel, and A. M. Bayen, "Scaling the mobile millennium system in the cloud," in *Proceedings of the 2nd ACM Symposium on Cloud Computing*, 2011, pp. 1–8.
- [28] J. Yuan, Y. Zheng, X. Xie, and G. Sun, "Driving with knowledge from the physical world," in *Proceedings of the 17th ACM SIGKDD international conference on Knowledge discovery and data mining*, 2011, pp. 316–324.
- [29] J. Yuan, Y. Zheng, C. Zhang, W. Xie, X. Xie, G. Sun, and Y. Huang, "T-drive: driving directions based on taxi trajectories," in *Proceedings of the 18th SIGSPATIAL International conference on advances in geographic information systems*, 2010, pp. 99–108.
- [30] L. Tang, X. Yang, Z. Dong, and Q. Li, "Clric: Collecting lane-based road information via crowdsourcing," *IEEE Transactions on Intelligent Transportation Systems*, vol. 17, no. 9, pp. 2552–2562, 2016.
- [31] D. P. Kreil, M. K. Kopp, and al., "The surprising efficiency of framing geo-spatial time series forecasting as a video prediction task – insights from the iarai Traffic4cast competition at neurips 2019," in *Proceedings of the NeurIPS 2019 Competition and Demonstration Track*, ser. Proceedings of Machine Learning Research, H. J. Escalante and R. Hadsell, Eds., vol. 123. PMLR, 08–14 Dec 2020, pp. 232–241. [Online]. Available: <https://proceedings.mlr.press/v123/kreil20a.html>
- [32] M. Kopp, D. Kreil, and al., "Traffic4cast at neurips 2020 - yet more on the unreasonable effectiveness of gridded geo-spatial processes," in *Proceedings of the NeurIPS 2020 Competition and Demonstration Track*, ser. Proceedings of Machine Learning Research, H. J. Escalante and K. Hofmann, Eds., vol. 133. PMLR, 06–12 Dec 2021, pp. 325–343. [Online]. Available: <https://proceedings.mlr.press/v133/kopp21a.html>
- [33] C. Eichenberger, M. Neun, and al., "Traffic4cast at neurips 2021 - temporal and spatial few-shot transfer learning in gridded geo-spatial processes," in *Proceedings of the NeurIPS 2021 Competitions and Demonstrations Track*, ser. Proceedings of Machine Learning Research, D. Kiela, M. Ciccone, and B. Caputo, Eds., vol. 176. PMLR, 06–14 Dec 2022, pp. 97–112. [Online]. Available: <https://proceedings.mlr.press/v176/eichenberger22a.html>
- [34] M. Neun, C. Eichenberger, Y. Xin, C. Fu, N. Wiedemann, H. Martin, M. Tomko, L. Ambühl, L. Hermes, and M. Kopp, "Metropolitan segment traffic speeds from massive floating car data in 10 cities – supplementary material," 2023. [Online]. Available: <https://github.com/iarai/MeTS-10>
- [35] "About – openstreetmap," 2022, last accessed 11 October 2022. [Online]. Available: <https://www.openstreetmap.org/about>
- [36] G. Boeing, "Osmnx: New methods for acquiring, constructing, analyzing, and visualizing complex street networks," *Computers, Environment and Urban Systems*, vol. 65, pp. 126–139, 2017. [Online]. Available: <https://www.sciencedirect.com/science/article/pii/S0198971516303970>
- [37] M. Neun, C. Eichenberger, H. Martin, M. Spanring, R. Siripurapu, D. Springer, L. Deng, C. Wu, D. Lian, M. Zhou, M. Lumiste, A. Ilie, X. Wu, C. Lyu, Q.-L. Lu, V. Mahajan, Y. Lu, J. Li, J. Li, Y.-J. Gong, F. Grötschla, J. Mathys, Y. Wei, H. Haitao, H. Fang, K. Malm, F. Tang, M. Kopp, D. Kreil, and S. Hochreiter, "Traffic4cast at neurips 2022 – predict dynamics along graph edges from sparse node data: Whole city traffic and eta from stationary vehicle detectors," 2023.
- [38] Y. Zheng, "Trajectory data mining: An overview," *ACM Trans. Intell. Syst. Technol.*, vol. 6, no. 3, may 2015. [Online]. Available: <https://doi.org/10.1145/2743025>
- [39] S. Parafina, "Mapping Traffic Congestion - HERE Developer," last accessed 2022-06-07. [Online]. Available: <https://developer.here.com/blog/mapping-traffic-congestion>
- [40] "Uber movement," last accessed 17 October 2022. [Online]. Available: <https://movement.uber.com/>
- [41] "Here launches advanced real-time traffic service," October 2021, last accessed 11 October 2022. [Online]. Available: <https://www.here.com/about/press-releases/en/here-launches-advanced-real-time-traffic-service>
- [42] "Real time traffic – developer guide – here traffic api – here developer," last accessed 11 October 2022. [Online]. Available: https://developer.here.com/documentation/traffic-api/dev_guide/topics/concepts/real-time-traffic.html
- [43] "Terms and conditions — here developer," September 2020, last accessed 11 October 2022. [Online]. Available: <https://developer.here.com/terms-and-conditions>
- [44] "Fhwa: Traffic analysis tools." last accessed 2023-04-13. [Online]. Available: https://ops.fhwa.dot.gov/trafficanalyisistools/tat_vol3/sect5.htm
- [45] P. Wagner, R. Hoffmann, and A. Leich, "Observations on the Relationship between Crash Frequency and Traffic Flow," *Safety*, vol. 7, no. 1, p. 3, Mar. 2021, number: 1 Publisher: Multidisciplinary Digital Publishing Institute. Last accessed 2022-04-05. [Online]. Available: <https://www.mdpi.com/2313-576X/7/1/3>
- [46] W. P. van den Haak and M. Emde, "Validation of google floating car data for applications in traffic management," 2016. [Online]. Available: <http://resolver.tudelft.nl/uuid:b720bedd-1cc9-4fb1-b874-3ae5860736b8>
- [47] "Verkehrsdetektion berlin," last accessed 23 November 2022. [Online]. Available: <https://daten.berlin.de/datensatze/verkehrsdetektion-berlin>
- [48] "Tfl open data, tims," last accessed 23 November 2022. [Online]. Available: <https://roads.data.tfl.gov.uk/>
- [49] "Webtris," last accessed 23 November 2022. [Online]. Available: <https://webtris.highwaysengland.co.uk/>
- [50] "Madrid open data, historical traffic data," last accessed 23 November 2022. [Online]. Available: <https://datos.madrid.es/egob/catalogo/208627-0-transporte-ptomedida-historico>
- [51] M. M. Bruwer, I. Walker, and S. J. Andersen, "The impact of probe sample bias on the accuracy of commercial floating car data speeds," *Transportation Planning and Technology*, vol. 0, no. 0, pp. 1–18, 2022. [Online]. Available: <https://doi.org/10.1080/03081060.2022.2150858>
- [52] Y.-A. Montjoye, C. Hidalgo, M. Verleysen, and V. Blondel, "Unique in the crowd: The privacy bounds of human mobility," *Scientific reports*, vol. 3, p. 1376, 03 2013.
- [53] A. Krause, E. Horvitz, A. Kansal, and F. Zhao, "Toward community sensing," in *2008 International Conference on Information Processing in Sensor Networks (ipsn 2008)*, 2008, pp. 481–492.
- [54] J. Krumm, "Inference attacks on location tracks," in *Pervasive Computing, A. LaMarca, M. Langheinrich, and K. N. Truong, Eds. Berlin, Heidelberg: Springer Berlin Heidelberg*, 2007, pp. 127–143.
- [55] S. Rass, S. Fuchs, M. Schaffer, and K. Kyamakya, "How to protect privacy in floating car data systems," in *Proceedings of the Fifth ACM International Workshop on VehiculAr Inter-NETworking*, ser. VANET '08. New York, NY, USA: Association for Computing Machinery, 2008, p. 17–22. [Online]. Available: <https://doi.org/10.1145/1410043.1410047>
- [56] C. A. Ardagna, M. Cremonini, S. D. C. di Vimercati, and P. Samarati, "An obfuscation-based approach for protecting location privacy," *IEEE Transactions on Dependable and Secure Computing*, vol. 8, pp. 13–27, 2011.
- [57] B. Liu, W. Zhou, T. Zhu, L. Gao, and Y. Xiang, "Location privacy and its applications: A systematic study," *IEEE Access*, vol. 6, pp. 17606–17624, 2018.
- [58] W. Jiang and L. Zhang, "Geospatial data to images: A deep-learning framework for traffic forecasting," *Tinshhua Sci. Technol.*, vol. 24, no. 1, pp. 52–64, Feb. 2019. [Online]. Available: <https://ieeexplore.ieee.org/document/8526506/>
- [59] S. Saki and T. Hagen, "A practical guide to an open-source map-matching approach for big gps data," *SN Computer Science*, vol. 3, 08 2022.
- [60] "The hdf5@ library & file format - the hdf group," last accessed 11 October 2022. [Online]. Available: <https://www.hdfgroup.org/solutions/hdf5/>
- [61] "Hierarchical data format," last accessed 11 October 2022. [Online]. Available: https://en.wikipedia.org/wiki/Hierarchical_Data_Format
- [62] "Elements – openstreetmap wiki," 2022, last accessed 11 October 2022. [Online]. Available: <https://wiki.openstreetmap.org/wiki/Elements>
- [63] "Licence — openstreetmap foundation," 2022, last accessed 11 October 2022. [Online]. Available: <https://wiki.osmfoundation.org/w/index.php?title=Licence&oldid=8605>
- [64] "Overpass api – openstreetmap wiki," 2022, last accessed 11 October 2022. [Online]. Available: https://wiki.openstreetmap.org/wiki/Overpass_API
- [65] "Apache license, version 2.0," last accessed 10 October 2022. [Online]. Available: <https://www.apache.org/licenses/LICENSE-2.0>

- [66] S. Marshall, J. Gil, K. Kropf, M. Tomko, and L. Figueiredo, "Street network studies: from networks to models and their representations," *Networks and Spatial Economics*, vol. 18, no. 3, pp. 735–749, Sep. 2018.
- [67] "Key:highway," last accessed 23 November 2022. [Online]. Available: <https://wiki.openstreetmap.org/wiki/Key:highway>

Moritz Neun Researcher and director of research engineering at IARAI. His background is geo-spatial big data processing and analytics, geo-spatial search and transport optimization.

Christian Eichenberger Researcher and engineer at IARAI. His background is theoretical computer science (algebraic information theory) and transport engineering.

Yanan Xin Lead at the Mobility Information Engineering(MIE) Lab as a postdoctoral researcher at the Chair of Geoinformation Engineering, ETH Zurich. Her background is in Geographic Information Science.

Cheng Fu Group Leader of Urban Geoinformatics and Lecturer in the Department of Geography, University of Zurich (UZH), Switzerland. His background is in Geography, Remote Sensing and GIS.

Nina Wiedemann PhD student at the Mobility Information Engineering (MIE) lab at ETH Zurich. Her Background is in Cognitive Science and Data Science with a focus on machine learning and optimisation theory.

Henry Martin PhD student at the Mobility Information Engineering (MIE) lab at ETH Zurich and at IARAI. He has a Master's in Electrical Engineering and Information Technology from the Technical University of Munich.

Martin Tomko Associate Professor in Spatial Information Science at the University of Melbourne. His research covers spatial data science, trajectory analytics and spatial data management.

Lukas Ambühl Post-Doctoral Researcher at Research Group of Traffic Engineering, Institute for Transport Planning and Systems, ETHZ. His background is civil engineering and management, technology, and economics.

Luca Hermes PhD Student at Machine Learning Group, Bielefeld University. His background is in machine learning with a focus on graph representation learning.

Michael Kopp Founding director of IARAI. His background is in pure mathematics, mathematical modelling in finance and machine learning.

Supplementary Material: Metropolitan Segment Traffic Speeds from Massive Floating Car Data in 10 Cities

SUPPLEMENT A

COMPLEMENTS ON INPUT DATA AND DATA PIPELINE

A. Input Data

Here, we describe the two input data sources in terms of their data model, collection, provisioning, and license.

1) Traffic Map Movies:

a) *Dataset presentation*: Raw GPS data face privacy issues if individual users' behavior can be deduced from the data [52]–[54]. There are methods to preserve privacy by transforming the data, such as obfuscation, aggregation, privacy thresholds or snipping [55]–[57]. HERE Traffic Map Movies use spatio-temporal aggregation and privacy thresholding – we use the term *spot binning* for this aggregation method. Another motivation for framing a geo-spatial time series forecasting as a video prediction task [31] is to leverage state-of-the-art deep-learning methodologies in image and video processing [58]. The data was made available for the *Traffic4cast* competition series [31]–[33] at NeurIPS, an annual machine learning conference. A third motivation for bringing up GPS data in a map-free form is that spatio-temporal binning of GPS probes is computationally cheap in contrast to map-matching, and that it is also applicable in situations where no appropriate maps are available or not accurate enough [59].

Traffic Map Movies Data are provisioned in HDF5 (.h5), a format for typed multidimensional arrays [60], [61]. It can be downloaded for free from the HERE sample data website [19]. The data must be used solely for academic and non-commercial purposes and under standard HERE terms & conditions [43], which in particular explicitly forbid redistribution of HERE materials or derivatives thereof in combination with any open source or open data licenses.

b) *Dataset generation*: GPS probes are binned spatially for each heading direction quadrant of North–East (heading 0°–90°), North–West (heading 270°–0°), South–East (heading 90°–180°), and South–West (heading 180°–270°) into an 8-channel encoding (see Figure 10), where two features are calculated :

- Volume: The number of probe points recorded from the collection of HERE sources capped both above and below and normalized and discretized to an integer number between 0 and 255 (\mathbb{Z}_{256}).
- Mean speed: The average speed from the collected probe points. The values are capped at a maximum level and then discretized to $\{1, 2, \dots, 255\}$, by linearly scaling the capping speed to 255 and rounding the resulting values to the nearest integer. If no probes were collected (*i.e.* the volume is 0), the speed value is 0. This has to be taken into account when averaging speeds.

More formally, a GPS probe $(t, x, y, \alpha, v) \in \mathbb{R} \times \mathbb{R} \times [0, 360] \times \mathbb{R}^+$ consists of a timestamp t , a position (x, y) , an angle α

and a speed v . A spatio-temporal binning is a projection π to bins $(day, t, row, col, heading) \in \mathbb{N} \times \mathbb{Z}_{288} \times \mathbb{Z}_{495} \times \mathbb{Z}_{436} \times \{\text{NE, NW, SE, SW}\}$. The aggregation of a set P of GPS probes produces

$$vol_{d,t,r,c,h} = \lceil \left(\left| \left\{ \pi(tt, x, y, \alpha, v) = (d, t, r, c) \right\} \right| - \theta \right) \lceil_{\perp 0} \frac{255}{\kappa} \rceil \lrcorner \quad (1)$$

and

$$speed_{d,t,r,c,h} = \begin{cases} \lceil \left(\overline{\left\{ v \lceil_{\perp 0}^{120} : \pi(tt, x, y, \alpha, v) = (d, t, r, c) \right\}} \right) \lrcorner \frac{255}{120} \rceil & \text{if } vol_{d,t,r,c,h} > 0 \\ 0 & \text{if } vol_{d,t,r,c,h} = 0 \end{cases} \quad (2)$$

where clipping below is denoted by $x_{\perp b} = \max(x, b)$, clipping above by $x^{\lrcorner a} = \min(x, a)$, integer rounding as $\lceil \cdot \rceil$, and where θ is a privacy volume threshold and κ a volume cutoff. This means volume is set to 0 if the probe volume does not reach the privacy threshold.

Intuitively, this *spot binning* favors lower speeds as slower cars stay longer in the same spatio-temporal bin and are counted multiple times. Under idealized conditions (see Supplement B), the spatio-temporally aggregated speed $speed_B$ represents the total distance divided by the total travel time (see Eq. (4)), which is the harmonic sum of the speeds of Eq. (3), *i.e.*

$$speed_B = \frac{\sum_k 1}{\sum_k v_k^{-1}} \quad (3)$$

$$= \frac{s \cdot \sum_k 1}{\sum_k t_k} \quad (4)$$

for a bin B covering a road segment of length s and for virtual vehicles indexed by k at speeds v_k taking time t_k . In particular, this requires controlling the probe rate of vehicles and depends on traffic volume and homogeneity. Future work could establish bounds to control these factors, *e.g.* through simulations.

2) *OpenStreetMap*: OpenStreetMap (OSM) is a database of GIS data built by an open community of contributors [35]. Its data model [62] has three main elements: *nodes* represent a specific point on the earth's surface (id number and a pair of coordinates), *ways* define polylines (ordered list of nodes), and *relations* between two or more data elements (nodes, ways, and/or other relations), optionally with different *roles*. Hence, the OSM data model does not directly describe a road graph, a traversable graph needs to be derived from the OSM elements. OSM data comes under the Open Database License (ODbL) [63], requiring attribution of public use, share-alike (under the same license) and open redistribution. We use the Overpass API [64] to download OSM data.

B. Data Pipeline

Referring to Figure 9, we now describe the steps of our data pipeline in more detail. Each step is prefixed by $dp\langle N \rangle$ and corresponds to a standalone Python script in our public GitHub repo (see *Data and Code Availability* below). Our code is released under Apache License 2.0 [65]. This allows our

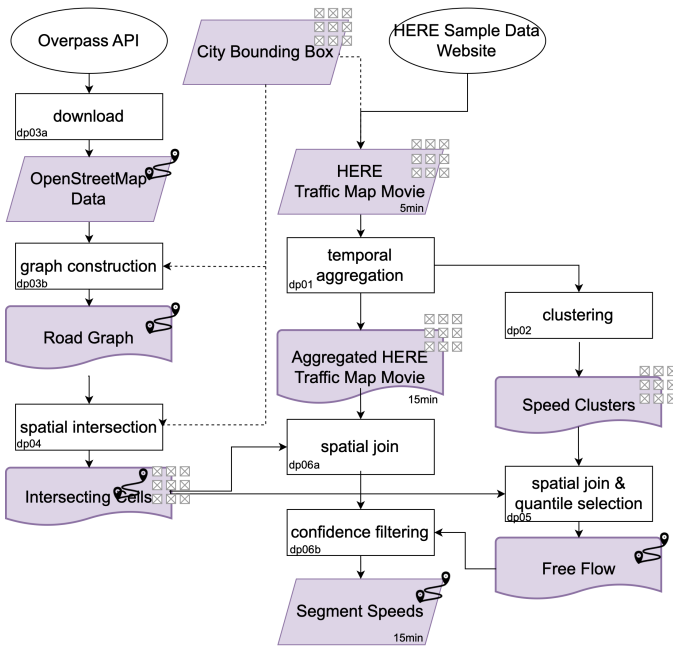


Fig. 9: Methods and data flowchart. Rectangles represent processing steps; ovals represent data repositories; rhomboids represent input and output; rectangles with wavy base represent data artifacts. There are two reference schemes (top-right of rectangles): spatial grid and road graph; both are georeferenced to allow for spatial joining. The temporal resolution is marked bottom-right on rectangles. Arrows represent data flow. Processing steps are labeled by $dp\langle N \rangle$ bottom left referring to the prefix of the corresponding Python script of the data pipeline (some processing steps are implemented in the same script, indicated by suffixes a/b).

method and code to be used and improved permissively in research and even in commercial use cases. The GitHub repo also contains a more technical data specification of all the (intermediate) data formats.

1) *OpenStreetMap Data Download and Road Graph Construction (dp03)*: The resulting graph is a primal (road junctions are vertices and road links are edges), non-planar, weighted multidigraph with self-loops and preserves one-way directionality [36], [66]. Formally, an edge is uniquely identified by a triplet (u, v, g) where u, v are node ids and where g is a road geometry; we use OSM node IDs for u, v and an integer hash of the road geometry for g .

In addition, we add the legal speed limit as an edge attribute. The source is the OSM `maxspeed` tag. Due to graph simplification, multiple such `maxspeed` values can be present per edge or can be missing. By default, we use the `OSMnx` implementation which assigns the mean of multiple values. In some cases (e.g. in Madrid) the `OSMnx` implementation sees parsing errors. Therefore, we also provide an alternative implementation that takes the max if multiple values are present. In the presence of missing values, the `OSMnx` implementation imputes the mean of the corresponding OSM highway type in the data, whereas our implementation uses hard-coded defaults for different OSM highway types.

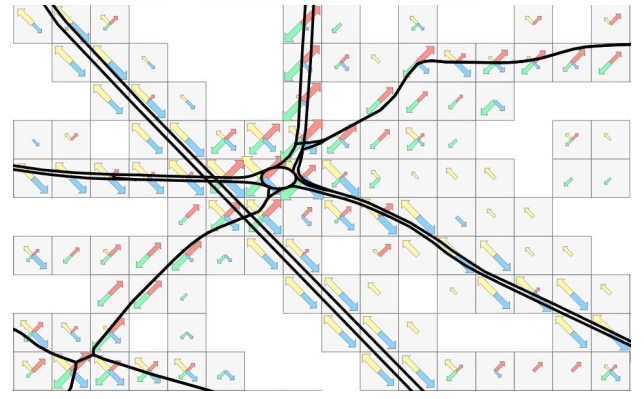


Fig. 10: Probe data and road network example from London. Black lines are the road centerline segments, grey boxes show grid cells with probe data, the sizes of the arrows correspond to the summed volumes of a sample day along the 4 headings, each heading with a different color. Only the data aligned with the road are mapped to the edge. There are some cells with data but without a road graph intersecting.

Note that any other road graph present in this form could be used instead of a road graph downloaded from OSM.

2) *Spatial Intersection of Road Graph and City Cells (dp04)*: This step generates lists of intersecting cells for each road segment in the corresponding Traffic Movie Grid. By interpolation over the edge geometries with a constant step size, we get a list of $(row, column, heading, fraction)$ where $(row, column, heading)$ denotes a directed cell and $fraction$ is the percentage of the length of the segment overlapping with this cell. The fraction can be zero as we add data from neighboring cells (up to a margin of $0.0005^\circ \sim 5$ m by default), and the sum of fractions in the intersecting cells can be larger than one as we add data from neighboring headings (margin of 10° by default); for edges going over the city boundary, the sum of fractions can also be smaller than one, obviously. See illustration in Figures 10–11. These fractions are currently not used in our pipeline, but they could be used for a weighting the contributions of different intersecting cells.

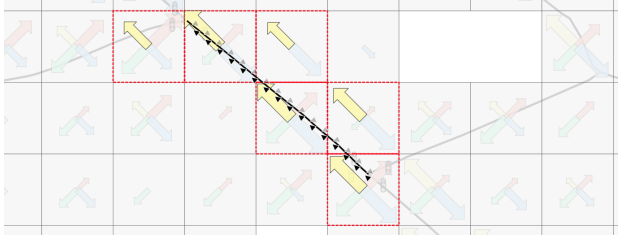
3) *Temporal Aggregation of HERE Traffic Map Movies (dp01)*: By default, we aggregate 3 consecutive 5-minute movie time bins into 15-minute bins by summing volumes and taking the mean of speeds after invalidating speeds with zero volume.

4) *Confidence Filtering of Segment Speeds (dp06b)*: The confidence-based filtering $conf$ is given by

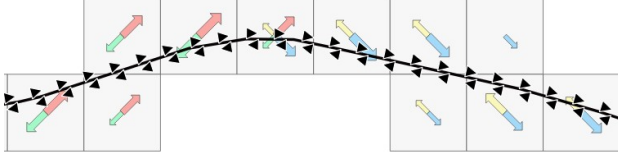
$$conf(ssp, vol, ff) = \begin{cases} \text{nan} & \text{if } vol < 5 \text{ or } cf < 0.4 \\ \text{nan} & \text{elif } vol < 3 \text{ or } cf < 0.8 \\ \text{nan} & \text{elif } vol < 1 \\ ssp & \text{else} \end{cases} \quad (5)$$

for median segment speed ssp , probe volume vol , free flow ff (opt. normalized) and congestion factor

$$cf = \frac{ssp}{ff}. \quad (6)$$



(a) Intersecting cells for one road segment in only one direction (bottom right to top left as indicated by the black arrow heads). The red boxes and yellow arrows in the foreground show the intersecting cells of this road segment. The data from non-intersecting cells of this road segment are greyed out – only the data along the NW heading are mapped on this road segment as the road segment is well aligned with the NW heading.



(b) Intersecting cells of both the two road segments going from left to right and from right to left (as indicated by the arrow heads in both directions). When the road is close to horizontal, data from NE and SE are used for the direction left to right while both NW and SW are used for right to left. When the road is close to the diagonal, there is only data from the corresponding headings. On the upper right, there is also one cell not intersecting with the road segment but within the 5m margin, so its data is mapped onto the corresponding direction of the edge as well. In this example, all data shown are mapped to either one of the two road segments.

Fig. 11: Intersecting cells example from London illustrating the mapping for individual roads.

In order not to need to keep the intermediate results, confidence filtering is implemented in the same script dp06 as the derivation of median speeds.

5) *Speed Clustering (dp02) and Free Flow speeds from Spatial Join and Quantile Selection (dp05)*: Here, we describe the derivation of free flow speeds from the data. This step derives free-flow speeds for each road segment using the speeds clusters in the Traffic4cast Movie Grid data.

We compute the 5 most dominant speeds clusters for every cell and heading from the aggregated 15 minute traffic map movies. By default, all speed values from 20 days of data are clustered using the K-means clustering algorithm for every cell/heading combination (495x436x4~860K). Hence, this process is computationally expensive and can easily take 2–3 hours per city on a standard consumer laptop. We then take the cluster median as the center representation of the speed clusters. More formally, for each directed cell, the output is a list of 5 pairs consisting of $(center, size)$, *i.e.* a $(495, 436, 4, 5, 2)$ tensor per city.

For each road segment, we start by merging the speed clusters from the intersecting cells by collecting all speed cluster medians from all the intersecting cells and sorting them. We then take as free flow the 80% percentile of these cluster medians based on the corresponding volumes; we default to 20 if there is no data; and we clip above to the

signalized speed limit from OSM. More formally, for an edge with intersecting cells $intersecting_cells$, speed limit sl and for $cl(r, ch)$ denoting the 5 clusters (structures with attributes center and size) computed above, we derive its free flow speed as

$$center \left(q_{0.8,20} \left(\bigcup_{\substack{(r,c,h) \in \\ intersecting_cells}} cl(r, c, h), size \right) \right)^{\top sl} \quad (7)$$

where $q_{v,d}(X, a)$ is the v quantile of the set X based on attribute a defaulting to d if $X = \emptyset$ and $(X)^{\top b} = \{\min(x, b) : x \in X\}$.

Optionally, we normalize free flow speed before computing the congestion factor. In normalization, we first use the signalized speed limit to make sure the free flow speed ff is not below the signalized limit sl from OSM and not above 60% of that speed limit:

$$\begin{cases} \max(\text{clip}(ff)_{20}^{sl}, 0.6 \cdot sl) & \text{if } sl \geq 5 \\ \max(\text{clip}(ff)_{20}, 0.6 \cdot sl) & \text{else} \end{cases} \quad (8)$$

where $\text{clip}(x)_l^u = \min(\max(x, l), u)$.

SUPPLEMENT B ANALYSIS OF SPOT BINNING UNDER IDEALIZED CONDITIONS

Here, we give details on Spot Binning as introduced in Section IV-A1 of the main text. Consider the following idealized conditions. For vehicles i in a bin B and r_i the number of their readings within B ,

- (i) all vehicles travel the same distance $s = s_i$
- (ii) constant speed $v_{ij} = v_i$ for all readings ij of vehicle i
- (iii) vehicles not fully covering the distance negligible, *i.e.* for every vehicle not traveling the full distance s_i within the temporal extension of B , there is another vehicle compensating with the same speed (not having left is compensated by another vehicle leaving). Technically, we have classes of vehicles $[i]$ merged together, so we can re-index vehicles i (possibly partially covering the full distance within the temporal extension of B) to virtual vehicles k going the full distance during the temporal extension of B , $v_k = v_{[i]} = v_i$ and $r_k = \sum_{ij:[i]=k} 1$.
- (iv) same probe rate R , *i.e.* a vehicle with speed v will have $r = c \cdot v^{-1}$ readings

Then,

$$speed_B = \frac{\sum_{ij} v_{ij}}{\sum_{ij} 1} \quad (9)$$

$$\stackrel{(ii)}{=} \frac{\sum_i r_i v_i}{\sum_i r_i} \quad (10)$$

$$\stackrel{(iii)}{\approx} \frac{\sum_k r_k v_k}{\sum_k r_k} \quad (11)$$

$$\stackrel{(iv)}{=} \frac{\sum_k \frac{c}{v_k} v_k}{\sum_k \frac{c}{v_k}} \quad (12)$$

$$= \frac{\sum_k 1}{\sum_k v_k^{-1}} \quad (13)$$

$$\stackrel{(i)}{=} \frac{\sum_k 1}{\sum_k \frac{t_k}{s}} \quad (14)$$

$$= \frac{s \cdot \sum_k 1}{\sum_k t_k} \quad (15)$$

Hence, under these assumptions, the spatio-temporally aggregated speed $speed_B$ represents the total distance divided by the total travel time as per Eq. (15), which is the harmonic sum of the speeds of Eq. (13). Assumption (iii) depends on the temporal and spatial extension of bins and on the probe rate. Assumption (iv) is hard to control in many settings; if vehicles do not have the same probe rate (iv) or even a correlation between speed and probe rate, then this can have a substantial impact in low-flow situations. This analysis shows the importance to control homogeneity of probe rates, the probe frequency and the bin extensions in time and space, especially under low-flow conditions.

SUPPLEMENT C

COMPLEMENTS ON VALIDATION

A. Comparison with Uber Movement Speeds

1) *Historic Road Graph*: Uber matches their data to the OSM data of the time of collection [14], only storing the OSM node and way IDs of the segments without feature attributes like position. Therefore, we download the historic OSM data closest to the collection period and take OSM start node ID, end node ID, and OSM way ID from the Uber data and match it with the OSM data to construct the same structure as issuing from dp03 above. We then run our pipeline on this road graph. Notice that this road graph is potentially incomplete due to divergences between the OSM IDs in Uber and the OSM data snapshot; in addition, as this approach does not use the OSM_nx road graph simplification, its segments are shorter in general. We refer to the Supplementary Material [34] for the key figures of the road graph properties and the *MeTS-10* speeds.

2) *Spatial and Temporal Coverage*: Figure 12 shows the difference in spatial temporal coverage between the Uber and *MeTS-10* datasets for London (color coded). Spatially, we see

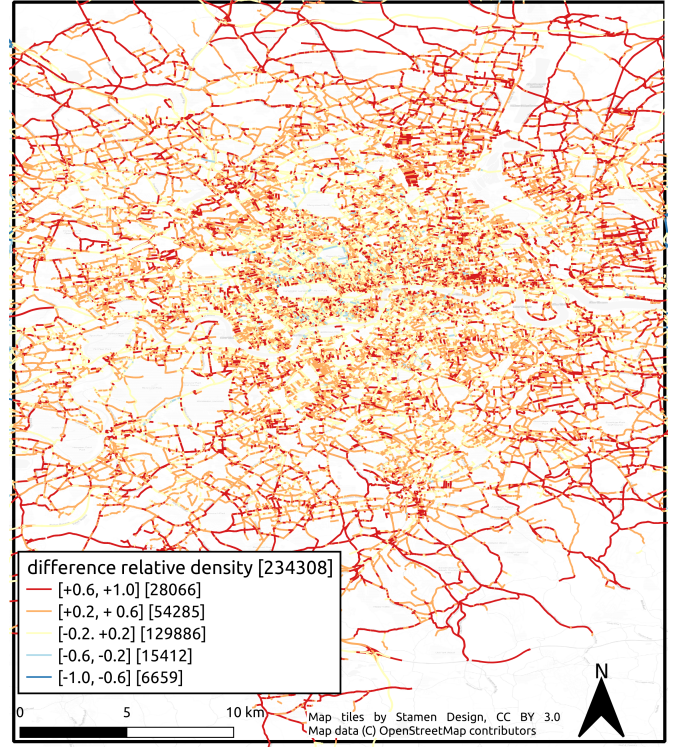


Fig. 12: Segment density differences of Uber and *MeTS-10* on the historic road graph London (8am–6pm). The color encoding shows the edge density difference, higher values mean higher temporal coverage of *MeTS-10*. In particular, the negative values outside of the bounding box are due only Uber having data there. The numbers of edges are shown in brackets.

that Uber has data outside of the *MeTS-10* bounding box, mainly including roads that lead to the airports outside of the city. Roughly speaking, we see similar temporal coverage in the city center (light yellow and light green colors), higher coverage of *MeTS-10* in the outer city areas, and negative values outside of the *Traffic4cast* bounding box.

Figure 13 shows a comparison of the temporal coverage of all three cities. It shows that temporal coverage in Barcelona and Berlin is in general higher in *MeTS-10* than in Uber. *MeTS-10* has high coverage for many segments in Berlin and low coverage for Uber. For London, many segments have similar temporal coverage, but also a considerable amount of segments with differences – slightly more segments with better coverage in *MeTS-10*. We refer to the Supplementary Material [34] for additional figures.

3) *Speed Differences*: We match the 1h Uber and *MeTS-10* segment speeds for one week of data in London, achieving a high number of samples that overlap spatio-temporally, namely 3.1 M data points. This corresponds to 77% of the 4.67 M data points for Uber within the bounding box, and to 47% of 6.63 M data points for *MeTS-10*; the higher absolute number of data points and the lower matching rate for *MeTS-10* is plausible in light of the previous paragraph. See Figure 14.

a) *Speed Differences: Qualitative Analysis*: Figure 15 shows the concentration of Uber and *MeTS-10* speeds along the diagonal. There are few cases with much higher *MeTS-10*

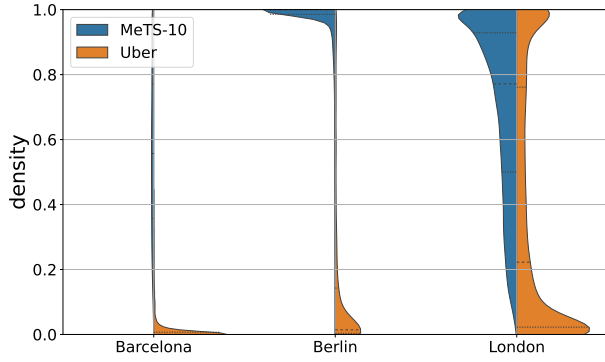


Fig. 13: Distribution of segment-wise temporal coverage of Uber and *MeTS-10* data for the 3 cities Barcelona, Berlin and London, bounding box only.

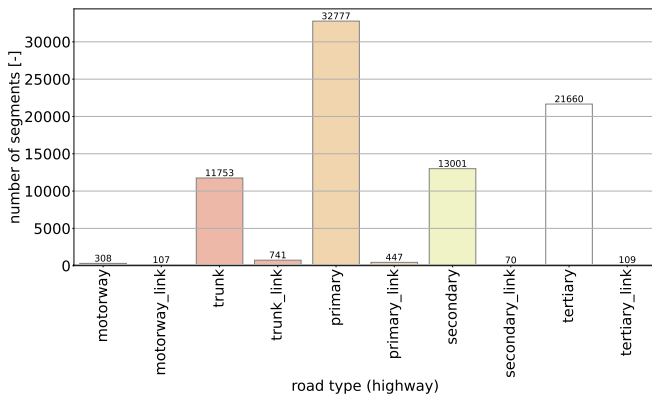


Fig. 14: Segment counts *MeTS-10* – Uber matched data.

speeds (bumps lower right) – inspection of examples shows that these tend to be due to high-speed GPS outliers above the signaled speed in low-flow situations which are not smoothed out by our median approach. On the other hand, there are many cases with *MeTS-10* close to zero and higher Uber speeds (bumps on the left) – here, an inspection of examples shows these tend to happen in junction situations, where spot binning of GPS probes from standing vehicles leads to much lower aggregated speed values compared to the per-vehicle mean speeds on the segment.

b) *Speed Differences: Quantitative Analysis:* The qualitative interpretation is confirmed by the quantitative analysis of Figure 16 and Figure 17: longer and non-link segments tend to have lower absolute percentage error comparing *MeTS-10* to Uber. We use absolute percentage error as used in the traffic simulation calibration literature [44]: in this context, a rule of thumbs asks for 85% of the counts measured in the simulation should deviate less than 15%.

c) *Speed Differences: Effect of Segment Length:* In order to also quantitatively assert the effect of segment length on APE, we further distinguish three ad-hoc sizes in Figure 17: S for segments up to 100 m, M for segments between 100 m and 500 m, and L for segments longer than 500 m. Apart from the link road types (with higher variance as discussed in Section V and low number of segments as per Figure 14), we see that longer segments tend to be better aligned with Uber

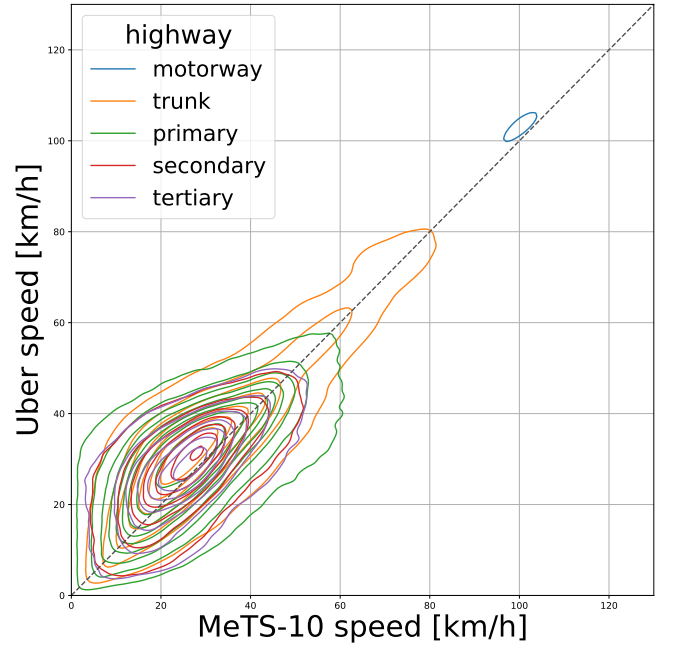


Fig. 15: Kernel density estimation of speeds of *MeTS-10* and Uber on the historic road graph London daytime (8am–6pm) on the matching data, *i. e.* within *MeTS-10* bounding box only and where data is available at the same time and segment, for the most important road types.

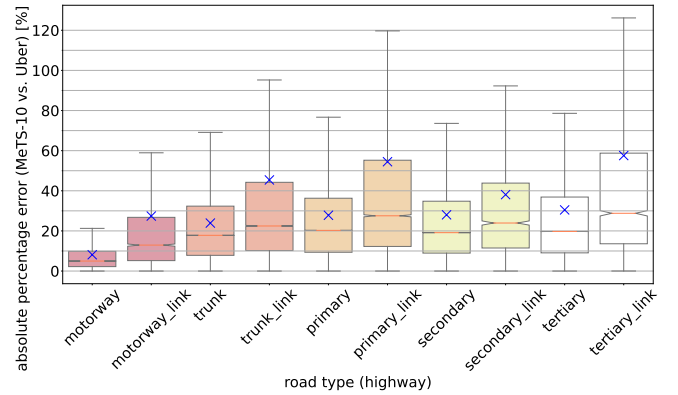


Fig. 16: London absolute percentage error *MeTS-10* vs. Uber by road type. Blue crosses indicate the mean per road type.

than shorter ones.

d) *Speed Differences: Effect of Road Segment Complexity:* In order to quantitatively assert the sensitivity to complex road situations, we differentiate between complex and non-complex road segments: we consider those road segments as complex which have at least one intersecting cell shared by at least 4 further road segments. The case of sharing with 1 further segment is trivial as this happens for every node not exactly at a cell border. See Figure 18 and Figure 19.

B. Comparison with Stationary Vehicle Detector Data

The sensor locations were matched to the *MeTS-10* road graph in order to find the corresponding road segment. The

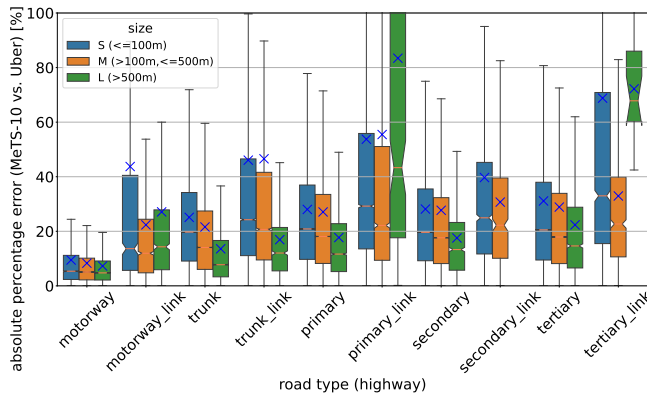


Fig. 17: London absolute percentage error *MeTS-10* vs. Uber by road type and segment length. Blue crosses indicate the mean per road type.

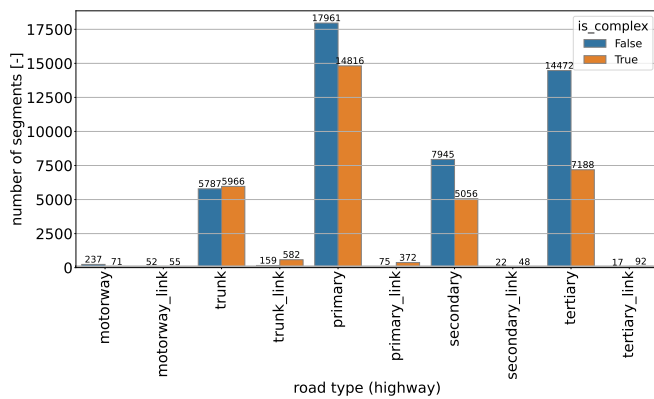


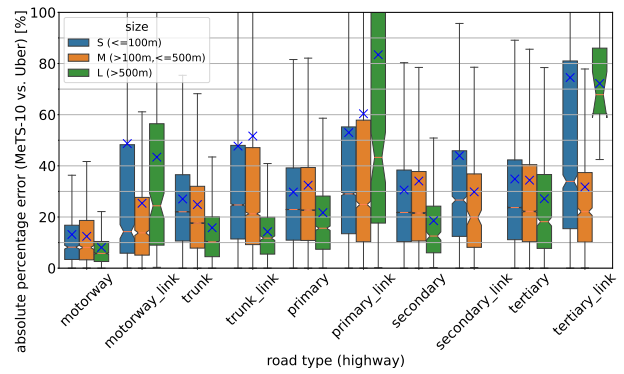
Fig. 18: Segment counts *MeTS-10* – Uber matched data.

TABLE V: Percentage and absolute count of matched stationary vehicle detector with *MeTS-10* speed measurements by OpenStreetMap highway type [67]).

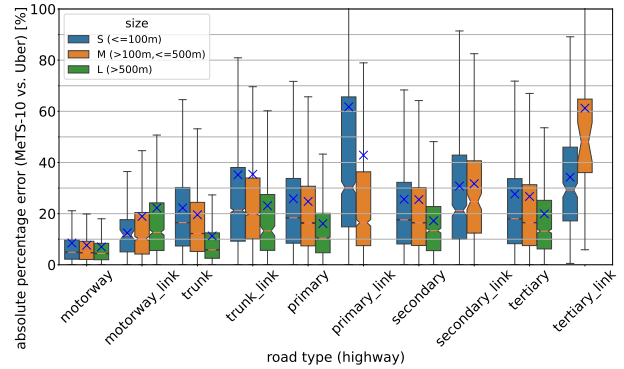
	Berlin		London		Madrid	
motorway	1 %	4	95 %	237	85 %	345
trunk	1 %	6	5 %	12	5 %	21
primary	41 %	218			4 %	16
secondary	52 %	280				
tertiary	4 %	22			1 %	4
other	1 %	8			4 %	18

matching logic uses the distance as well as, if provided, the heading angle and/or the name of the segment for determining the best match.

The spatial distribution of the speed sensors can be seen in Figure 20. These different distributions are also clearly visible in the differences in covered highway types in Table V. In Berlin, sensors cover the whole city with the majority of them located on primary and secondary roads. In contrast, in London and Madrid, speed sensors are mostly located on motorways and trunks. In London, these motorways are only located on the outskirts of the city where roads have fewer tunnels and overall higher speeds. In Madrid, the available speed counter data is mostly for motorways of the inner-city ring road, where we see more significant speed limits and other



(a) complex road segments



(b) non-complex road segments

Fig. 19: London absolute percentage error *MeTS-10* vs. Uber by road type and segment length. Blue crosses indicate the mean per road type.

effects of traffic control. We consider sensors on motorways that are not disturbed by traffic lights or other effects to be close to real ground truth values. This ignores the quality of the sensor, malfunctioning sensors, and potential temporal aggregation effects.



Fig. 20: Distribution of Vehicle Detectors with speed measurement in the corresponding *MeTS-10* bounding boxes.

Erroneous sensor readings were filtered before comparing the speed measurements. There were two main sources of erroneous readings: a) values at night due to maintenance

TABLE VI: Percentage and absolute count (matched/total) of stationary vehicle detector with Uber Movement Speeds by OpenStreetMap highway type [67]).

	Berlin		London	
motorway	1 %	4	95 %	210/237
trunk		0/6	5 %	11/12
primary	41 %	192/218		
secondary	53 %	249/280		
tertiary	4 %	19/22		
other	1 %	3		

or impaired averaging when no speed was detected in the measurement interval. Hence, we only looked at readings between 6 am and 11 pm. b) readings in situations where GPS signals are disturbed, such as tunnels. Hence, sensors in tunnels were filtered out as well. For more details on the pre-processing, see our code base referenced in *Data and Code Availability* below.

C. Baseline comparison of Uber Movement Speeds with Stationary Vehicle Detector Data

As a baseline of the used validation datasets we compare here the Uber Movement Speeds with the speed readings from the Stationary Vehicle Detectors. This was done for Berlin and London where we had overlapping time ranges for the comparison.

The same matching procedure was used as for the comparison of the *MeTS-10* speeds with the stationary vehicle detectors. Table VI shows the statistics of the used vehicle detectors with matching Uber speeds. Uber coverage is lower, hence compared to *MeTS-10* (see also Table V) less counters did have a corresponding Uber speed on the associated street segment.

Figure 21 shows the Binned Kernel Distribution Estimation (KDE) Plots of Uber and the detectors as well as box plots of the speed differences between Uber Movement Speeds and vehicle detector speeds.

In both cities we see a good alignment with the majority of the points along the diagonals in the KDE plots. The shapes of the plots are very similar to the KDE plots in the comparison between *MeTS-10* and the detectors. Hence, also here we see the differences in sensor placement on predominantly inner city roads (Berlin) vs mostly motorways (London) as shown in Table VI. In the box plots by highway type (Figure 21 bottom; Figure 22) we can see a very good alignment for this higher class highway types in London as well as for the lower class highway types in Berlin.

In the side-by-side (SxS) comparisons in Figure 22, both *MeTS-10* and Uber show the same speed level difference for motorways in Berlin. This only affects 4 motorway counters and hence seems to be a systematic difference for the type of counter or location. Note, the plots here only show counters on segments where both Uber and *MeTS-10* had data points. Therefore, for example the trunk type segments are not shown as they only had data in the *MeTS-10* dataset.

The good general visual alignment in the box plots is also confirmed by the quantitative comparisons in Table VII

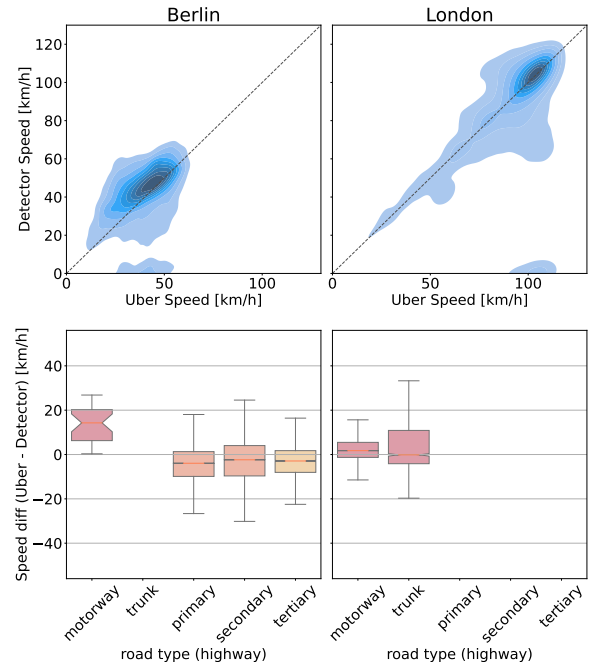


Fig. 21: Comparisons of Uber Movement Speeds and vehicle detector speeds (30 days of data matched to the Uber OSM road graph). Top: Binned Kernel Distribution Estimation Plots of speeds; Bottom: Box plots of speed differences by highway type (OSM carto color scheme)

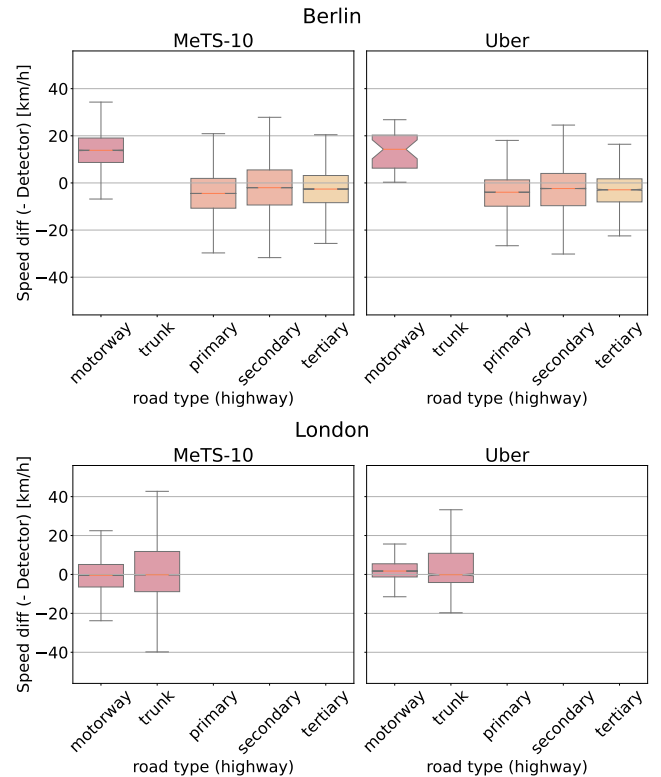


Fig. 22: SxS of *MeTS-10*-Detector and Uber-Detector Differences by highway type (OSM carto color scheme).

and VIII as well as in the histograms in Figure 23. These

TABLE VII: Berlin differences of Uber/*MeTS-10* speeds at stationary vehicle detector locations

highway	Uber – Detector			<i>MeTS-10</i> – Detector			Uber – <i>MeTS-10</i>			# values
	diff mean	diff std	diff median	diff mean	diff std	diff median	diff mean	diff std	diff median	
motorway	13.483067	7.795273	14.2730	12.686667	7.246002	12.182353	0.796400	5.414309	-0.223706	30
primary	-3.084538	13.618173	-3.9420	-3.610773	12.903032	-5.332353	0.526235	6.378054	0.787451	69214
residential	-4.955351	7.833748	-2.3000	-7.877973	7.149825	-5.766667	2.922622	4.547528	2.402353	57
secondary	-2.004949	15.230711	-2.3785	-1.881549	14.190849	-2.976471	-0.123400	6.207306	0.194863	49526
tertiary	-2.247903	10.411396	-2.9145	-2.196423	10.097512	-2.988235	-0.051480	5.857588	-0.034078	3466
TOTAL	-2.620424	14.225456	-3.3330	-2.868381	13.397577	-4.319608	0.247957	6.302485	0.503647	122293

TABLE VIII: London differences of Uber/*MeTS-10* speeds at stationary vehicle detector locations

highway	Uber – Detector			<i>MeTS-10</i> – Detector			Uber – <i>MeTS-10</i>			# values
	diff mean	diff std	diff median	diff mean	diff std	diff median	diff mean	diff std	diff median	
motorway	5.253279	17.986759	1.739697	2.196420	18.520102	-0.463783	3.056858	6.926557	2.273585	50777
motorway_link	-10.143697	10.655478	-9.506371	8.156388	13.872980	9.457262	-18.300085	15.978163	-16.496598	3275
trunk	8.395831	22.285910	-0.150473	4.489668	24.107821	-0.287161	3.906163	11.074098	2.583295	1834
trunk_link	-12.372454	20.987359	-14.653041	15.267473	22.729794	15.082768	-27.639927	12.654695	-27.497865	339
TOTAL	4.352669	18.243336	1.384032	2.697190	18.602136	-0.276012	1.655479	9.667750	1.873293	56225

comparisons show the speed differences between Uber, *MeTS-10* and detector readings for all detectors with both Uber and *MeTS-10* data available during 30 consecutive days.

In Berlin (see Table VII), the majority of the detectors is on roads of type primary and secondary. On these two road types, we see also a very good alignment of the Uber and *MeTS-10* speeds with a speed diff of 0.5 ± 6.4 km/h and -0.1 ± 6.2 km/h (average \pm standard deviation), respectively.

In London, almost all counters are along motorways. Here, we see a small but stable difference of 3.1 ± 6.9 km/h.

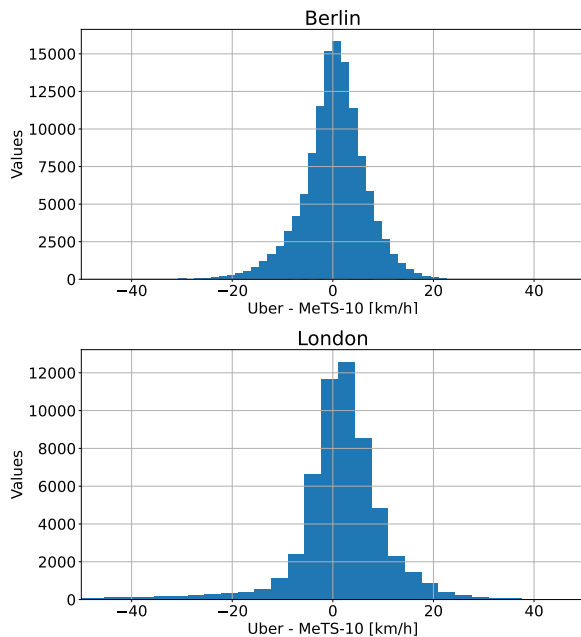


Fig. 23: Histogram of Uber/*MeTS-10* speed differences at stationary vehicle detector locations (Uber - *MeTS-10*)

SUPPLEMENT D COMPLEMENTS ON DISCUSSION

A. Complements Spatial Intersection (*dp04*)

In Table IX, we contrast edges whose geometry is along the N/E/S/W axis (horizontal/diagonal $\pm 10^\circ$) or along the NE/SE/SW/NE (diagonal $\pm 10^\circ$). We sample 10 days of speed data. We see that the coverage along the diagonal is slightly lower. This is plausible in light of the horizontal/diagonal edges getting values from two headings.

SUPPLEMENT E EXTENDED DATASET OVERVIEW

Referring to Table X, the dataset comprises 10 cities with data from 108 up to 361 days publicly available: **t4c year** is the competition year which the was published for by HERE (relevant for download); **days** is the number of full days of data (288 5 minute bins of full bounding box each); **date ranges** are the corresponding date ranges – in the 2022 competition, every second week in the date range was held back for tests in the competition, so there is not a consecutive range of dates available; **Traffic4cast** bounding box is given by **lat_min, lat_max, lon_min, lon_max**; number of **nodes** and **edges** in the road graph; **total segment length** is the sum of all lengths of all directed edges; **ratio covered edges** is the ratio of edges in the road graph with at least one speed value (from 20 sampled days); **mapped ratio** is the ratio of GPS probes mapped to the road graph; **daily fcd volume** is the daily GPS probe volume sum (from 20 sampled days); **8–18 coverage** is the ratio of edges with speed values between 8am and 6pm (from 20 sampled days); **mean segment volume** is mean volume sum of all intersecting cells for segments with speed value (from 20 sample days).

TABLE IX: Coverage for segments along the diagonals vs. segments along the horizontal/vertical axes.

city (year)	#edges	#N/E/S/W	#NE/SE/SW/NW	coverage	coverage N/E/S/W	coverage NE/SE/SW/NW	difference
Antwerp (2021)	81667	17349 (21.2%)	21443 (26.3%)	0.13	0.16	0.11	+0.03
Bangkok (2021)	694818	201316 (29.0%)	91609 (13.2%)	0.03	0.04	0.03	+0.00
Barcelona (2021)	118813	22003 (18.5%)	34724 (29.2%)	0.06	0.07	0.06	+0.01
Berlin (2021)	88882	20875 (23.5%)	19940 (22.4%)	0.29	0.37	0.29	+0.08
Chicago (2021)	187570	118970 (63.4%)	9399 (5.0%)	0.07	0.07	0.10	-0.00
Istanbul (2021)	270109	61255 (22.7%)	61564 (22.8%)	0.52	0.61	0.48	+0.09
Melbourne (2021)	230654	103833 (45.0%)	31915 (13.8%)	0.05	0.05	0.04	+0.00
Moscow (2021)	47877	10177 (21.3%)	13259 (27.7%)	0.69	0.71	0.67	+0.03
London (2022)	271075	59654 (22.0%)	65380 (24.1%)	0.15	0.19	0.15	+0.04
Madrid (2022)	143402	32018 (22.3%)	35551 (24.8%)	0.33	0.39	0.32	+0.06
Melbourne (2022)	230654	103833 (45.0%)	31915 (13.8%)	0.05	0.06	0.04	+0.01

TABLE X: Extended dataset overview.

city (t4c year)	days	date ranges	lat_min, lat_max, lon_min, lon_max	nodes	edges	total segment length [m]	mean segment length [m]	ratio covered edges	mapped ratio	daily fcd data	8-18 cover- age	mean segment volume
Antwerp (2021)	361	2019-01-2019-06, 2020-01-2020-06	(51.001, 51.437, 4.153, 4.648)	34722	81667	13833313.7	169.4	0.99	0.89	3.247e+06	0.17	7.10
Bangkok (2021)	361	2019-01-2019-06, 2020-01-2020-06	(13.554, 14.049, 100.308, 100.744)	317797	694818	58792833.8	84.6	0.76	0.91	4.576e+06	0.05	7.50
Barcelona (2021)	361	2019-01-2019-06, 2020-01-2020-06	(41.253, 41.748, 1.925, 2.361)	58106	118813	14081313.2	118.5	0.97	0.81	1.811e+06	0.09	6.24
Berlin (2021)	180	2019-01-2019-06	(52.359, 52.854, 13.189, 13.625)	34308	88882	14045121.9	158.0	1.00	0.94	6.270e+07	0.36	57.31
Chicago (2021)	180	2019-01-2019-06	(41.601, 42.096, -87.945, -87.509)	68430	187570	27117716.0	144.6	0.98	0.93	4.684e+06	0.11	9.82
Istanbul (2021)	180	2019-01-2019-06	(40.81, 41.305, 28.794, 29.23)	102754	270109	22126616.3	81.9	1.00	0.96	7.065e+07	0.63	24.53
Melbourne (2021)	180	2019-01-2019-06	(-38.106, -37.611, 144.757, 145.193)	103062	230654	24277388.0	105.3	0.95	0.93	2.519e+06	0.08	5.56
Moscow (2021)	361	2019-01-2019-06, 2020-01-2020-06	(55.506, 55.942, 37.358, 37.853)	22627	47877	10906823.2	227.8	1.00	0.81	7.292e+07	0.71	46.88
London (2022)	110	2019-07-2019-12, 2020-01	(51.205, 51.7, -0.369, 0.067)	116304	271075	26738400.4	98.6	0.99	0.95	1.119e+07	0.24	8.15
Madrid (2022)	109	2021-06-2021-12	(40.177, 40.672, -3.927, -3.491)	71757	143402	15799502.4	110.2	0.99	0.93	2.977e+07	0.36	22.05
Melbourne (2022)	108	2020-06-2020-12	(-38.106, -37.611, 144.757, 145.193)	103062	230654	24277388.0	105.3	0.95	0.90	2.086e+06	0.08	4.52

SUPPLEMENT F

KEY FIGURES

When a city has appeared in multiple competition years, we add the competition year for data download. The code to reproduce the figures, as well as additional figures can be found in our code repository.

A. Key Figures Antwerp (2021)

1) Road graph map Antwerp (2021):

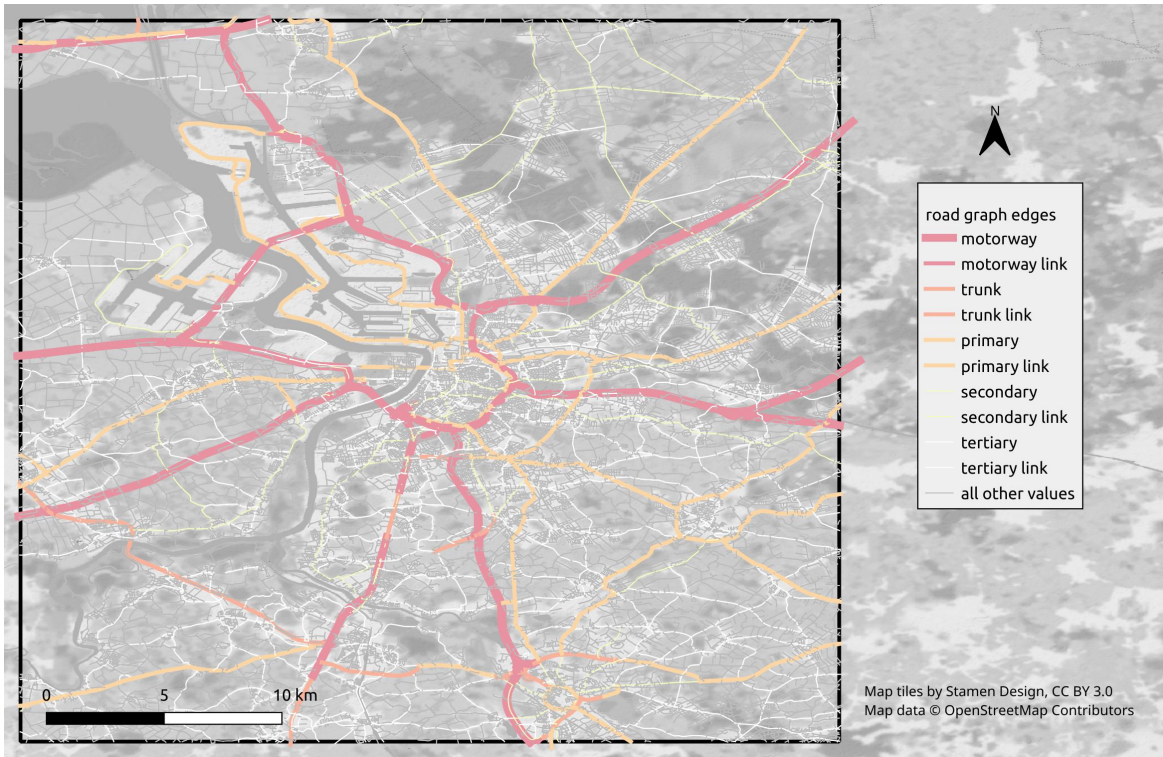


Fig. 24: Road graph Antwerp, OSM color scheme (2021).

2) Static data Antwerp (2021) :

Attribute	mean	std	median	q01	q99	data points	sum
bounding box						4.153–4.648 / 51.001–51.437	
num_edges						81'667	
motorway						232	
motorway_link						483	
trunk						274	
trunk_link						67	
primary						2798	
primary_link						152	
secondary						3348	
secondary_link						69	
tertiary						10929	
tertiary_link						42	
unclassified						11700	
residential						51573	
num_nodes						34722	
num_edges_per_cell	1.0	0.2	1.0	1.0	2.0	385'170	
num_intersecting_cells	4.9	5.1	4.0	1.0	25.0	81'667	
node_degree	2.7	0.9	3.0	1.0	4.0	34'722	
length_meters	169.4	240.4	100.8	6.6	1'113.6	81'667	1.4e+07
motorway	1'496.8	1'426.3	954.9	93.1	6'717.8	232	3.5e+05
motorway_link	313.5	330.0	218.0	11.0	1'684.1	483	1.5e+05
trunk	370.6	468.1	184.0	7.6	2'112.0	274	1.0e+05
trunk_link	162.4	156.1	121.7	15.4	646.1	67	1.1e+04
primary	201.6	273.3	106.4	5.4	1'393.4	2'798	5.6e+05
primary_link	49.6	66.0	24.4	4.1	288.3	152	7.5e+03
secondary	171.1	246.4	95.5	5.5	1'142.0	3'348	5.7e+05
secondary_link	63.1	69.7	42.6	6.7	300.2	69	4.4e+03
tertiary	176.7	237.1	103.4	5.4	1'116.8	10'929	1.9e+06
tertiary_link	52.2	42.7	39.7	15.8	207.5	42	2.2e+03
unclassified	299.4	348.2	184.3	7.2	1'541.1	11'700	3.5e+06

residential	128.7	137.1	92.4	6.9	650.5	51'573	6.6e+06
speed_kph	42.0	12.0	36.3	30.0	80.0	81'667	
motorway	109.2	15.9	120.0	50.0	120.0	232	
motorway_link	82.6	16.6	81.4	50.0	120.0	483	
trunk	77.9	14.4	70.0	50.0	120.0	274	
trunk_link	61.5	9.0	61.2	50.0	90.0	67	
primary	61.7	11.0	66.5	30.0	80.0	2'798	
primary_link	55.5	5.7	55.5	50.0	70.0	152	
secondary	56.0	9.4	50.0	30.0	70.0	3'348	
secondary_link	58.4	7.9	59.2	43.6	76.4	69	
tertiary	49.6	9.7	50.0	30.0	70.0	10'929	
tertiary_link	49.7	7.0	48.9	30.0	70.0	42	
unclassified	48.1	6.6	48.2	30.0	70.0	11'700	
residential	36.1	6.8	36.3	30.0	50.0	51'573	
free_flow_kph	38.9	18.0	35.8	5.6	116.7	77'109	
motorway	109.6	12.9	117.1	71.5	120.0	232	
motorway_link	87.4	28.5	93.9	26.3	120.0	483	
trunk	66.5	22.9	65.2	23.3	120.0	272	
trunk_link	74.1	25.1	74.6	27.1	120.0	67	
primary	52.2	16.3	50.5	24.0	95.8	2'798	
primary_link	41.4	23.1	36.8	7.4	92.0	148	
secondary	49.4	16.8	46.6	20.7	108.8	3'344	
secondary_link	53.8	31.4	41.8	13.6	118.4	68	
tertiary	46.0	15.5	43.8	19.8	104.0	10'915	
tertiary_link	43.9	18.6	41.2	21.1	95.0	42	
unclassified	44.1	21.7	41.9	3.5	119.5	10'392	
residential	33.6	13.9	32.0	3.3	80.0	48'348	
free_flow_kph-speed_kph	-3.3	15.8	-3.9	-36.6	53.6	77'109	
motorway	0.4	11.9	-1.4	-25.2	42.8	232	
motorway_link	4.9	28.8	6.8	-55.6	62.1	483	
trunk	-11.5	19.8	-7.2	-57.4	30.5	272	
trunk_link	12.6	24.8	10.8	-34.1	70.0	67	
primary	-9.5	14.5	-7.9	-44.3	23.9	2'798	
primary_link	-14.1	23.7	-15.5	-55.7	38.9	148	
secondary	-6.7	16.1	-7.2	-39.3	48.9	3'344	
secondary_link	-4.6	30.2	-17.6	-45.6	58.4	68	
tertiary	-3.6	14.2	-3.9	-32.4	48.6	10'915	
tertiary_link	-5.9	20.2	-7.7	-37.1	46.1	42	
unclassified	-4.0	21.6	-6.1	-45.4	71.1	10'392	
residential	-2.5	14.1	-3.2	-33.1	42.3	48'348	

TABLE XI: Key figures Antwerp for the generated data from 20 randomly sampled days. **num_edges** number of edges in the street network graph; **num_nodes** number of nodes in the street network graph; **num_edges_per_cell** number of edges a cell (row,col,heading) has in its intersecting cells; **num_intersecting_cells** number of cells (row,col,heading) in an edge's intersecting cells; **node_degree** number of (unique) neighbor nodes per node; **length_meters** free flow speed derived from data; **speed_kph** signalled speed; **free_flow_kph** free flow speed derived from data; **free_flow_kph-speed_kph** difference

3) *Segment density map Antwerp (2021):*

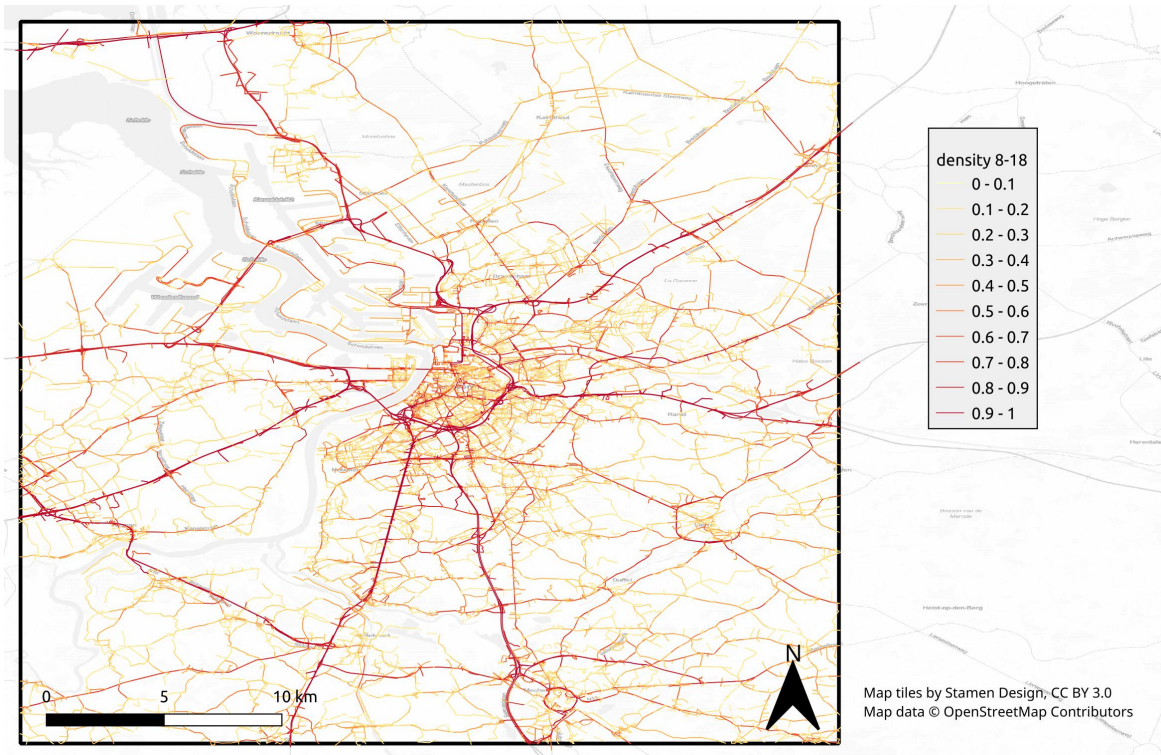


Fig. 25: Segment-wise density 8am–6pm Antwerp from 20 randomly sampled days.

4) Daily density profile Antwerp (2021) :

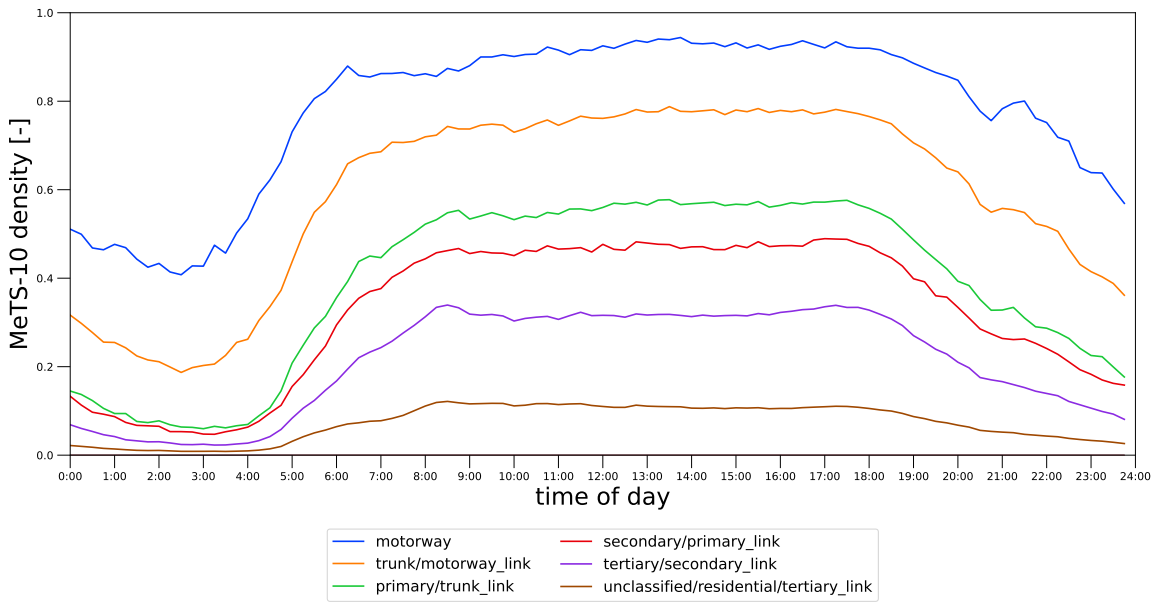


Fig. 26: Daily density profile for different road types for Antwerp . Data from 20 randomly sampled days.

5) Daily speed profile Antwerp (2021) :

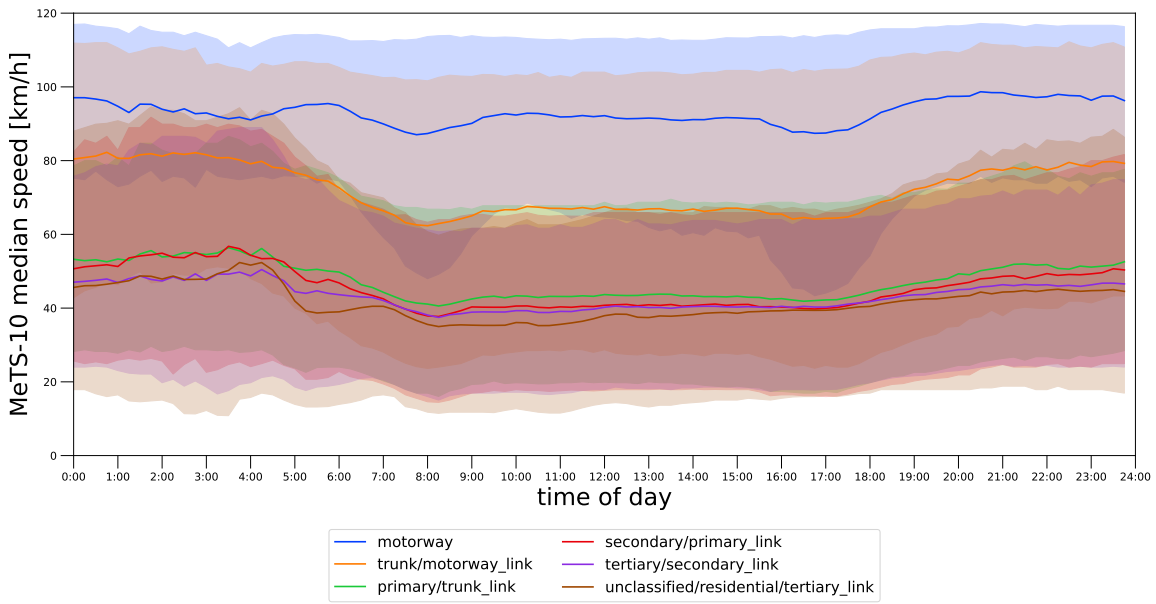


Fig. 27: Daily median 15 min speeds of all intersecting cells profile for different road types for Antwerp . The error hull is the 80% data interval [10.0–90.0 percentiles] of daily means from 20 randomly sampled days.

B. Key Figures Bangkok (2021)

1) Road graph map Bangkok (2021):



Fig. 28: Road graph Bangkok, OSM color scheme (2021).

2) Static data Bangkok (2021) :

Attribute	mean	std	median	q01	q99	data points	sum
bounding box						100.308–100.744 / 13.554–14.049	
num_edges						694'818	
motorway						378	
motorway_link						878	
trunk						1579	
trunk_link						682	
primary						7160	
primary_link						1974	
secondary						15319	
secondary_link						1510	
tertiary						25096	
tertiary_link						342	
unclassified						16290	
residential						623610	
num_nodes						317797	
num_edges_per_cell	1.2	0.7	1.0	1.0	5.0	1'827'614	
num_intersecting_cells	3.1	2.5	2.0	1.0	12.0	694'818	
node_degree	2.3	1.1	3.0	1.0	4.0	317'797	
length_meters	84.6	118.3	49.6	5.2	538.4	694'818	5.9e+07
motorway	1'443.2	1'511.9	961.7	36.7	7'006.2	378	5.5e+05
motorway_link	366.4	357.8	297.5	9.2	1'518.2	878	3.2e+05
trunk	299.6	439.6	115.9	6.4	2'025.4	1'579	4.7e+05
trunk_link	138.9	189.5	76.1	11.1	914.0	682	9.5e+04

primary	159.8	263.3	78.3	5.1	1'190.7	7'160	1.1e+06
primary_link	112.9	202.2	52.6	6.6	864.2	1'974	2.2e+05
secondary	107.7	148.3	59.3	4.0	773.0	15'319	1.6e+06
secondary_link	111.4	178.4	45.2	6.5	837.9	1'510	1.7e+05
tertiary	87.9	125.2	49.5	3.5	635.1	25'096	2.2e+06
tertiary_link	57.2	121.8	14.8	4.9	752.7	342	2.0e+04
unclassified	124.7	175.4	63.6	3.7	877.5	16'290	2.0e+06
residential	80.0	95.0	49.0	5.5	463.3	623'610	5.0e+07
speed_kph	31.8	7.5	29.7	29.7	67.0	694'818	
motorway	108.3	10.6	109.0	40.6	120.0	378	
motorway_link	40.6	0.0	40.6	40.6	40.6	878	
trunk	54.9	1.4	54.9	54.9	54.9	1'579	
trunk_link	54.9	0.0	54.9	54.9	54.9	682	
primary	62.8	2.3	62.9	50.0	62.9	7'160	
primary_link	43.8	1.4	43.8	43.8	43.8	1'974	
secondary	67.0	2.1	67.0	67.0	67.0	15'319	
secondary_link	54.9	0.8	54.9	54.9	54.9	1'510	
tertiary	36.4	1.9	36.4	30.0	36.4	25'096	
tertiary_link	54.9	0.0	54.9	54.9	54.9	342	
unclassified	49.7	1.6	49.7	49.7	49.7	16'290	
residential	29.7	0.6	29.7	29.7	29.7	623'610	
free_flow_kph	34.9	24.3	29.6	0.0	120.0	350'957	
motorway	83.3	17.3	81.5	37.8	120.0	378	
motorway_link	74.4	21.3	77.4	16.9	120.0	877	
trunk	57.1	16.0	53.6	28.5	91.3	1'579	
trunk_link	63.6	19.9	68.7	9.3	93.6	682	
primary	54.5	17.6	51.8	19.8	89.9	7'156	
primary_link	58.5	22.3	60.2	8.5	93.3	1'965	
secondary	54.1	20.1	50.8	18.8	100.6	15'314	
secondary_link	59.0	22.4	60.7	8.5	96.9	1'507	
tertiary	44.3	19.9	40.0	15.6	120.0	24'594	
tertiary_link	50.9	21.8	49.2	10.7	96.9	327	
unclassified	41.8	20.9	37.6	5.6	120.0	13'506	
residential	31.5	23.7	26.4	0.0	119.1	283'072	
free_flow_kph-speed_kph	1.2	23.5	-3.3	-34.1	83.6	350'957	
motorway	-25.0	20.7	-28.1	-71.2	37.4	378	
motorway_link	33.8	21.3	36.8	-23.7	79.4	877	
trunk	2.2	16.1	-1.3	-26.5	36.4	1'579	
trunk_link	8.7	19.9	13.8	-45.6	38.7	682	
primary	-8.3	17.4	-11.1	-43.1	27.0	7'156	
primary_link	14.7	22.3	16.4	-35.3	49.5	1'965	
secondary	-12.9	20.2	-16.4	-48.2	40.0	15'314	
secondary_link	4.0	22.4	5.8	-46.4	42.0	1'507	
tertiary	7.9	19.8	3.6	-20.9	83.6	24'594	
tertiary_link	-4.0	21.8	-5.7	-44.2	42.0	327	
unclassified	-7.9	20.9	-12.1	-44.1	70.3	13'506	
residential	1.8	23.7	-3.3	-29.7	89.4	283'072	

TABLE XII: Key figures Bangkok for the generated data from 20 randomly sampled days. **num_edges** number of edges in the street network graph; **num_nodes** number of nodes in the street network graph; **num_edges_per_cell** number of edges a cell (row,col,heading) has in its intersecting cells; **num_intersecting_cells** number of cells (row,col,heading) in an edge's intersecting cells; **node_degree** number of (unique) neighbor nodes per node; **length_meters** free flow speed derived from data; **speed_kph** signalled speed; **free_flow_kph** free flow speed derived from data; **free_flow_kph-speed_kph** difference

3) Segment density map Bangkok (2021):

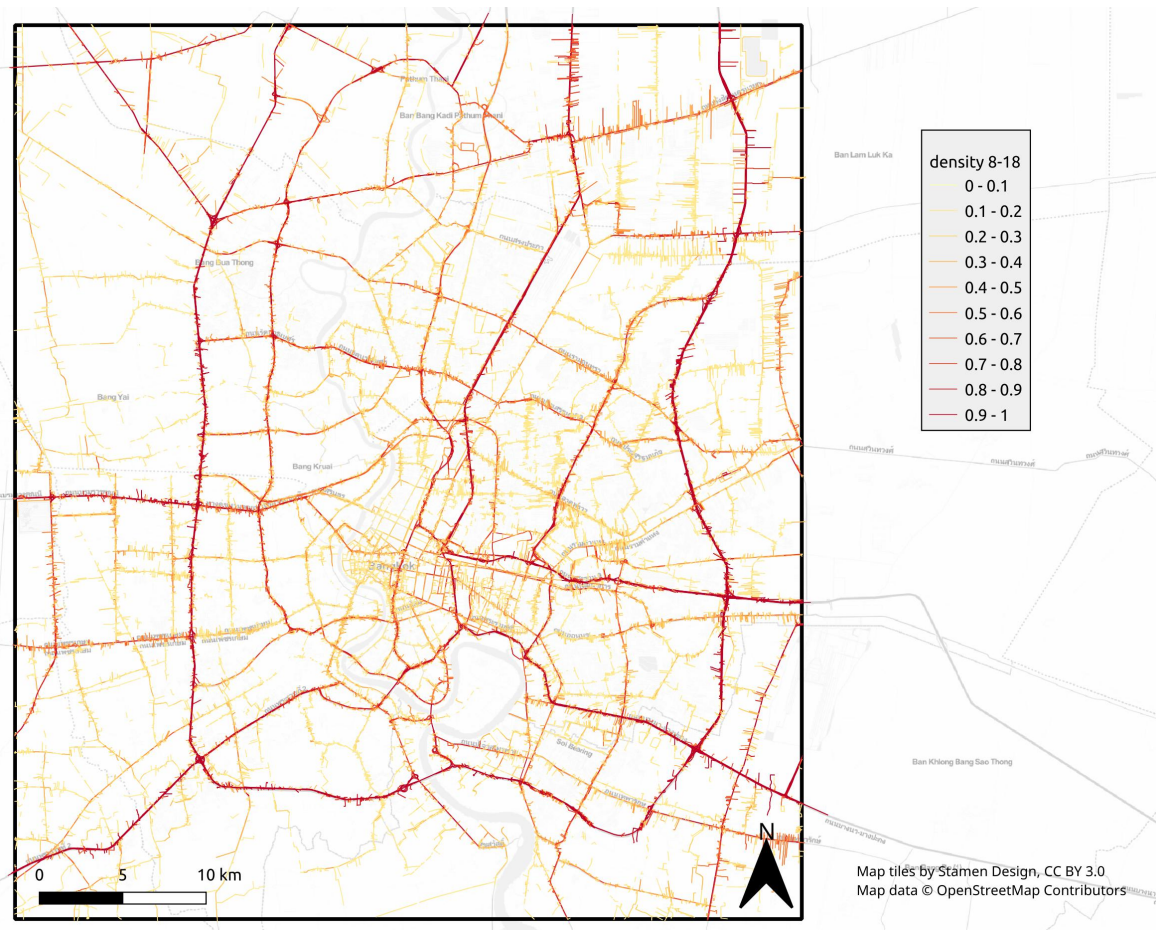


Fig. 29: Segment-wise density 8am–6pm Bangkok from 20 randomly sampled days.

4) Daily density profile Bangkok (2021) :

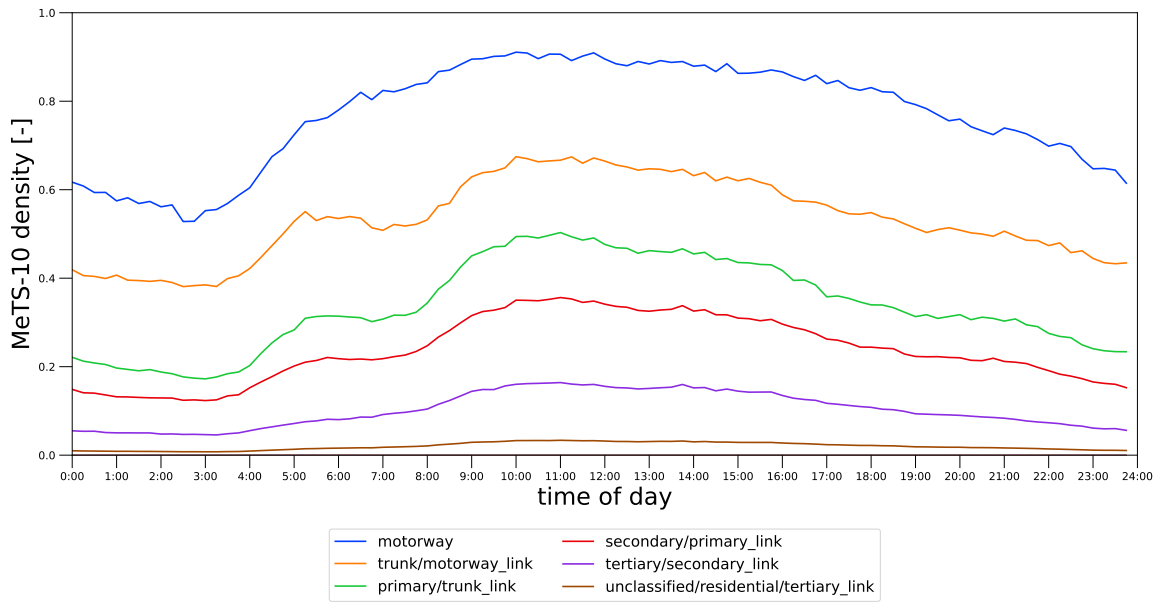


Fig. 30: Daily density profile for different road types for Bangkok . Data from 20 randomly sampled days.

5) Daily speed profile Bangkok (2021) :

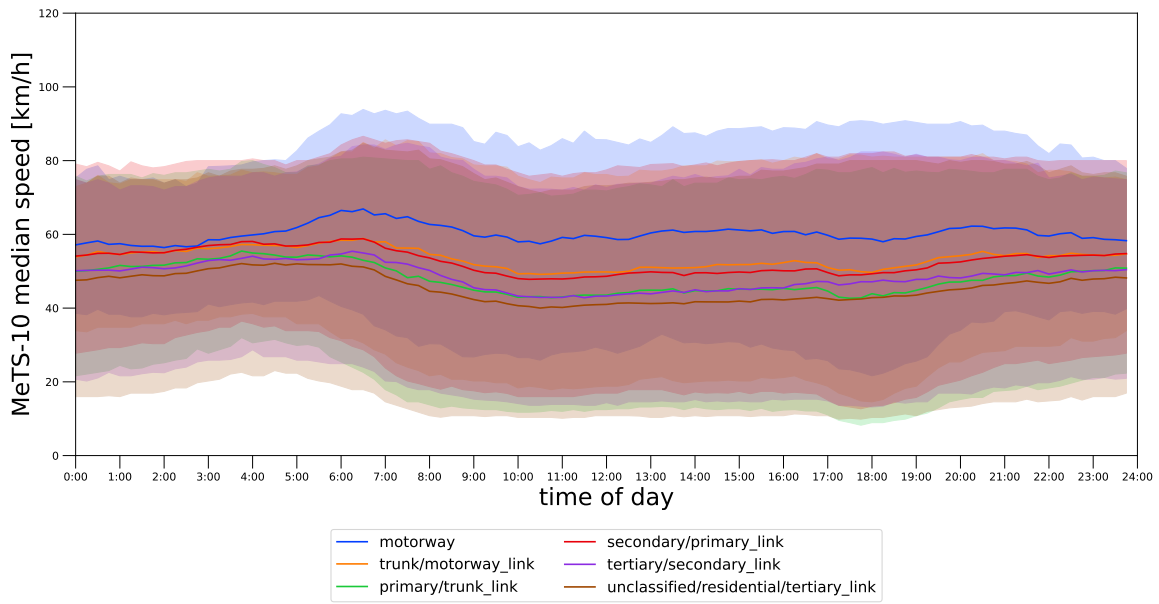


Fig. 31: Daily median 15 min speeds of all intersecting cells profile for different road types for Bangkok . The error hull is the 80% data interval [10.0–90.0 percentiles] of daily means from 20 randomly sampled days.

C. Key Figures Barcelona (2021)

1) Road graph map Barcelona (2021):

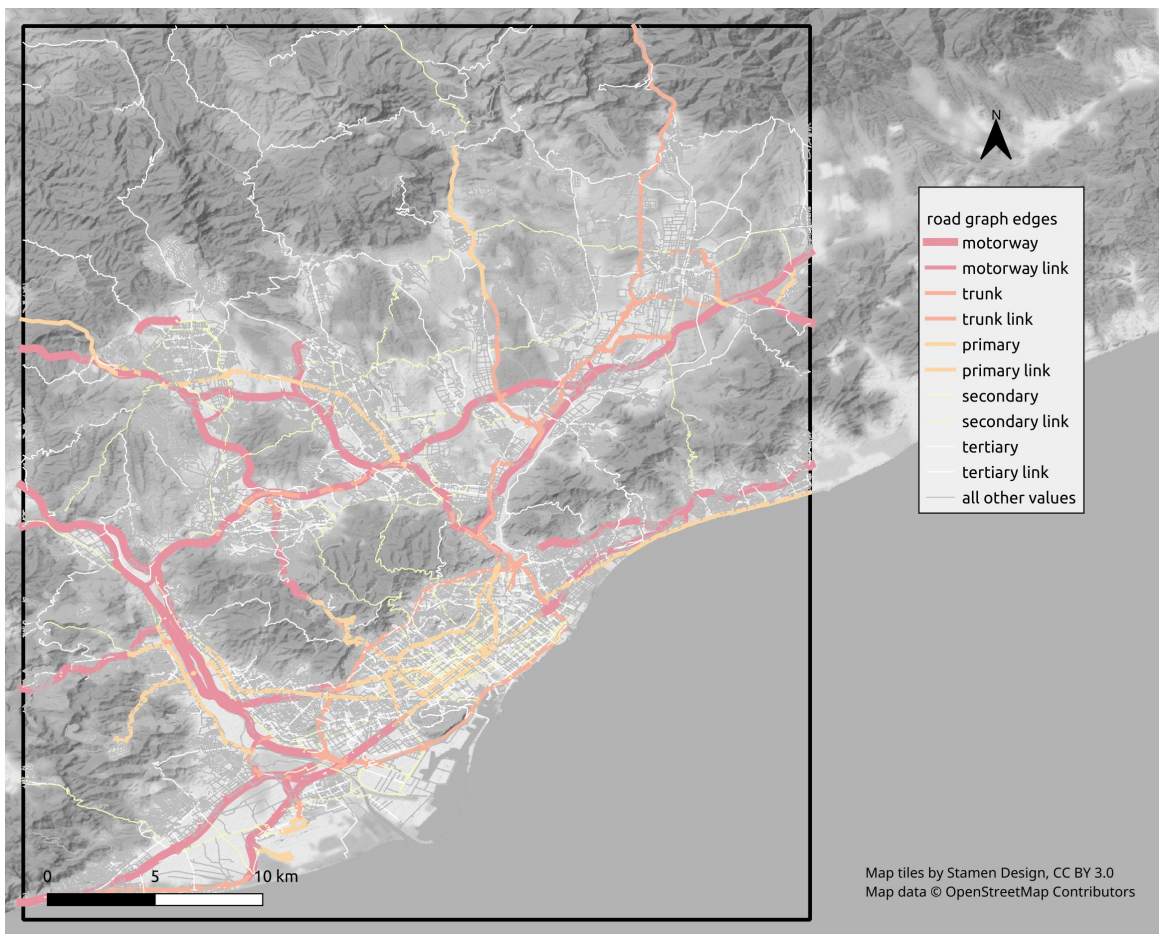


Fig. 32: Road graph Barcelona, OSM color scheme (2021).

2) Static data Barcelona (2021) :

Attribute	mean	std	median	q01	q99	data points	sum
bounding box						1.925–2.361 / 41.253–41.748	
num_edges						118'813	
motorway						442	
motorway_link						700	
trunk						613	
trunk_link						860	
primary						2126	
primary_link						690	
secondary						5525	
secondary_link						879	
tertiary						14875	
tertiary_link						1250	
unclassified						3840	
residential						87013	
num_nodes						58106	
num_edges_per_cell	1.1	0.4	1.0	1.0	3.0	410'314	
num_intersecting_cells	3.7	4.6	3.0	1.0	18.0	118'813	
node_degree	3.0	0.8	3.0	1.0	4.0	58'106	
length_meters	118.5	215.0	74.0	4.5	808.4	118'813	1.4e+07
motorway	987.6	954.8	708.9	38.7	5'246.0	442	4.4e+05
motorway_link	315.6	295.8	262.0	12.6	1'313.0	700	2.2e+05
trunk	456.4	428.8	355.4	13.5	2'071.3	613	2.8e+05
trunk_link	199.6	163.0	165.8	9.5	734.7	860	1.7e+05

primary	122.2	227.6	63.1	3.4	1'054.5	2'126	2.6e+05
primary_link	81.5	106.4	45.4	4.4	450.3	690	5.6e+04
secondary	122.6	268.5	52.9	3.7	1'083.5	5'525	6.8e+05
secondary_link	54.9	80.4	29.9	3.1	365.3	879	4.8e+04
tertiary	122.3	361.2	55.2	3.1	1'192.1	14'875	1.8e+06
tertiary_link	46.2	60.3	27.8	3.4	301.6	1'250	5.8e+04
unclassified	238.8	458.7	101.7	5.1	2'086.6	3'840	9.2e+05
residential	105.0	112.4	76.6	5.2	550.9	87'013	9.1e+06
speed_kph	37.2	9.4	33.9	30.0	80.0	118'813	
motorway	100.0	19.9	100.0	40.0	120.0	442	
motorway_link	63.7	13.6	63.3	40.0	120.0	700	
trunk	81.5	15.5	80.0	40.0	100.0	613	
trunk_link	58.5	10.9	58.6	30.0	100.0	860	
primary	48.0	9.6	50.0	20.0	80.0	2'126	
primary_link	46.8	7.0	50.0	20.0	60.0	690	
secondary	49.5	10.7	50.0	30.0	90.0	5'525	
secondary_link	46.2	6.5	46.7	30.0	60.0	879	
tertiary	43.3	8.1	44.2	30.0	60.0	14'875	
tertiary_link	38.7	6.9	38.5	30.0	50.0	1'250	
unclassified	40.9	5.1	41.0	30.0	50.0	3'840	
residential	33.7	3.7	33.9	30.0	50.0	87'013	
free_flow_kph	34.5	21.6	29.6	0.0	117.4	103'177	
motorway	105.3	12.3	104.0	71.4	120.0	442	
motorway_link	94.3	22.7	99.8	35.3	120.0	699	
trunk	87.4	16.0	89.9	39.9	118.6	613	
trunk_link	81.6	20.2	86.6	24.1	119.3	858	
primary	47.1	18.6	42.8	18.5	100.7	2'126	
primary_link	52.9	21.9	49.9	14.5	109.1	686	
secondary	43.6	17.3	39.5	17.9	102.3	5'519	
secondary_link	44.4	19.4	40.9	14.0	102.8	865	
tertiary	39.0	18.4	34.8	12.7	104.9	14'706	
tertiary_link	42.9	22.7	36.7	10.9	120.0	1'215	
unclassified	42.1	26.0	35.3	0.0	120.0	3'228	
residential	29.7	18.6	26.4	0.0	104.9	72'220	
free_flow_kph-speed_kph	-3.1	19.4	-6.6	-33.9	70.0	103'177	
motorway	5.3	15.7	0.0	-24.0	40.0	442	
motorway_link	30.6	22.6	35.1	-27.5	70.0	699	
trunk	5.9	13.1	4.0	-25.0	43.2	613	
trunk_link	23.1	21.1	28.0	-34.5	61.4	858	
primary	-0.9	17.5	-3.9	-30.7	53.6	2'126	
primary_link	6.0	22.3	0.9	-33.1	58.8	686	
secondary	-5.9	17.3	-8.4	-42.2	53.4	5'519	
secondary_link	-1.7	19.1	-4.4	-35.9	59.2	865	
tertiary	-4.3	18.8	-7.8	-34.0	64.9	14'706	
tertiary_link	4.1	23.0	-1.8	-30.7	80.0	1'215	
unclassified	1.0	26.5	-5.7	-41.0	79.0	3'228	
residential	-3.9	18.7	-7.1	-33.9	71.0	72'220	

TABLE XIII: Key figures Barcelona for the generated data from 20 randomly sampled days. **num_edges** number of edges in the street network graph; **num_nodes** number of nodes in the street network graph; **num_edges_per_cell** number of edges a cell (row,col,heading) has in its intersecting cells; **num_intersecting_cells** number of cells (row,col,heading) in an edge's intersecting cells; **node_degree** number of (unique) neighbor nodes per node; **length_meters** free flow speed derived from data; **speed_kph** signalled speed; **free_flow_kph** free flow speed derived from data; **free_flow_kph-speed_kph** difference

3) Segment density map Barcelona (2021):

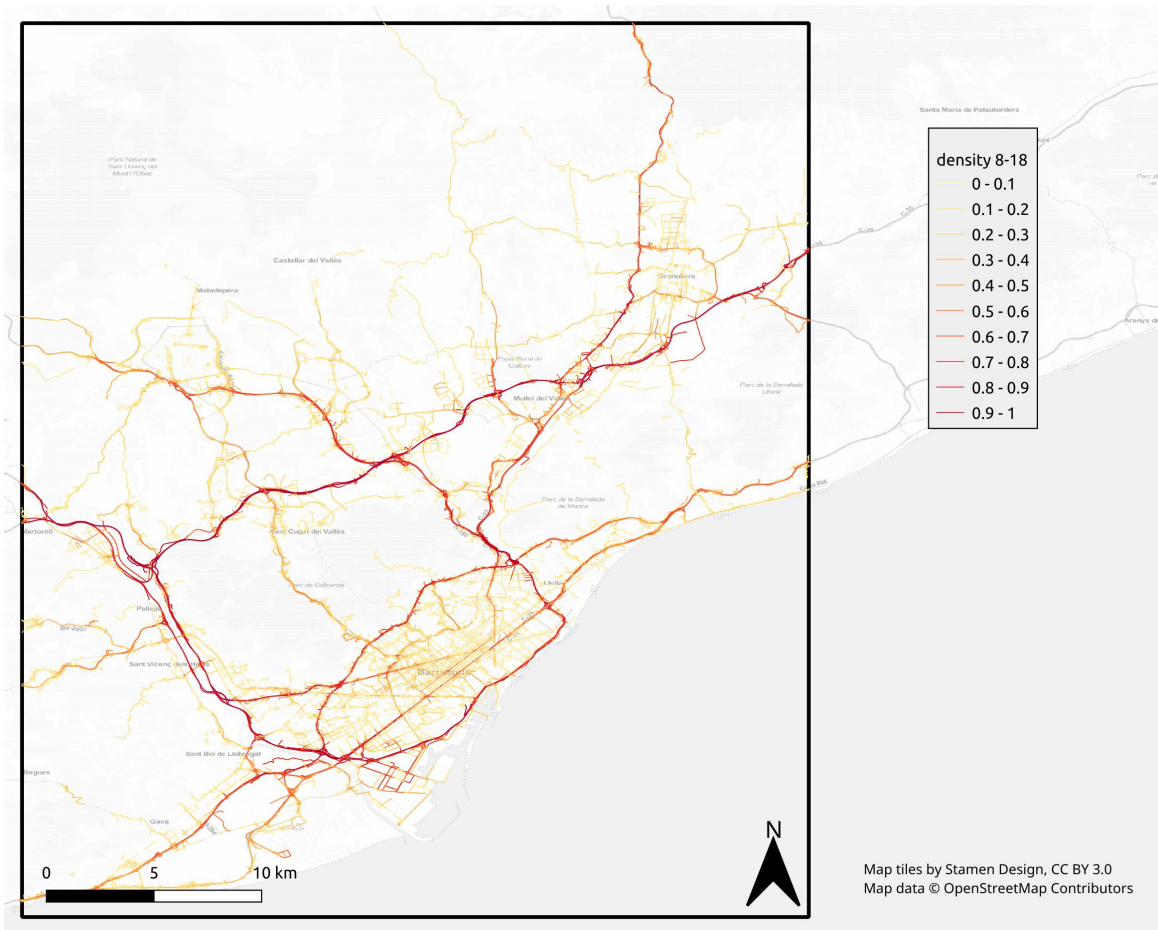


Fig. 33: Segment-wise density 8am–6pm Barcelona from 20 randomly sampled days.

4) Daily density profile Barcelona (2021) :

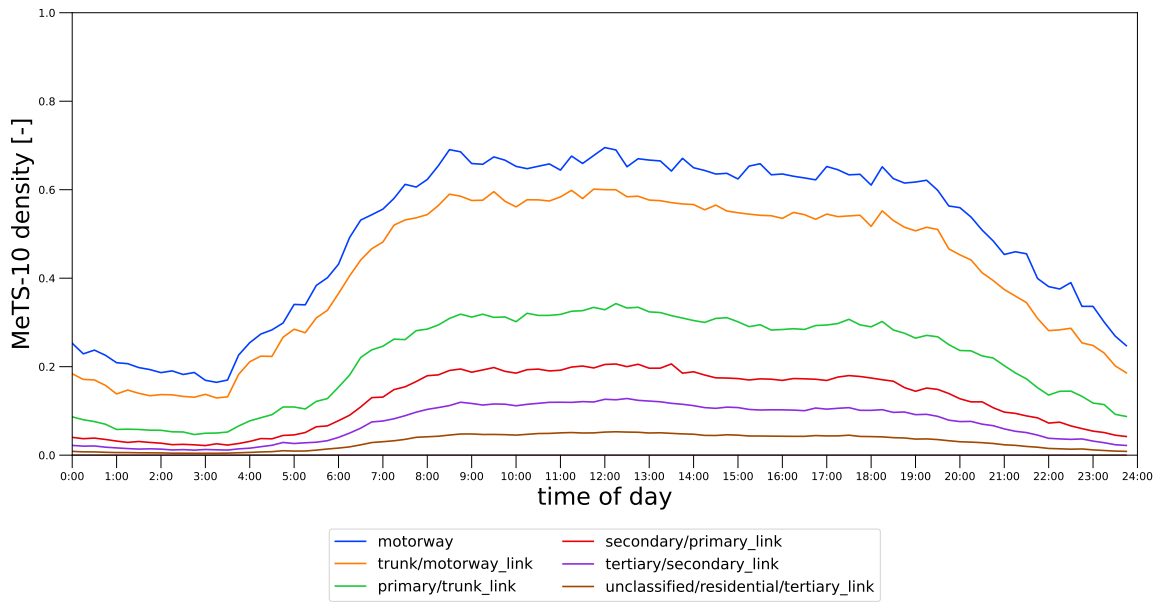


Fig. 34: Daily density profile for different road types for Barcelona . Data from 20 randomly sampled days.

5) Daily speed profile Barcelona (2021) :

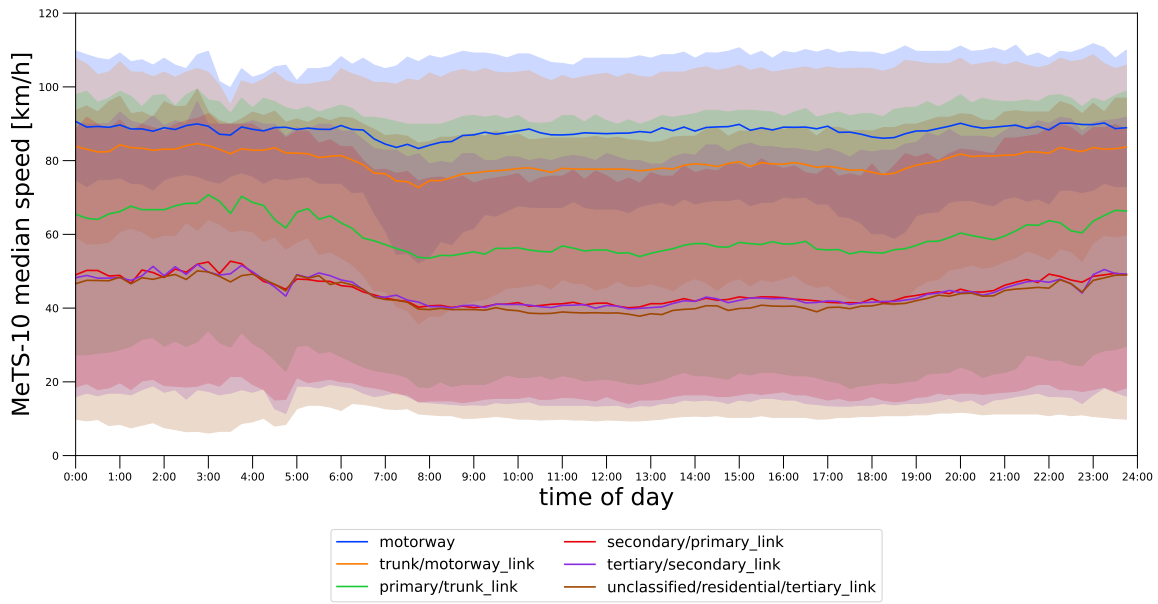


Fig. 35: Daily median 15 min speeds of all intersecting cells profile for different road types for Barcelona . The error hull is the 80% data interval [10.0–90.0 percentiles] of daily means from 20 randomly sampled days.

D. Key Figures Berlin (2021)

1) Road graph map Berlin (2021):

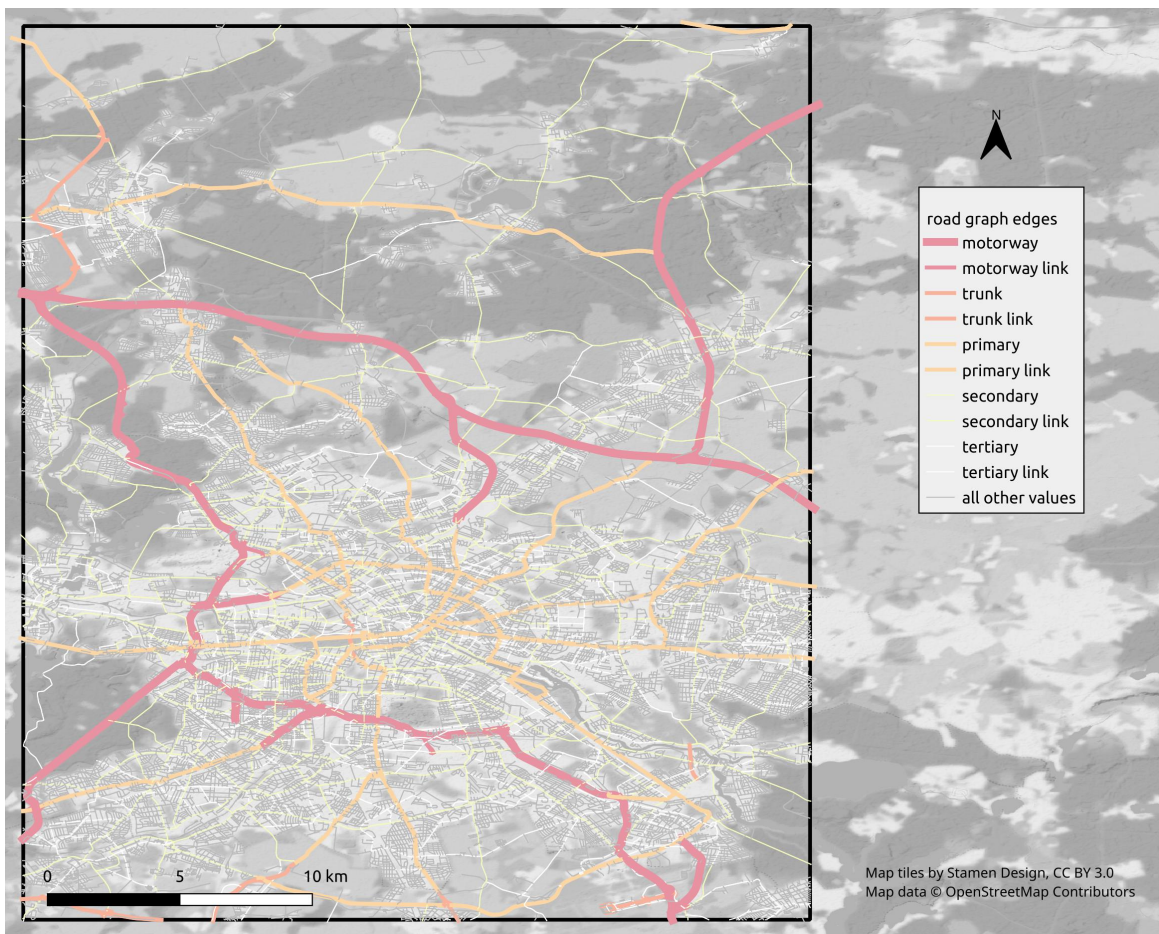


Fig. 36: Road graph Berlin, OSM color scheme (2021).

2) Static data Berlin (2021) :

Attribute	mean	std	median	q01	q99	data points	sum
bounding box						13.189–13.625 / 52.359–52.854	
num_edges						88'882	
motorway						279	
motorway_link						469	
trunk						75	
trunk_link						77	
primary						2754	
primary_link						150	
secondary						10292	
secondary_link						280	
tertiary						8486	
tertiary_link						61	
unclassified						1766	
residential						64193	
num_nodes						34308	
num_edges_per_cell	1.0	0.2	1.0	1.0	2.0	405'500	
num_intersecting_cells	4.7	4.3	4.0	1.0	20.0	88'882	
node_degree	2.9	0.9	3.0	1.0	4.0	34'308	
length_meters	158.0	202.0	119.3	8.5	784.2	88'882	1.4e+07
motorway	1'058.1	1'232.4	585.3	88.1	5'875.6	279	3.0e+05
motorway_link	256.9	257.1	216.8	14.3	1'456.1	469	1.2e+05
trunk	846.4	959.8	516.8	44.1	5'038.1	75	6.3e+04
trunk_link	214.3	117.7	220.9	13.5	532.3	77	1.6e+04

primary	191.6	292.9	119.1	7.7	1'583.0	2'754	5.3e+05
primary_link	52.6	73.4	18.0	7.2	302.2	150	7.9e+03
secondary	174.3	300.9	111.5	7.6	1'554.5	10'292	1.8e+06
secondary_link	25.5	31.5	14.6	7.0	149.6	280	7.1e+03
tertiary	155.1	216.5	113.0	7.3	951.6	8'486	1.3e+06
tertiary_link	23.3	34.8	12.9	7.2	160.2	61	1.4e+03
unclassified	310.2	439.8	171.5	9.5	2'386.5	1'766	5.5e+05
residential	145.6	116.1	120.1	9.0	547.1	64'193	9.3e+06
speed_kph	35.7	10.1	30.0	30.0	60.0	88'882	
motorway	85.4	17.1	80.0	60.0	120.0	279	
motorway_link	61.7	14.7	60.0	40.0	120.0	469	
trunk	87.5	32.5	100.0	30.0	120.0	75	
trunk_link	52.6	8.5	52.5	30.0	72.4	77	
primary	49.5	8.3	50.0	30.0	80.0	2'754	
primary_link	48.9	7.8	50.0	30.0	70.0	150	
secondary	48.7	6.5	50.0	30.0	70.0	10'292	
secondary_link	48.2	5.2	50.0	30.0	60.0	280	
tertiary	46.4	8.5	50.0	30.0	60.0	8'486	
tertiary_link	46.4	8.3	50.0	22.0	54.0	61	
unclassified	42.6	10.0	43.1	10.0	70.0	1'766	
residential	30.8	4.4	30.0	20.0	50.0	64'193	
free_flow_kph	37.4	14.1	35.3	12.0	87.5	85'074	
motorway	92.2	15.7	87.8	68.4	119.5	279	
motorway_link	78.4	20.0	80.6	31.4	119.0	469	
trunk	90.5	25.2	99.1	47.4	118.6	75	
trunk_link	83.7	26.8	82.4	18.6	118.3	77	
primary	48.8	12.1	48.5	24.0	89.8	2'754	
primary_link	44.8	18.5	41.9	13.2	96.4	150	
secondary	46.9	11.3	47.5	21.5	84.7	10'283	
secondary_link	34.8	16.7	33.6	11.8	80.9	280	
tertiary	44.2	10.7	43.8	21.6	83.0	8'484	
tertiary_link	32.8	15.1	33.4	11.3	61.8	59	
unclassified	43.9	17.0	42.8	16.0	105.4	1'689	
residential	33.4	11.8	32.0	10.4	73.5	60'475	
free_flow_kph-speed_kph	1.5	12.6	0.6	-28.4	42.2	85'074	
motorway	6.9	16.6	6.6	-48.4	37.0	279	
motorway_link	16.7	20.9	19.2	-29.0	59.1	469	
trunk	3.0	13.4	-0.1	-35.2	34.3	75	
trunk_link	31.1	26.1	29.8	-33.9	65.8	77	
primary	-0.7	10.8	-0.5	-26.2	31.8	2'754	
primary_link	-4.1	19.6	-7.2	-52.1	39.7	150	
secondary	-1.8	11.5	-1.1	-29.3	33.2	10'283	
secondary_link	-13.4	17.9	-15.3	-42.1	30.9	280	
tertiary	-2.2	11.4	-2.2	-28.4	31.9	8'484	
tertiary_link	-13.5	19.6	-14.6	-37.8	40.4	59	
unclassified	1.3	18.1	-0.3	-32.1	59.7	1'689	
residential	2.5	12.3	1.3	-27.2	42.9	60'475	

TABLE XIV: Key figures Berlin for the generated data from 20 randomly sampled days. **num_edges** number of edges in the street network graph; **num_nodes** number of nodes in the street network graph; **num_edges_per_cell** number of edges a cell (row,col,heading) has in its intersecting cells; **num_intersecting_cells** number of cells (row,col,heading) in an edge's intersecting cells; **node_degree** number of (unique) neighbor nodes per node; **length_meters** free flow speed derived from data; **speed_kph** signalled speed; **free_flow_kph** free flow speed derived from data; **free_flow_kph-speed_kph** difference

3) Segment density map Berlin (2021):

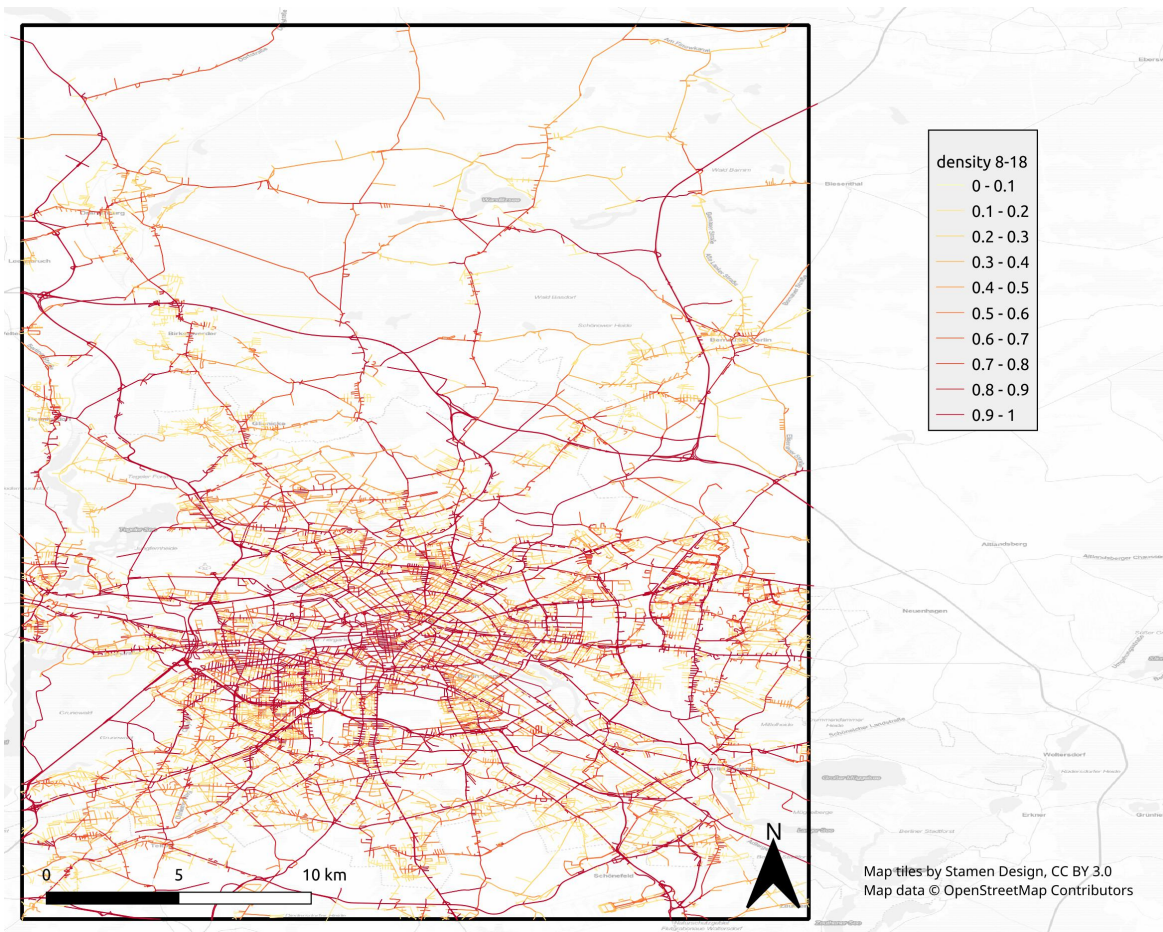


Fig. 37: Segment-wise density 8am–6pm Berlin from 20 randomly sampled days.

4) Daily density profile Berlin (2021) :

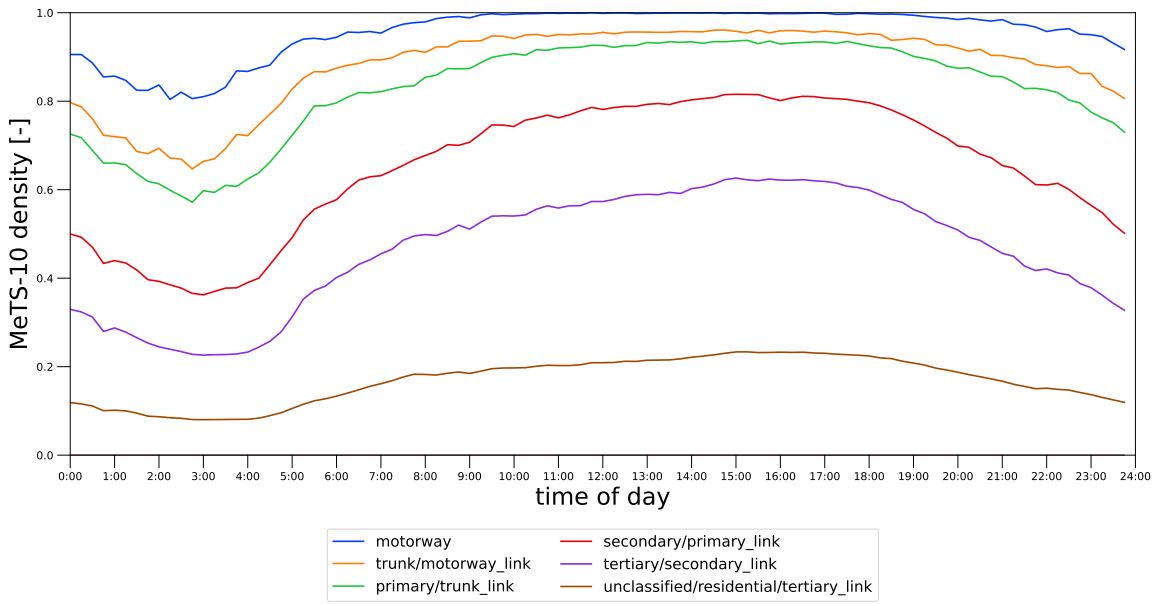


Fig. 38: Daily density profile for different road types for Berlin . Data from 20 randomly sampled days.

5) Daily speed profile Berlin (2021) :

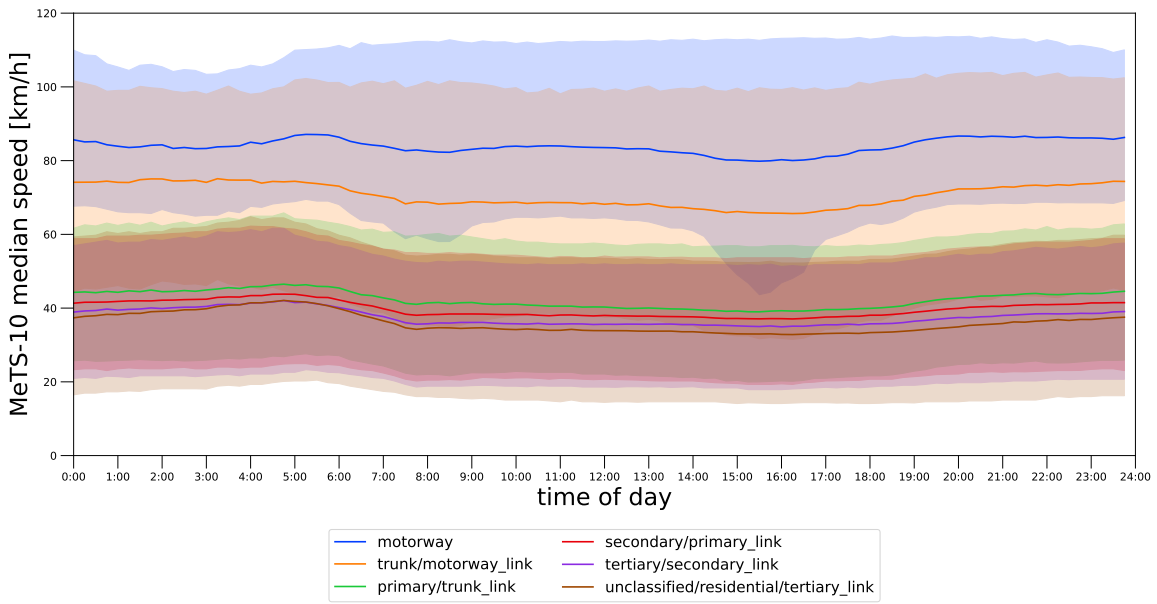


Fig. 39: Daily median 15 min speeds of all intersecting cells profile for different road types for Berlin . The error hull is the 80% data interval [10.0–90.0 percentiles] of daily means from 20 randomly sampled days.

E. Key Figures Chicago (2021)

1) Road graph map Chicago (2021):

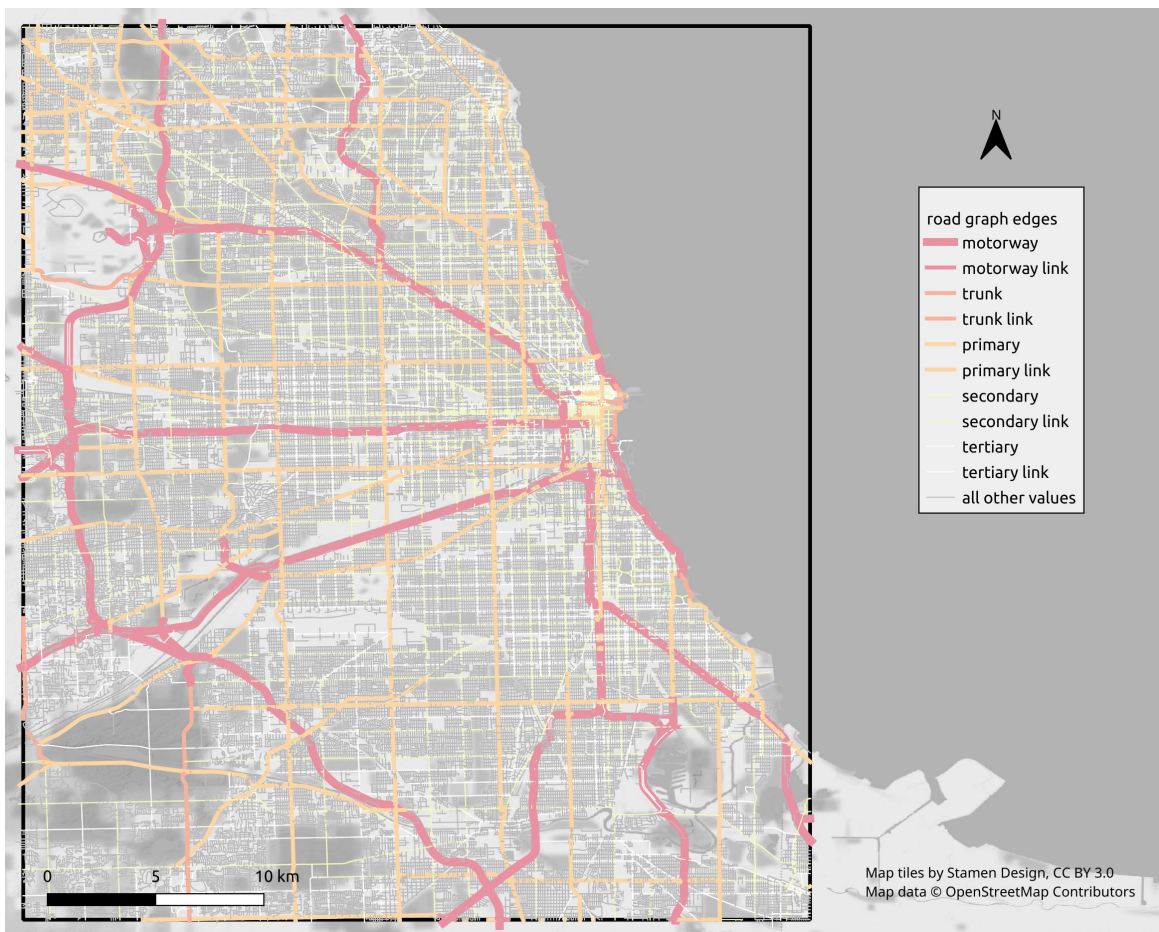


Fig. 40: Road graph Chicago, OSM color scheme (2021).

2) Static data Chicago (2021) :

Attribute	mean	std	median	q01	q99	data points	sum
bounding box						-87.945—87.509 / 41.601—42.096	
num_edges						187'570	
motorway						822	
motorway_link						1178	
trunk						207	
trunk_link						73	
primary						10439	
primary_link						387	
secondary						22812	
secondary_link						208	
tertiary						16603	
tertiary_link						71	
unclassified						1069	
residential						133701	
num_nodes						68430	
num_edges_per_cell	1.1	0.3	1.0	1.0	3.0	966'289	
num_intersecting_cells	5.5	3.3	4.0	1.0	16.0	187'570	
node_degree	3.2	0.9	3.0	1.0	4.0	68'430	
length_meters	144.6	134.2	103.9	9.7	583.7	187'570	2.7e+07
motorway	778.1	872.2	559.2	22.6	4'295.7	822	6.4e+05
motorway_link	329.9	265.3	301.3	10.2	1'229.2	1'178	3.9e+05
trunk	370.4	431.5	262.0	7.6	1'872.6	207	7.7e+04
trunk_link	106.8	102.1	59.3	4.6	371.3	73	7.8e+03

primary	141.9	158.8	102.1	6.9	797.0	10'439	1.5e+06
primary_link	70.4	72.8	52.5	10.2	404.8	387	2.7e+04
secondary	128.0	111.6	101.5	7.2	588.6	22'812	2.9e+06
secondary_link	61.2	66.2	43.8	8.7	346.1	208	1.3e+04
tertiary	140.2	148.4	102.3	8.2	674.1	16'603	2.3e+06
tertiary_link	40.3	31.5	30.6	6.4	131.5	71	2.9e+03
unclassified	229.4	297.9	126.5	4.8	1'519.1	1'069	2.5e+05
residential	142.0	95.5	106.8	10.3	452.4	133'701	1.9e+07
speed_kph	41.0	8.0	36.8	36.8	83.8	187'570	
motorway	87.7	6.9	88.5	72.4	112.7	822	
motorway_link	83.7	3.0	83.8	83.8	83.8	1'178	
trunk	75.1	8.8	74.4	48.3	88.5	207	
trunk_link	57.1	0.0	57.1	57.1	57.1	73	
primary	55.6	3.4	55.8	48.3	64.4	10'439	
primary_link	57.1	0.0	57.1	57.1	57.1	387	
secondary	50.9	1.9	50.9	48.3	56.3	22'812	
secondary_link	32.2	0.0	32.2	32.2	32.2	208	
tertiary	44.7	2.5	44.7	32.2	56.3	16'603	
tertiary_link	48.3	0.0	48.3	48.3	48.3	71	
unclassified	56.3	2.7	56.3	56.3	56.3	1'069	
residential	36.8	0.6	36.8	36.8	36.8	133'701	
free_flow_kph	45.1	19.0	42.8	4.2	111.2	162'191	
motorway	99.4	12.9	98.1	52.3	118.6	822	
motorway_link	91.4	20.9	95.5	29.6	118.9	1'178	
trunk	68.8	17.9	70.6	32.1	98.8	207	
trunk_link	67.4	17.8	76.7	26.4	91.4	73	
primary	55.2	13.6	54.1	30.1	98.4	10'427	
primary_link	52.4	17.2	51.8	12.7	96.4	384	
secondary	49.6	14.6	46.6	25.9	99.8	22'787	
secondary_link	51.7	21.0	48.5	13.7	110.0	208	
tertiary	48.9	16.7	45.6	21.2	111.1	16'538	
tertiary_link	48.4	20.2	46.6	19.4	110.9	69	
unclassified	47.6	24.9	46.5	3.3	118.0	988	
residential	41.5	18.5	39.2	2.7	107.3	108'510	
free_flow_kph-speed_kph	3.4	17.7	0.9	-33.5	64.5	162'191	
motorway	11.8	12.8	10.6	-35.5	40.4	822	
motorway_link	7.7	21.0	11.7	-54.2	36.2	1'178	
trunk	-6.3	14.9	-3.7	-44.6	18.3	207	
trunk_link	10.3	17.8	19.6	-30.7	34.3	73	
primary	-0.4	13.3	-1.2	-26.2	42.1	10'427	
primary_link	-4.7	17.2	-5.3	-44.4	39.3	384	
secondary	-1.2	14.6	-4.1	-25.0	48.9	22'787	
secondary_link	19.5	21.0	16.3	-18.5	77.8	208	
tertiary	4.2	16.7	1.2	-23.5	66.4	16'538	
tertiary_link	0.1	20.2	-1.7	-28.9	62.6	69	
unclassified	-8.7	24.8	-9.7	-53.0	61.7	988	
residential	4.7	18.5	2.3	-34.0	70.6	108'510	

TABLE XV: Key figures Chicago for the generated data from 20 randomly sampled days. **num_edges** number of edges in the street network graph; **num_nodes** number of nodes in the street network graph; **num_edges_per_cell** number of edges a cell (row,col,heading) has in its intersecting cells; **num_intersecting_cells** number of cells (row,col,heading) in an edge's intersecting cells; **node_degree** number of (unique) neighbor nodes per node; **length_meters** free flow speed derived from data; **speed_kph** signalled speed; **free_flow_kph** free flow speed derived from data; **free_flow_kph-speed_kph** difference

3) Segment density map Chicago (2021):

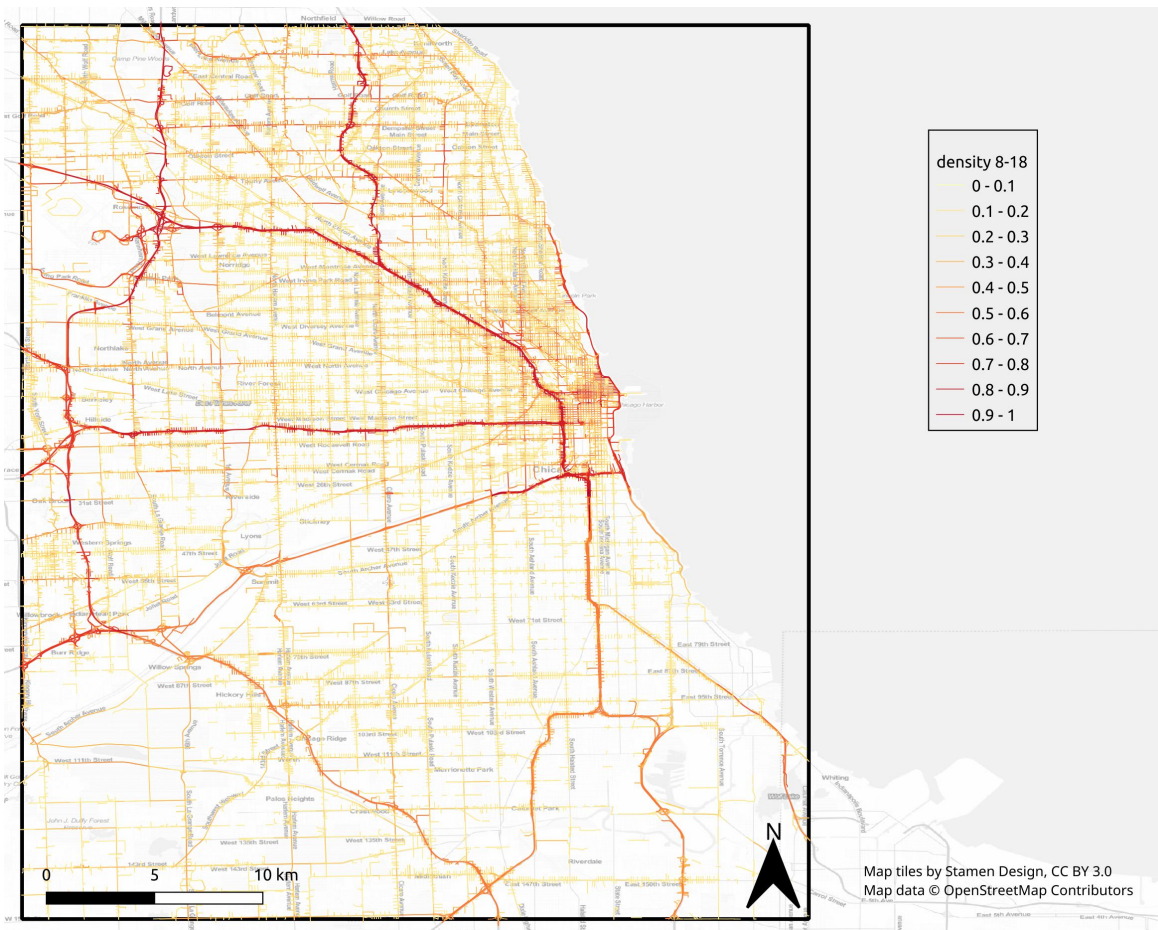


Fig. 41: Segment-wise density 8am–6pm Chicago from 20 randomly sampled days.

4) Daily density profile Chicago (2021) :

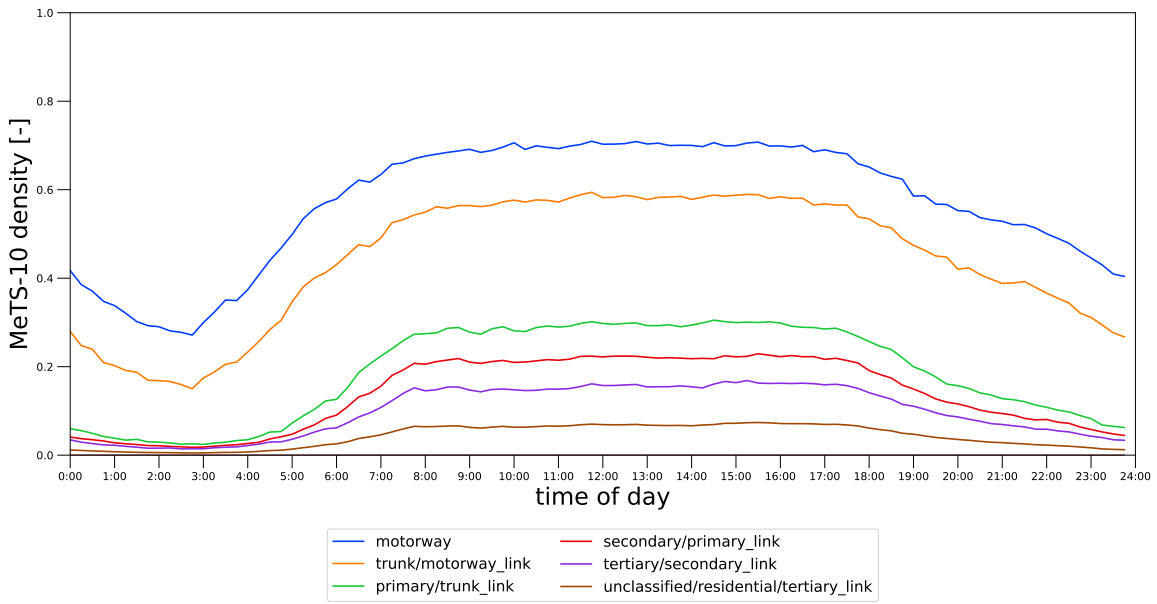


Fig. 42: Daily density profile for different road types for Chicago . Data from 20 randomly sampled days.

5) Daily speed profile Chicago (2021) :

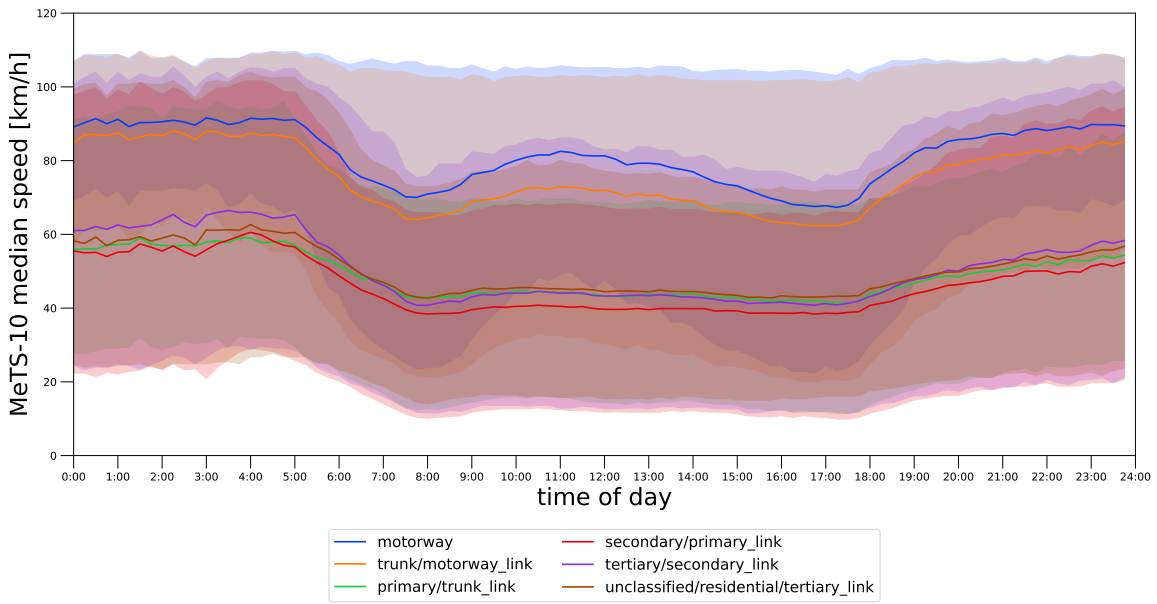


Fig. 43: Daily median 15 min speeds of all intersecting cells profile for different road types for Chicago . The error hull is the 80% data interval [10.0–90.0 percentiles] of daily means from 20 randomly sampled days.

F. Key Figures Istanbul (2021)

1) Road graph map Istanbul (2021):

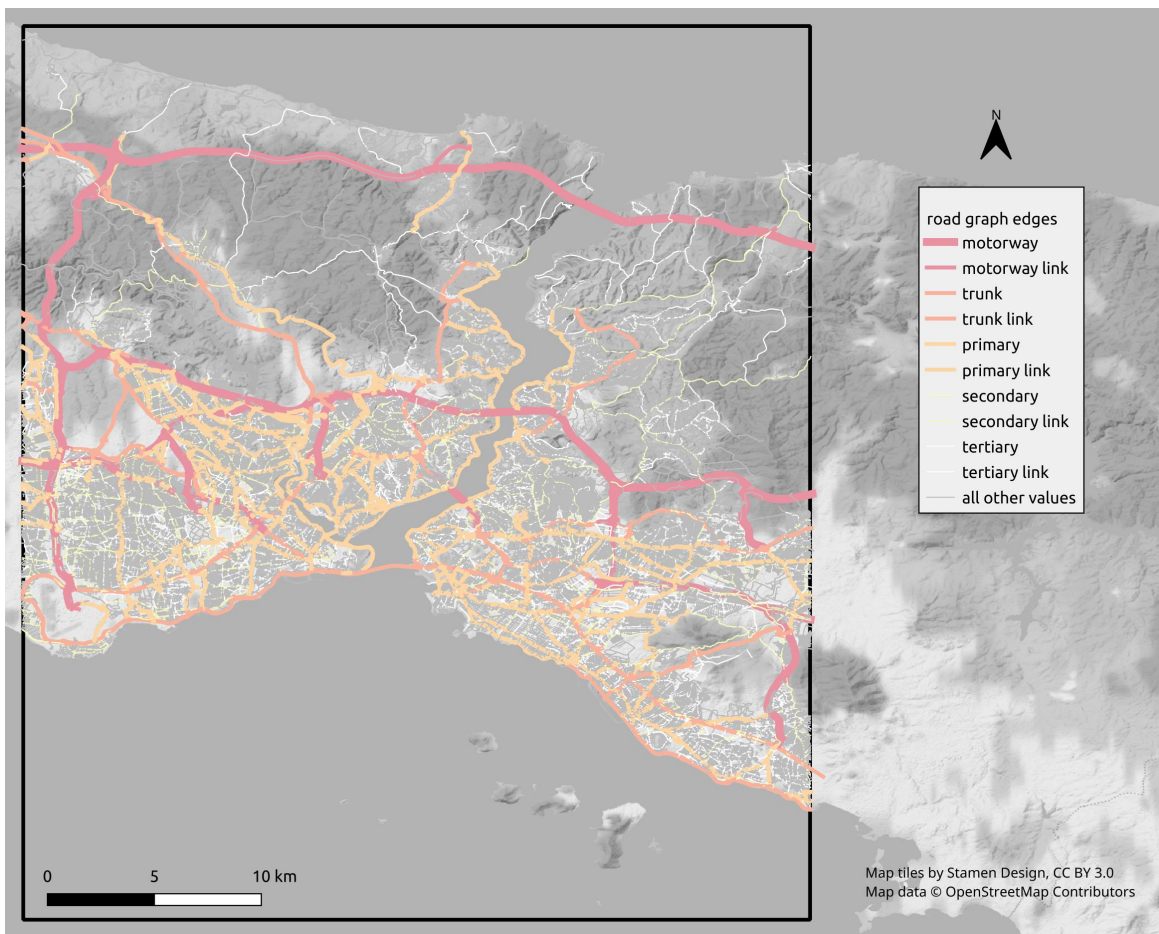


Fig. 44: Road graph Istanbul, OSM color scheme (2021).

2) Static data Istanbul (2021) :

Attribute	mean	std	median	q01	q99	data points	sum
bounding box						28.794–29.23 / 40.81–41.305	
num_edges						270'109	
motorway						338	
motorway_link						699	
trunk						1156	
trunk_link						1529	
primary						9242	
primary_link						2430	
secondary						17014	
secondary_link						1403	
tertiary						30221	
tertiary_link						625	
unclassified						5422	
residential						200030	
num_nodes						102754	
num_edges_per_cell	1.1	0.6	1.0	1.0	4.0	734'722	
num_intersecting_cells	3.1	2.9	2.0	1.0	12.0	270'109	
node_degree	3.0	0.8	3.0	1.0	4.0	102'754	
length_meters	81.9	135.0	53.3	5.9	479.4	270'109	2.2e+07
motorway	1'066.1	1'693.6	647.9	42.4	8'557.5	338	3.6e+05
motorway_link	361.1	312.1	277.1	11.8	1'505.5	699	2.5e+05
trunk	394.2	522.6	216.3	9.5	2'387.7	1'156	4.6e+05
trunk_link	162.4	148.9	126.8	7.7	677.8	1'529	2.5e+05

primary	104.8	160.3	57.2	5.6	723.8	9'242	9.7e+05
primary_link	65.0	78.0	37.4	5.7	378.0	2'430	1.6e+05
secondary	74.6	128.1	42.2	5.0	507.6	17'014	1.3e+06
secondary_link	48.6	75.7	28.1	4.6	308.9	1'403	6.8e+04
tertiary	73.5	153.4	43.8	4.8	515.8	30'221	2.2e+06
tertiary_link	30.4	32.4	20.1	3.9	170.2	625	1.9e+04
unclassified	217.9	370.2	104.7	7.1	1'861.4	5'422	1.2e+06
residential	74.6	67.7	55.0	6.5	317.6	200'030	1.5e+07
speed_kph	35.4	6.2	33.2	22.3	50.0	270'109	
motorway	107.1	9.9	107.3	80.0	120.0	338	
motorway_link	47.5	8.8	46.6	30.0	90.0	699	
trunk	75.3	10.8	76.4	30.0	100.0	1'156	
trunk_link	42.3	4.8	42.4	30.0	50.0	1'529	
primary	44.9	4.5	44.9	30.0	50.0	9'242	
primary_link	32.4	2.8	32.4	30.0	32.4	2'430	
secondary	38.1	2.9	38.1	30.0	50.0	17'014	
secondary_link	30.5	1.8	30.6	20.0	30.6	1'403	
tertiary	45.1	2.2	45.2	33.2	50.0	30'221	
tertiary_link	31.6	1.4	31.6	30.0	31.6	625	
unclassified	22.4	1.2	22.3	22.3	33.2	5'422	
residential	33.2	1.1	33.2	33.2	33.2	200'030	
free_flow_kph	24.7	12.4	20.9	10.4	75.8	268'548	
motorway	81.4	14.2	83.9	18.9	106.3	338	
motorway_link	69.4	16.7	71.7	24.4	98.1	698	
trunk	61.7	14.7	64.5	19.6	91.1	1'156	
trunk_link	53.9	18.2	56.5	10.8	87.4	1'529	
primary	36.4	12.4	34.4	16.5	75.9	9'242	
primary_link	33.6	13.9	31.5	11.3	77.1	2'430	
secondary	31.2	14.4	26.8	14.3	82.3	17'014	
secondary_link	32.0	16.9	26.8	10.7	82.5	1'403	
tertiary	26.1	10.2	24.0	12.7	67.8	30'195	
tertiary_link	24.7	10.7	22.0	10.1	76.5	625	
unclassified	29.7	16.4	25.6	8.0	89.1	4'735	
residential	22.5	10.4	19.8	9.9	68.2	199'183	
free_flow_kph-speed_kph	-10.7	12.1	-13.7	-29.5	37.7	268'548	
motorway	-25.8	15.6	-23.3	-88.4	2.1	338	
motorway_link	21.9	17.6	24.5	-26.7	53.6	698	
trunk	-13.6	15.8	-11.4	-57.6	25.1	1'156	
trunk_link	11.6	18.0	14.5	-31.6	44.6	1'529	
primary	-8.5	12.6	-10.3	-30.3	29.7	9'242	
primary_link	1.2	14.1	-0.6	-22.2	43.6	2'430	
secondary	-6.9	14.6	-11.3	-25.2	44.4	17'014	
secondary_link	1.5	16.9	-3.5	-19.9	51.9	1'403	
tertiary	-18.9	10.4	-21.0	-33.0	22.1	30'195	
tertiary_link	-6.9	10.8	-9.6	-22.5	44.9	625	
unclassified	7.3	16.5	3.3	-15.9	66.8	4'735	
residential	-10.8	10.4	-13.4	-23.3	35.0	199'183	

TABLE XVI: Key figures Istanbul for the generated data from 20 randomly sampled days. **num_edges** number of edges in the street network graph; **num_nodes** number of nodes in the street network graph; **num_edges_per_cell** number of edges a cell (row,col,heading) has in its intersecting cells; **num_intersecting_cells** number of cells (row,col,heading) in an edge's intersecting cells; **node_degree** number of (unique) neighbor nodes per node; **length_meters** free flow speed derived from data; **speed_kph** signalled speed; **free_flow_kph** free flow speed derived from data; **free_flow_kph-speed_kph** difference

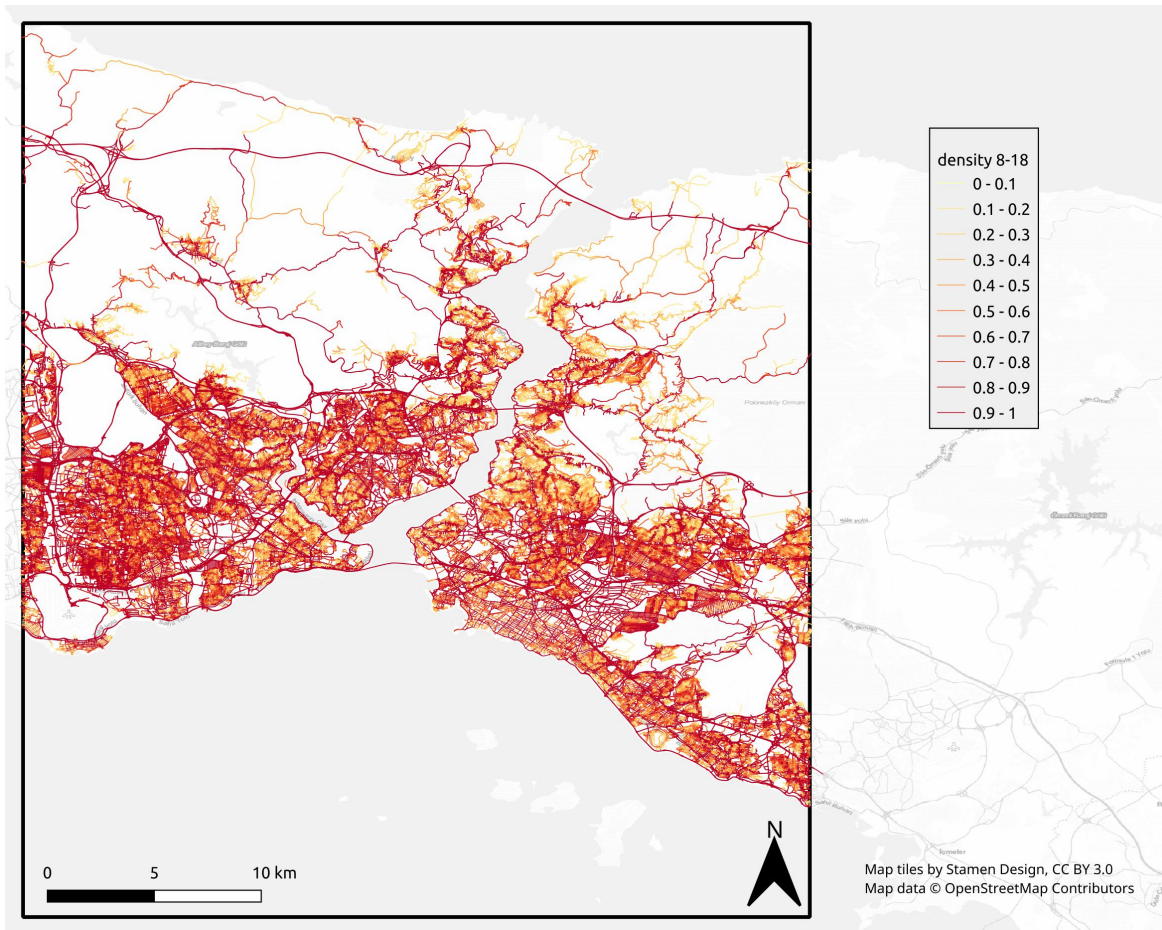
3) *Segment density map Istanbul (2021):*

Fig. 45: Segment-wise density 8am–6pm Istanbul from 20 randomly sampled days.

4) Daily density profile Istanbul (2021) :

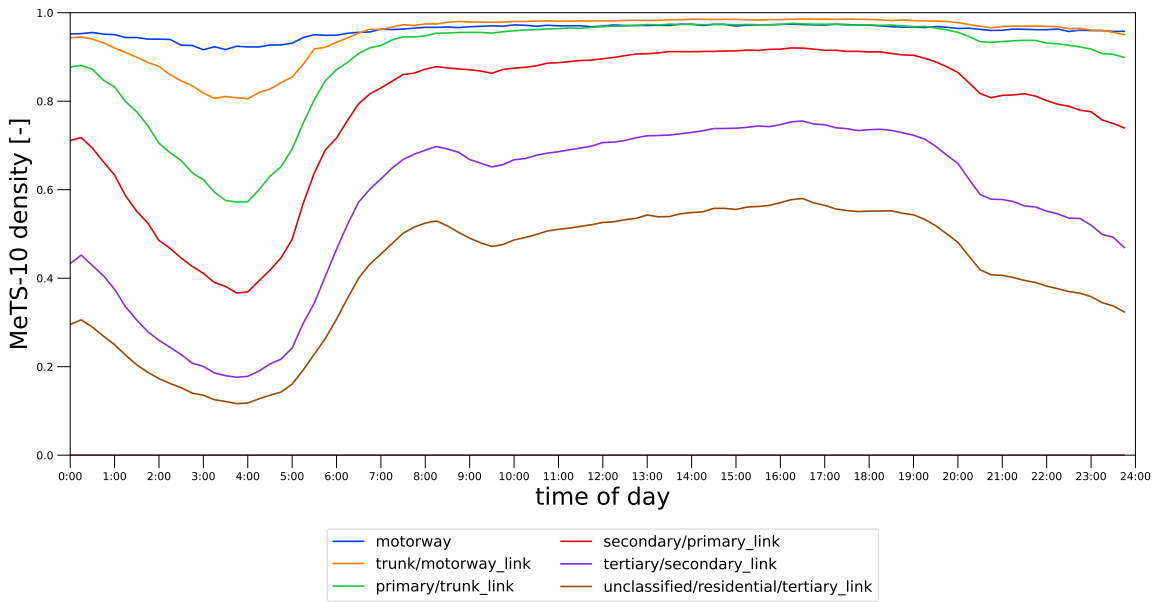


Fig. 46: Daily density profile for different road types for Istanbul . Data from 20 randomly sampled days.

5) Daily speed profile Istanbul (2021) :

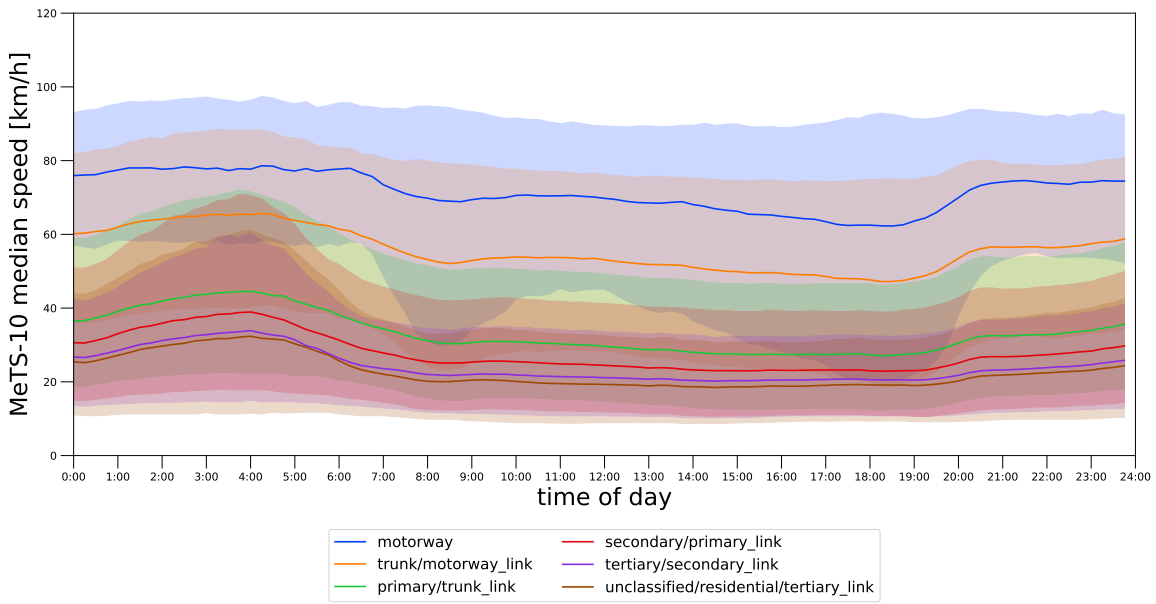


Fig. 47: Daily median 15 min speeds of all intersecting cells profile for different road types for Istanbul . The error hull is the 80% data interval [10.0–90.0 percentiles] of daily means from 20 randomly sampled days.

G. Key Figures Melbourne (2021)

1) Road graph map Melbourne (2021):

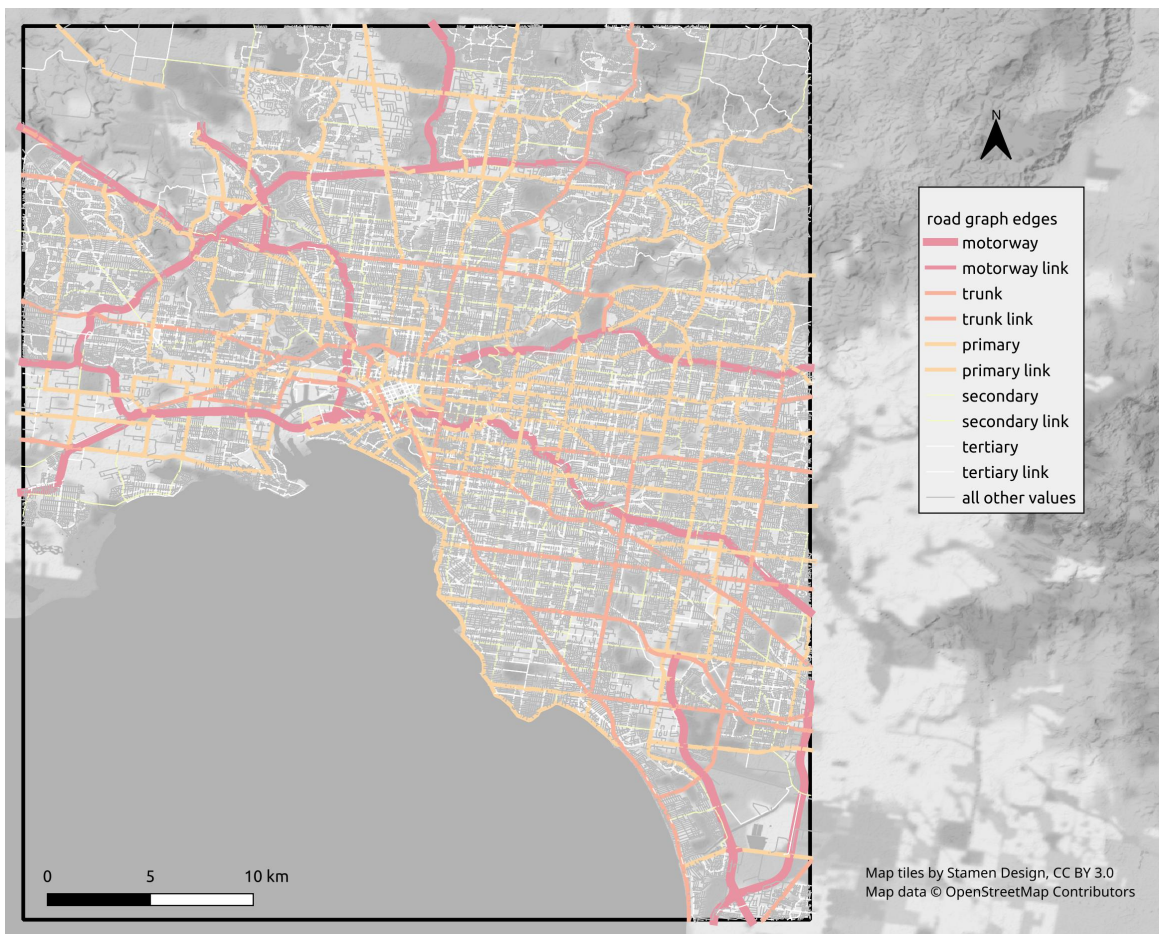


Fig. 48: Road graph Melbourne, OSM color scheme (2021).

2) Static data Melbourne (2021) :

Attribute	mean	std	median	q01	q99	data points	sum
bounding box						144.757–145.193 / -38.106–37.611	
num_edges						230'654	
motorway						354	
motorway_link						891	
trunk						5383	
trunk_link						766	
primary						13917	
primary_link						1574	
secondary						10342	
secondary_link						394	
tertiary						30552	
tertiary_link						1007	
unclassified						7301	
residential						158173	
num_nodes						103062	
num_edges_per_cell	1.1	0.4	1.0	1.0	3.0	891'475	
num_intersecting_cells	4.2	3.1	4.0	1.0	14.0	230'654	
node_degree	2.8	0.8	3.0	1.0	4.0	103'062	
length_meters	105.3	123.1	81.5	2.7	497.8	230'654	2.4e+07
motorway	1'102.6	774.5	976.5	26.1	4'090.9	354	3.9e+05
motorway_link	261.5	319.2	102.2	10.1	1'525.0	891	2.3e+05
trunk	105.4	139.8	68.1	3.9	657.1	5'383	5.7e+05
trunk_link	36.2	39.8	22.9	7.8	182.2	766	2.8e+04

primary	99.4	115.9	69.4	3.0	565.5	13'917	1.4e+06
primary_link	30.5	34.3	17.0	6.2	146.5	1'574	4.8e+04
secondary	86.5	104.6	64.2	2.3	457.6	10'342	9.0e+05
secondary_link	40.3	28.6	37.1	5.1	124.3	394	1.6e+04
tertiary	78.5	111.2	54.4	1.6	421.8	30'552	2.4e+06
tertiary_link	23.2	25.0	12.7	2.0	117.5	1'007	2.3e+04
unclassified	153.4	235.0	89.3	3.7	1'066.3	7'301	1.1e+06
residential	108.6	99.5	87.7	3.1	444.9	158'173	1.7e+07
speed_kph	51.1	6.8	48.7	40.0	80.0	230'654	
motorway	93.6	9.5	100.0	80.0	100.0	354	
motorway_link	77.2	11.0	78.9	50.0	100.0	891	
trunk	68.6	9.5	70.0	40.0	80.0	5'383	
trunk_link	65.2	5.0	65.4	50.0	80.0	766	
primary	62.5	8.3	60.0	40.0	80.0	13'917	
primary_link	57.1	3.3	57.0	40.0	70.0	1'574	
secondary	58.8	5.9	60.0	40.0	80.0	10'342	
secondary_link	59.4	2.5	59.6	50.0	70.0	394	
tertiary	51.4	5.8	51.4	40.0	70.0	30'552	
tertiary_link	54.4	3.0	54.6	40.0	60.0	1'007	
unclassified	49.1	4.8	49.0	20.0	60.0	7'301	
residential	48.7	2.4	48.7	40.0	50.0	158'173	
free_flow_kph	40.6	18.7	39.5	0.0	96.7	187'487	
motorway	91.4	10.0	96.0	65.0	100.7	348	
motorway_link	76.9	22.7	82.6	24.2	99.8	879	
trunk	56.4	13.4	56.9	26.8	80.8	5'380	
trunk_link	47.2	19.8	49.9	4.3	85.6	747	
primary	51.0	13.1	52.7	23.1	82.8	13'913	
primary_link	46.4	19.6	47.4	3.8	94.4	1'516	
secondary	49.5	13.3	51.1	20.8	94.6	10'301	
secondary_link	43.1	15.7	41.2	7.7	93.9	387	
tertiary	42.1	13.0	41.6	16.9	84.7	29'619	
tertiary_link	39.8	16.4	38.6	6.6	76.2	941	
unclassified	37.9	18.5	33.9	3.3	94.6	6'868	
residential	37.1	19.4	35.8	0.0	96.9	116'588	
free_flow_kph-speed_kph	-11.0	17.6	-11.2	-48.7	44.5	187'487	
motorway	-2.1	9.0	-2.1	-30.0	17.2	348	
motorway_link	-0.3	22.8	0.4	-54.7	38.8	879	
trunk	-12.3	12.2	-9.2	-45.6	12.7	5'380	
trunk_link	-18.0	20.0	-15.4	-61.1	19.7	747	
primary	-11.5	12.5	-8.5	-44.0	19.5	13'913	
primary_link	-10.7	19.8	-9.1	-53.2	36.5	1'516	
secondary	-9.3	13.1	-7.8	-38.6	36.9	10'301	
secondary_link	-16.4	16.0	-18.7	-51.9	34.3	387	
tertiary	-9.3	12.7	-9.5	-35.4	32.8	29'619	
tertiary_link	-14.6	16.4	-15.8	-50.0	21.6	941	
unclassified	-11.2	18.8	-15.1	-47.1	44.6	6'868	
residential	-11.5	19.5	-12.8	-48.7	47.8	116'588	

TABLE XVII: Key figures Melbourne for the generated data from 20 randomly sampled days. **num_edges** number of edges in the street network graph; **num_nodes** number of nodes in the street network graph; **num_edges_per_cell** number of edges a cell (row,col,heading) has in its intersecting cells; **num_intersecting_cells** number of cells (row,col,heading) in an edge's intersecting cells; **node_degree** number of (unique) neighbor nodes per node; **length_meters** free flow speed derived from data; **speed_kph** signalled speed; **free_flow_kph** free flow speed derived from data; **free_flow_kph-speed_kph** difference

3) Segment density map Melbourne (2021):

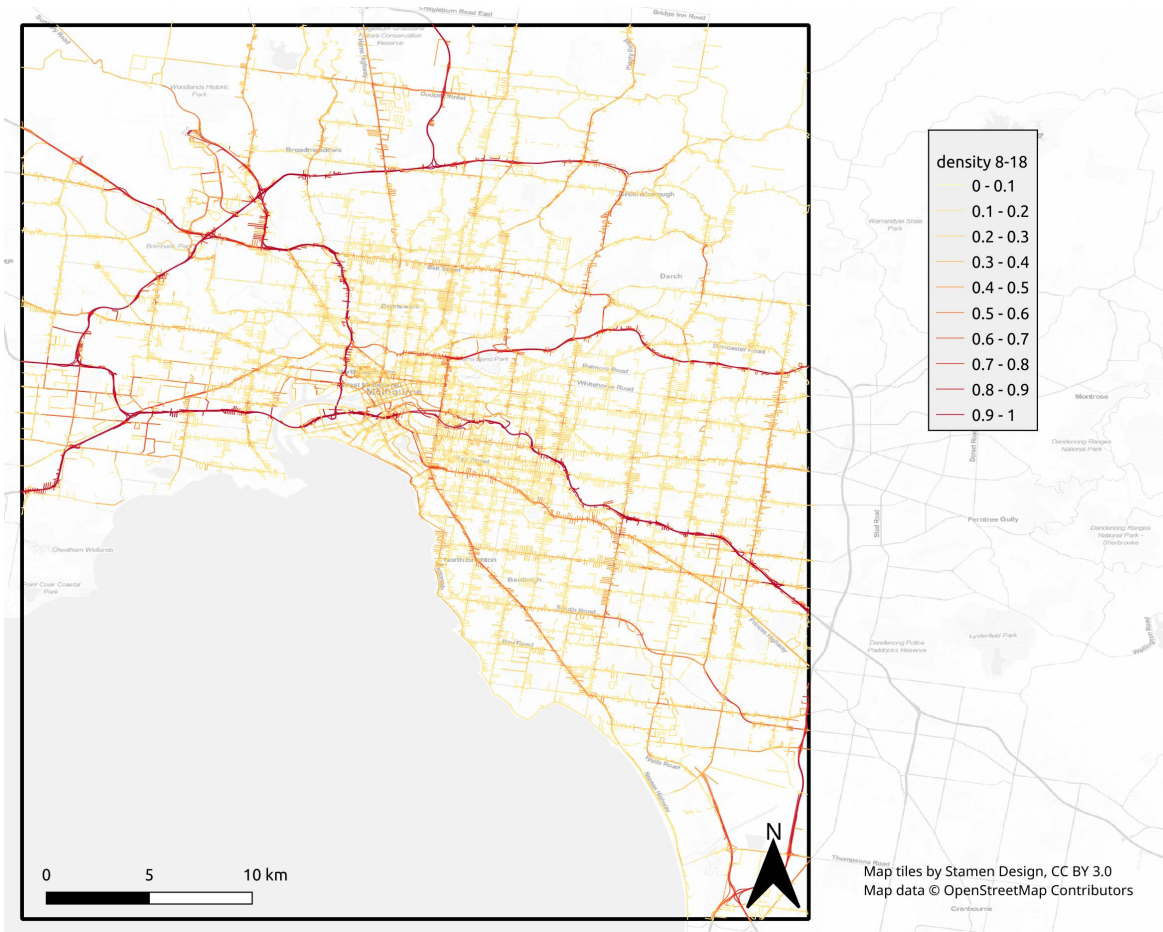


Fig. 49: Segment-wise density 8am–6pm Melbourne from 20 randomly sampled days.

4) Daily density profile Melbourne (2021) :

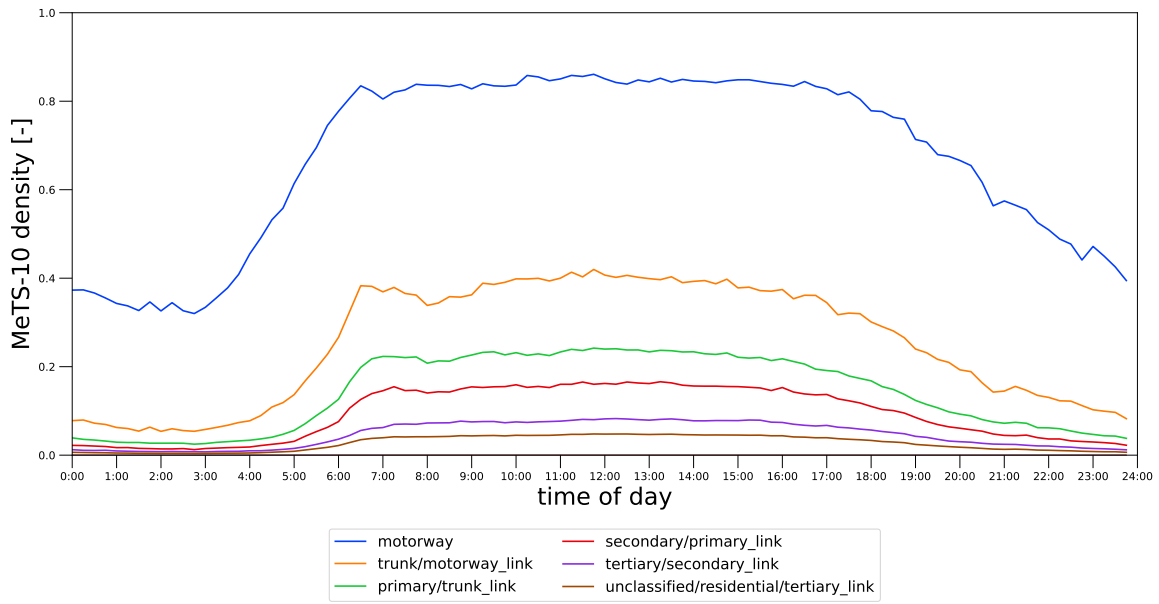


Fig. 50: Daily density profile for different road types for Melbourne . Data from 20 randomly sampled days.

5) Daily speed profile Melbourne (2021) :

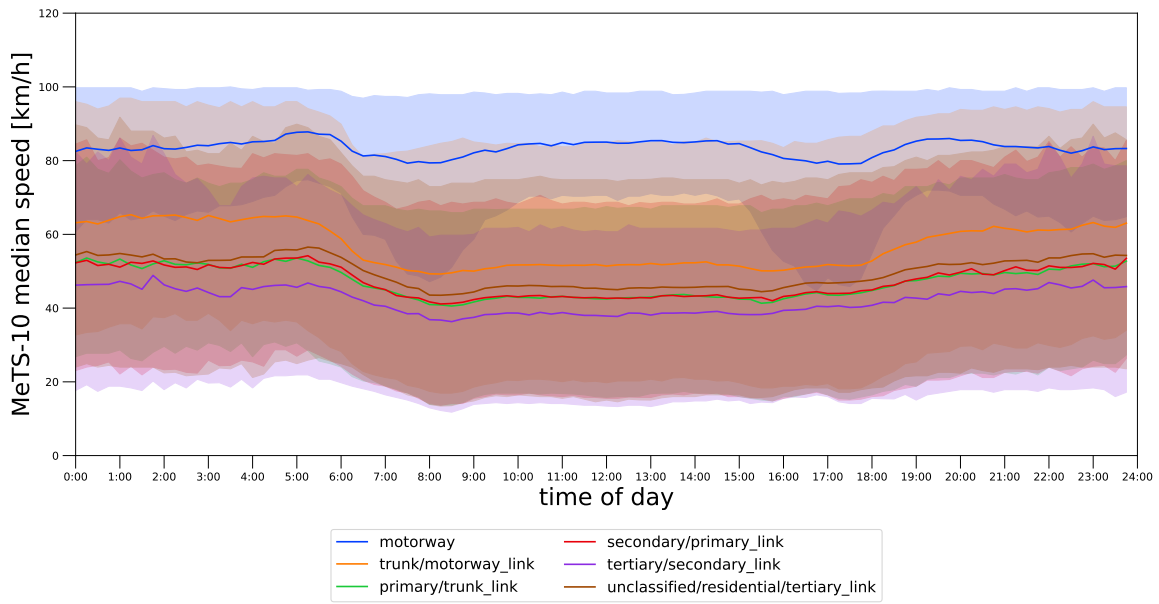


Fig. 51: Daily median 15 min speeds of all intersecting cells profile for different road types for Melbourne . The error hull is the 80% data interval [10.0–90.0 percentiles] of daily means from 20 randomly sampled days.

H. Key Figures Moscow (2021)

1) Road graph map Moscow (2021):

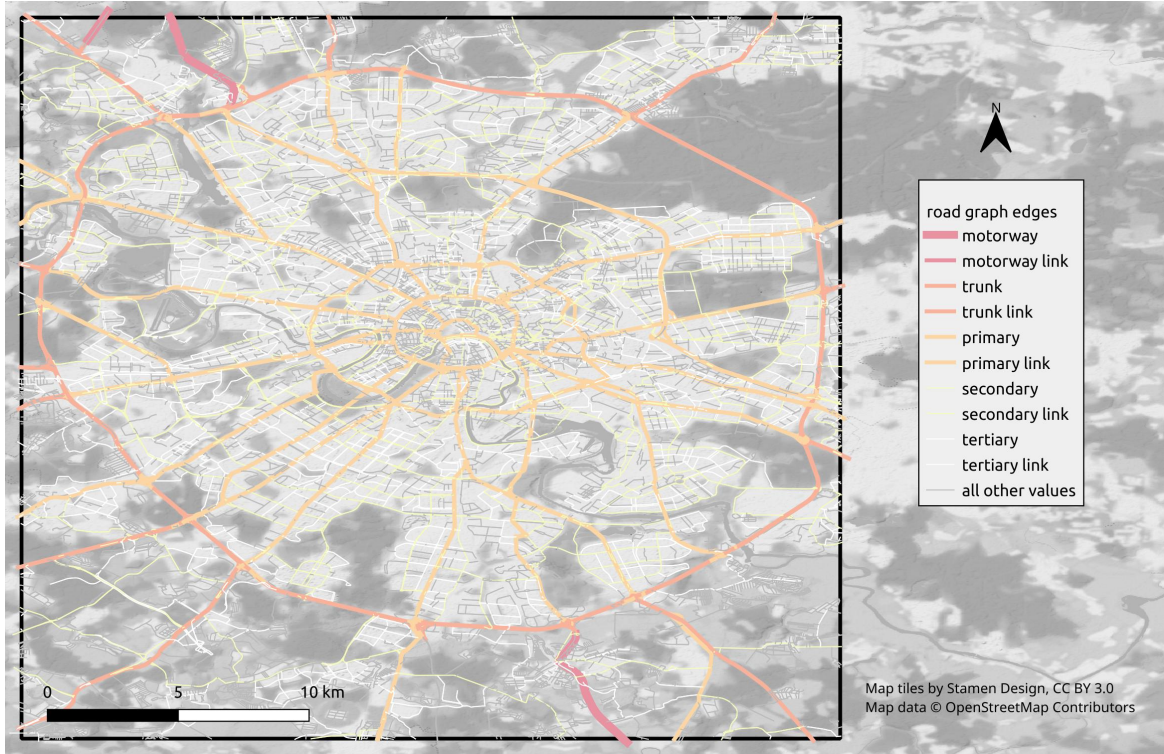


Fig. 52: Road graph Moscow, OSM color scheme (2021).

2) Static data Moscow (2021) :

Attribute	mean	std	median	q01	q99	data points	sum
bounding box						37.358–37.853 / 55.506–55.942	
num_edges						47'877	
motorway						14	
trunk						653	
trunk_link						150	
primary						2766	
primary_link						575	
secondary						9406	
secondary_link						1461	
tertiary						11198	
tertiary_link						806	
unclassified						6407	
residential						14441	
num_nodes						22627	
num_edges_per_cell	1.0	0.2	1.0	1.0	2.0	293'771	
num_intersecting_cells	6.3	6.2	4.0	1.0	30.0	47'877	
node_degree	2.9	0.8	3.0	1.0	4.0	22'627	
length_meters	227.8	280.2	140.5	7.6	1'272.5	47'877	1.1e+07
motorway	1'970.2	1'889.5	869.5	175.3	4'800.2	14	2.8e+04
trunk	561.1	840.2	293.3	18.5	3'519.5	653	3.7e+05
trunk_link	363.9	332.4	268.5	15.6	1'560.7	150	5.5e+04
primary	294.2	371.6	174.6	8.3	1'723.0	2'766	8.1e+05
primary_link	238.1	242.6	164.0	9.4	1'165.3	575	1.4e+05
secondary	209.8	255.6	115.8	6.2	1'204.2	9'406	2.0e+06
secondary_link	138.4	165.0	75.8	9.2	810.4	1'461	2.0e+05
tertiary	231.5	270.7	134.7	7.8	1'276.1	11'198	2.6e+06
tertiary_link	97.5	123.9	54.8	8.5	619.4	806	7.9e+04
unclassified	220.6	277.7	131.1	6.5	1'348.2	6'407	1.4e+06
residential	224.9	217.1	161.8	8.8	1'070.7	14'441	3.2e+06
speed_kph	48.6	11.3	49.0	20.0	94.7	47'877	

motorway	71.1	16.4	73.2	40.0	105.2	14
trunk	94.1	12.0	100.0	50.0	110.0	653
trunk_link	54.1	5.6	54.5	30.0	60.0	150
primary	73.8	6.5	74.1	50.0	90.0	2'766
primary_link	45.2	4.7	45.1	27.4	60.0	575
secondary	53.5	5.5	53.5	30.0	60.0	9'406
secondary_link	50.6	3.8	50.4	40.0	60.0	1'461
tertiary	49.6	5.3	49.0	30.0	60.0	11'198
tertiary_link	52.6	3.2	52.4	40.0	60.0	806
unclassified	36.9	5.3	36.6	20.0	60.0	6'407
residential	42.5	4.5	42.6	20.0	60.0	14'441
free_flow_kph	35.4	15.8	32.5	8.9	79.8	47'501
motorway	93.0	9.7	92.0	76.9	105.9	14
trunk	73.8	10.7	76.5	43.5	92.4	653
trunk_link	63.0	11.7	62.4	37.2	85.0	150
primary	51.6	12.5	51.8	23.4	77.2	2'766
primary_link	53.4	13.3	53.9	22.1	82.1	575
secondary	41.5	12.5	40.5	19.6	72.9	9'406
secondary_link	47.1	15.3	47.4	14.6	81.8	1'461
tertiary	35.9	11.9	34.0	16.5	73.2	11'198
tertiary_link	44.3	18.0	42.8	11.8	83.3	806
unclassified	29.4	14.1	26.4	7.1	73.8	6'363
residential	25.7	12.3	23.3	6.6	68.2	14'109
free_flow_kph-speed_kph	-13.3	14.2	-15.6	-40.4	28.8	47'501
motorway	21.9	22.0	18.6	-12.9	65.9	14
trunk	-20.3	12.1	-20.9	-47.6	11.5	653
trunk_link	8.9	12.9	7.7	-19.7	37.0	150
primary	-22.2	12.1	-21.0	-50.8	1.8	2'766
primary_link	8.2	14.0	8.7	-25.1	37.2	575
secondary	-12.0	13.2	-13.0	-36.3	20.9	9'406
secondary_link	-3.5	15.5	-3.3	-35.8	33.8	1'461
tertiary	-13.7	12.6	-15.4	-36.7	24.4	11'198
tertiary_link	-8.4	18.0	-9.6	-40.6	31.0	806
unclassified	-7.5	14.5	-10.2	-35.1	36.8	6'363
residential	-16.8	13.0	-19.5	-38.3	26.3	14'109

TABLE XVIII: Key figures Moscow for the generated data from 20 randomly sampled days. **num_edges** number of edges in the street network graph; **num_nodes** number of nodes in the street network graph; **num_edges_per_cell** number of edges a cell (row,col,heading) has in its intersecting cells; **num_intersecting_cells** number of cells (row,col,heading) in an edge's intersecting cells; **node_degree** number of (unique) neighbor nodes per node; **length_meters** free flow speed derived from data; **speed_kph** signalled speed; **free_flow_kph** free flow speed derived from data; **free_flow_kph-speed_kph** difference

3) *Segment density map Moscow (2021):*



Fig. 53: Segment-wise density 8am–6pm Moscow from 20 randomly sampled days.

4) Daily density profile Moscow (2021) :

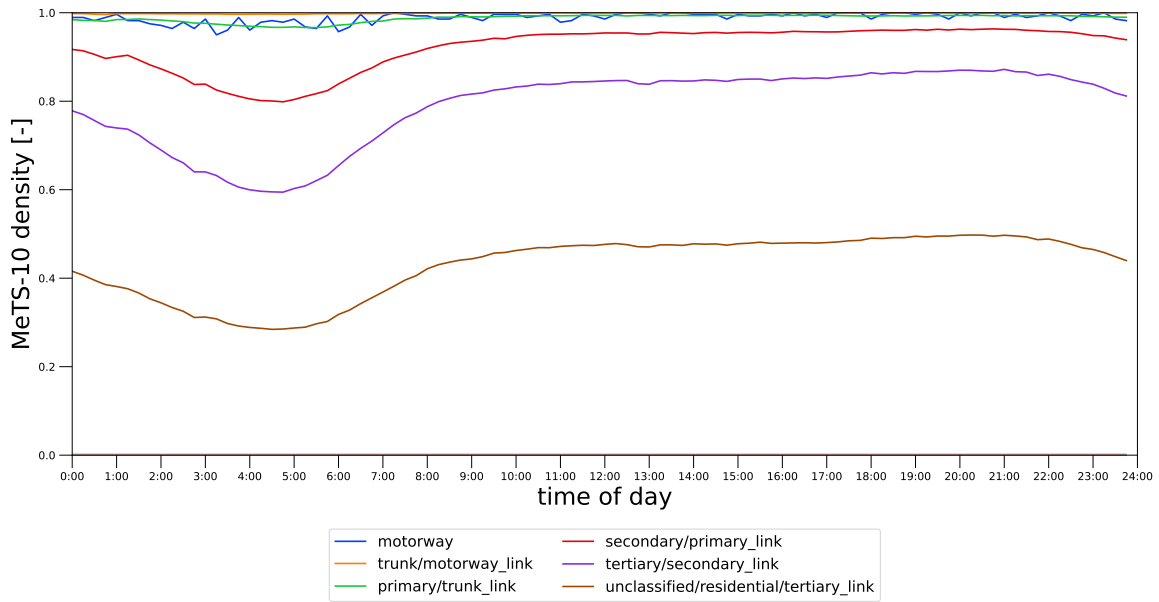


Fig. 54: Daily density profile for different road types for Moscow . Data from 20 randomly sampled days.

5) Daily speed profile Moscow (2021) :

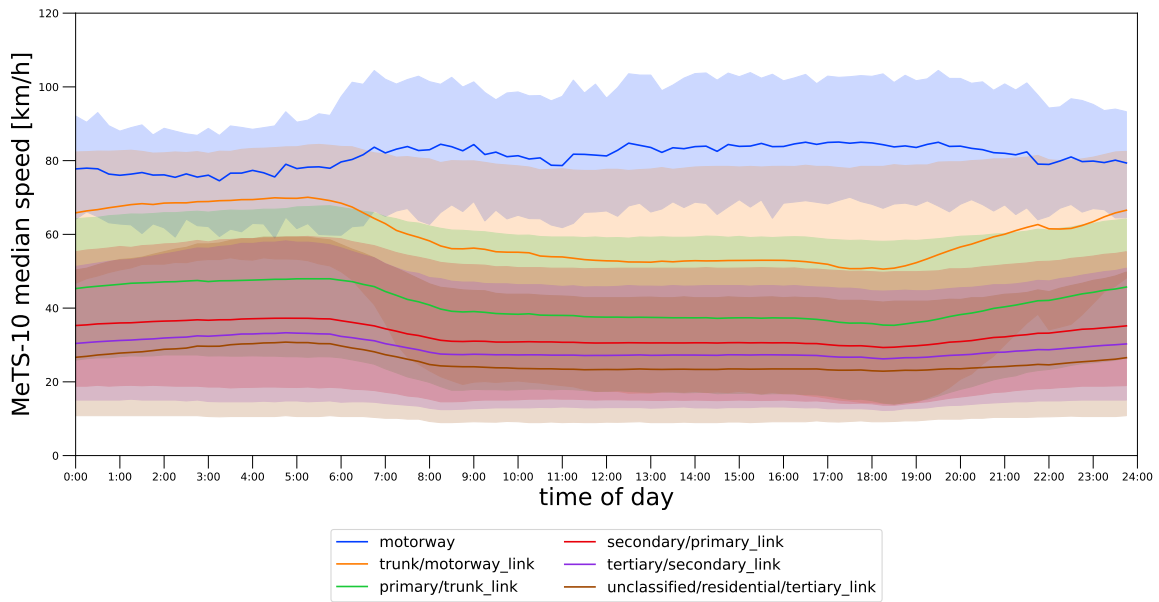


Fig. 55: Daily median 15 min speeds of all intersecting cells profile for different road types for Moscow . The error hull is the 80% data interval [10.0–90.0 percentiles] of daily means from 20 randomly sampled days.

I. Key Figures London (2022)

1) Road graph map London (2022):

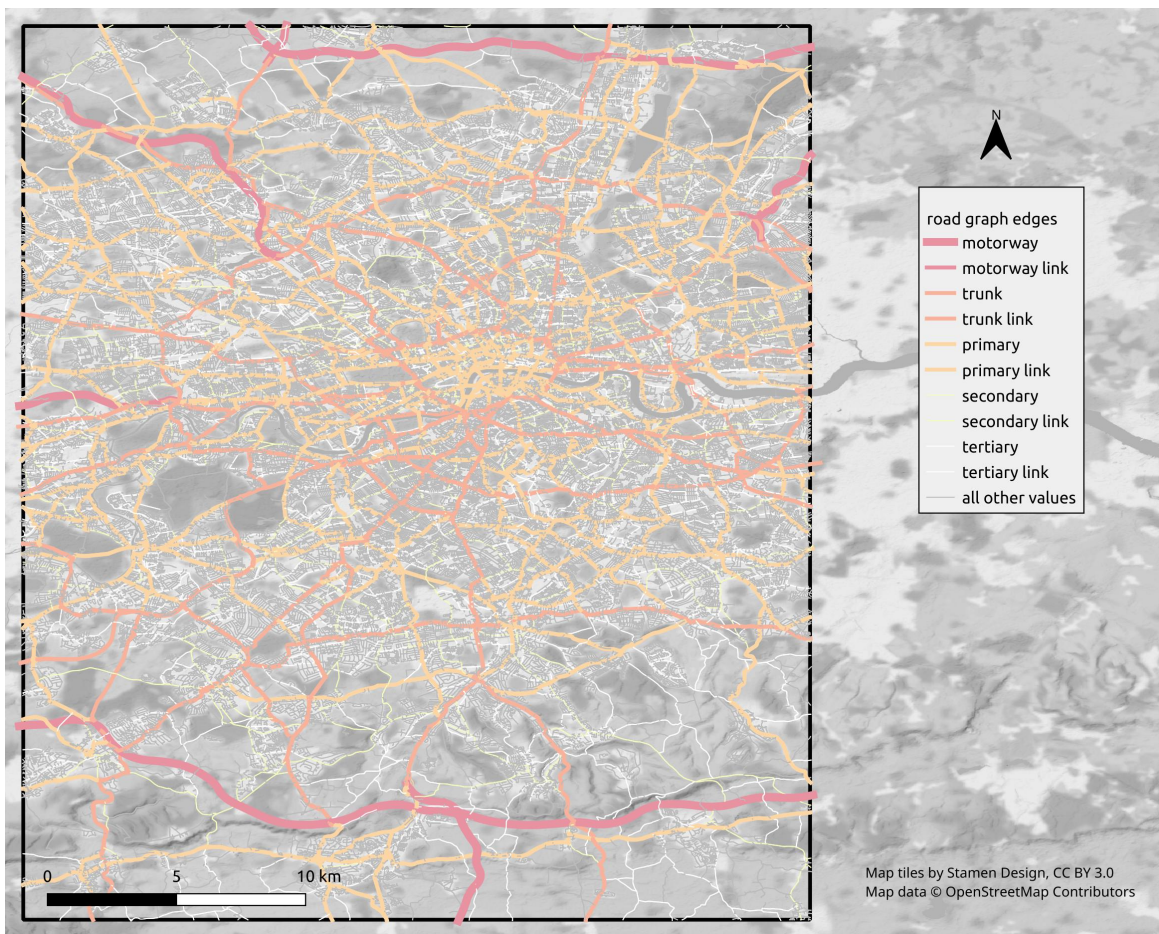


Fig. 56: Road graph London, OSM color scheme (2022).

2) Static data London (2022) :

Attribute	mean	std	median	q01	q99	data points	sum
bounding box						-0.369-0.067 / 51.205-51.7	
num_edges						271'075	
motorway						79	
motorway_link						82	
trunk						8629	
trunk_link						686	
primary						25189	
primary_link						411	
secondary						11275	
secondary_link						110	
tertiary						23878	
tertiary_link						124	
unclassified						16513	
residential						184099	
num_nodes						116304	
num_edges_per_cell	1.1	0.3	1.0	1.0	3.0	912'914	
num_intersecting_cells	3.6	3.0	3.0	1.0	13.0	271'075	
node_degree	2.5	0.9	3.0	1.0	4.0	116'304	
length_meters	98.6	127.4	69.4	5.2	496.3	271'075	2.7e+07
motorway	2'516.4	2'181.2	1'699.3	332.5	10'264.8	79	2.0e+05
motorway_link	520.9	373.5	463.0	28.6	1'615.7	82	4.3e+04
trunk	114.3	205.3	57.4	3.7	1'001.6	8'629	9.9e+05
trunk_link	124.8	135.0	56.8	6.6	521.9	686	8.6e+04

primary	83.2	116.4	56.4	3.6	505.1	25'189	2.1e+06
primary_link	40.8	48.2	28.1	6.2	242.2	411	1.7e+04
secondary	96.8	131.4	66.5	3.9	597.7	11'275	1.1e+06
secondary_link	28.3	21.2	24.9	7.2	119.8	110	3.1e+03
tertiary	112.9	166.6	73.2	5.0	835.6	23'878	2.7e+06
tertiary_link	40.4	34.5	29.9	8.1	189.0	124	5.0e+03
unclassified	117.2	188.0	68.2	5.1	943.9	16'513	1.9e+06
residential	95.5	85.8	71.6	6.1	402.9	184'099	1.8e+07
speed_kph	36.8	7.9	32.2	32.2	64.4	271'075	
motorway	106.2	15.6	112.7	60.9	112.7	79	
motorway_link	104.4	16.6	112.7	48.3	112.7	82	
trunk	51.1	12.4	48.3	32.2	96.6	8'629	
trunk_link	57.0	14.3	48.3	32.2	112.7	686	
primary	42.0	9.6	48.3	32.2	64.4	25'189	
primary_link	44.2	8.1	48.3	32.2	64.4	411	
secondary	38.9	8.5	32.2	32.2	64.4	11'275	
secondary_link	39.4	8.5	40.0	32.2	64.4	110	
tertiary	38.5	8.4	32.2	32.2	64.4	23'878	
tertiary_link	46.1	11.9	47.0	32.2	96.6	124	
unclassified	35.4	6.9	32.2	24.1	64.4	16'513	
residential	35.1	5.5	32.2	32.2	48.3	184'099	
free_flow_kph	30.0	11.8	28.7	6.8	68.7	263'309	
motorway	104.3	14.4	110.4	60.6	118.3	79	
motorway_link	92.3	20.2	99.0	36.6	117.6	82	
trunk	39.5	12.9	36.2	19.2	81.8	8'629	
trunk_link	53.5	20.7	57.9	13.6	85.9	682	
primary	35.3	9.6	32.9	17.9	64.9	25'189	
primary_link	31.6	14.3	28.7	8.9	76.6	411	
secondary	34.9	9.7	32.9	17.9	65.9	11'275	
secondary_link	27.4	9.4	26.8	4.7	50.3	110	
tertiary	35.0	10.2	32.9	17.9	67.3	23'872	
tertiary_link	34.7	14.0	30.2	18.0	76.7	124	
unclassified	28.0	13.0	26.4	6.1	72.0	16'213	
residential	27.8	11.1	26.8	5.6	63.1	176'643	
free_flow_kph-speed_kph	-6.9	11.5	-6.4	-33.7	27.5	263'309	
motorway	-1.9	12.5	-1.6	-33.7	35.9	79	
motorway_link	-12.1	17.4	-11.1	-68.8	13.2	82	
trunk	-11.6	10.6	-11.4	-45.7	10.9	8'629	
trunk_link	-3.5	18.8	-3.6	-45.6	32.6	682	
primary	-6.7	10.0	-5.5	-30.5	16.5	25'189	
primary_link	-12.5	14.2	-15.6	-36.0	28.4	411	
secondary	-4.0	9.5	-3.5	-27.6	20.4	11'275	
secondary_link	-12.1	10.5	-11.0	-35.3	10.6	110	
tertiary	-3.5	9.6	-3.5	-26.7	23.8	23'872	
tertiary_link	-11.4	16.8	-12.3	-69.8	28.5	124	
unclassified	-7.3	12.8	-8.2	-33.7	33.0	16'213	
residential	-7.2	11.7	-7.3	-33.7	28.5	176'643	

TABLE XIX: Key figures London for the generated data from 20 randomly sampled days. **num_edges** number of edges in the street network graph; **num_nodes** number of nodes in the street network graph; **num_edges_per_cell** number of edges a cell (row,col,heading) has in its intersecting cells; **num_intersecting_cells** number of cells (row,col,heading) in an edge's intersecting cells; **node_degree** number of (unique) neighbor nodes per node; **length_meters** free flow speed derived from data; **speed_kph** signalled speed; **free_flow_kph** free flow speed derived from data; **free_flow_kph-speed_kph** difference

3) Segment density map London (2022):

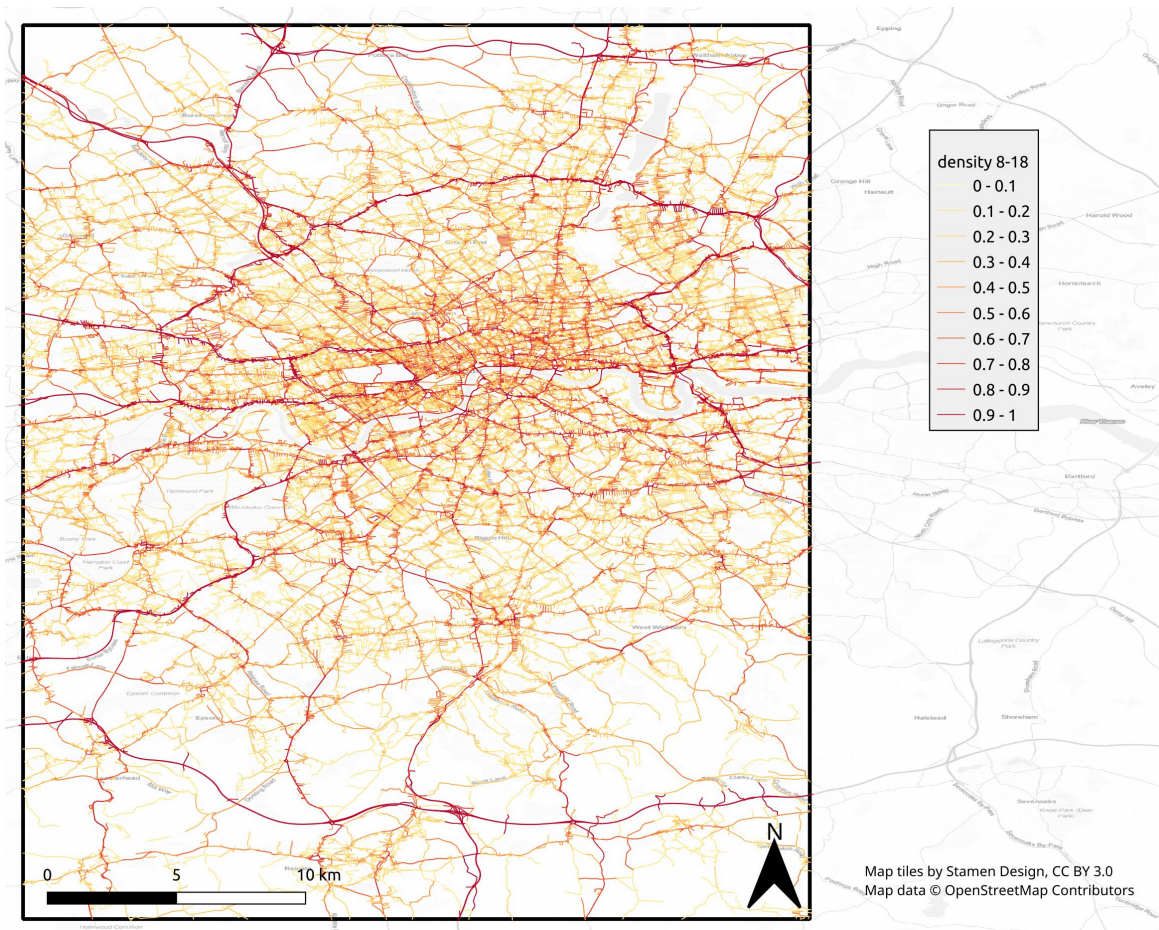


Fig. 57: Segment-wise density 8am–6pm London from 20 randomly sampled days.

4) Daily density profile London (2022) :

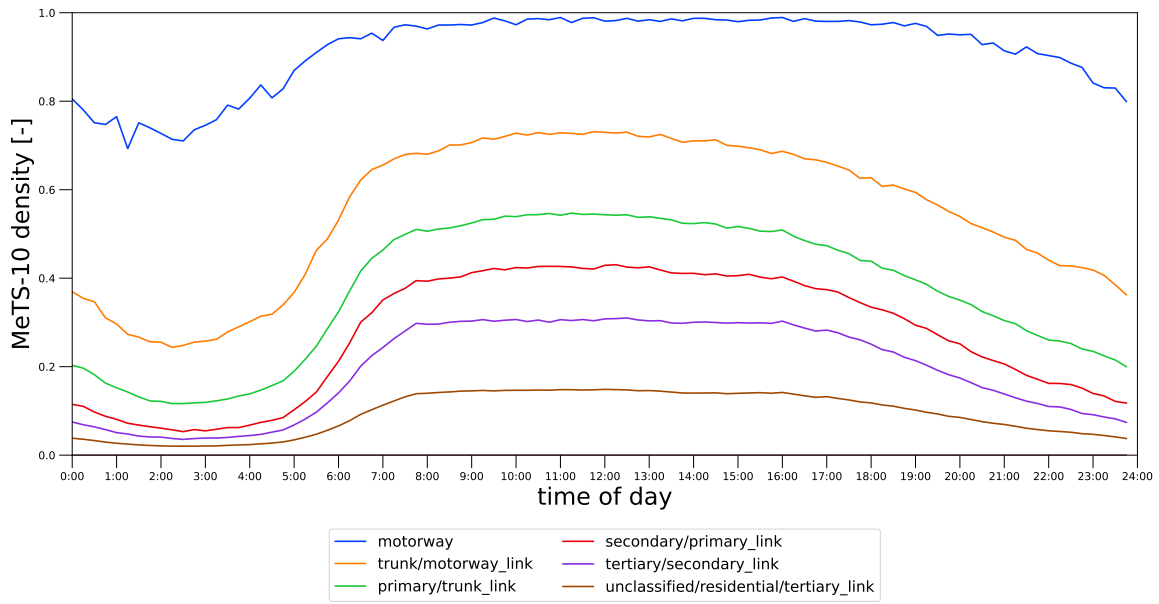


Fig. 58: Daily density profile for different road types for London . Data from 20 randomly sampled days.

5) Daily speed profile London (2022) :

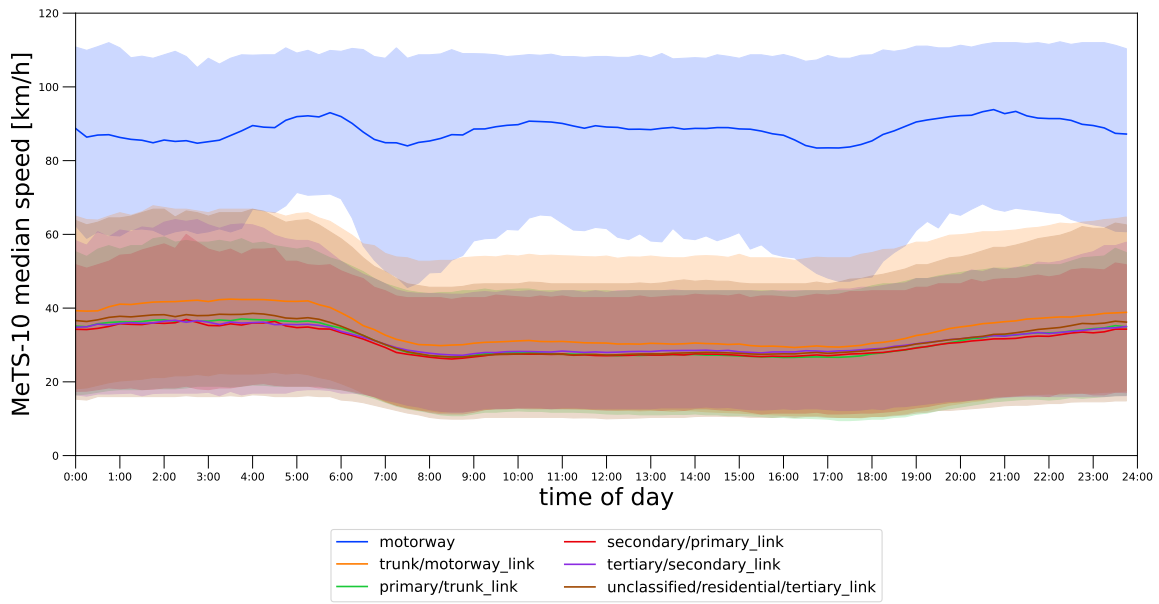


Fig. 59: Daily median 15 min speeds of all intersecting cells profile for different road types for London . The error hull is the 80% data interval [10.0–90.0 percentiles] of daily means from 20 randomly sampled days.

J. Key Figures Madrid (2022)

1) Road graph map Madrid (2022):

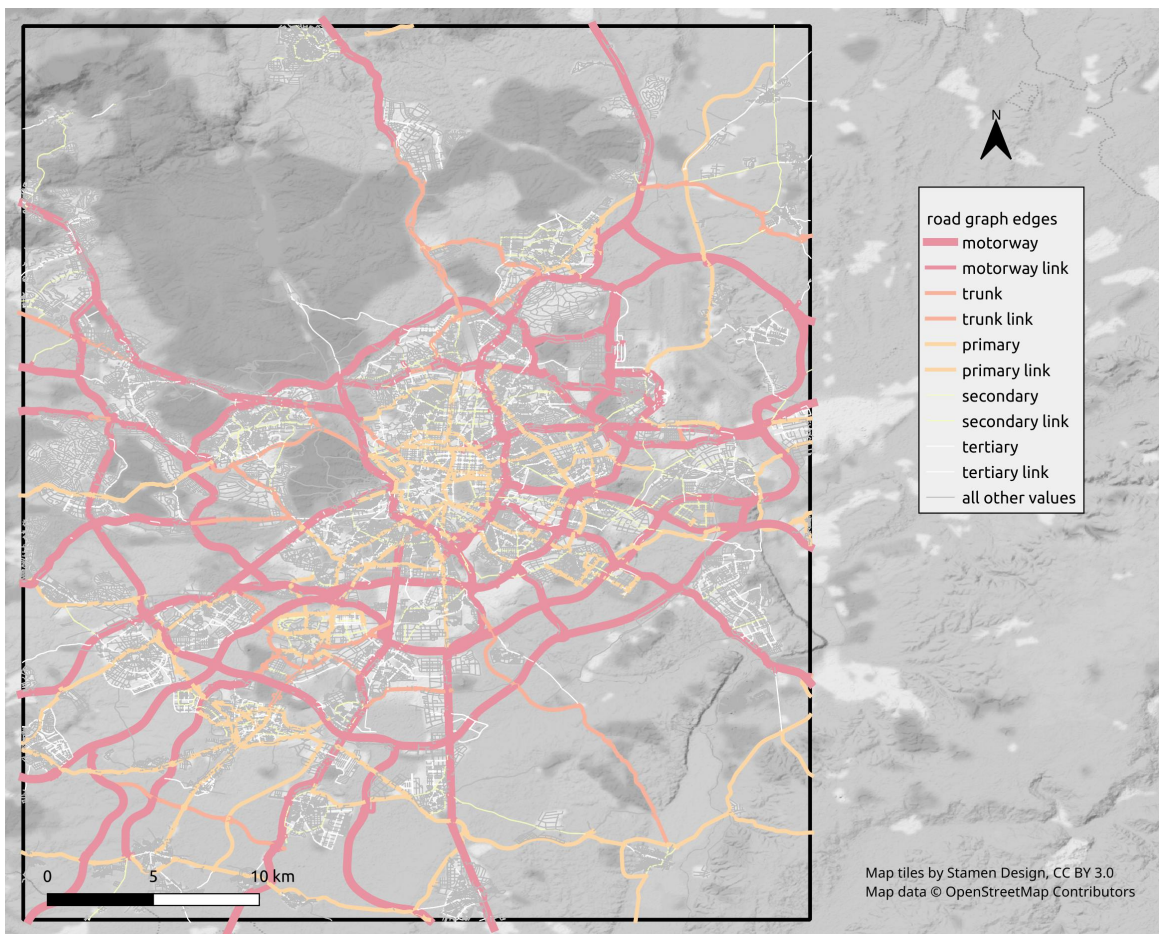


Fig. 60: Road graph Madrid, OSM color scheme (2022).

2) Static data Madrid (2022) :

Attribute	mean	std	median	q01	q99	data points	sum
bounding box						-3.927—3.491 / 40.177—40.672	
num_edges						143'402	
motorway						1277	
motorway_link						2647	
trunk						1017	
trunk_link						373	
primary						6265	
primary_link						475	
secondary						6855	
secondary_link						276	
tertiary						16147	
tertiary_link						310	
unclassified						5669	
residential						102091	
num_nodes						71757	
num_edges_per_cell	1.1	0.4	1.0	1.0	3.0	467'013	
num_intersecting_cells	3.5	3.7	3.0	1.0	16.0	143'402	
node_degree	3.0	0.7	3.0	1.0	4.0	71'757	
length_meters	110.2	193.2	66.0	4.7	776.8	143'402	1.6e+07
motorway	878.7	842.8	660.3	13.2	4'440.7	1'277	1.1e+06
motorway_link	343.5	287.4	286.5	15.6	1'344.9	2'647	9.1e+05
trunk	254.4	483.3	60.4	4.9	2'285.9	1'017	2.6e+05
trunk_link	227.4	235.6	175.3	12.4	923.6	373	8.5e+04

primary	130.1	335.0	44.6	3.3	1'346.9	6'265	8.1e+05
primary_link	132.5	135.1	85.7	8.1	654.7	475	6.3e+04
secondary	94.2	247.8	41.0	3.2	686.8	6'855	6.5e+05
secondary_link	73.9	94.8	38.2	6.0	420.4	276	2.0e+04
tertiary	88.6	147.2	45.6	3.2	602.5	16'147	1.4e+06
tertiary_link	77.3	112.8	35.7	6.5	581.5	310	2.4e+04
unclassified	169.9	331.4	76.3	5.6	1'687.0	5'669	9.6e+05
residential	92.7	92.4	68.0	5.2	452.5	102'091	9.5e+06
speed_kph	68.6	1'334.2	76.6	20.0	151.3	143'402	
motorway	98.1	15.5	100.0	50.0	120.0	1'277	
motorway_link	60.4	13.0	59.2	40.0	100.0	2'647	
trunk	63.8	19.1	71.2	30.0	100.0	1'017	
trunk_link	52.8	9.2	52.1	40.0	82.8	373	
primary	87.7	50.7	50.0	30.0	151.3	6'265	
primary_link	48.9	6.8	49.0	40.0	90.0	475	
secondary	56.5	120.6	61.3	30.0	70.0	6'855	
secondary_link	45.1	4.7	45.3	30.0	60.0	276	
tertiary	44.6	5.8	44.8	20.0	50.0	16'147	
tertiary_link	41.7	5.7	41.8	20.0	60.0	310	
unclassified	40.6	4.2	40.5	20.0	60.0	5'669	
residential	73.8	1'580.9	76.6	20.0	76.6	102'091	
free_flow_kph	34.8	17.9	30.6	9.9	101.2	141'365	
motorway	93.3	15.4	95.2	51.2	120.0	1'277	
motorway_link	86.7	18.0	90.4	32.1	120.0	2'645	
trunk	57.1	24.0	49.4	24.0	102.7	1'017	
trunk_link	76.8	18.3	81.4	28.7	105.7	373	
primary	42.2	15.9	38.6	17.9	95.2	6'261	
primary_link	61.4	24.2	61.6	10.7	101.0	474	
secondary	37.9	13.3	35.3	18.4	88.8	6'855	
secondary_link	49.6	20.1	46.6	9.1	87.9	272	
tertiary	36.2	13.6	33.9	16.9	91.9	16'144	
tertiary_link	47.3	22.0	41.9	11.7	101.6	307	
unclassified	43.9	25.0	34.8	8.9	107.0	5'448	
residential	30.8	13.5	28.7	8.9	89.9	100'292	
free_flow_kph-speed_kph	-33.7	1'343.9	-36.6	-108.0	46.4	141'365	
motorway	-4.8	14.1	-4.6	-46.5	26.0	1'277	
motorway_link	26.3	19.5	29.3	-26.3	60.8	2'645	
trunk	-6.7	20.4	-3.3	-44.4	40.5	1'017	
trunk_link	24.1	19.3	27.2	-30.5	60.7	373	
primary	-45.5	50.0	-18.0	-129.7	23.6	6'261	
primary_link	12.6	24.7	12.6	-41.7	53.0	474	
secondary	-18.6	120.7	-17.5	-41.9	28.3	6'855	
secondary_link	4.5	20.0	2.3	-36.8	42.4	272	
tertiary	-8.3	14.5	-10.9	-31.2	48.1	16'144	
tertiary_link	5.6	22.3	-0.6	-31.2	59.8	307	
unclassified	3.2	24.7	-5.7	-31.6	67.3	5'448	
residential	-43.0	1'595.0	-44.6	-67.0	22.7	100'292	

TABLE XX: Key figures Madrid for the generated data from 20 randomly sampled days. **num_edges** number of edges in the street network graph; **num_nodes** number of nodes in the street network graph; **num_edges_per_cell** number of edges a cell (row,col,heading) has in its intersecting cells; **num_intersecting_cells** number of cells (row,col,heading) in an edge's intersecting cells; **node_degree** number of (unique) neighbor nodes per node; **length_meters** free flow speed derived from data; **speed_kph** signalled speed; **free_flow_kph** free flow speed derived from data; **free_flow_kph-speed_kph** difference

3) Segment density map Madrid (2022):



Fig. 61: Segment-wise density 8am–6pm Madrid from 20 randomly sampled days.

4) Daily density profile Madrid (2022) :

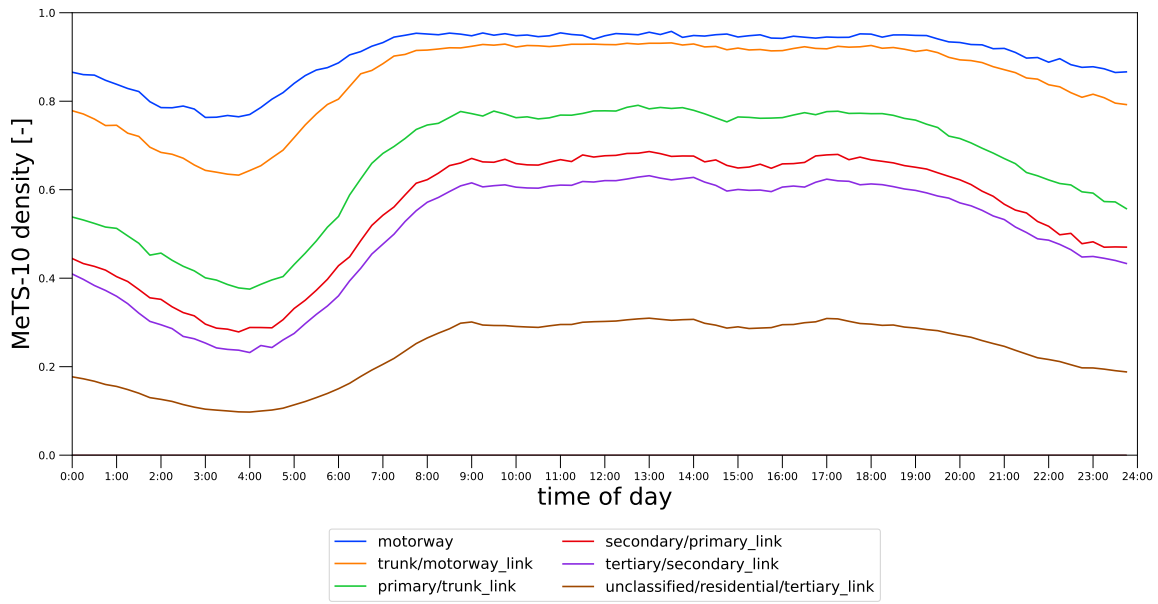


Fig. 62: Daily density profile for different road types for Madrid . Data from 20 randomly sampled days.

5) Daily speed profile Madrid (2022) :

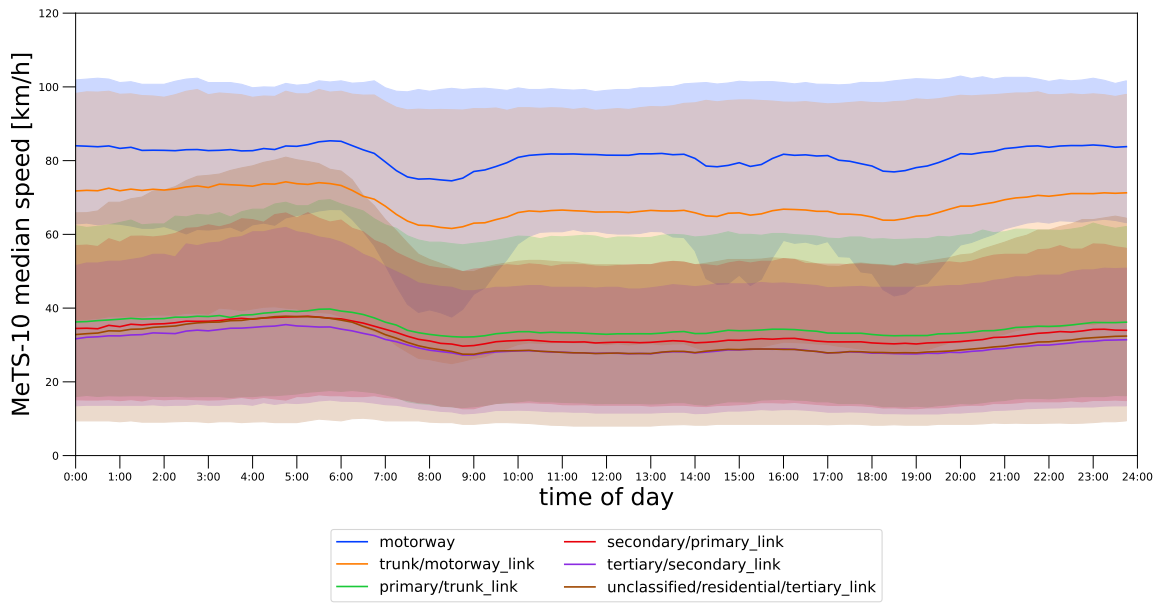


Fig. 63: Daily median 15 min speeds of all intersecting cells profile for different road types for Madrid . The error hull is the 80% data interval [10.0–90.0 percentiles] of daily means from 20 randomly sampled days.

K. Key Figures Melbourne (2022)

1) Road graph map Melbourne (2022):

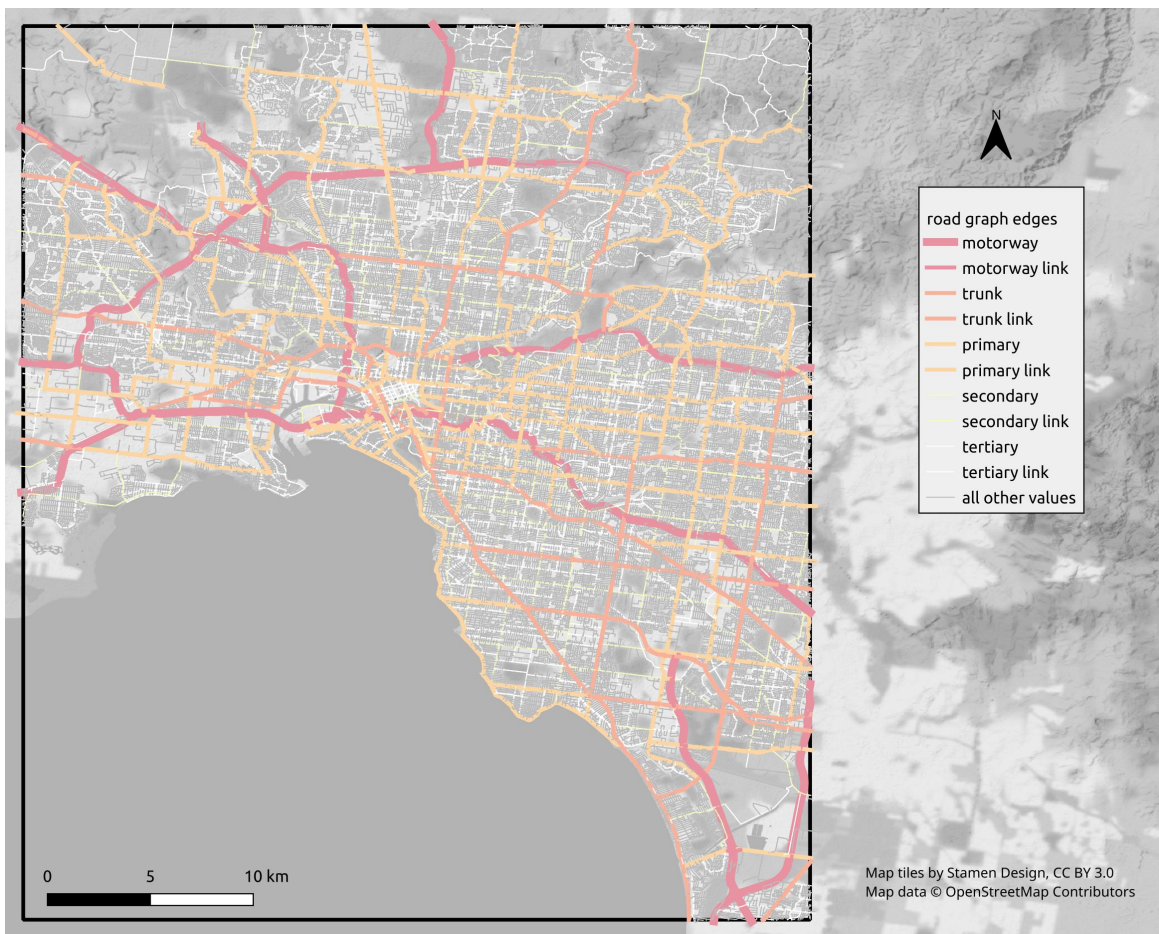


Fig. 64: Road graph Melbourne, OSM color scheme (2022).

2) Static data Melbourne (2022) :

Attribute	mean	std	median	q01	q99	data points	sum
bounding box						144.757–145.193 / -38.106–37.611	
num_edges						230'654	
motorway						354	
motorway_link						896	
trunk						5382	
trunk_link						762	
primary						13913	
primary_link						1574	
secondary						10342	
secondary_link						394	
tertiary						30557	
tertiary_link						1001	
unclassified						7381	
residential						158098	
num_nodes						103062	
num_edges_per_cell	1.1	0.4	1.0	1.0	3.0	891'475	
num_intersecting_cells	4.2	3.1	4.0	1.0	14.0	230'654	
node_degree	2.8	0.8	3.0	1.0	4.0	103'062	
length_meters	105.3	123.1	81.5	2.7	497.8	230'654	2.4e+07
motorway	1'102.6	774.5	976.5	26.1	4'090.9	354	3.9e+05
motorway_link	260.7	318.6	102.0	10.2	1'524.8	896	2.3e+05
trunk	105.4	139.8	68.1	3.9	657.1	5'382	5.7e+05
trunk_link	36.0	39.8	22.8	7.8	182.3	762	2.7e+04

primary	99.3	115.6	69.4	3.0	564.1	13'913	1.4e+06
primary_link	30.5	34.3	17.0	6.2	146.5	1'574	4.8e+04
secondary	86.5	104.6	64.2	2.3	457.6	10'342	9.0e+05
secondary_link	40.3	28.6	37.1	5.1	124.3	394	1.6e+04
tertiary	78.5	111.2	54.4	1.6	421.8	30'557	2.4e+06
tertiary_link	22.9	24.5	12.7	2.0	105.6	1'001	2.3e+04
unclassified	155.5	235.7	91.0	3.7	1'068.5	7'381	1.1e+06
residential	108.5	99.3	87.6	3.1	443.9	158'098	1.7e+07
speed_kph	51.1	6.8	48.7	40.0	80.0	230'654	
motorway	93.6	9.5	100.0	80.0	100.0	354	
motorway_link	77.2	11.0	78.9	50.0	100.0	896	
trunk	68.6	9.5	70.0	40.0	80.0	5'382	
trunk_link	65.2	5.0	65.4	50.0	80.0	762	
primary	62.5	8.3	60.0	40.0	80.0	13'913	
primary_link	57.1	3.3	57.0	40.0	70.0	1'574	
secondary	58.8	5.9	60.0	40.0	80.0	10'342	
secondary_link	59.4	2.5	59.6	50.0	70.0	394	
tertiary	51.4	5.8	51.4	40.0	70.0	30'557	
tertiary_link	54.4	3.0	54.6	40.0	60.0	1'001	
unclassified	49.1	4.8	49.0	20.0	60.0	7'381	
residential	48.7	2.4	48.7	40.0	50.0	158'098	
free_flow_kph	37.7	18.3	37.2	0.0	82.8	190'471	
motorway	87.6	15.0	94.0	16.7	99.8	354	
motorway_link	73.0	23.1	80.0	16.9	98.8	894	
trunk	54.9	13.1	56.0	25.3	77.9	5'381	
trunk_link	44.8	20.3	46.2	0.0	80.5	748	
primary	49.8	12.9	51.8	24.0	80.0	13'906	
primary_link	45.2	19.1	44.7	1.1	92.5	1'527	
secondary	47.6	12.6	49.9	19.6	85.6	10'326	
secondary_link	41.7	14.5	40.9	12.3	82.6	385	
tertiary	39.5	12.2	39.1	10.1	73.9	29'809	
tertiary_link	37.6	15.4	36.7	0.0	74.6	930	
unclassified	36.0	18.6	32.2	0.0	92.2	7'035	
residential	33.7	18.6	32.9	0.0	80.0	119'176	
free_flow_kph-speed_kph	-13.9	17.0	-13.8	-50.0	29.9	190'471	
motorway	-6.0	14.9	-2.1	-80.1	17.1	354	
motorway_link	-4.1	23.3	-1.2	-62.0	37.9	894	
trunk	-13.7	12.1	-10.4	-47.4	6.4	5'381	
trunk_link	-20.4	20.5	-18.8	-65.4	22.9	748	
primary	-12.6	12.3	-9.6	-43.9	18.6	13'906	
primary_link	-11.9	19.1	-11.5	-55.9	31.3	1'527	
secondary	-11.2	12.4	-9.2	-39.5	30.6	10'326	
secondary_link	-17.8	14.8	-18.7	-49.4	23.0	385	
tertiary	-11.9	11.7	-11.9	-42.5	19.2	29'809	
tertiary_link	-16.8	15.3	-17.5	-54.6	20.2	930	
unclassified	-13.1	18.9	-16.5	-49.0	42.7	7'035	
residential	-14.8	18.7	-15.5	-50.0	31.9	119'176	

TABLE XXI: Key figures Melbourne for the generated data from 20 randomly sampled days. **num_edges** number of edges in the street network graph; **num_nodes** number of nodes in the street network graph; **num_edges_per_cell** number of edges a cell (row,col,heading) has in its intersecting cells; **num_intersecting_cells** number of cells (row,col,heading) in an edge's intersecting cells; **node_degree** number of (unique) neighbor nodes per node; **length_meters** free flow speed derived from data; **speed_kph** signalled speed; **free_flow_kph** free flow speed derived from data; **free_flow_kph-speed_kph** difference

3) Segment density map Melbourne (2022):

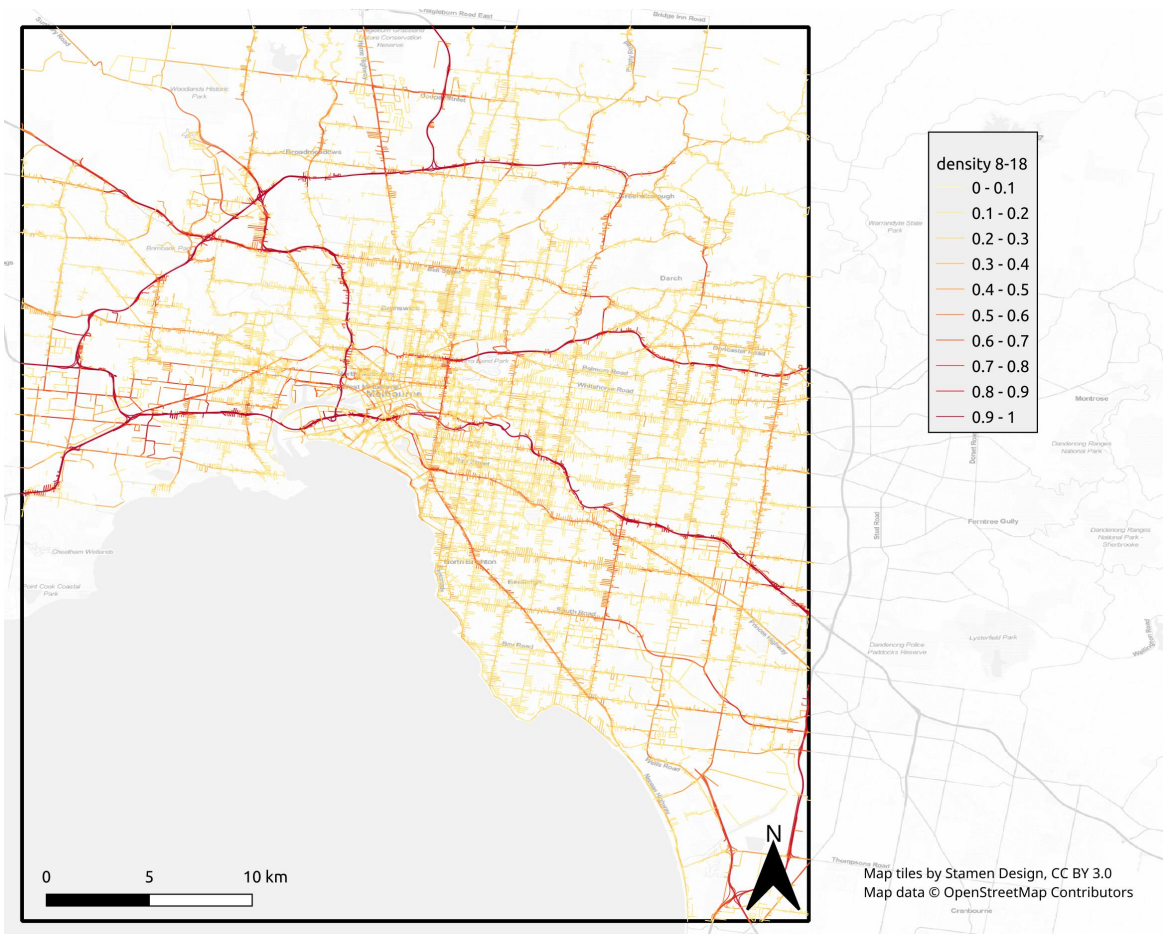


Fig. 65: Segment-wise density 8am–6pm Melbourne from 20 randomly sampled days.

4) Daily density profile Melbourne (2022) :

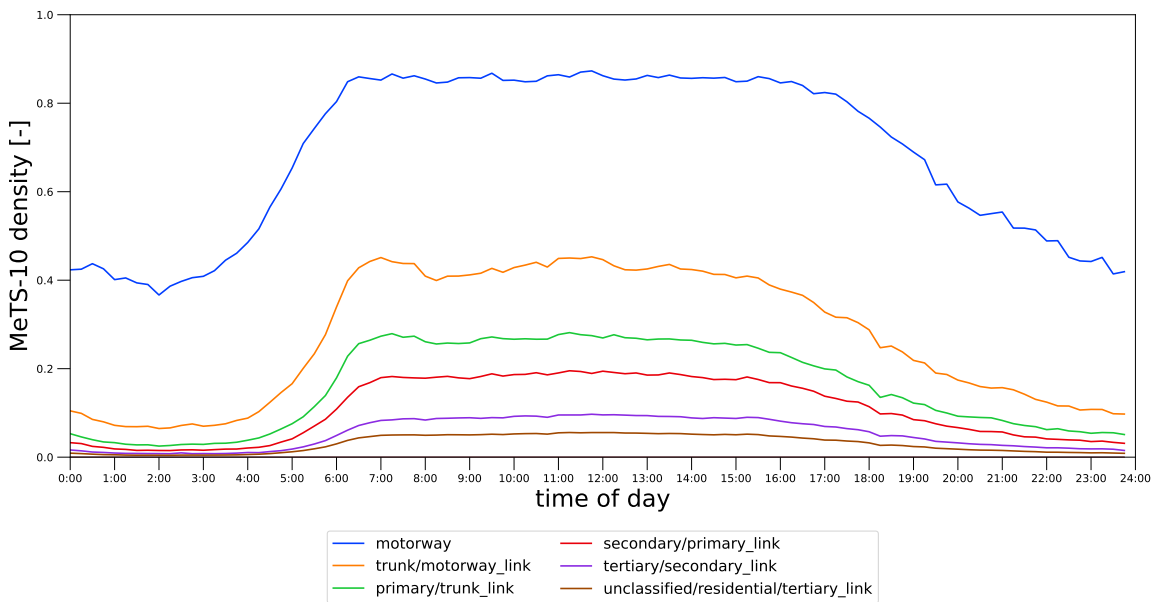


Fig. 66: Daily density profile for different road types for Melbourne . Data from 20 randomly sampled days.

5) Daily speed profile Melbourne (2022) :

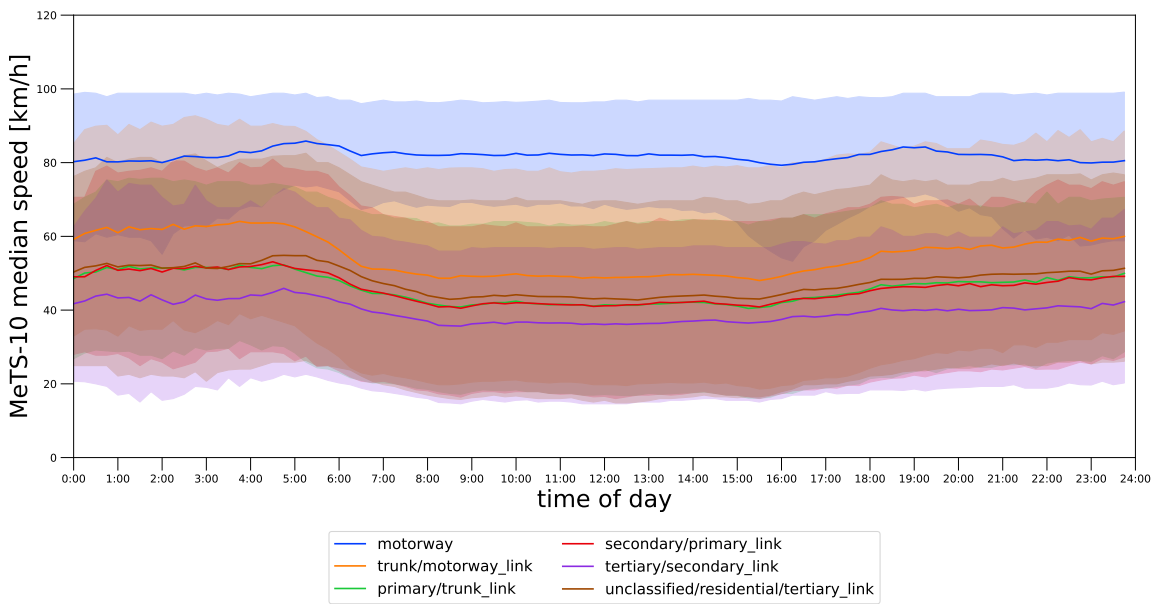


Fig. 67: Daily median 15 min speeds of all intersecting cells profile for different road types for Melbourne . The error hull is the 80% data interval [10.0–90.0 percentiles] of daily means from 20 randomly sampled days.

SUPPLEMENT G
KEY FIGURES UBER VALIDATION HISTORIC ROAD GRAPH

A. Key Figures London

1) Road graph map London:

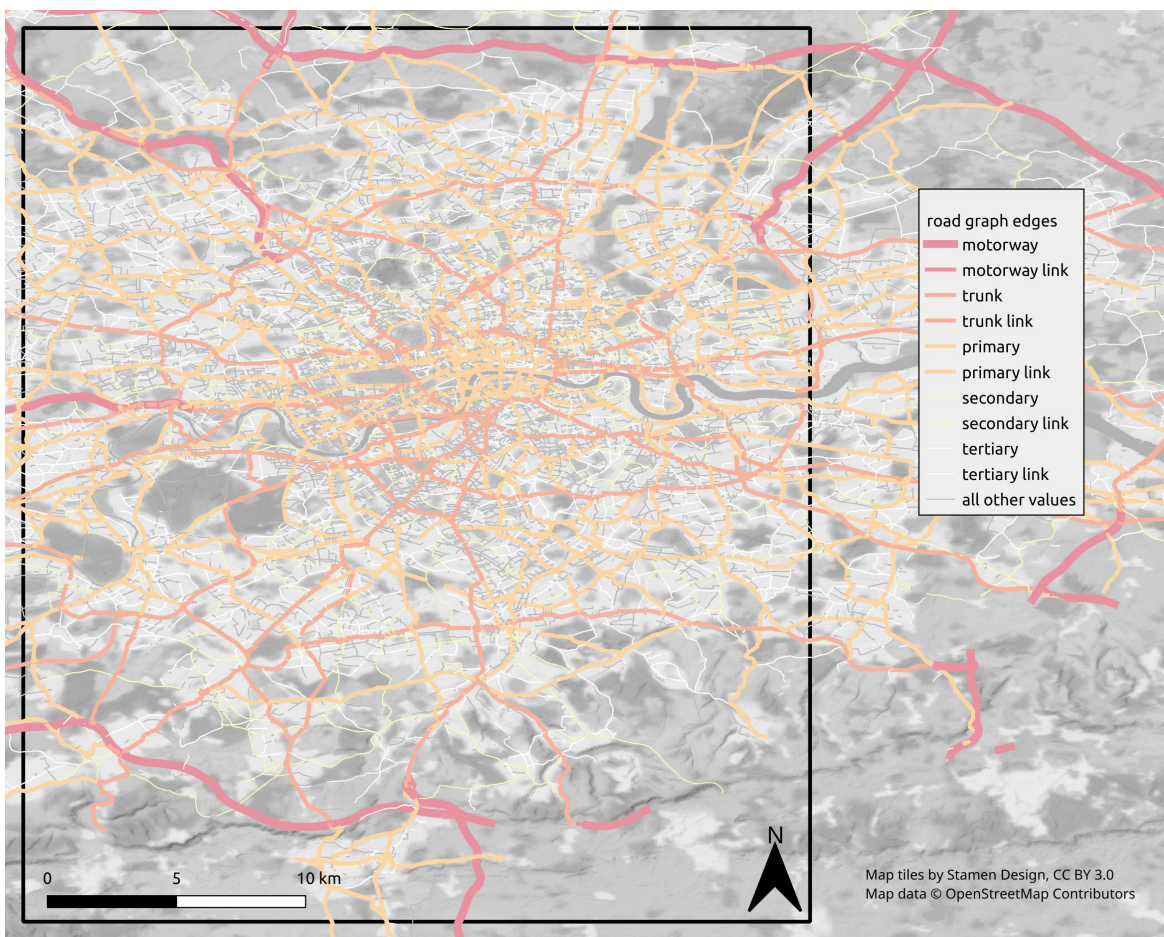


Fig. 68: Road graph London, OSM color scheme.

2) Static data London (full historic road graph):

Attribute	mean	std	median	q01	q99	data points	sum
bounding box (full historic road graph)						-0.369-0.067 / 51.205-51.7	
num_edges (full historic road graph)						234'308	
motorway						1520	
motorway_link						894	
trunk						17347	
trunk_link						1600	
primary						62005	
primary_link						907	
secondary						28003	
secondary_link						135	
tertiary						59977	
tertiary_link						257	
unclassified						12447	
residential						49110	
living_street						58	
service						44	
cycleway						1	
road						2	

construction								1
num_nodes (full historic road graph)								140412
num_edges_per_cell (full historic road graph)	1.1	0.4	1.0	1.0	3.0			355'950
num_intersecting_cells (full historic road graph)	1.7	2.2	1.0	0.0	9.0			234'308
node_degree (full historic road graph)	2.2	0.6	2.0	1.0	4.0			140'412
length_meters (full historic road graph)	108.2	172.9	65.6	4.7	748.0			234'308 2.5e+07
motorway	691.1	1'030.4	286.2	19.1	4'846.2		1'520	1.1e+06
motorway_link	293.3	308.7	182.6	14.3	1'437.8		894	2.6e+05
trunk	144.1	271.7	63.2	5.0	1'332.8		17'347	2.5e+06
trunk_link	178.8	198.2	97.1	8.9	834.9		1'600	2.9e+05
primary	91.0	129.0	55.0	4.3	620.1		62'005	5.6e+06
primary_link	84.0	104.8	48.8	5.2	572.8		907	7.6e+04
secondary	104.5	143.8	63.2	4.6	721.5		28'003	2.9e+06
secondary_link	54.7	60.9	33.6	6.3	294.2		135	7.4e+03
tertiary	104.9	129.4	68.5	4.8	628.2		59'977	6.3e+06
tertiary_link	77.3	91.4	47.6	4.1	426.4		257	2.0e+04
unclassified	104.1	152.4	60.9	4.4	776.5		12'447	1.3e+06
residential	101.6	94.8	76.6	5.0	469.3		49'110	5.0e+06
living_street	68.2	52.7	49.7	4.8	207.9		58	4.0e+03
service	66.6	83.8	30.0	4.7	337.7		44	2.9e+03
cycleway	31.0	nan	31.0	31.0	31.0		1	3.1e+01
road	45.8	1.8	45.8	44.6	47.1		2	9.2e+01
construction	14.8	nan	14.8	14.8	14.8		1	1.5e+01
speed_kph (full historic road graph)	47.3	16.1	48.3	32.2	112.7			234'308
motorway	110.6	8.3	112.7	64.4	112.7		1'520	
motorway_link	106.0	14.2	112.7	64.4	112.7		894	
trunk	62.1	21.5	48.3	32.2	112.7		17'347	
trunk_link	72.9	21.6	72.8	32.2	112.7		1'600	
primary	50.4	13.5	48.3	32.2	96.6		62'005	
primary_link	54.2	13.9	48.3	32.2	96.6		907	
secondary	48.5	14.2	48.3	32.2	96.6		28'003	
secondary_link	47.9	14.2	48.3	32.2	91.1		135	
tertiary	46.2	12.9	46.2	32.2	96.6		59'977	
tertiary_link	52.2	12.7	52.0	32.2	96.6		257	
unclassified	40.4	10.3	40.4	32.2	96.6		12'447	
residential	36.3	6.1	32.2	32.2	48.3		49'110	
living_street	33.1	3.6	32.2	32.2	48.3		58	
service	33.8	3.3	33.6	32.2	48.3		44	
cycleway	32.2	nan	32.2	32.2	32.2		1	
road	52.8	0.0	52.8	52.8	52.8		2	
construction	32.2	nan	32.2	32.2	32.2		1	
free_flow_kph (full historic road graph)	34.0	11.8	32.0	15.3	77.2			136'149
motorway	103.2	14.4	109.2	59.8	117.6		311	
motorway_link	89.0	21.2	94.8	41.5	117.5		125	
trunk	41.2	14.2	38.1	20.2	85.6		11'928	
trunk_link	54.7	19.7	57.9	18.7	102.0		779	
primary	35.8	10.0	32.9	18.4	67.4		33'921	
primary_link	44.0	19.0	38.6	17.9	80.4		511	
secondary	35.1	10.0	32.9	17.9	67.8		14'742	
secondary_link	32.2	14.7	28.7	17.8	78.1		88	
tertiary	34.6	10.2	32.5	17.9	67.8		28'749	
tertiary_link	48.9	20.0	46.6	19.8	78.6		134	
unclassified	28.9	11.7	27.1	11.8	75.8		7'505	
residential	28.8	8.4	27.8	12.7	54.6		37'281	
living_street	23.1	4.3	24.9	12.9	28.6		53	
service	28.0	18.2	19.8	13.4	76.8		19	
road	26.4	0.7	26.4	25.9	26.8		2	
construction	14.1	nan	14.1	14.1	14.1		1	
free_flow_kph-speed_kph (full historic road graph)	-7.6	10.1	-6.3	-31.4	18.6			136'149
motorway	-4.4	12.0	-2.6	-46.4	23.9		311	
motorway_link	-12.9	19.1	-7.8	-64.9	12.7		125	

trunk	-11.5	9.9	-11.3	-39.2	10.0	11'928
trunk_link	-6.4	18.2	-5.5	-48.2	32.5	779
primary	-9.2	10.1	-7.8	-30.9	13.6	33'921
primary_link	-5.8	16.7	-5.8	-37.6	29.8	511
secondary	-7.1	10.1	-5.4	-31.5	14.4	14'742
secondary_link	-10.2	14.5	-10.3	-30.4	29.5	88
tertiary	-6.0	10.2	-4.5	-29.5	20.9	28'749
tertiary_link	-0.3	19.6	-3.5	-31.1	36.8	134
unclassified	-7.9	11.5	-8.2	-32.8	31.5	7'505
residential	-6.3	8.8	-5.8	-29.7	17.5	37'281
living_street	-10.1	5.2	-8.0	-21.9	-3.6	53
service	-4.5	18.1	-12.4	-19.6	44.6	19
road	-26.4	0.7	-26.4	-26.9	-26.0	2
construction	-18.1	nan	-18.1	-18.1	-18.1	1

TABLE XXII: Key figures London for the generated data from 20 randomly sampled days (full historic road graph). **num_edges** number of edges in the street network graph; **num_nodes** number of nodes in the street network graph; **num_edges_per_cell** number of edges a cell (row,col,heading) has in its intersecting cells; **num_intersecting_cells** number of cells (row,col,heading) in an edge's intersecting cells; **node_degree** number of (unique) neighbor nodes per node; **length_meters** free flow speed derived from data; **speed_kph** signalled speed; **free_flow_kph** free flow speed derived from data; **free_flow_kph-speed_kph** difference

3) *Static data London (MeTS-10 extent (bounding box)):*

Attribute	mean	std	median	q01	q99	data points	sum
bounding box (MeTS-10 extent (bounding box))						-0.369-0.067 / 51.205-51.7	
num_edges (MeTS-10 extent (bounding box))						136'138	
motorway						311	
motorway_link						125	
trunk						11928	
trunk_link						779	
primary						33917	
primary_link						511	
secondary						14738	
secondary_link						88	
tertiary						28749	
tertiary_link						134	
unclassified						7506	
residential						37277	
living_street						53	
service						19	
road						2	
construction						1	
num_nodes (MeTS-10 extent (bounding box))						77427	
num_edges_per_cell (MeTS-10 extent (bounding box))	1.1	0.4	1.0	1.0	3.0	355'931	
num_intersecting_cells (MeTS-10 extent (bounding box))	2.9	2.2	2.0	1.0	10.0	136'138	
node_degree (MeTS-10 extent (bounding box))	2.2	0.6	2.0	1.0	4.0	77'427	
length_meters (MeTS-10 extent (bounding box))	92.4	124.6	62.4	4.6	521.7	136'138	1.3e+07
motorway	829.7	1'142.2	358.1	39.0	5'045.8	311	2.6e+05
motorway_link	429.7	421.9	343.9	30.6	1'768.6	125	5.4e+04
trunk	102.9	162.1	57.2	4.8	764.9	11'928	1.2e+06
trunk_link	112.9	132.8	57.8	6.9	628.9	779	8.8e+04
primary	74.2	88.6	50.7	4.2	435.2	33'917	2.5e+06
primary_link	71.0	86.0	42.9	7.1	408.4	511	3.6e+04
secondary	86.7	104.9	58.8	4.5	473.7	14'738	1.3e+06
secondary_link	44.3	49.9	29.6	5.9	244.1	88	3.9e+03
tertiary	95.4	105.3	66.8	5.1	515.2	28'749	2.7e+06
tertiary_link	75.5	89.4	46.0	4.6	443.7	134	1.0e+04
unclassified	85.6	110.3	56.2	4.2	540.6	7'506	6.4e+05

residential	99.7	92.2	75.2	4.9	461.4	37°277	3.7e+06
living_street	69.9	54.1	51.9	4.8	209.1	53	3.7e+03
service	46.9	62.2	19.6	5.1	210.4	19	8.9e+02
road	45.8	1.8	45.8	44.6	47.1	2	9.2e+01
construction	14.8	nan	14.8	14.8	14.8	1	1.5e+01
speed_kph (MeTS-10 extent (bounding box))	41.6	10.9	40.4	32.2	80.5	136°138	
motorway	107.6	13.2	112.7	64.4	112.7	311	
motorway_link	101.9	18.0	112.7	48.3	112.7	125	
trunk	52.7	12.4	48.3	32.2	96.6	11°928	
trunk_link	61.1	14.9	64.4	32.2	112.7	779	
primary	45.0	9.2	48.3	32.2	64.4	33°917	
primary_link	49.8	11.4	48.3	32.2	80.5	511	
secondary	42.1	9.8	48.3	32.2	64.4	14°738	
secondary_link	42.4	9.5	48.1	32.2	66.5	88	
tertiary	40.6	9.2	46.2	32.2	64.4	28°749	
tertiary_link	49.1	11.5	48.3	32.2	80.5	134	
unclassified	36.8	7.3	32.2	24.1	48.3	7°506	
residential	35.2	5.3	32.2	32.2	48.3	37°277	
living_street	33.2	3.7	32.2	32.2	48.3	53	
service	32.6	0.6	32.2	32.2	33.6	19	
road	52.8	0.0	52.8	52.8	52.8	2	
construction	32.2	nan	32.2	32.2	32.2	1	
free_flow_kph (MeTS-10 extent (bounding box))	34.0	11.8	32.0	15.3	77.2	136°137	
motorway	103.2	14.4	109.2	59.8	117.6	311	
motorway_link	89.0	21.2	94.8	41.5	117.5	125	
trunk	41.2	14.2	38.1	20.2	85.6	11°928	
trunk_link	54.7	19.7	57.9	18.7	102.0	779	
primary	35.8	10.0	32.9	18.4	67.4	33°917	
primary_link	44.0	19.0	38.6	17.9	80.4	511	
secondary	35.1	10.0	32.9	17.9	67.8	14°738	
secondary_link	32.2	14.7	28.7	17.8	78.1	88	
tertiary	34.6	10.2	32.5	17.9	67.8	28°749	
tertiary_link	48.9	20.0	46.6	19.8	78.6	134	
unclassified	28.9	11.7	27.1	11.8	75.8	7°505	
residential	28.8	8.4	27.8	12.7	54.6	37°277	
living_street	23.1	4.3	24.9	12.9	28.6	53	
service	28.0	18.2	19.8	13.4	76.8	19	
road	26.4	0.7	26.4	25.9	26.8	2	
construction	14.1	nan	14.1	14.1	14.1	1	
free_flow_kph-speed_kph (MeTS-10 extent (bounding box))	-7.6	10.1	-6.3	-31.4	18.6	136°137	
motorway	-4.4	12.0	-2.6	-46.4	23.9	311	
motorway_link	-12.9	19.1	-7.8	-64.9	12.7	125	
trunk	-11.5	9.9	-11.3	-39.2	10.0	11°928	
trunk_link	-6.4	18.2	-5.5	-48.2	32.5	779	
primary	-9.2	10.1	-7.8	-30.9	13.6	33°917	
primary_link	-5.8	16.7	-5.8	-37.6	29.8	511	
secondary	-7.1	10.1	-5.4	-31.4	14.4	14°738	
secondary_link	-10.2	14.5	-10.3	-30.4	29.5	88	
tertiary	-6.0	10.2	-4.5	-29.5	20.9	28°749	
tertiary_link	-0.3	19.6	-3.5	-31.1	36.8	134	
unclassified	-7.9	11.5	-8.2	-32.8	31.5	7°505	
residential	-6.3	8.8	-5.8	-29.7	17.5	37°277	
living_street	-10.1	5.2	-8.0	-21.9	-3.6	53	
service	-4.5	18.1	-12.4	-19.6	44.6	19	
road	-26.4	0.7	-26.4	-26.9	-26.0	2	
construction	-18.1	nan	-18.1	-18.1	-18.1	1	

TABLE XXIII: Key figures London for the generated data from 20 randomly sampled days (MeTS-10 extent (bounding box)). **num_edges** number of edges in the street network graph; **num_nodes** number of nodes in the street network graph; **num_edges_per_cell** number of edges a cell (row,col,heading) has in its intersecting cells; **num_intersecting_cells** number of cells (row,col,heading) in an edge's intersecting cells; **node_degree** number of (unique) neighbor nodes per node; **length_meters** free flow speed derived from data; **speed_kph** signalled speed; **free_flow_kph** free flow speed derived from data; **free_flow_kph-speed_kph** difference

4) Segment density map London:

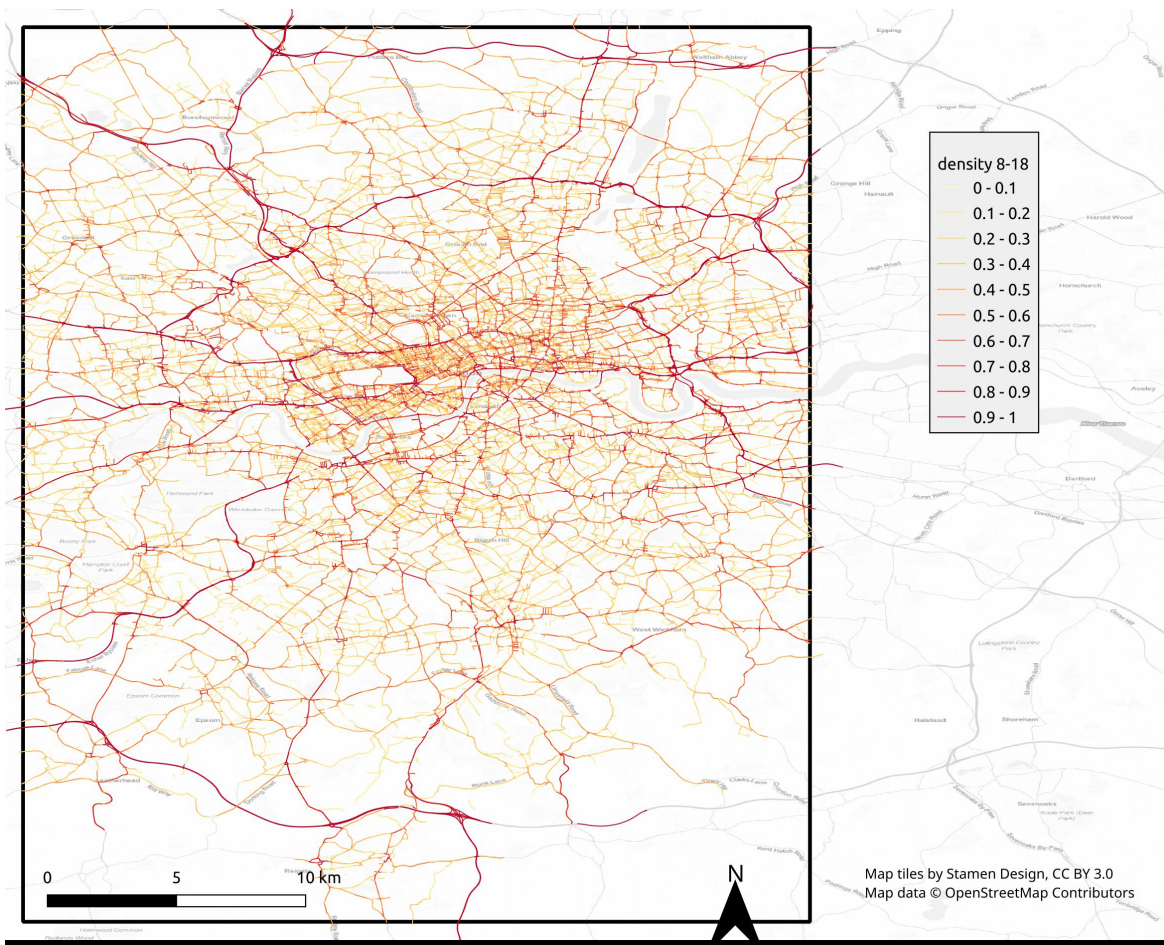


Fig. 69: Segment-wise density 8am–6pm London from 20 randomly sampled days.

5) Daily density profile London (full historic road graph):

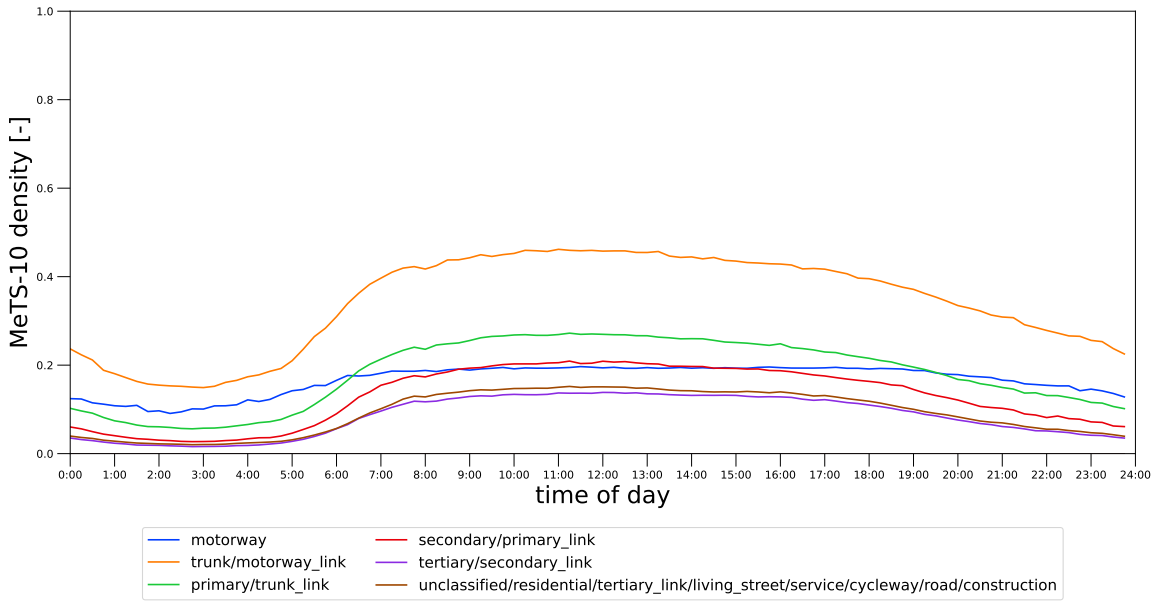


Fig. 70: Daily density profile for different road types for London (full historic road graph). Data from 20 randomly sampled days.

6) Daily speed profile London (full historic road graph):

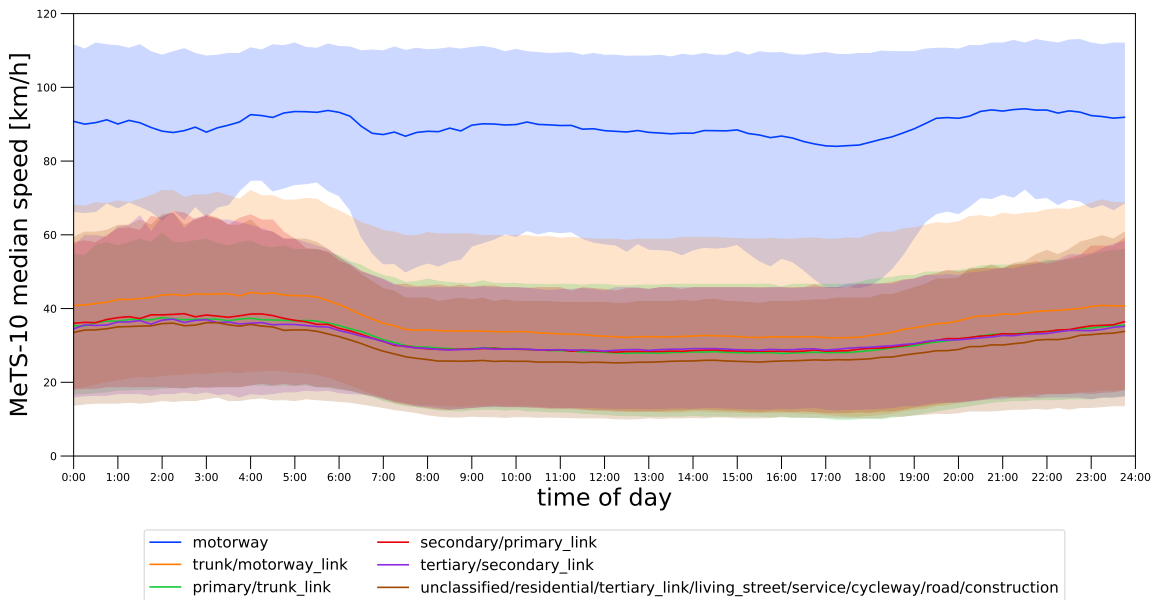


Fig. 71: Daily median 15 min speeds of all intersecting cells profile for different road types for London (full historic road graph). The error hull is the 80% data interval [10.0–90.0 percentiles] of daily means from 20 randomly sampled days.

7) Daily density profile London (MeTS-10 extent (bounding box)):

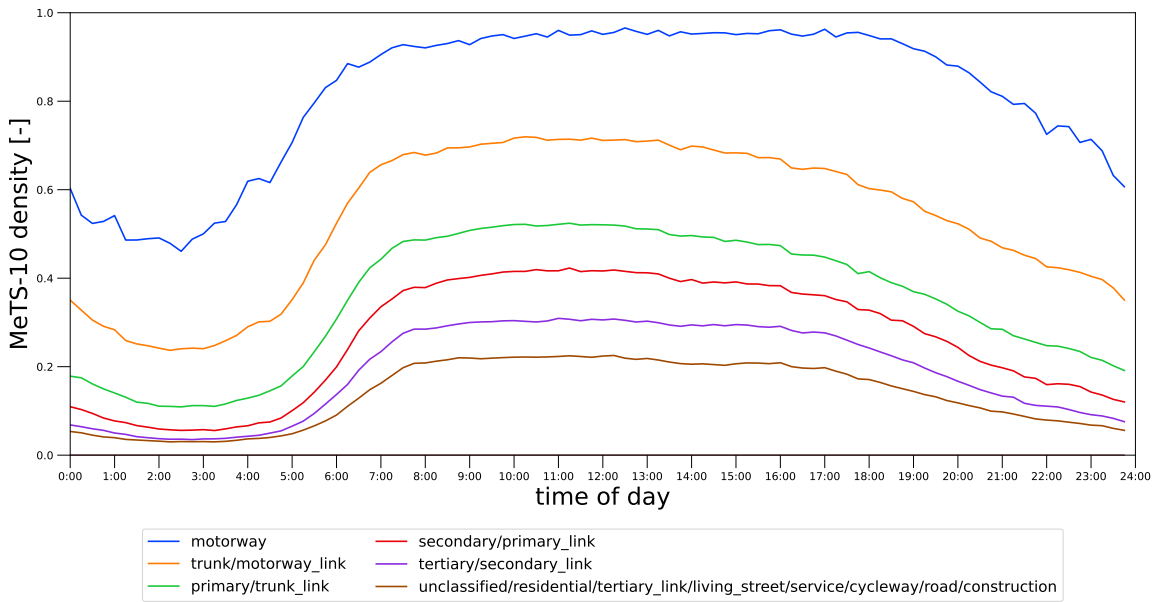


Fig. 72: Daily density profile for different road types for London (MeTS-10 extent (bounding box)). Data from 20 randomly sampled days.

8) Daily speed profile London (MeTS-10 extent (bounding box)):

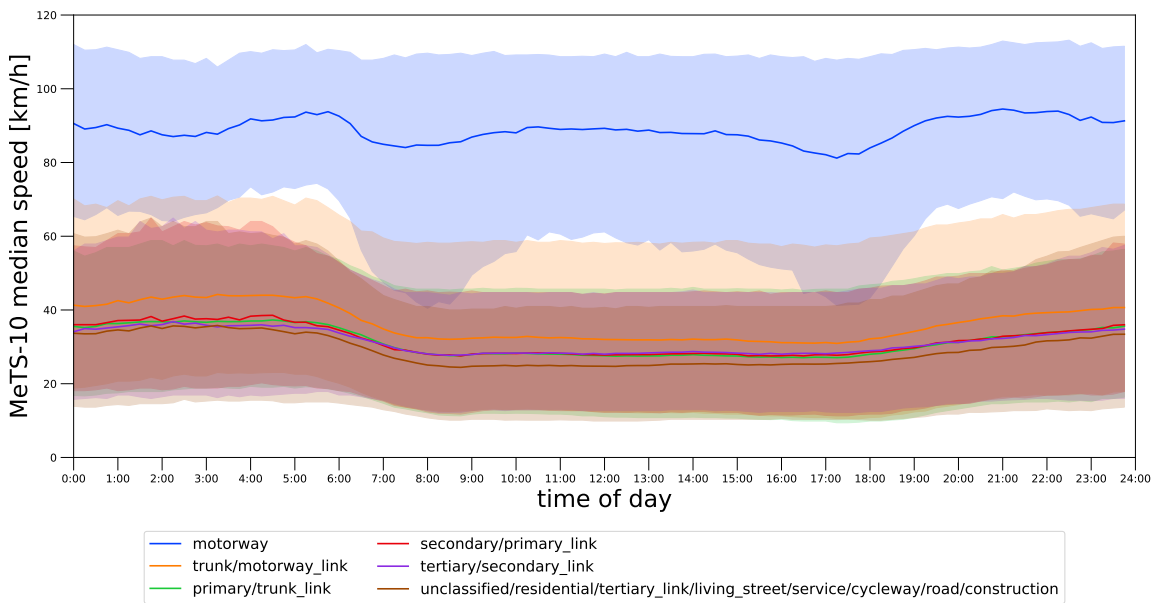


Fig. 73: Daily median 15 min speeds of all intersecting cells profile for different road types for London (MeTS-10 extent (bounding box)). The error hull is the 80% data interval [10.0–90.0 percentiles] of daily means from 20 randomly sampled days.

B. Key Figures Berlin

1) Road graph map Berlin:

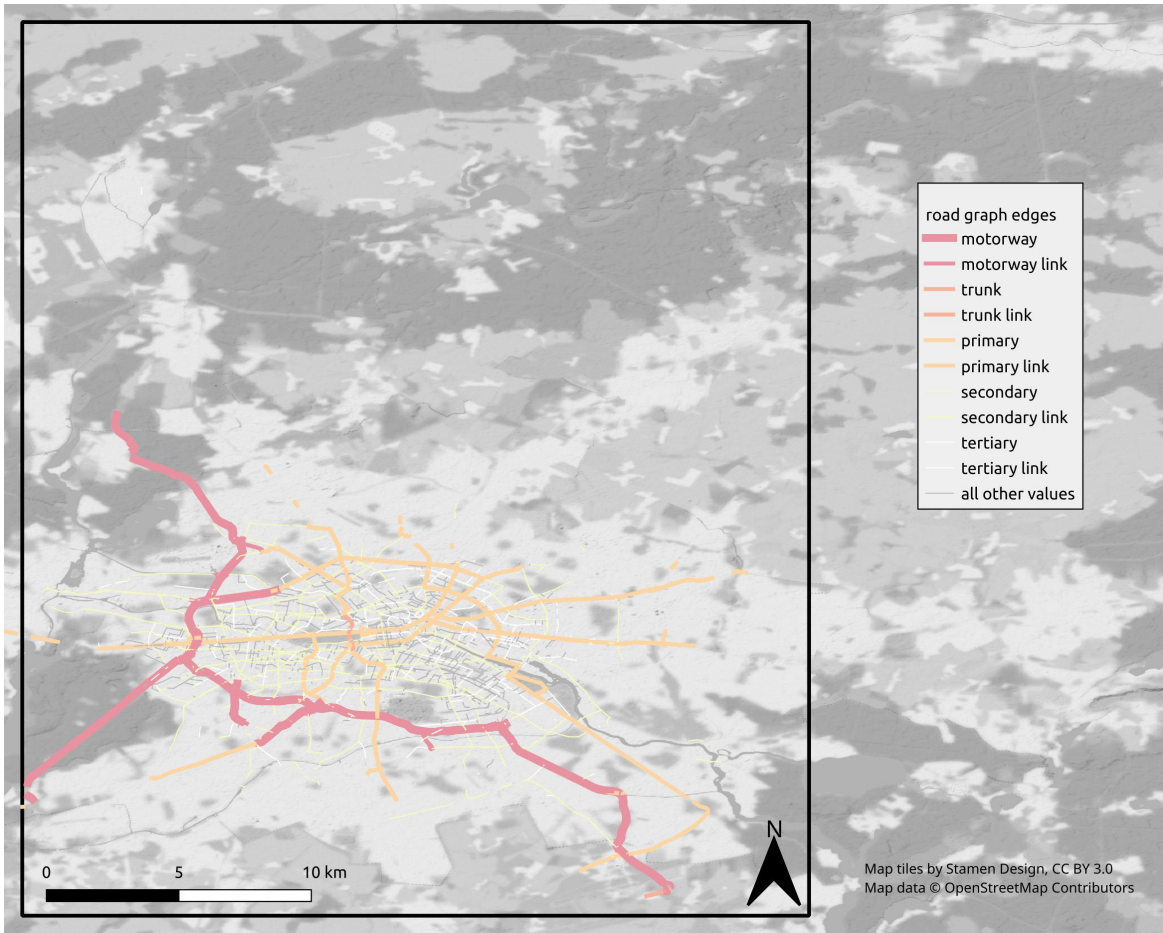


Fig. 74: Road graph Berlin, OSM color scheme.

2) Static data Berlin (full historic road graph):

Attribute	mean	std	median	q01	q99	data points	sum
bounding box (full historic road graph)						13.189–13.625 / 52.359–52.854	
num_edges (full historic road graph)						16'279	
motorway						515	
motorway_link						384	
trunk						72	
trunk_link						4	
primary						2937	
primary_link						15	
secondary						6464	
secondary_link						21	
tertiary						2782	
tertiary_link						2	
unclassified						56	
residential						2934	
living_street						91	
construction						2	
num_nodes (full historic road graph)						12655	
num_edges_per_cell (full historic road graph)	1.1	0.3	1.0	1.0	3.0	46'509	

num_intersecting_cells (full historic road graph)	3.1	2.2	2.0	1.0	12.0	16'279	
node_degree (full historic road graph)	2.2	0.7	2.0	1.0	4.0	12'655	
length_meters (full historic road graph)	103.4	120.9	71.8	5.2	536.7	16'279	1.7e+06
motorway	269.5	322.6	166.2	13.9	1'670.6	515	1.4e+05
motorway_link	144.0	118.0	116.4	13.2	531.2	384	5.5e+04
trunk	337.4	572.4	162.9	3.7	2'542.3	72	2.4e+04
trunk_link	87.3	97.4	54.2	12.1	224.5	4	3.5e+02
primary	105.3	116.2	72.0	5.6	603.9	2'937	3.1e+05
primary_link	36.3	32.9	23.3	10.7	122.0	15	5.4e+02
secondary	91.4	89.8	66.2	5.5	413.8	6'464	5.9e+05
secondary_link	50.7	47.3	27.3	15.4	148.3	21	1.1e+03
tertiary	90.2	85.8	65.8	4.9	378.2	2'782	2.5e+05
tertiary_link	19.2	0.0	19.2	19.2	19.2	2	3.8e+01
unclassified	75.9	80.8	46.1	4.3	351.9	56	4.2e+03
residential	101.2	86.4	77.1	4.2	373.4	2'934	3.0e+05
living_street	111.4	96.5	88.3	6.9	369.8	91	1.0e+04
construction	36.7	0.0	36.7	36.7	36.7	2	7.3e+01
speed_kph (full historic road graph)	46.6	11.2	50.0	30.0	80.0	16'279	
motorway	77.3	11.8	80.0	40.0	120.0	515	
motorway_link	60.1	10.0	60.0	40.0	80.0	384	
trunk	70.6	22.0	65.0	50.0	100.0	72	
trunk_link	30.0	0.0	30.0	30.0	30.0	4	
primary	48.8	6.0	50.0	30.0	60.0	2'937	
primary_link	48.0	7.7	50.0	30.0	58.6	15	
secondary	48.8	5.3	50.0	30.0	60.0	6'464	
secondary_link	50.0	0.0	50.0	50.0	50.0	21	
tertiary	45.7	8.1	50.0	30.0	50.0	2'782	
tertiary_link	50.0	0.0	50.0	50.0	50.0	2	
unclassified	37.7	10.3	30.0	20.0	50.0	56	
residential	32.5	7.7	30.0	10.0	50.0	2'934	
living_street	50.0	0.0	50.0	50.0	50.0	91	
construction	50.0	0.0	50.0	50.0	50.0	2	
free_flow_kph (full historic road graph)	45.1	13.5	43.5	22.1	89.9	16'229	
motorway	84.3	10.5	85.2	56.8	115.1	515	
motorway_link	77.6	14.2	81.5	36.7	114.7	384	
trunk	59.5	19.6	52.9	33.2	96.0	46	
primary	47.1	8.8	47.1	28.7	70.8	2'919	
primary_link	42.9	11.7	41.1	25.9	64.8	15	
secondary	45.9	9.2	45.6	26.5	80.3	6'464	
secondary_link	41.6	14.0	39.8	20.2	77.2	21	
tertiary	41.4	8.8	40.9	23.4	75.6	2'780	
tertiary_link	38.8	0.0	38.8	38.8	38.8	2	
unclassified	44.8	7.8	46.1	21.8	54.3	56	
residential	34.2	7.7	33.9	18.8	55.9	2'934	
living_street	26.0	6.1	24.9	16.5	37.9	91	
construction	42.4	0.0	42.4	42.4	42.4	2	
free_flow_kph-speed_kph (full historic road graph)	-1.4	10.8	-1.3	-26.0	30.2	16'229	
motorway	7.0	7.5	6.9	-9.6	29.0	515	
motorway_link	17.5	13.1	20.6	-15.5	38.7	384	
trunk	2.9	10.1	2.9	-16.8	26.0	46	
primary	-1.6	8.2	-1.1	-20.5	19.2	2'919	
primary_link	-5.1	16.7	-8.9	-24.1	34.2	15	
secondary	-2.9	9.9	-3.4	-23.4	31.5	6'464	
secondary_link	-8.4	14.0	-10.2	-29.8	27.2	21	
tertiary	-4.4	10.8	-5.3	-26.0	25.6	2'780	
tertiary_link	-11.2	0.0	-11.2	-11.2	-11.2	2	
unclassified	7.1	13.6	12.4	-28.2	23.3	56	
residential	1.6	10.6	2.5	-29.6	26.2	2'934	
living_street	-24.0	6.1	-25.1	-33.5	-12.1	91	
construction	-7.6	0.0	-7.6	-7.6	-7.6	2	

TABLE XXIV: Key figures Berlin for the generated data from 20 randomly sampled days (full historic road graph). **num_edges** number of edges in the street network graph; **num_nodes** number of nodes in the street network graph; **num_edges_per_cell** number of edges a cell (row,col,heading) has in its intersecting cells; **num_intersecting_cells** number of cells (row,col,heading) in an edge's intersecting cells; **node_degree** number of (unique) neighbor nodes per node; **length_meters** free flow speed derived from data; **speed_kph** signalled speed; **free_flow_kph** free flow speed derived from data; **free_flow_kph-speed_kph** difference

3) *Static data Berlin (MeTS-10 extent (bounding box)):*

Attribute	mean	std	median	q01	q99	data points	sum
bounding box (MeTS-10 extent (bounding box))						13.189–13.625 / 52.359–52.854	
num_edges (MeTS-10 extent (bounding box))						16'229	
motorway						515	
motorway_link						384	
trunk						46	
primary						2919	
primary_link						15	
secondary						6464	
secondary_link						21	
tertiary						2780	
tertiary_link						2	
unclassified						56	
residential						2934	
living_street						91	
construction						2	
num_nodes (MeTS-10 extent (bounding box))						12603	
num_edges_per_cell (MeTS-10 extent (bounding box))	1.1	0.3	1.0	1.0	3.0	46'509	
num_intersecting_cells (MeTS-10 extent (bounding box))	3.1	2.2	2.0	1.0	12.0	16'229	
node_degree (MeTS-10 extent (bounding box))	2.2	0.7	2.0	1.0	4.0	12'603	
length_meters (MeTS-10 extent (bounding box))	102.6	114.6	71.7	5.2	531.4	16'229	1.7e+06
motorway	269.5	322.6	166.2	13.9	1'670.6	515	1.4e+05
motorway_link	144.0	118.0	116.4	13.2	531.2	384	5.5e+04
trunk	191.8	209.7	114.0	3.6	835.0	46	8.8e+03
primary	105.4	116.5	72.0	5.6	605.4	2'919	3.1e+05
primary_link	36.3	32.9	23.3	10.7	122.0	15	5.4e+02
secondary	91.4	89.8	66.2	5.5	413.8	6'464	5.9e+05
secondary_link	50.7	47.3	27.3	15.4	148.3	21	1.1e+03
tertiary	90.2	85.8	65.8	4.9	378.3	2'780	2.5e+05
tertiary_link	19.2	0.0	19.2	19.2	19.2	2	3.8e+01
unclassified	75.9	80.8	46.1	4.3	351.9	56	4.2e+03
residential	101.2	86.4	77.1	4.2	373.4	2'934	3.0e+05
living_street	111.4	96.5	88.3	6.9	369.8	91	1.0e+04
construction	36.7	0.0	36.7	36.7	36.7	2	7.3e+01
speed_kph (MeTS-10 extent (bounding box))	46.5	11.0	50.0	30.0	80.0	16'229	
motorway	77.3	11.8	80.0	40.0	120.0	515	
motorway_link	60.1	10.0	60.0	40.0	80.0	384	
trunk	56.5	11.4	50.0	50.0	80.0	46	
primary	48.8	6.0	50.0	30.0	60.0	2'919	
primary_link	48.0	7.7	50.0	30.0	58.6	15	
secondary	48.8	5.3	50.0	30.0	60.0	6'464	
secondary_link	50.0	0.0	50.0	50.0	50.0	21	
tertiary	45.7	8.1	50.0	30.0	50.0	2'780	
tertiary_link	50.0	0.0	50.0	50.0	50.0	2	
unclassified	37.7	10.3	30.0	20.0	50.0	56	
residential	32.5	7.7	30.0	10.0	50.0	2'934	
living_street	50.0	0.0	50.0	50.0	50.0	91	
construction	50.0	0.0	50.0	50.0	50.0	2	

free_flow_kph (MeTS-10 extent (bounding box))	45.1	13.5	43.5	22.1	89.9	16'229
motorway	84.3	10.5	85.2	56.8	115.1	515
motorway_link	77.6	14.2	81.5	36.7	114.7	384
trunk	59.5	19.6	52.9	33.2	96.0	46
primary	47.1	8.8	47.1	28.7	70.8	2'919
primary_link	42.9	11.7	41.1	25.9	64.8	15
secondary	45.9	9.2	45.6	26.5	80.3	6'464
secondary_link	41.6	14.0	39.8	20.2	77.2	21
tertiary	41.4	8.8	40.9	23.4	75.6	2'780
tertiary_link	38.8	0.0	38.8	38.8	38.8	2
unclassified	44.8	7.8	46.1	21.8	54.3	56
residential	34.2	7.7	33.9	18.8	55.9	2'934
living_street	26.0	6.1	24.9	16.5	37.9	91
construction	42.4	0.0	42.4	42.4	42.4	2
free_flow_kph-speed_kph (MeTS-10 extent (bounding box))	-1.4	10.8	-1.3	-26.0	30.2	16'229
motorway	7.0	7.5	6.9	-9.6	29.0	515
motorway_link	17.5	13.1	20.6	-15.5	38.7	384
trunk	2.9	10.1	2.9	-16.8	26.0	46
primary	-1.6	8.2	-1.1	-20.5	19.2	2'919
primary_link	-5.1	16.7	-8.9	-24.1	34.2	15
secondary	-2.9	9.9	-3.4	-23.4	31.5	6'464
secondary_link	-8.4	14.0	-10.2	-29.8	27.2	21
tertiary	-4.4	10.8	-5.3	-26.0	25.6	2'780
tertiary_link	-11.2	0.0	-11.2	-11.2	-11.2	2
unclassified	7.1	13.6	12.4	-28.2	23.3	56
residential	1.6	10.6	2.5	-29.6	26.2	2'934
living_street	-24.0	6.1	-25.1	-33.5	-12.1	91
construction	-7.6	0.0	-7.6	-7.6	-7.6	2

TABLE XXV: Key figures Berlin for the generated data from 20 randomly sampled days (MeTS-10 extent (bounding box)). **num_edges** number of edges in the street network graph; **num_nodes** number of nodes in the street network graph; **num_edges_per_cell** number of edges a cell (row,col,heading) has in its intersecting cells; **num_intersecting_cells** number of cells (row,col,heading) in an edge's intersecting cells; **node_degree** number of (unique) neighbor nodes per node; **length_meters** free flow speed derived from data; **speed_kph** signalled speed; **free_flow_kph** free flow speed derived from data; **free_flow_kph-speed_kph** difference

4) Segment density map Berlin:

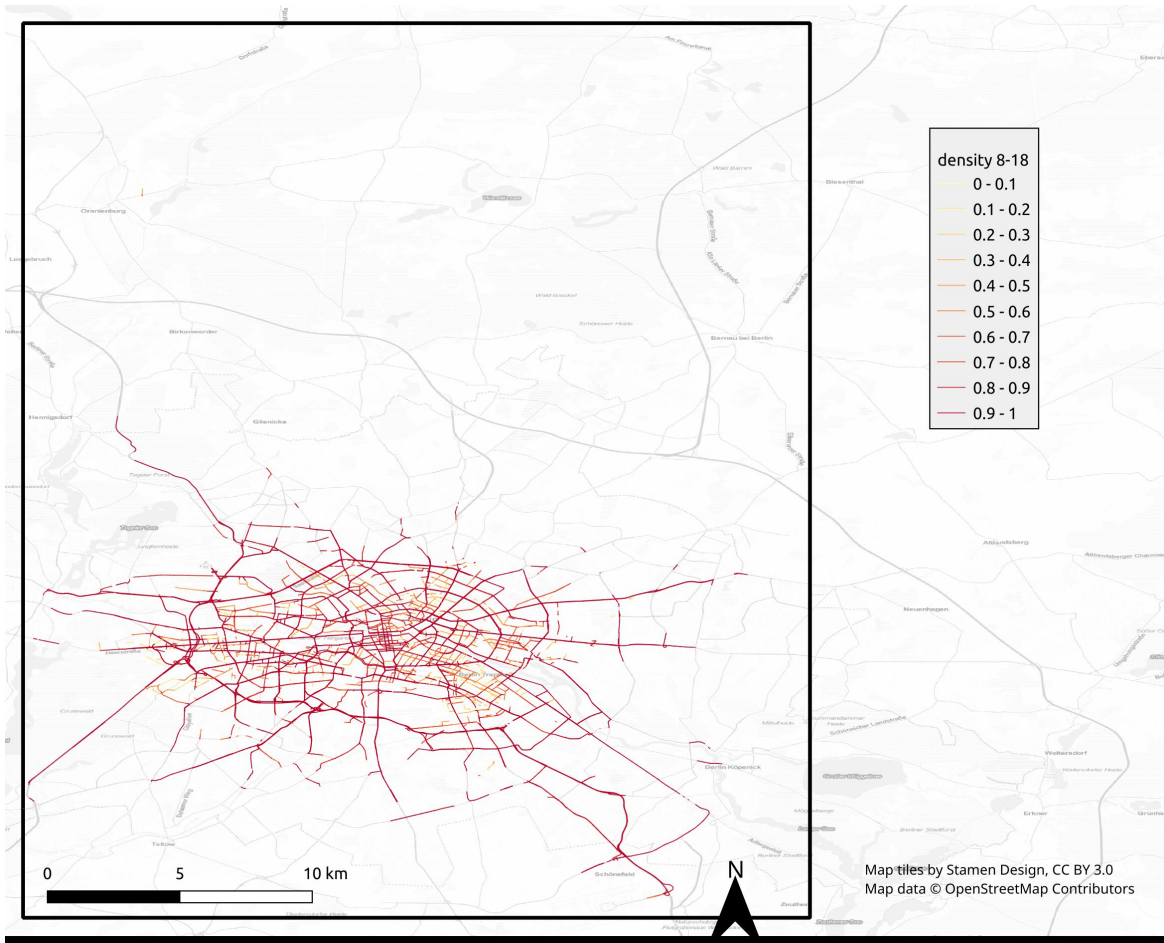


Fig. 75: Segment-wise density 8am–6pm Berlin from 20 randomly sampled days.

5) Daily density profile Berlin (full historic road graph):

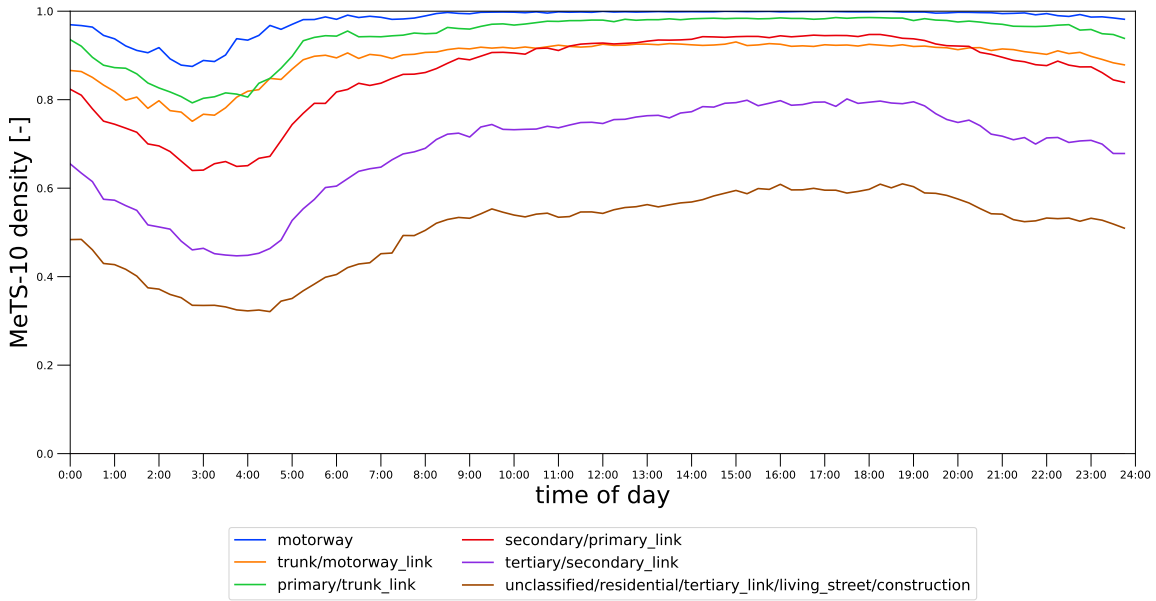


Fig. 76: Daily density profile for different road types for Berlin (full historic road graph). Data from 20 randomly sampled days.

6) Daily speed profile Berlin (full historic road graph):

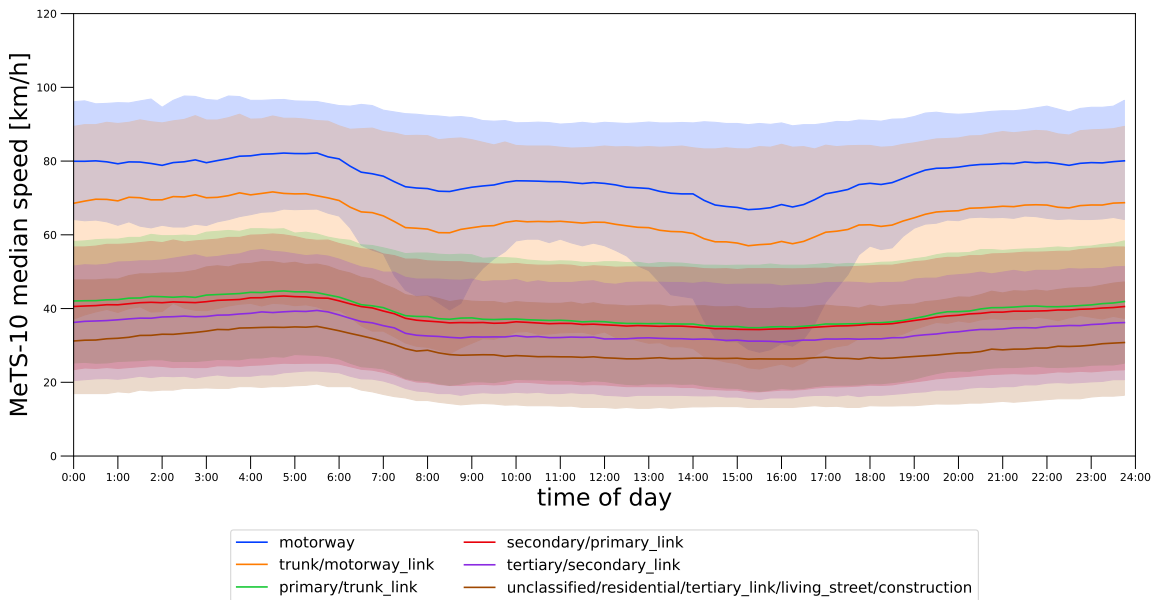


Fig. 77: Daily median 15 min speeds of all intersecting cells profile for different road types for Berlin (full historic road graph). The error hull is the 80% data interval [10.0–90.0 percentiles] of daily means from 20 randomly sampled days.

7) Daily density profile Berlin (MeTS-10 extent (bounding box)):

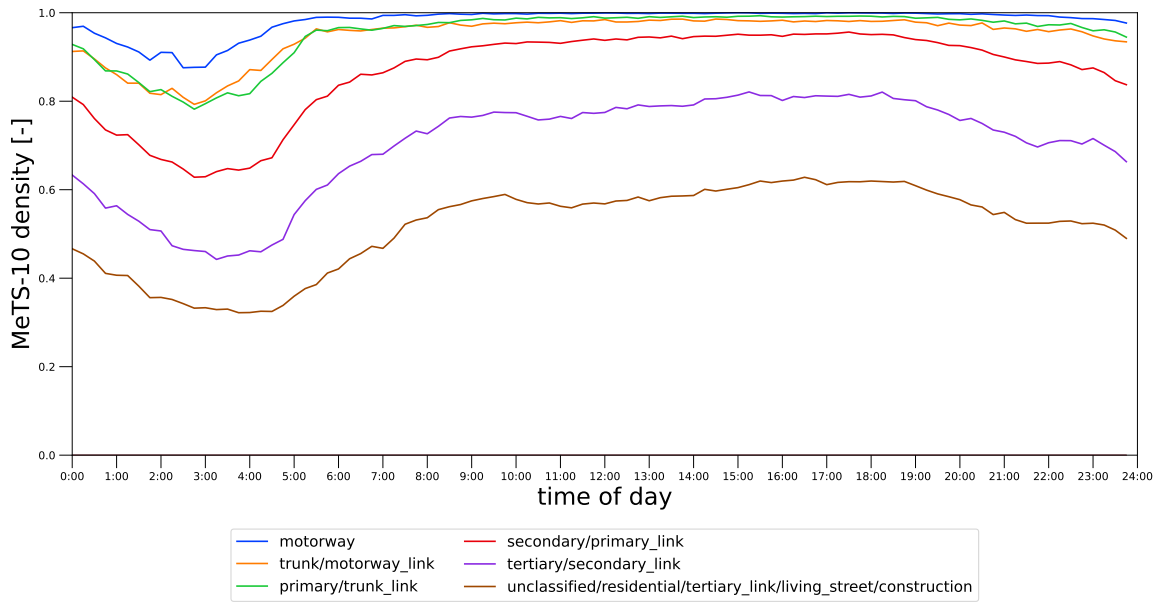


Fig. 78: Daily density profile for different road types for Berlin (MeTS-10 extent (bounding box)). Data from 20 randomly sampled days.

8) Daily speed profile Berlin (MeTS-10 extent (bounding box)):

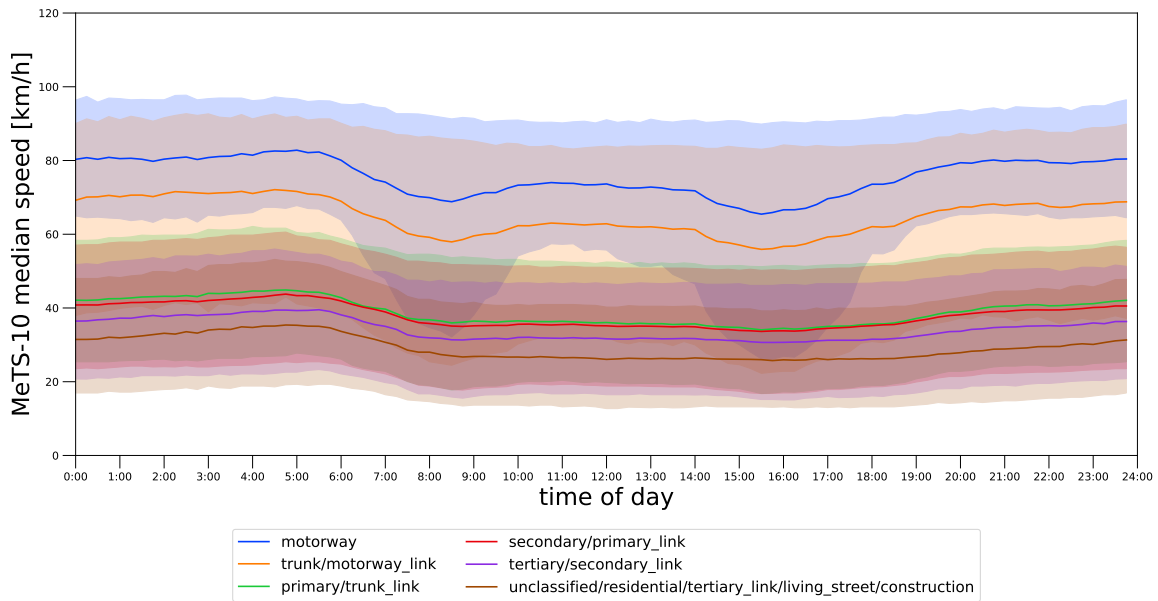


Fig. 79: Daily median 15 min speeds of all intersecting cells profile for different road types for Berlin (MeTS-10 extent (bounding box)). The error hull is the 80% data interval [10.0–90.0 percentiles] of daily means from 20 randomly sampled days.

C. Key Figures Barcelona

1) Road graph map Barcelona:

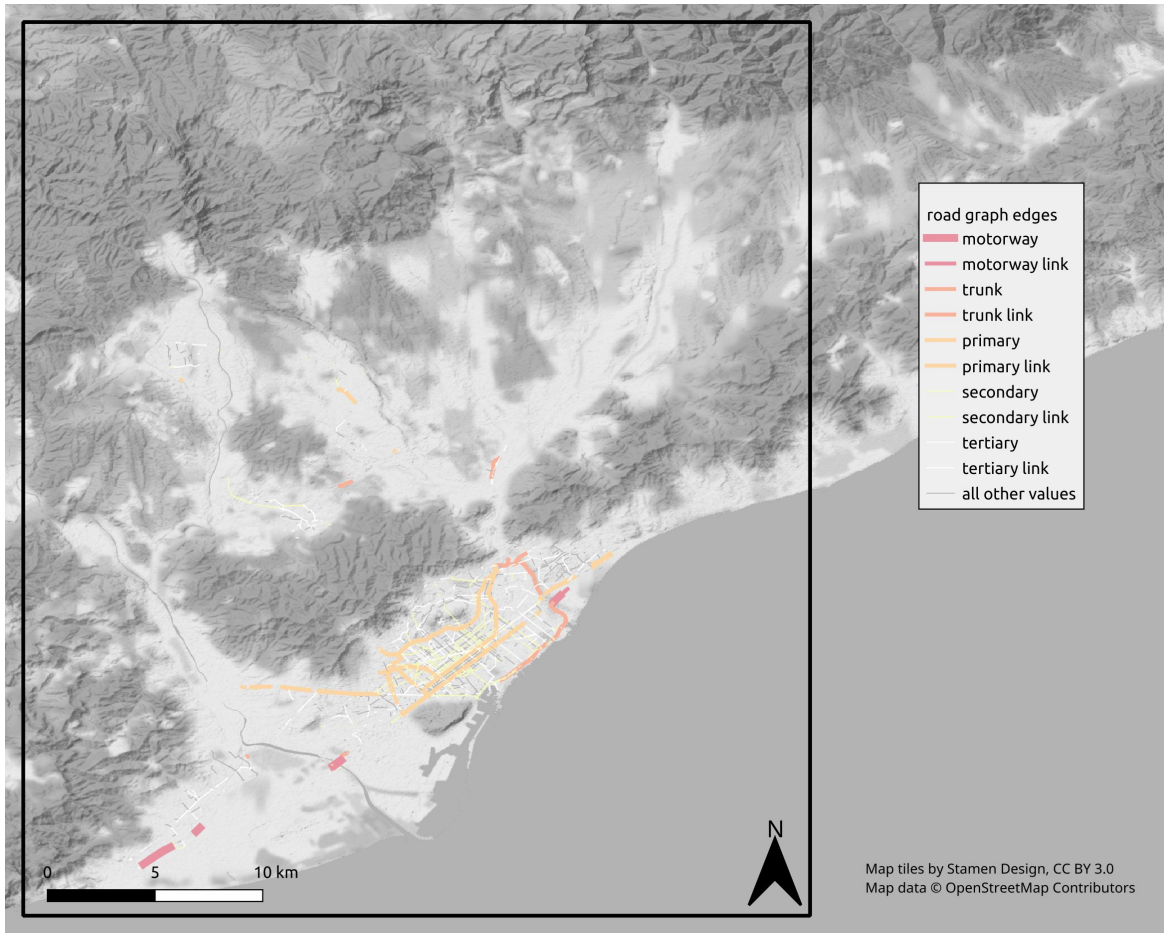


Fig. 80: Road graph Barcelona, OSM color scheme.

2) Static data Barcelona (full historic road graph):

Attribute	mean	std	median	q01	q99	data points	sum
bounding_box (full historic road graph)						1.925–2.361 / 41.253–41.748	
num_edges (full historic road graph)						5'943	
motorway						16	
motorway_link						3	
trunk						56	
trunk_link						44	
primary						709	
primary_link						216	
secondary						1278	
secondary_link						92	
tertiary						2014	
tertiary_link						130	
unclassified						20	
residential						1341	
living_street						24	
num_nodes (full historic road graph)						5530	
num_edges_per_cell (full historic road graph)	1.1	0.4	1.0	1.0	3.0	13'823	
num_intersecting_cells (full historic road graph)	2.5	1.5	2.0	1.0	8.0	5'943	

node_degree (full historic road graph)	2.0	0.7	2.0	1.0	4.0	5'530	
length_meters (full historic road graph)	80.0	74.0	61.9	3.9	327.3	5'943	4.8e+05
motorway	225.8	223.5	133.2	25.4	651.4	16	3.6e+03
motorway_link	202.8	130.0	196.9	78.3	333.0	3	6.1e+02
trunk	212.8	202.4	130.6	7.9	880.2	56	1.2e+04
trunk_link	122.5	102.9	90.1	18.7	439.1	44	5.4e+03
primary	83.5	78.4	69.0	4.3	350.4	709	5.9e+04
primary_link	71.6	65.1	44.5	4.6	274.5	216	1.5e+04
secondary	86.8	80.8	68.0	4.4	365.5	1'278	1.1e+05
secondary_link	52.3	70.4	32.1	2.7	279.8	92	4.8e+03
tertiary	73.1	62.2	56.0	3.6	275.8	2'014	1.5e+05
tertiary_link	67.6	70.3	33.4	3.6	258.8	130	8.8e+03
unclassified	89.9	99.5	48.1	7.1	366.2	20	1.8e+03
residential	77.8	58.6	65.5	4.0	266.4	1'341	1.0e+05
living_street	68.6	42.6	63.2	6.2	153.9	24	1.6e+03
speed_kph (full historic road graph)	47.3	7.3	49.7	30.0	80.0	5'943	
motorway	90.0	11.0	90.0	80.0	117.0	16	
motorway_link	56.7	5.8	60.0	50.2	60.0	3	
trunk	78.5	6.4	80.0	60.0	89.0	56	
trunk_link	57.3	9.9	57.4	40.0	80.0	44	
primary	49.7	2.5	50.0	30.8	50.0	709	
primary_link	47.2	7.3	50.0	20.0	58.5	216	
secondary	49.7	1.5	50.0	40.0	50.0	1'278	
secondary_link	49.1	3.2	50.0	30.0	50.0	92	
tertiary	49.5	2.6	50.0	31.3	50.0	2'014	
tertiary_link	49.3	3.0	50.0	30.0	50.0	130	
unclassified	41.4	6.0	41.4	30.0	50.0	20	
residential	38.6	5.4	38.6	30.0	50.0	1'341	
living_street	16.6	7.8	16.3	10.0	30.0	24	
free_flow_kph (full historic road graph)	37.1	14.8	35.3	14.4	91.4	5'943	
motorway	103.7	13.4	93.6	90.8	119.8	16	
motorway_link	85.4	17.2	94.7	66.2	96.0	3	
trunk	80.8	8.6	82.1	63.5	99.8	56	
trunk_link	74.9	12.9	76.7	39.9	92.7	44	
primary	41.6	11.4	42.1	20.9	90.2	709	
primary_link	46.2	13.2	47.5	18.9	81.7	216	
secondary	38.8	11.5	37.6	17.8	80.9	1'278	
secondary_link	39.0	14.8	35.3	18.4	85.0	92	
tertiary	35.7	13.6	32.9	15.1	88.5	2'014	
tertiary_link	35.9	11.5	34.1	14.3	78.8	130	
unclassified	47.4	29.2	36.7	19.2	117.1	20	
residential	30.0	12.2	28.7	11.5	83.0	1'341	
living_street	25.0	10.4	20.5	9.1	43.8	24	
free_flow_kph-speed_kph (full historic road graph)	-10.2	13.7	-11.9	-33.5	38.5	5'943	
motorway	13.7	13.5	11.9	-6.4	29.8	16	
motorway_link	28.8	11.4	34.7	16.0	36.0	3	
trunk	2.3	7.6	3.2	-13.3	19.8	56	
trunk_link	17.6	15.1	16.7	-14.2	52.7	44	
primary	-8.1	11.4	-7.3	-29.1	40.2	709	
primary_link	-1.0	15.8	-1.1	-31.0	50.0	216	
secondary	-10.9	11.8	-12.1	-32.0	31.2	1'278	
secondary_link	-10.1	15.5	-14.7	-29.0	45.0	92	
tertiary	-13.9	13.5	-16.1	-34.9	36.3	2'014	
tertiary_link	-13.4	12.2	-15.2	-35.0	29.7	130	
unclassified	6.0	29.9	-3.8	-22.2	75.7	20	
residential	-8.6	12.9	-9.4	-33.1	44.4	1'341	
living_street	8.4	17.0	5.0	-20.9	33.8	24	

TABLE XXVI: Key figures Barcelona for the generated data from 20 randomly sampled days (full historic road graph). **num_edges** number of edges in the street network graph; **num_nodes** number of nodes in the street network graph; **num_edges_per_cell** number of edges a cell (row,col,heading) has in its intersecting cells; **num_intersecting_cells** number of cells (row,col,heading) in an edge's intersecting cells; **node_degree** number of (unique) neighbor nodes per node; **length_meters** free flow speed derived from data; **speed_kph** signalled speed; **free_flow_kph** free flow speed derived from data; **free_flow_kph-speed_kph** difference

3) *Static data Barcelona (MeTS-10 extent (bounding box)):*

Attribute	mean	std	median	q01	q99	data points	sum	
bounding box (MeTS-10 extent (bounding box))	1.925–2.361 / 41.253–41.748							
num_edges (MeTS-10 extent (bounding box))							5'943	
motorway							16	
motorway_link							3	
trunk							56	
trunk_link							44	
primary							709	
primary_link							216	
secondary							1278	
secondary_link							92	
tertiary							2014	
tertiary_link							130	
unclassified							20	
residential							1341	
living_street							24	
num_nodes (MeTS-10 extent (bounding box))							5530	
num_edges_per_cell (MeTS-10 extent (bounding box))	1.1	0.4	1.0	1.0	3.0	13'823		
num_intersecting_cells (MeTS-10 extent (bounding box))	2.5	1.5	2.0	1.0	8.0	5'943		
node_degree (MeTS-10 extent (bounding box))	2.0	0.7	2.0	1.0	4.0	5'530		
length_meters (MeTS-10 extent (bounding box))	80.0	74.0	61.9	3.9	327.3	5'943	4.8e+05	
motorway	225.8	223.5	133.2	25.4	651.4	16	3.6e+03	
motorway_link	202.8	130.0	196.9	78.3	333.0	3	6.1e+02	
trunk	212.8	202.4	130.6	7.9	880.2	56	1.2e+04	
trunk_link	122.5	102.9	90.1	18.7	439.1	44	5.4e+03	
primary	83.5	78.4	69.0	4.3	350.4	709	5.9e+04	
primary_link	71.6	65.1	44.5	4.6	274.5	216	1.5e+04	
secondary	86.8	80.8	68.0	4.4	365.5	1'278	1.1e+05	
secondary_link	52.3	70.4	32.1	2.7	279.8	92	4.8e+03	
tertiary	73.1	62.2	56.0	3.6	275.8	2'014	1.5e+05	
tertiary_link	67.6	70.3	33.4	3.6	258.8	130	8.8e+03	
unclassified	89.9	99.5	48.1	7.1	366.2	20	1.8e+03	
residential	77.8	58.6	65.5	4.0	266.4	1'341	1.0e+05	
living_street	68.6	42.6	63.2	6.2	153.9	24	1.6e+03	
speed_kph (MeTS-10 extent (bounding box))	47.3	7.3	49.7	30.0	80.0	5'943		
motorway	90.0	11.0	90.0	80.0	117.0	16		
motorway_link	56.7	5.8	60.0	50.2	60.0	3		
trunk	78.5	6.4	80.0	60.0	89.0	56		
trunk_link	57.3	9.9	57.4	40.0	80.0	44		
primary	49.7	2.5	50.0	30.8	50.0	709		
primary_link	47.2	7.3	50.0	20.0	58.5	216		
secondary	49.7	1.5	50.0	40.0	50.0	1'278		
secondary_link	49.1	3.2	50.0	30.0	50.0	92		
tertiary	49.5	2.6	50.0	31.3	50.0	2'014		
tertiary_link	49.3	3.0	50.0	30.0	50.0	130		
unclassified	41.4	6.0	41.4	30.0	50.0	20		
residential	38.6	5.4	38.6	30.0	50.0	1'341		
living_street	16.6	7.8	16.3	10.0	30.0	24		

free_flow_kph (MeTS-10 extent (bounding box))	37.1	14.8	35.3	14.4	91.4	5'943
motorway	103.7	13.4	93.6	90.8	119.8	16
motorway_link	85.4	17.2	94.7	66.2	96.0	3
trunk	80.8	8.6	82.1	63.5	99.8	56
trunk_link	74.9	12.9	76.7	39.9	92.7	44
primary	41.6	11.4	42.1	20.9	90.2	709
primary_link	46.2	13.2	47.5	18.9	81.7	216
secondary	38.8	11.5	37.6	17.8	80.9	1'278
secondary_link	39.0	14.8	35.3	18.4	85.0	92
tertiary	35.7	13.6	32.9	15.1	88.5	2'014
tertiary_link	35.9	11.5	34.1	14.3	78.8	130
unclassified	47.4	29.2	36.7	19.2	117.1	20
residential	30.0	12.2	28.7	11.5	83.0	1'341
living_street	25.0	10.4	20.5	9.1	43.8	24
free_flow_kph-speed_kph (MeTS-10 extent (bounding box))	-10.2	13.7	-11.9	-33.5	38.5	5'943
motorway	13.7	13.5	11.9	-6.4	29.8	16
motorway_link	28.8	11.4	34.7	16.0	36.0	3
trunk	2.3	7.6	3.2	-13.3	19.8	56
trunk_link	17.6	15.1	16.7	-14.2	52.7	44
primary	-8.1	11.4	-7.3	-29.1	40.2	709
primary_link	-1.0	15.8	-1.1	-31.0	50.0	216
secondary	-10.9	11.8	-12.1	-32.0	31.2	1'278
secondary_link	-10.1	15.5	-14.7	-29.0	45.0	92
tertiary	-13.9	13.5	-16.1	-34.9	36.3	2'014
tertiary_link	-13.4	12.2	-15.2	-35.0	29.7	130
unclassified	6.0	29.9	-3.8	-22.2	75.7	20
residential	-8.6	12.9	-9.4	-33.1	44.4	1'341
living_street	8.4	17.0	5.0	-20.9	33.8	24

TABLE XXVII: Key figures Barcelona for the generated data from 20 randomly sampled days (MeTS-10 extent (bounding box)). **num_edges** number of edges in the street network graph; **num_nodes** number of nodes in the street network graph; **num_edges_per_cell** number of edges a cell (row,col,heading) has in its intersecting cells; **num_intersecting_cells** number of cells (row,col,heading) in an edge's intersecting cells; **node_degree** number of (unique) neighbor nodes per node; **length_meters** free flow speed derived from data; **speed_kph** signalled speed; **free_flow_kph** free flow speed derived from data; **free_flow_kph-speed_kph** difference

4) Segment density map Barcelona:

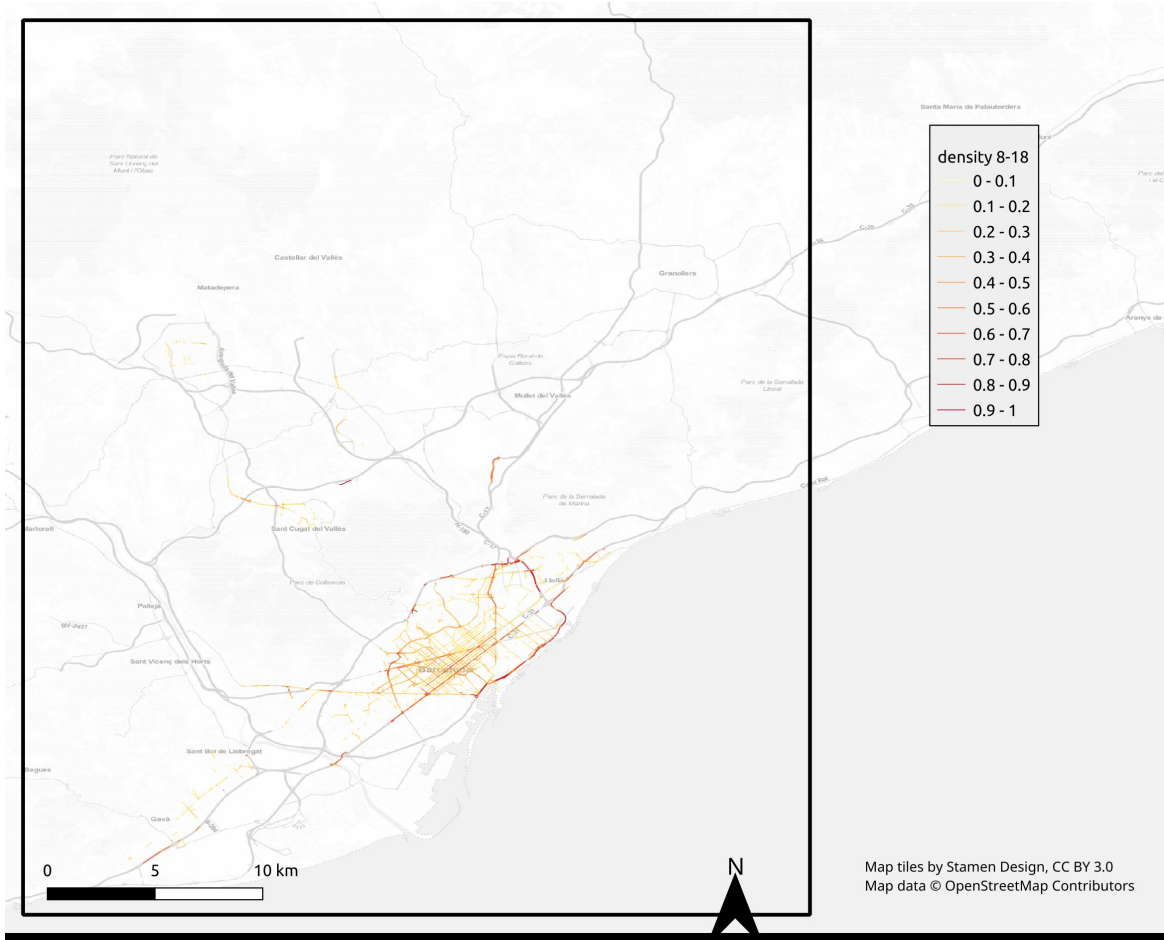


Fig. 81: Segment-wise density 8am–6pm Barcelona from 20 randomly sampled days.

5) Daily density profile Barcelona (full historic road graph):

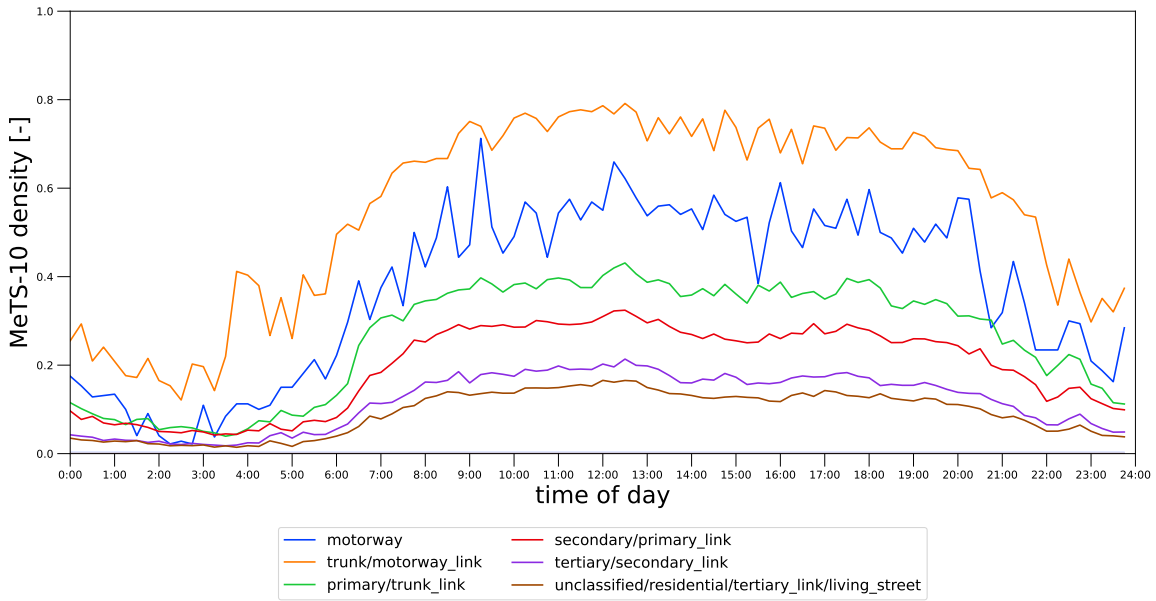


Fig. 82: Daily density profile for different road types for Barcelona (full historic road graph). Data from 20 randomly sampled days.

6) Daily speed profile Barcelona (full historic road graph):

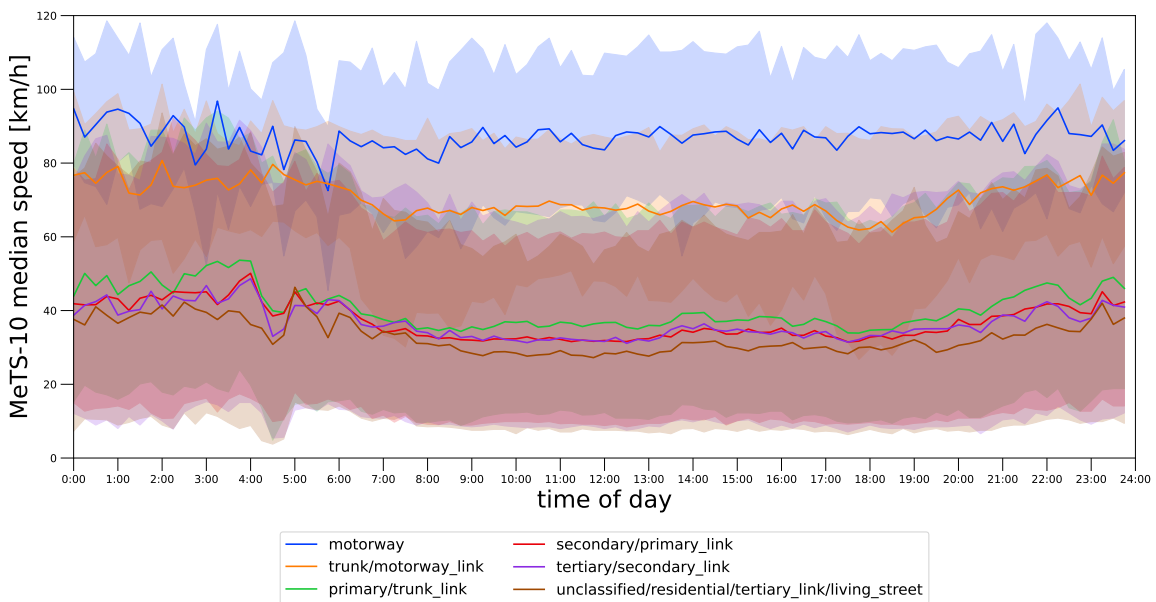


Fig. 83: Daily median 15 min speeds of all intersecting cells profile for different road types for Barcelona (full historic road graph). The error hull is the 80% data interval [10.0–90.0 percentiles] of daily means from 20 randomly sampled days.

7) Daily density profile Barcelona (MeTS-10 extent (bounding box)):

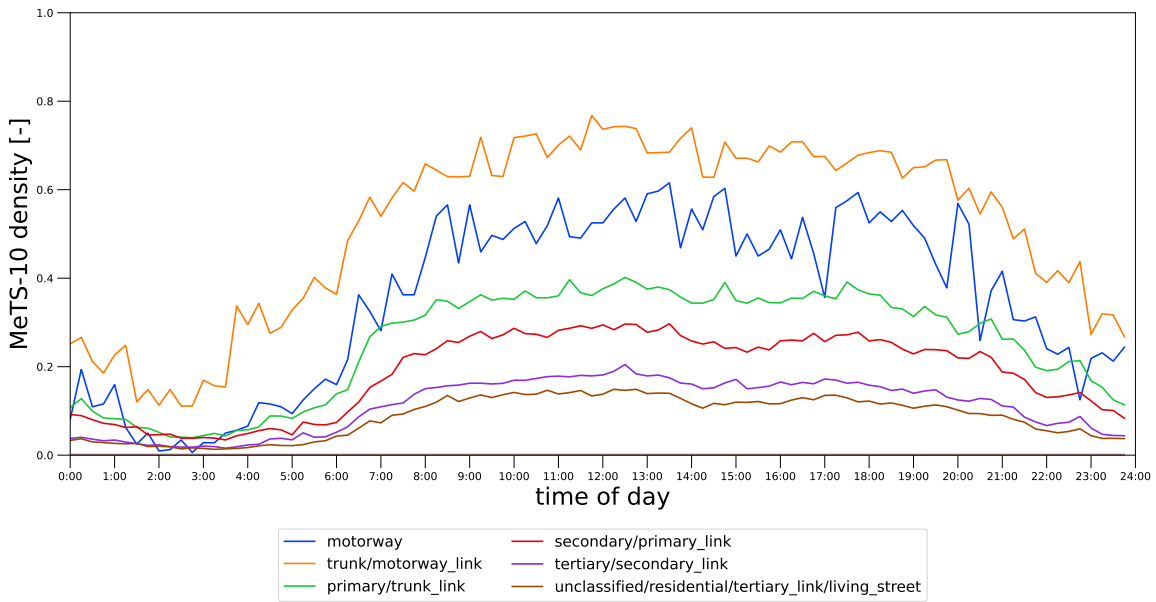


Fig. 84: Daily density profile for different road types for Barcelona (MeTS-10 extent (bounding box)). Data from 20 randomly sampled days.

8) Daily speed profile Barcelona (MeTS-10 extent (bounding box)):

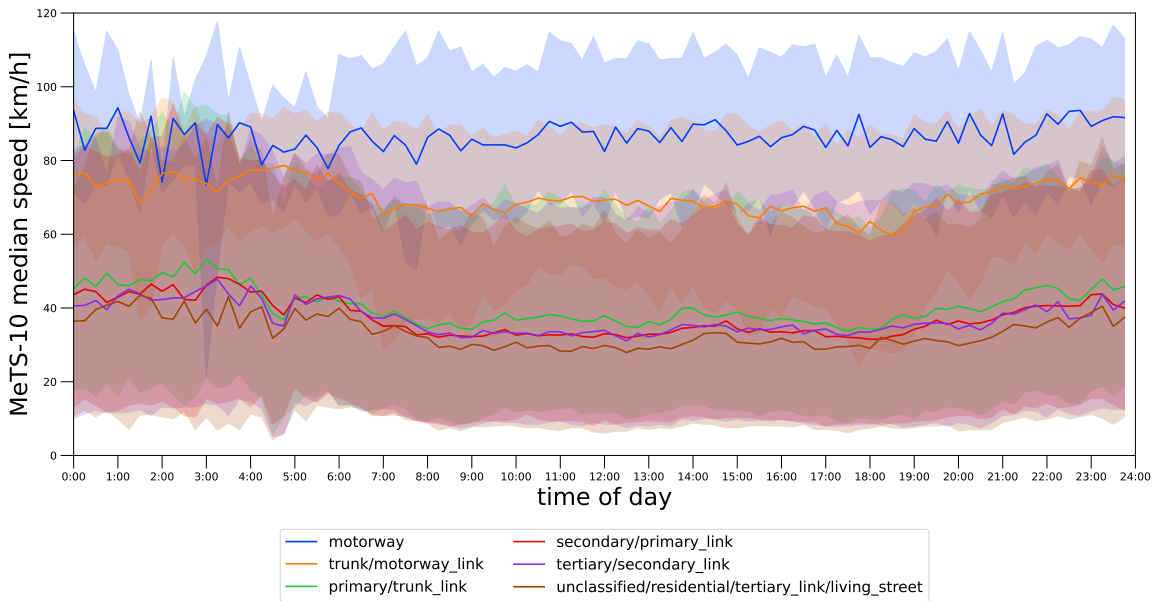
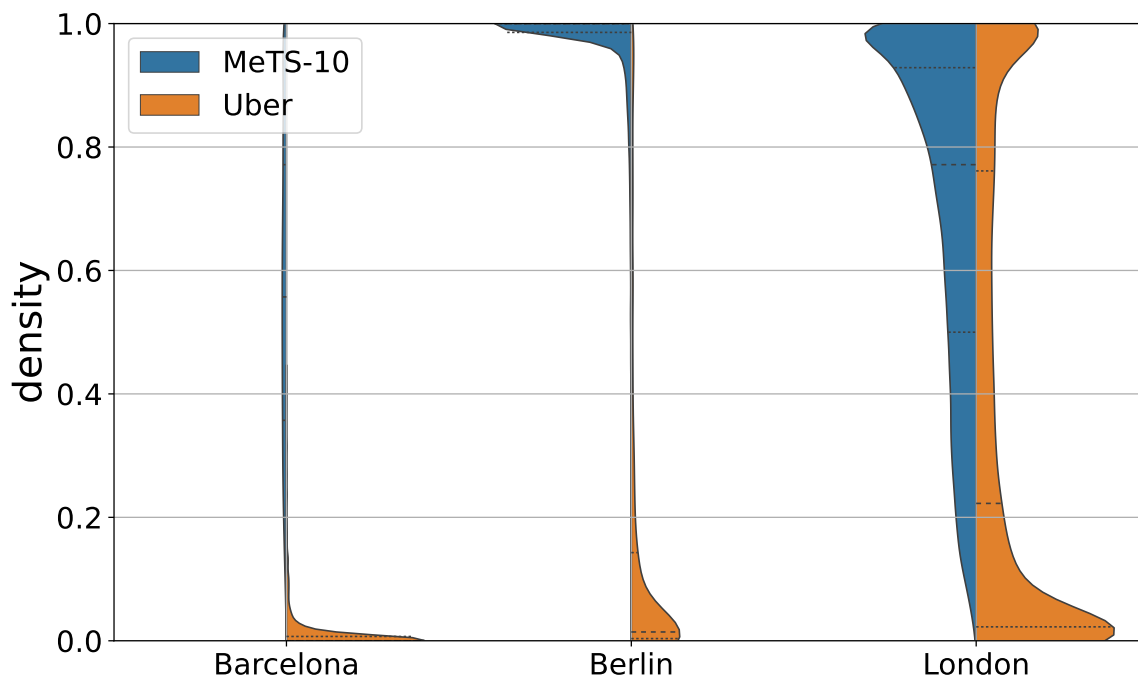


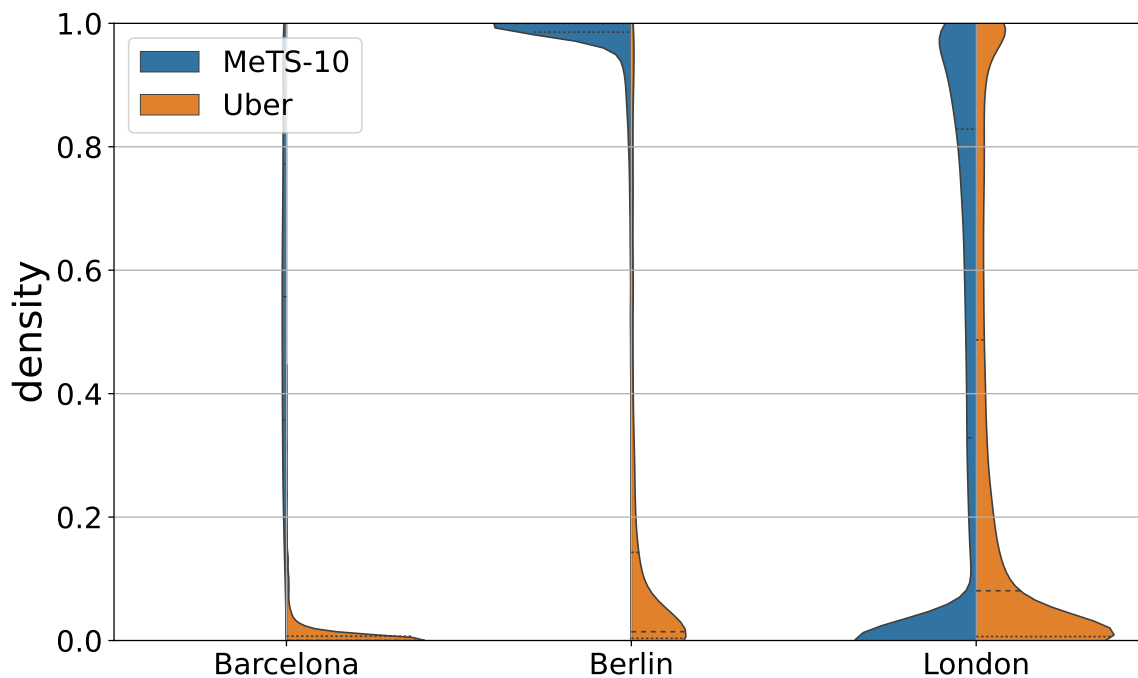
Fig. 85: Daily median 15 min speeds of all intersecting cells profile for different road types for Barcelona (MeTS-10 extent (bounding box)). The error hull is the 80% data interval [10.0–90.0 percentiles] of daily means from 20 randomly sampled days.

SUPPLEMENT H
KEY FIGURES UBER COMPARISON

A. Temporal coverage all 3 cities



(a) Uber segments in *Traffic4cast* bounding box only



(b) full historic road graph (all Uber segments)

Fig. 86: Violin plot of segment-wise temporal coverage for *MeTS-10* and Uber on the historic road graph for the 3 cities Barcelona, Berlin and London.

B. Barcelona

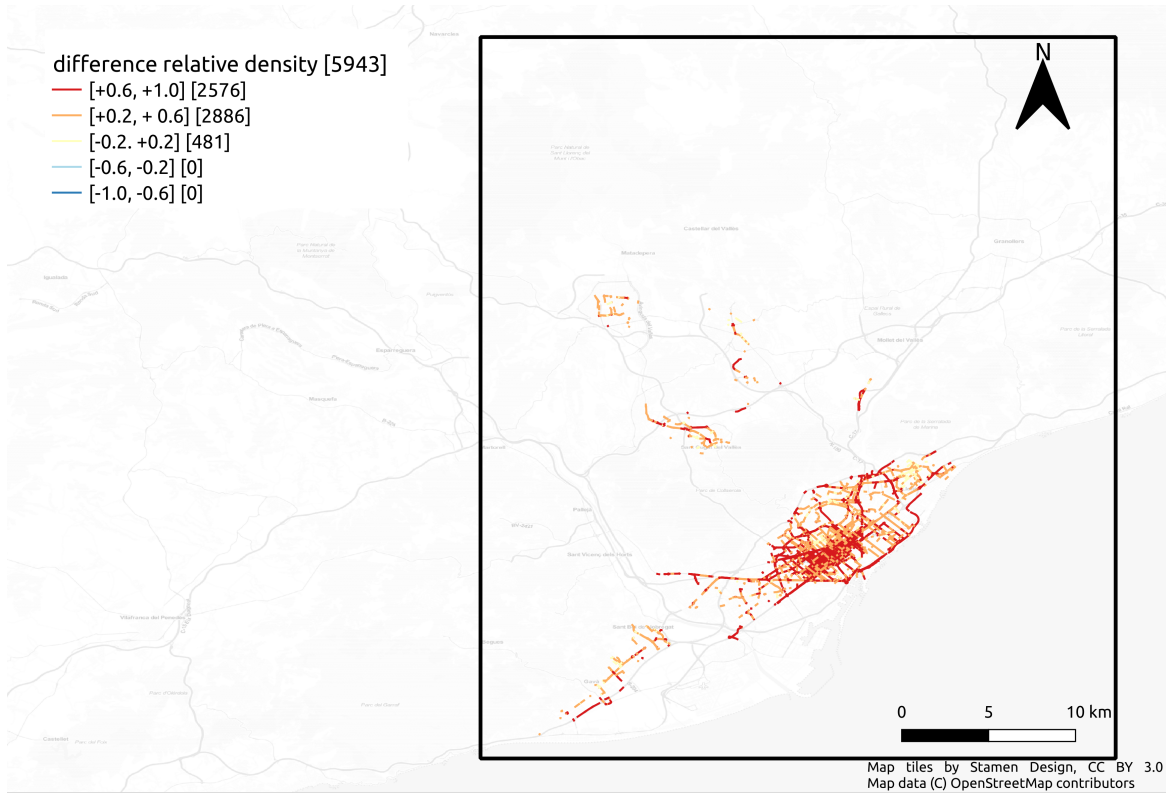


Fig. 87: Segment density differences of Uber and *MeTS-10* on the historic road graph Barcelona (8am–6pm). The color encoding shows the edge density difference, negative means higher temporal coverage of *MeTS-10* and positive values mean higher temporal coverage..

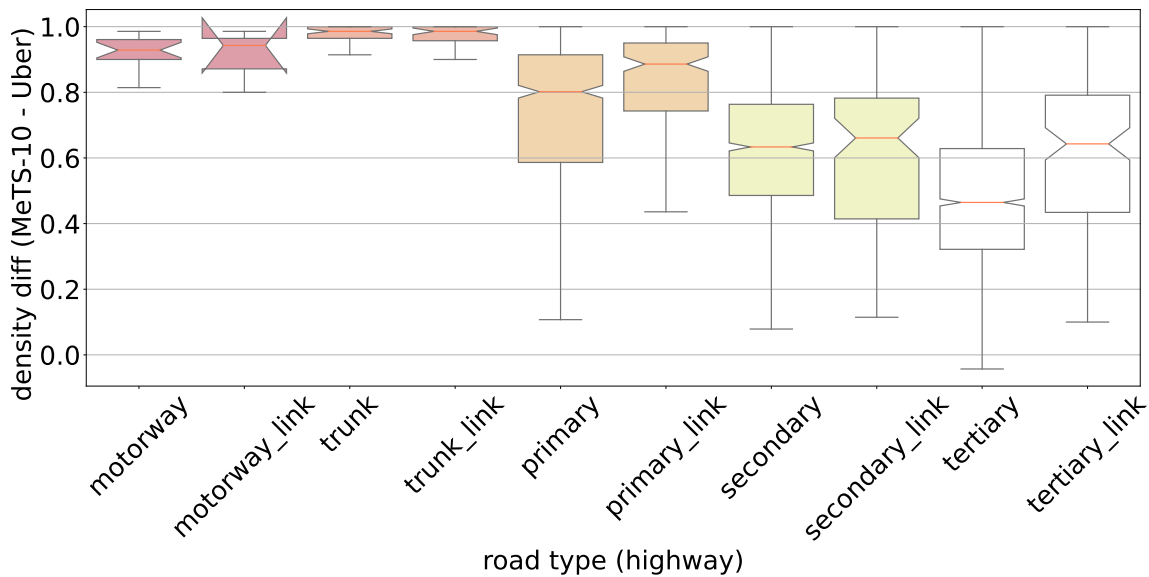


Fig. 88: Segment density differences Uber and *MeTS-10* on the historic road graph Barcelona daytime (8am–6pm, segments within 4c bounding box only). Mean density difference by road type (*i. e.* OSM highway attribute); positive density difference means higher temporal coverage of *MeTS-10* and negative mean higher temporal coverage.

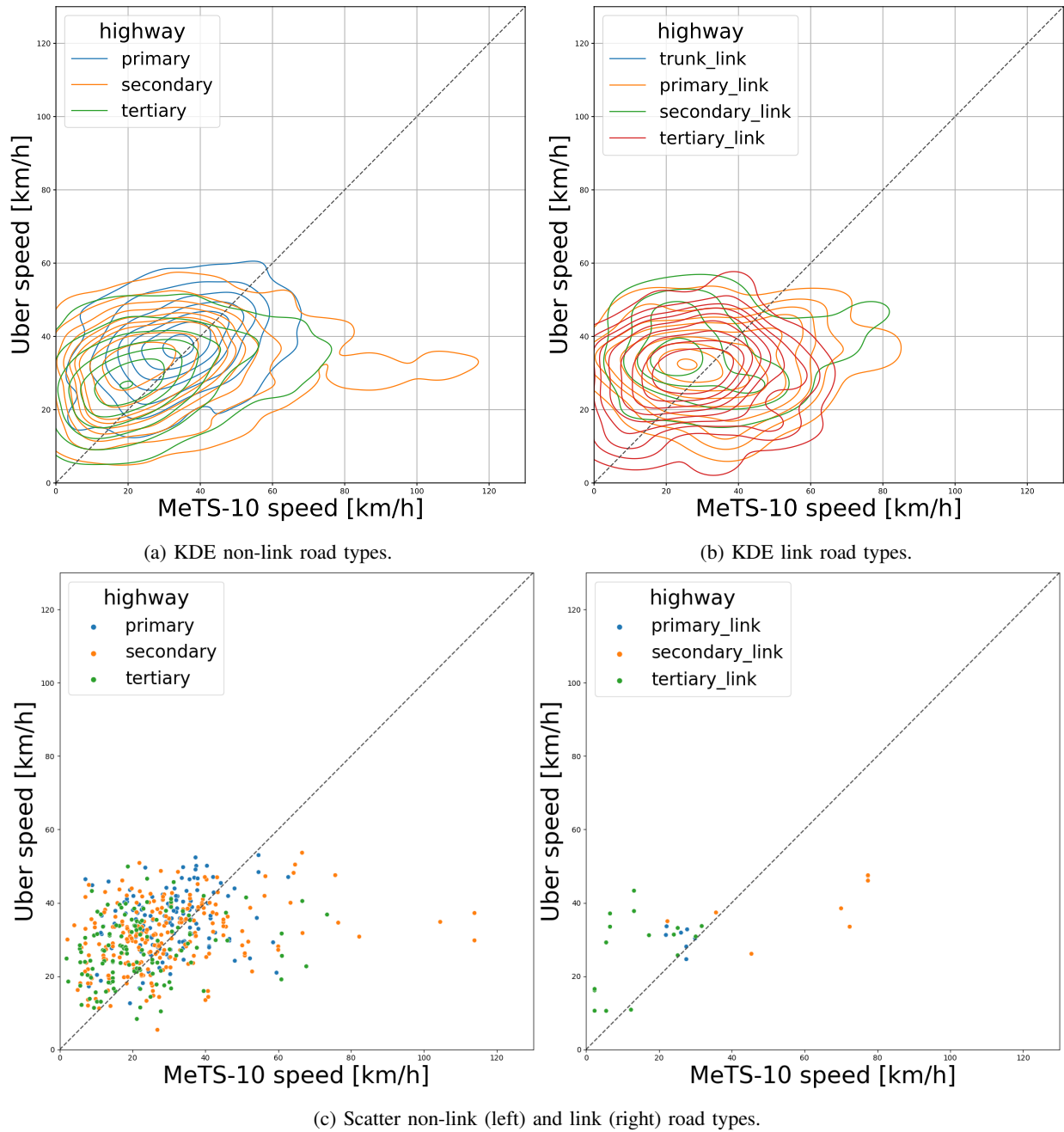


Fig. 89: Kernel Distribution Estimation and Scatter Plots of speeds of *MeTS-10* (x-axis, median_speed_kph) and Uber (y-axis, speed_kph_mean) on the historic road graph Barcelona daytime (8am–6pm) on the matching data, *i.e.* within *MeTS-10* bounding box only and where data is available at the same time and segment, for the most important road types.

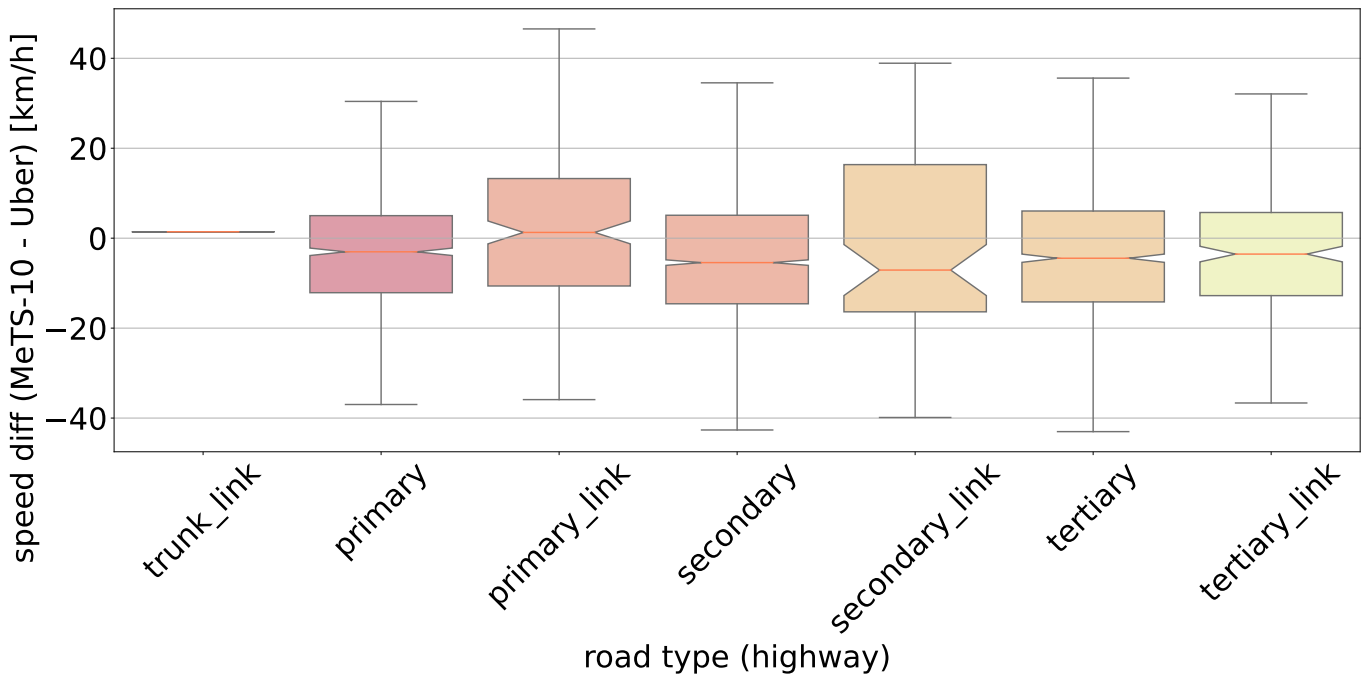


Fig. 90: Speed differences Uber and *MeTS-10* on the historic road graph Barcelona daytime (8am–6pm) on the matching data, *i. e.* within *MeTS-10* bounding box only and where data is available at the same time and segment. Mean difference by road class (OSM highway attribute). Positive speed difference means higher values in *MeTS-10*.

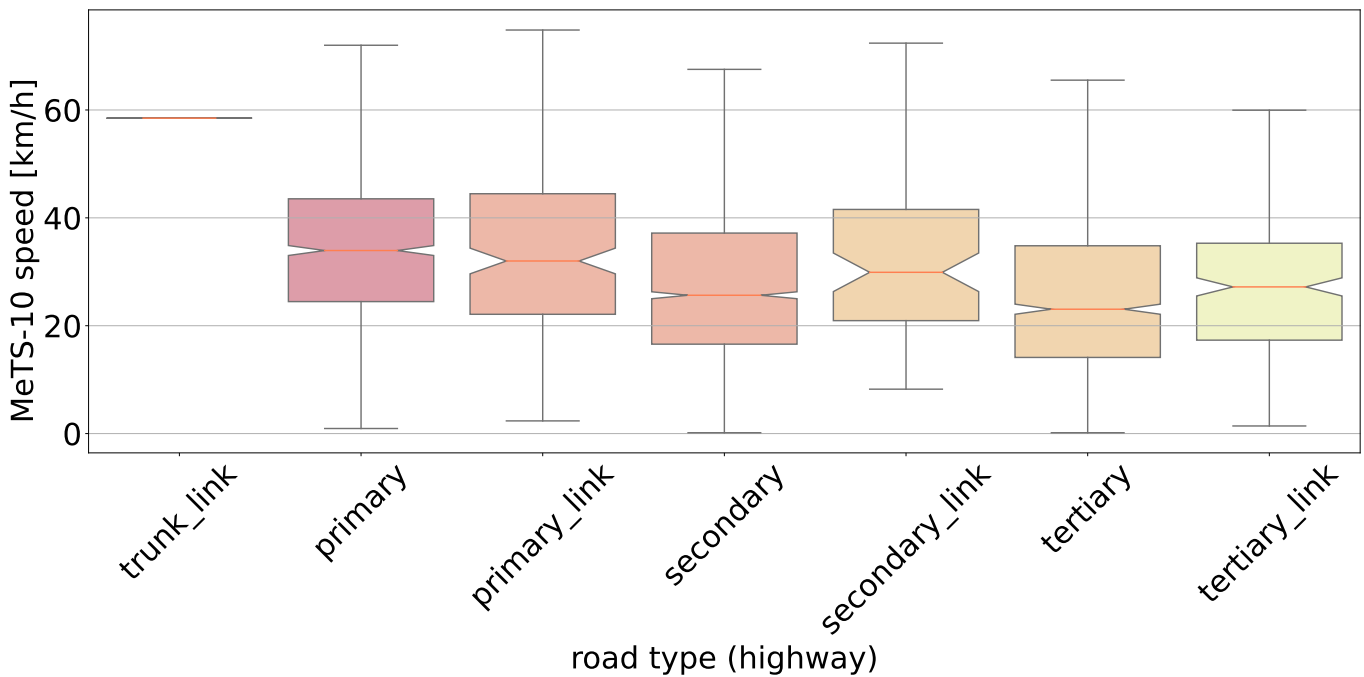


Fig. 91: *MeTS-10* speeds on the historic road graph Barcelona daytime (8am–6pm) on the matching data, *i. e.* within *MeTS-10* bounding box only and where data is available at the same time and segment. By road class (OSM highway attribute).

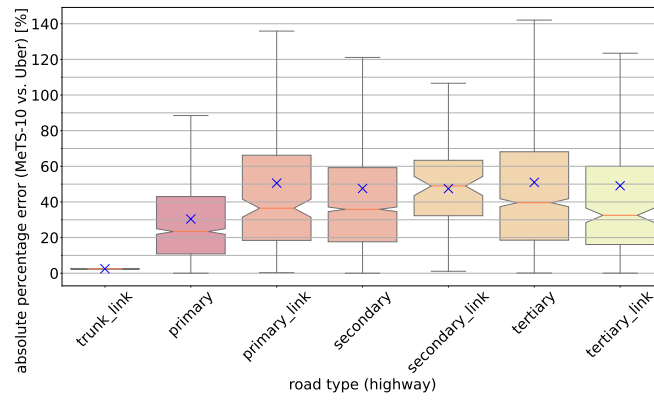


Fig. 92: Barcelona absolute percentage error *MeTS-10* vs. Uber by road type. Blue crosses indicate the mean per road type.

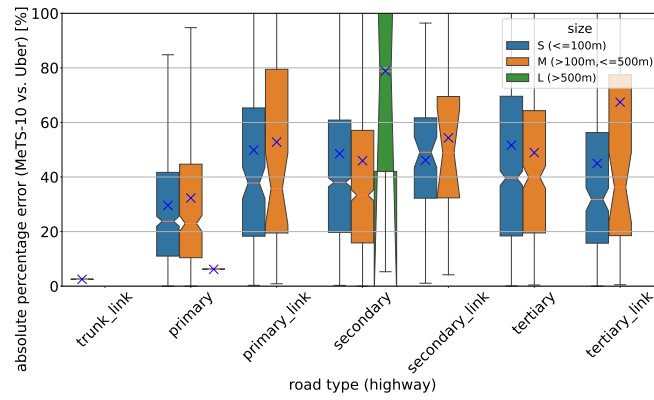


Fig. 93: Barcelona absolute percentage error *MeTS-10* vs. Uber by road type and segment length. Blue crosses indicate the mean per road type.

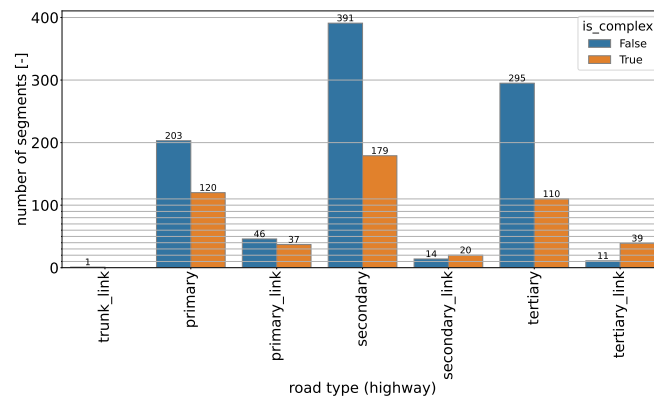


Fig. 94: Segment counts *MeTS-10* – Uber matched data.

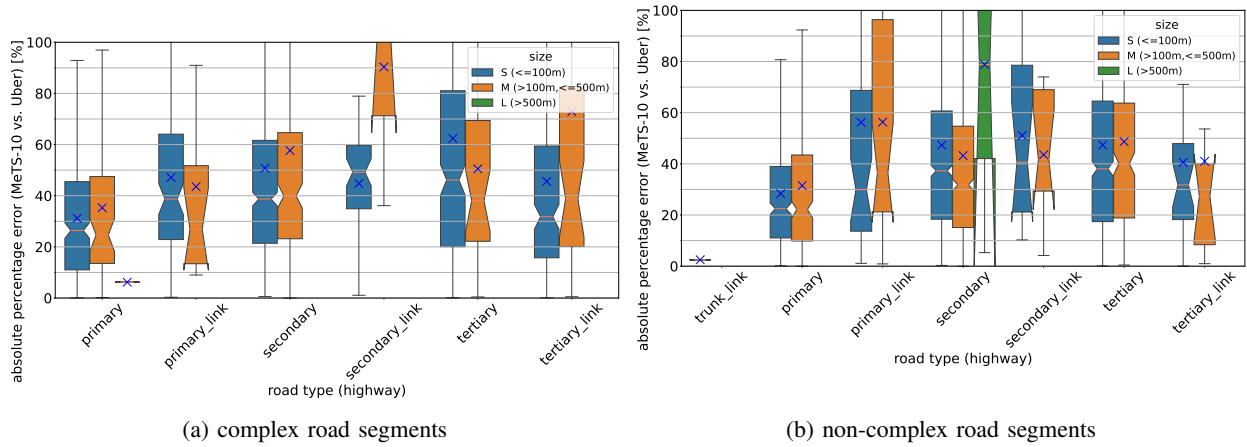


Fig. 95: Barcelona absolute percentage error *MeTS-10* vs. Uber by road type and segment length. Blue crosses indicate the mean per road type.

C. Berlin

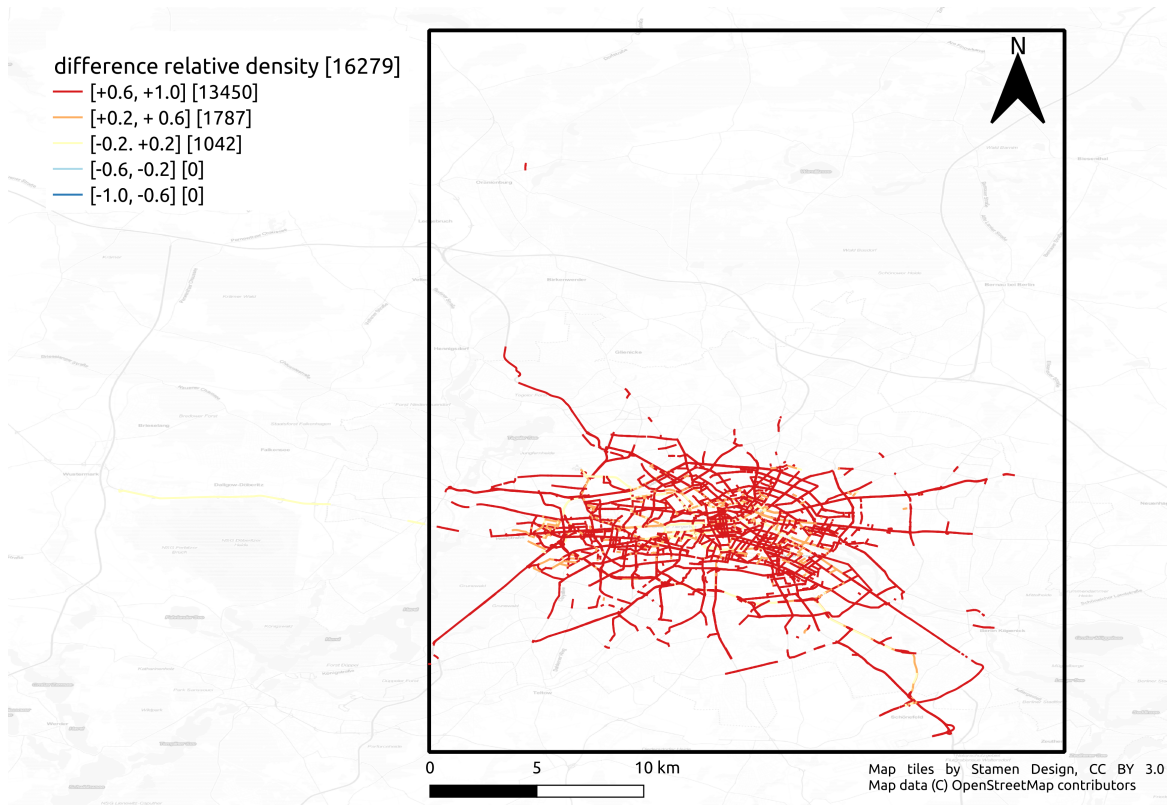


Fig. 96: Segment density differences of Uber and *MeTS-10* on the historic road graph Berlin (8am–6pm). The color encoding shows the edge density difference, negative means higher temporal coverage of *MeTS-10* and positive values mean higher temporal coverage..

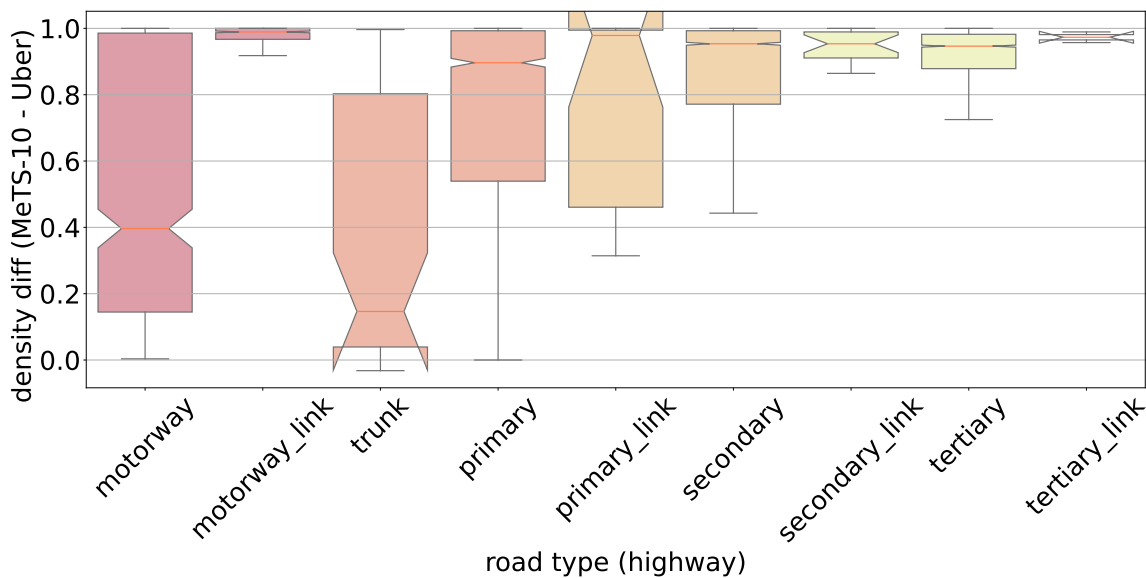
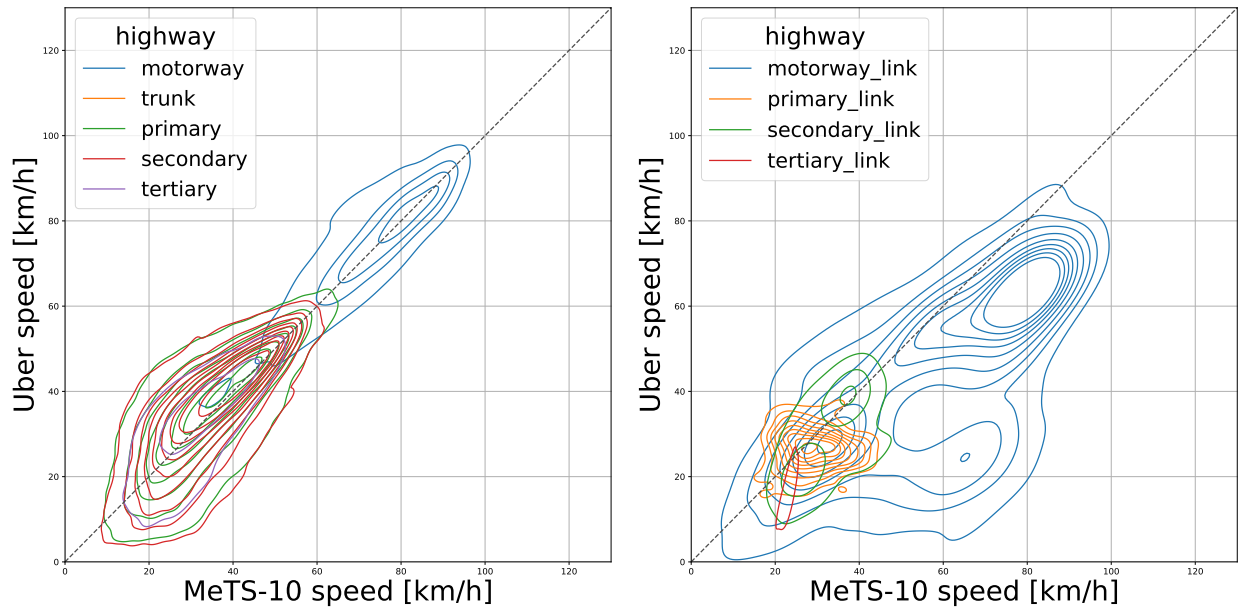
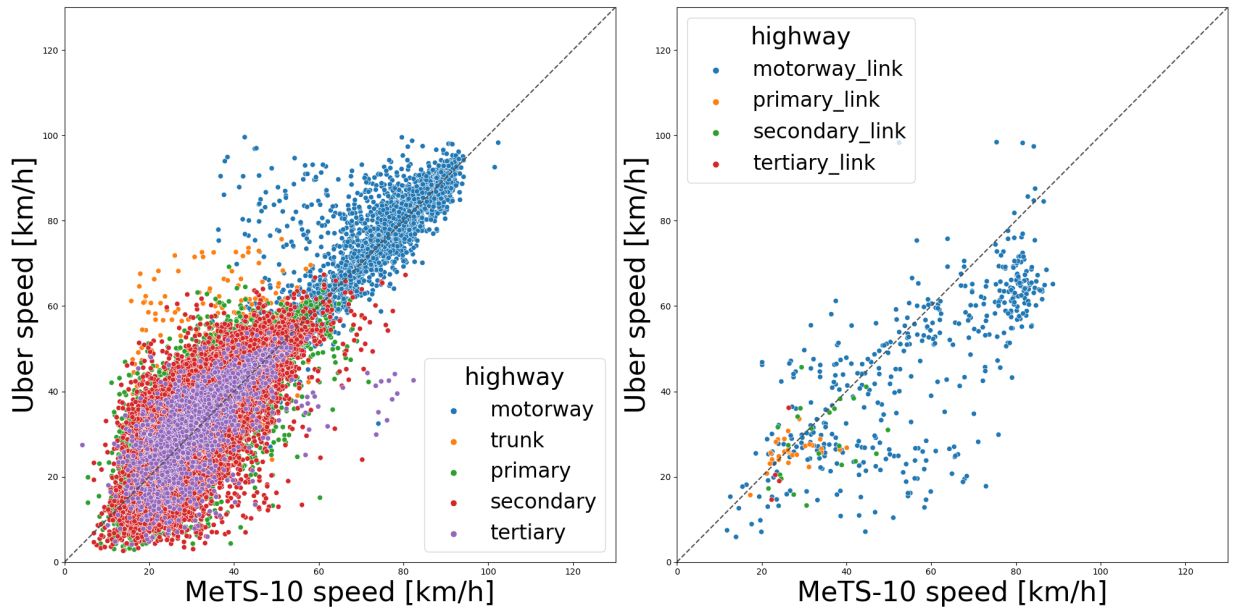


Fig. 97: Segment density differences Uber and *MeTS-10* on the historic road graph Berlin daytime (8am–6pm, segments within 4c bounding box only). Mean density difference by road class (*i. e.* OSM highway attribute); positive density difference means higher temporal coverage of *MeTS-10* and negative mean higher temporal coverage.



(a) KDE non-link road types.

(b) KDE link road types.



(c) Scatter non-link (left) and link (right) road types.

Fig. 98: Kernel Distribution Estimation and Scatter Plots of speeds of *MeTS-10* (x-axis, median_speed_kph) and Uber (y-axis, speed_kph_mean) on the historic road graph Berlin daytime (8am–6pm) on the matching data, *i. e.* within *MeTS-10* bounding box only and where data is available at the same time and segment, for the most important road types.

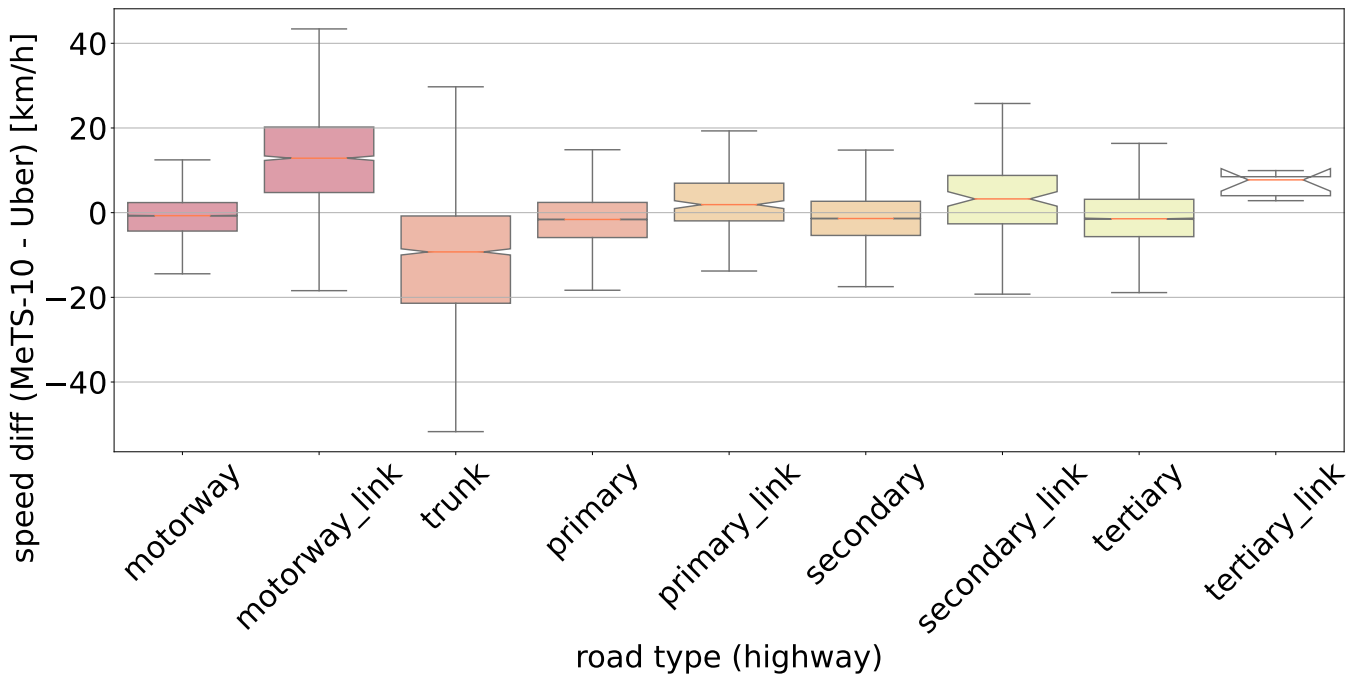


Fig. 99: Speed differences Uber and *MeTS-10* on the historic road graph Berlin daytime (8am–6pm) on the matching data, *i. e.* within *MeTS-10* bounding box only and where data is available at the same time and segment. Mean difference by road class (OSM highway attribute). Positive speed difference means higher values in *MeTS-10*.

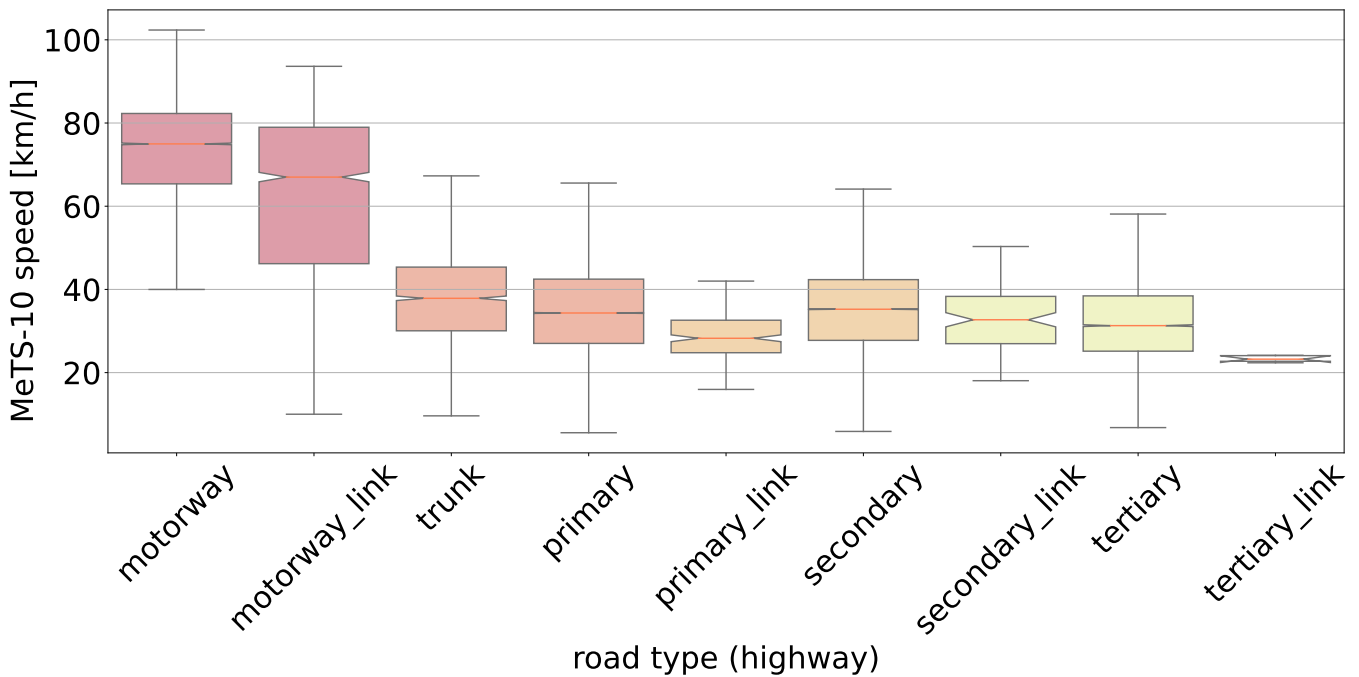


Fig. 100: *MeTS-10* speeds on the historic road graph Berlin daytime (8am–6pm) on the matching data, *i. e.* within *MeTS-10* bounding box only and where data is available at the same time and segment. By road class (OSM highway attribute).

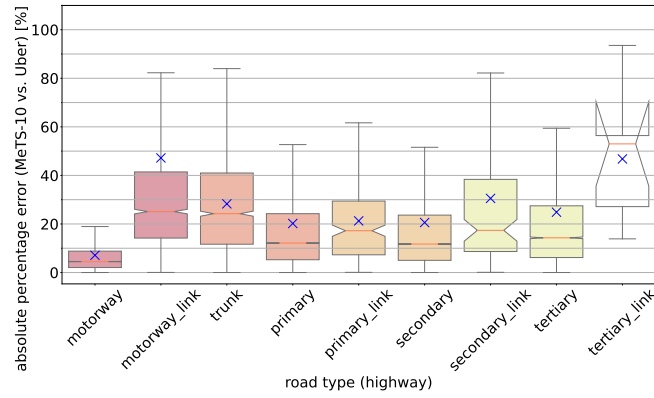


Fig. 101: Berlin absolute percentage error *MeTS-10* vs. Uber by road type. Blue crosses indicate the mean per road type.

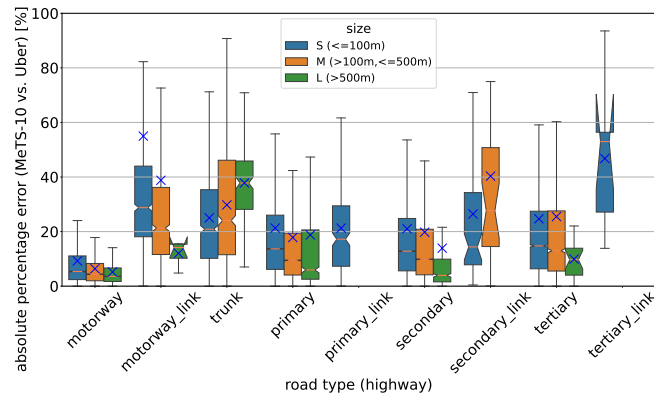


Fig. 102: Berlin absolute percentage error *MeTS-10* vs. Uber by road type and segment length. Blue crosses indicate the mean per road type.

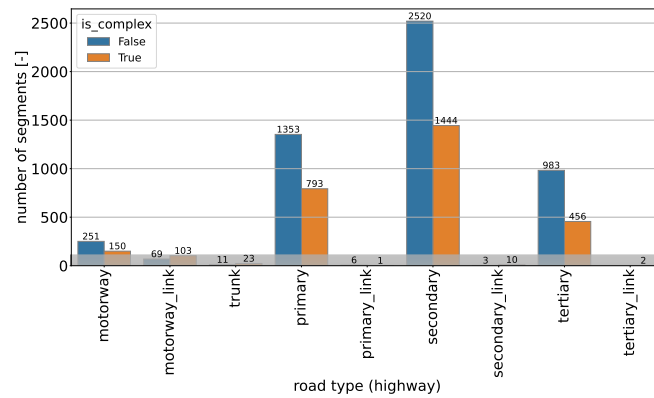


Fig. 103: Segment counts *MeTS-10* – Uber matched data.

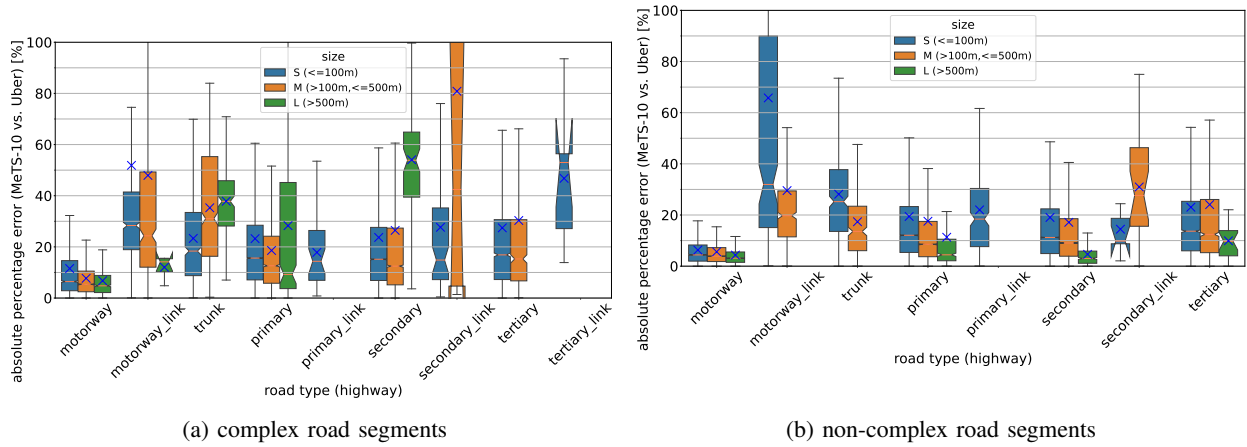


Fig. 104: Berlin absolute percentage error *MeTS-10* vs. Uber by road type and segment length. Blue crosses indicate the mean per road type.

D. London

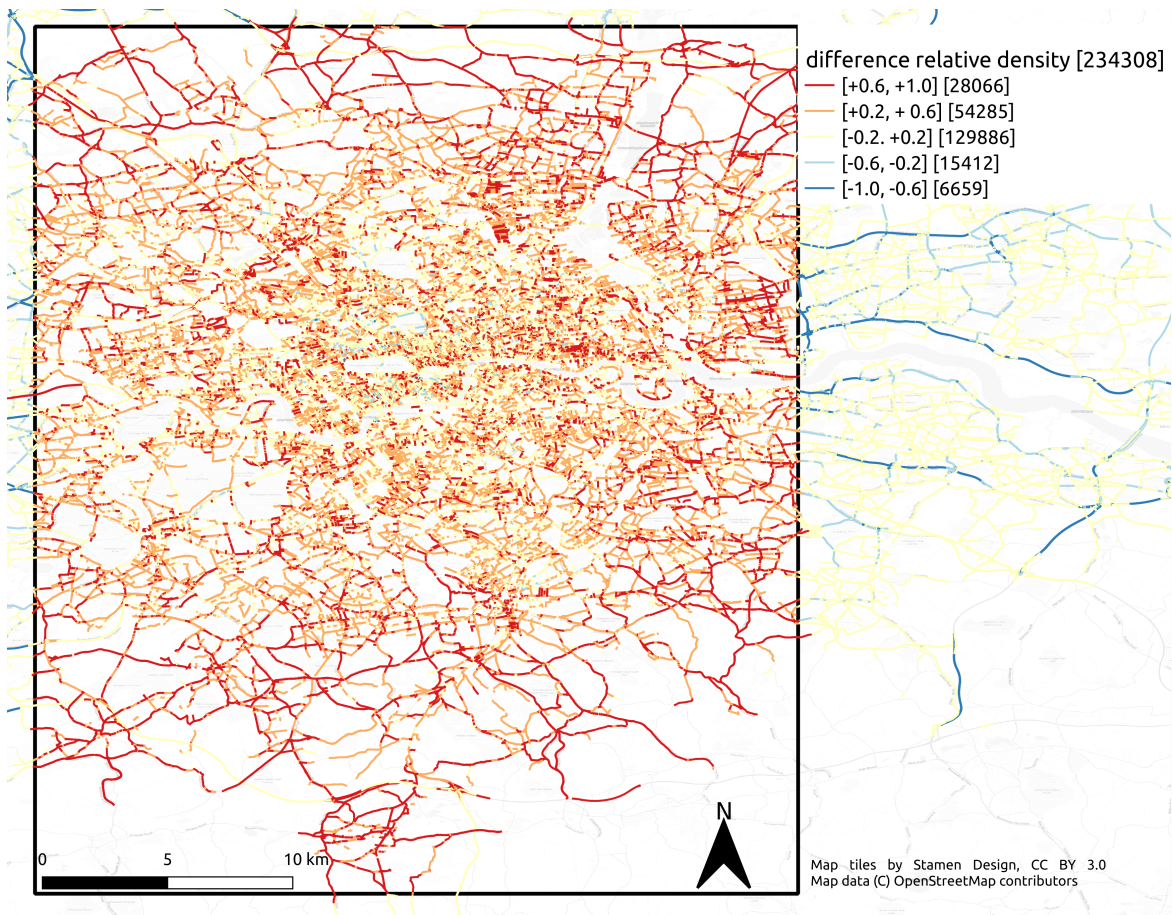


Fig. 105: Segment density differences of Uber and *MeTS-10* on the historic road graph London (8am–6pm). The color encoding shows the edge density difference, negative means higher temporal coverage of *MeTS-10* and positive values mean higher temporal coverage..

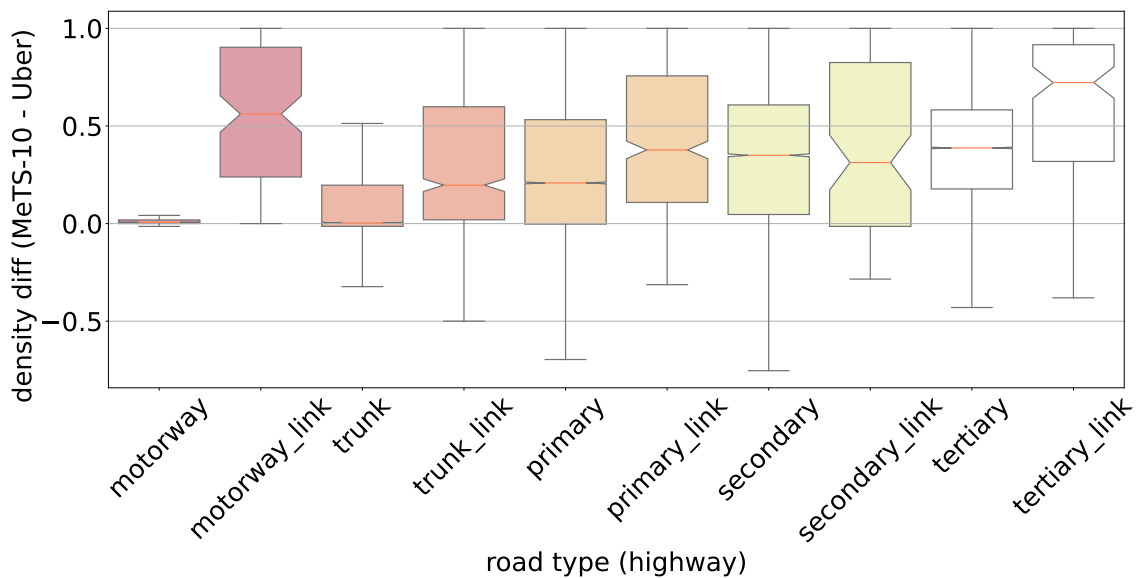
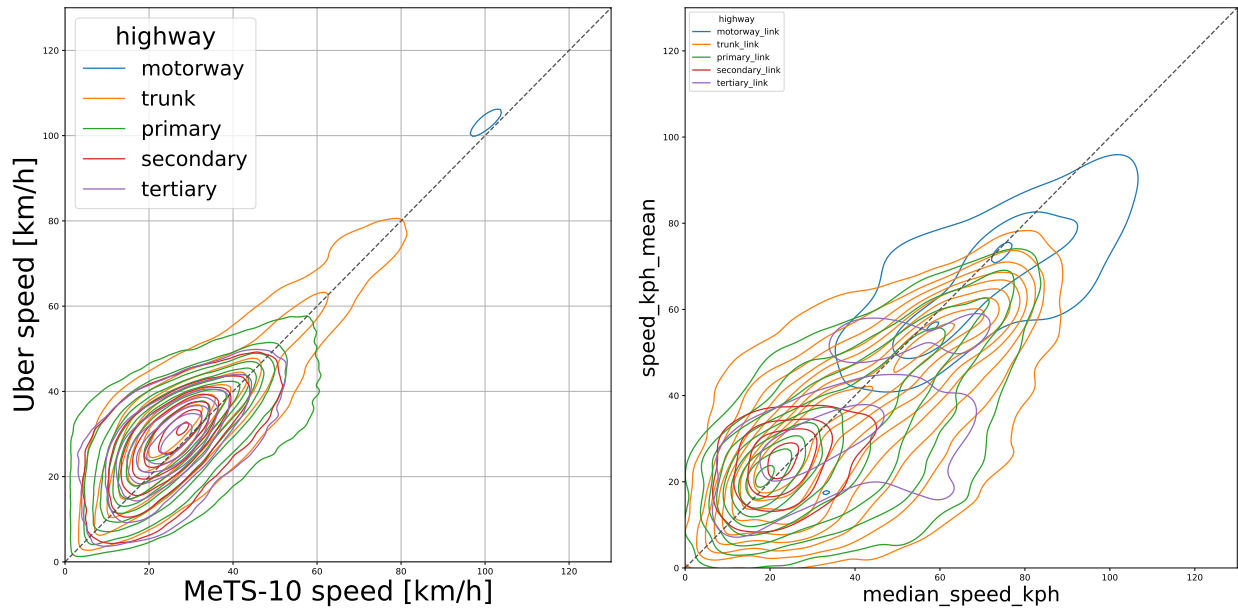
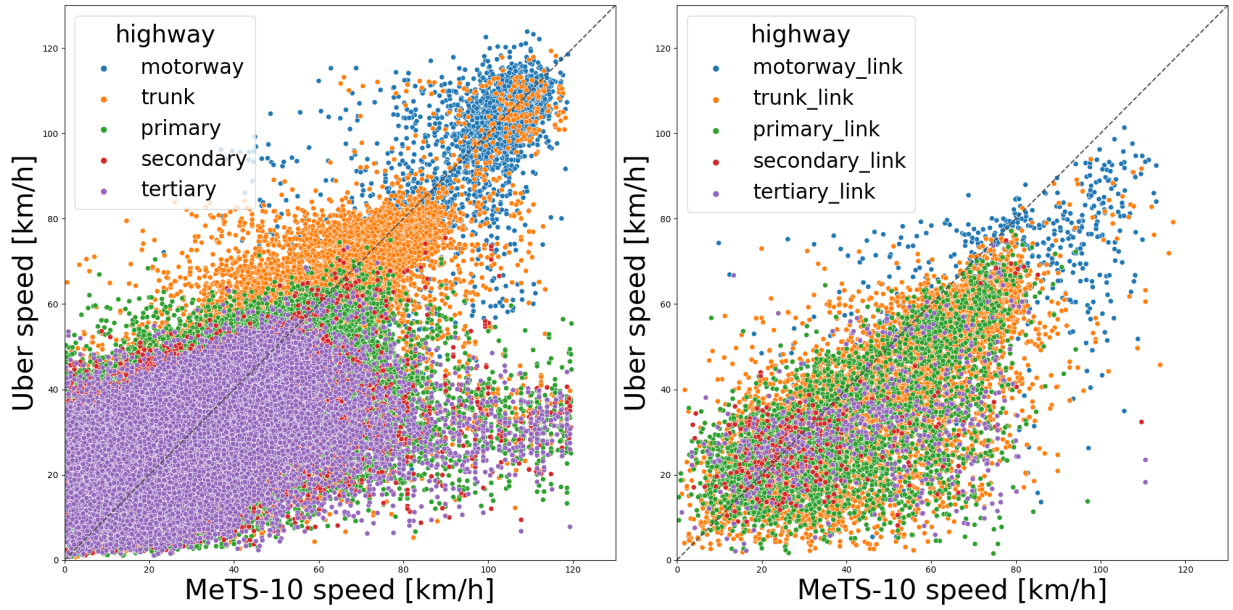


Fig. 106: Segment density differences Uber and *MeTS-10* on the historic road graph London daytime (8am–6pm, segments within 4c bounding box only). Mean density difference by road class (*i. e.* OSM highway attribute); positive density difference means higher temporal coverage of *MeTS-10* and negative mean higher temporal coverage.



(a) KDE non-link road types.

(b) KDE link road types.



(c) Scatter non-link (left) and link (right) road types.

Fig. 107: Kernel Distribution Estimation and Scatter Plots of speeds of *MeTS-10* (x-axis, median_speed_kph) and Uber (y-axis, speed_kph_mean) on the historic road graph London daytime (8am–6pm) on the matching data, *i. e.* within *MeTS-10* bounding box only and where data is available at the same time and segment, for the most important road types.

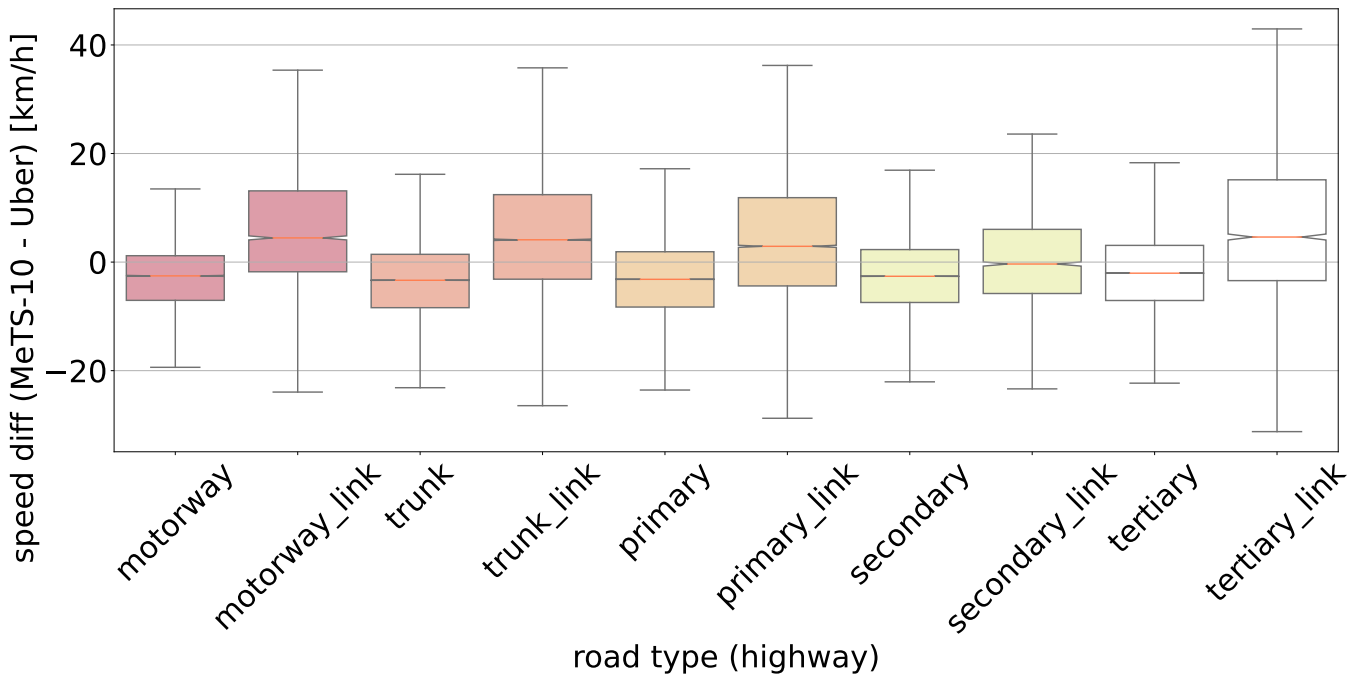


Fig. 108: Speed differences Uber and *MeTS-10* on the historic road graph London daytime (8am–6pm) on the matching data, *i.e.* within *MeTS-10* bounding box only and where data is available at the same time and segment. Mean difference by road class (OSM highway attribute). Positive speed difference means higher values in *MeTS-10*.

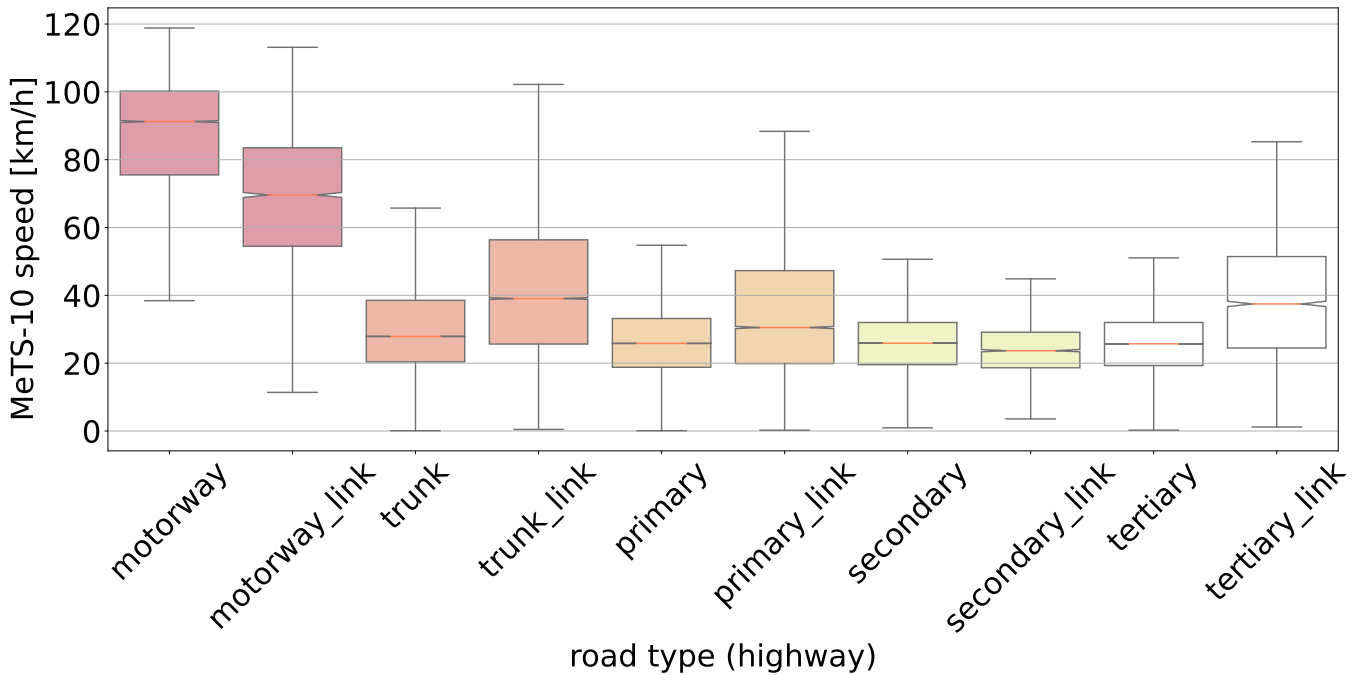


Fig. 109: *MeTS-10* speeds on the historic road graph London daytime (8am–6pm) on the matching data, *i.e.* within *MeTS-10* bounding box only and where data is available at the same time and segment. By road class (OSM highway attribute).

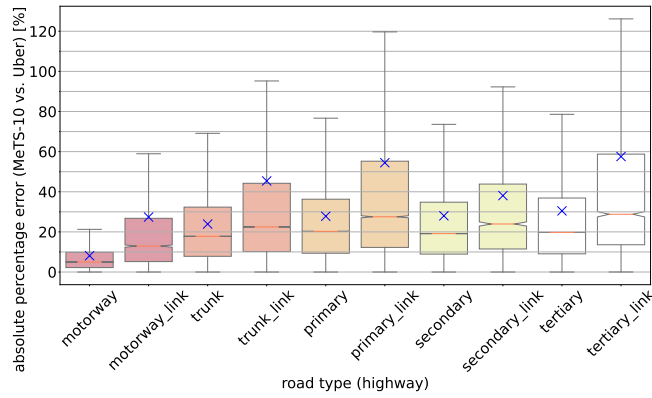


Fig. 110: London absolute percentage error *MeTS-10* vs. Uber by road type. Blue crosses indicate the mean per road type.

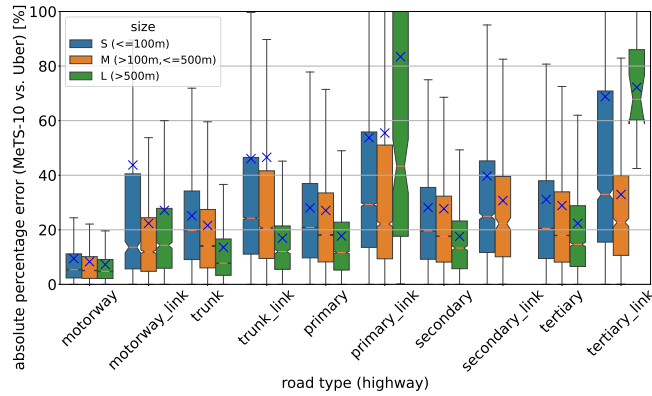


Fig. 111: London absolute percentage error *MeTS-10* vs. Uber by road type and segment length. Blue crosses indicate the mean per road type.

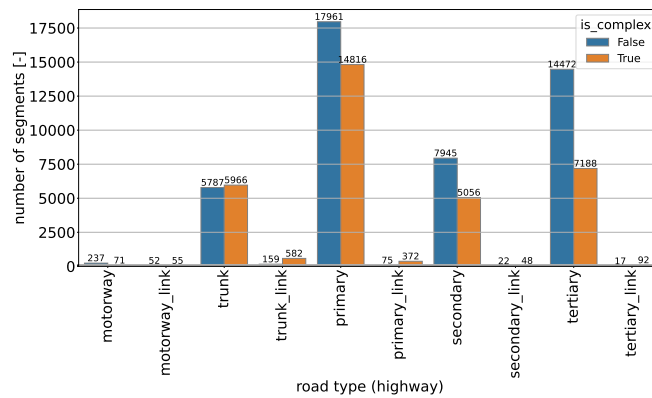
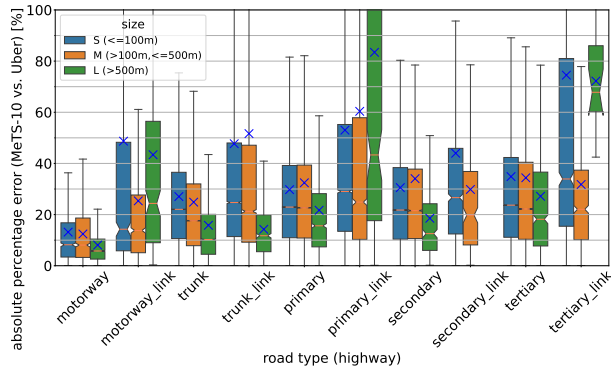
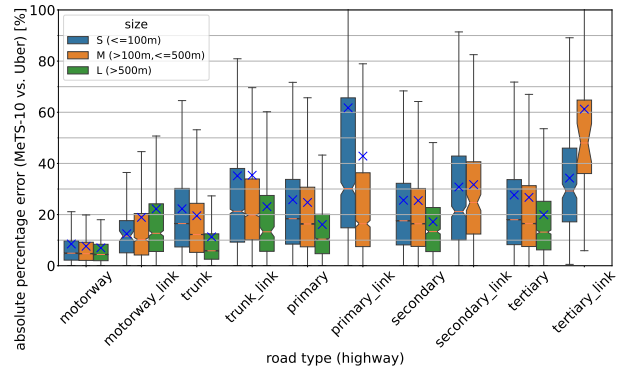


Fig. 112: Segment counts *MeTS-10* – Uber matched data.



(a) complex road segments



(b) non-complex road segments

Fig. 113: London absolute percentage error *MeTS-10* vs. Uber by road type and segment length. Blue crosses indicate the mean per road type.

CONTENTS

I	Introduction	1	Nina Wiedemann	11
II	Related Work	2	Henry Martin	11
	II-A Vehicle Detector Datasets	2	Martin Tomko	11
	II-B GPS Probes Datasets	3	Lukas Ambühl	11
III	The Dataset: Segment Median Speeds	3	Luca Hermes	11
IV	Input Data and Data Pipeline	3	Michael Kopp	11
	IV-A Input Data	4	Supplement A: Complements on Input Data and Data Pipeline	1
	IV-A1 Traffic Map Movies	4	A-A Input Data	1
	IV-A2 OpenStreetMap	4	A-A1 Traffic Map Movies	1
	IV-B Data Pipeline	4	A-A2 OpenStreetMap	1
	IV-B1 OpenStreetMap Data Download and Road Graph Construction (dp03)	4	A-B Data Pipeline	1
	IV-B2 Spatial Intersection of Road Graph and City Cells (dp04)	4	A-B1 OpenStreetMap Data Download and Road Graph Construction (dp03)	2
	IV-B3 Temporal Aggregation of HERE Traffic Map Movies (dp01)	4	A-B2 Spatial Intersection of Road Graph and City Cells (dp04)	2
	IV-B4 Segment Speeds from Spatial Join (dp06a)	4	A-B3 Temporal Aggregation of HERE Traffic Map Movies (dp01)	2
	IV-B5 Confidence Filtering of Segment Speeds (dp06b) Based on Speed Clustering (dp02) and Free Flow Speeds from Spatial Join and Quantile Selection (dp05)	5	A-B4 Confidence Filtering of Segment Speeds (dp06b)	2
V	Validation	5	A-B5 Speed Clustering (dp02) and Free Flow speeds from Spatial Join and Quantile Selection (dp05)	3
	V-A Comparison with Uber Movement Speeds	5	Supplement B: Analysis of Spot Binning under Idealized Conditions	3
	V-A1 Dataset Comparison	5	Supplement C: Complements on Validation	4
	V-A2 Spatial and Temporal Coverage	5	C-A Comparison with Uber Movement Speeds	4
	V-A3 Speed Differences	6	C-A1 Historic Road Graph	4
	V-B Comparison with Stationary Vehicle Detector Data	6	C-A2 Spatial and Temporal Coverage	4
	V-C Baseline comparison of Uber Movement Speeds with Stationary Vehicle Detector Data	7	C-A3 Speed Differences	4
VI	Discussion	7	C-B Comparison with Stationary Vehicle Detector Data	5
	VI-A Discussion of Method Design Choices	7	C-C Baseline comparison of Uber Movement Speeds with Stationary Vehicle Detector Data	7
	VI-B Discussion of Validations	8	Supplement D: Complements on Discussion	8
VII	Conclusion	8	D-A Complements Spatial Intersection (dp04)	8
Acknowledgment		9	Supplement E: Extended Dataset Overview	8
Author Contributions Statement		9	Supplement F: Key Figures	10
References		9	F-A Key Figures Antwerp (2021)	11
Biographies		11	F-A1 Road graph map Antwerp (2021)	11
	Moritz Neun	11	F-A2 Static data Antwerp (2021)	11
	Christian Eichenberger	11	F-A3 Segment density map Antwerp (2021)	13
	Yanan Xin	11	F-A4 Daily density profile Antwerp (2021)	14
	Cheng Fu	11	F-A5 Daily speed profile Antwerp (2021)	14
			F-B Key Figures Bangkok (2021)	15

F-B1	Road graph map Bangkok (2021)	15	F-G5	Daily speed profile Melbourne (2021)	38
F-B2	Static data Bangkok (2021)	15	F-H	Key Figures Moscow (2021)	39
F-B3	Segment density map Bangkok (2021)	17	F-H1	Road graph map Moscow (2021)	39
F-B4	Daily density profile Bangkok (2021)	18	F-H2	Static data Moscow (2021)	39
F-B5	Daily speed profile Bangkok (2021)	18	F-H3	Segment density map Moscow (2021)	41
F-C	Key Figures Barcelona (2021)	19	F-H4	Daily density profile Moscow (2021)	42
F-C1	Road graph map Barcelona (2021)	19	F-H5	Daily speed profile Moscow (2021)	42
F-C2	Static data Barcelona (2021)	19	F-I	Key Figures London (2022)	43
F-C3	Segment density map Barcelona (2021)	21	F-I1	Road graph map London (2022)	43
F-C4	Daily density profile Barcelona (2021)	22	F-I2	Static data London (2022)	43
F-C5	Daily speed profile Barcelona (2021)	22	F-I3	Segment density map London (2022)	45
F-D	Key Figures Berlin (2021)	23	F-I4	Daily density profile London (2022)	46
F-D1	Road graph map Berlin (2021)	23	F-I5	Daily speed profile London (2022)	46
F-D2	Static data Berlin (2021)	23	F-J	Key Figures Madrid (2022)	47
F-D3	Segment density map Berlin (2021)	25	F-J1	Road graph map Madrid (2022)	47
F-D4	Daily density profile Berlin (2021)	26	F-J2	Static data Madrid (2022)	47
F-D5	Daily speed profile Berlin (2021)	26	F-J3	Segment density map Madrid (2022)	49
F-E	Key Figures Chicago (2021)	27	F-J4	Daily density profile Madrid (2022)	50
F-E1	Road graph map Chicago (2021)	27	F-J5	Daily speed profile Madrid (2022)	50
F-E2	Static data Chicago (2021)	27	F-K	Key Figures Melbourne (2022)	51
F-E3	Segment density map Chicago (2021)	29	F-K1	Road graph map Melbourne (2022)	51
F-E4	Daily density profile Chicago (2021)	30	F-K2	Static data Melbourne (2022)	51
F-E5	Daily speed profile Chicago (2021)	30	F-K3	Segment density map Melbourne (2022)	53
F-F	Key Figures Istanbul (2021)	31	F-K4	Daily density profile Melbourne (2022)	54
F-F1	Road graph map Istanbul (2021)	31	F-K5	Daily speed profile Melbourne (2022)	54
F-F2	Static data Istanbul (2021)	31	Supplement G: Key Figures Uber Validation Historic Road Graph		
F-F3	Segment density map Istanbul (2021)	33	G-A	Key Figures London	55
F-F4	Daily density profile Istanbul (2021)	34	G-A1	Road graph map London	55
F-F5	Daily speed profile Istanbul (2021)	34	G-A2	Static data London (full historic road graph)	55
F-G	Key Figures Melbourne (2021)	35	G-A3	Static data London (MeTS-10 extent (bounding box))	57
F-G1	Road graph map Melbourne (2021)	35	G-A4	Segment density map London	59
F-G2	Static data Melbourne (2021)	35	G-A5	Daily density profile London (full historic road graph)	60
F-G3	Segment density map Melbourne (2021)	37	G-A6	Daily speed profile London (full historic road graph)	60
F-G4	Daily density profile Melbourne (2021)	38	G-A7	Daily density profile London (MeTS-10 extent (bounding box))	61

	G-A8	Daily speed profile London (MeTS-10 extent (bounding box))	61
G-B		Key Figures Berlin	62
	G-B1	Road graph map Berlin . . .	62
	G-B2	Static data Berlin (full historic road graph)	62
	G-B3	Static data Berlin (MeTS-10 extent (bounding box)) . . .	64
	G-B4	Segment density map Berlin	66
	G-B5	Daily density profile Berlin (full historic road graph) . .	67
	G-B6	Daily speed profile Berlin (full historic road graph) . .	67
	G-B7	Daily density profile Berlin (MeTS-10 extent (bounding box))	68
	G-B8	Daily speed profile Berlin (MeTS-10 extent (bounding box))	68
G-C		Key Figures Barcelona	69
	G-C1	Road graph map Barcelona .	69
	G-C2	Static data Barcelona (full historic road graph)	69
	G-C3	Static data Barcelona (MeTS-10 extent (bounding box))	71
	G-C4	Segment density map Barcelona	73
	G-C5	Daily density profile Barcelona (full historic road graph)	74
	G-C6	Daily speed profile Barcelona (full historic road graph)	74
	G-C7	Daily density profile Barcelona (MeTS-10 extent (bounding box))	75
	G-C8	Daily speed profile Barcelona (MeTS-10 extent (bounding box))	75
Supplement H: Key Figures Uber Comparison			76
	H-A	Temporal coverage all 3 cities	76
	H-B	Barcelona	77
	H-C	Berlin	81
	H-D	London	86